DIETARY FLAVONOIDS REDUCE CARCINOGEN-INDUCED DNA DAMAGE IN BRONCHIAL EPITHELIAL CELLS IN VITRO

By

Tharindu Lakshan Suraweera Arachchilage

Submitted in fulfillment of the requirements

for the degree of Master of Science

at

Dalhousie University

Halifax, Nova Scotia

June 2022

Dalhousie University is located in Mi'kma'ki, the

ancestral and unceded territory of the Mi'kmaq.

We are all Treaty people.

TABLE OF CONTENTS

LIST OF TABLES

LIST OF FIGURES

ABSTRACT

The potential of selected flavonoids in reducing carcinogen-induced reactive oxygen species (ROS) and DNA damage through the activation of nuclear factor erythroid 2 p45 (NF-E2)-related factor (Nrf2)/antioxidant response element (ARE) pathway was studied *in vitro*. Dose-dependent effects of pre-incubated flavonoids on pro-carcinogen 4-[(acetoxymethyl)nitrosamino]-1-(3-pyridyl)-1-butanone (NNKAc)-induced ROS and DNA damage in human bronchial epithelial cells were studied in comparison to non-flavonoids. The most effective flavonoids were assessed for the activation of Nrf2/ARE pathway. Genistein, procyanidin B2 (PCB2), and quercetin significantly suppressed the NNKAc-induced ROS and DNA damage. PCB2 significantly upregulated the activation of Nrf2 and protein kinase B through phosphorylation. Genistein and PCB2 significantly upregulated the phospho-Nrf2 nuclear translocation and catalase activity. In summary, quercetin, genistein, and PCB2 reduced the NNKAc-induced ROS and DNA damage in concert with activation of Nrf2. Further studies are required to understand the role of dietary flavonoids on the regulation of Nrf2/ARE pathway in relation to carcinogenesis.

Keywords: *Dietary flavonoids, DNA damage, lung epithelial cells, Nrf2/ARE pathway, Reactive oxygen species*

LIST OF ABBREVIATIONS AND SYMBOLS USED

α	Alpha
β	Beta
γ	Gamma
ºC	Degree Celsius
%	Percentage
<	Less than
>	Greater than
µL	Micro litre
µM	Micro molar
nM	Nano molar
cm	Centimeter
cm^2	Square centimeter
h	Hour
min	Minute
mL	Milliliter
mM	Millimolar
mg	Milligram
g	Gram
V	Volt
W	Watt
A	Ampere
U	Enzyme unit

6-OHDA	6-Hydroxydopamine
ABTS	2,2′-Azino-bis-3-ethylbenzothiazoline-6-sulfonic acid
Akt	Protein kinase B
AMPK	5′ Adenosine monophosphate-activated protein kinase
ANOVA	One-way analysis of variance
Asp	Aspartate
ATM	Ataxia-telangiectasia mutated protein
ATR	Ataxia telangiectasia and rad 3 related protein
BSA	Bovine serum albumin
BRACA1	Breast cancer gene 1
BRACA2	Breast cancer gene 2
BrdU	Bromodeoxyuridine
C3G	Cyanidin-3-*O*-glucoside
CA	Comet assay
CAT	Catalase
Cat	Catalogue number
Chk1	Checkpoint kinase 1
Chk2	Checkpoint kinase 2
CTNF	Corrected total nuclear fluorescence
Cul3	Cullin3
CYP	Cytochrome p450
Cys	Cysteine
DAPI	4′,6-Diamidino-2-phenylindol

DCFDA	2' 7'-Dichlorofluorescein diacetate
DDR	DNA damage response
DFEA	DNA fragmentation ELISA assay
DMEM	Dulbecco's modified eagle medium
DMF	Dimethyl fumarate
DMSO	Dimethyl sulfoxide
DNA	Deoxyribonucleic acid
DPP3	Dipeptidyl peptidase III
DPPH	2,2-diphenyl-1-picrylhydrazyl
DSB	Double strand break
EDTA	Ethylenediaminetetraacetic acid
ELISA	Enzyme-linked immunosorbent assay
ERK	Extracellular signal-regulated protein kinase
FBS	Fetal bovine serum
G	Genistein
GCLM	Glutamate-cysteine ligase modifier
GPx	Glutathione peroxidase
GR	Glutathione reductase
GSH	Glutathione
GSK-3β	Glycogen synthase kinase 3 beta
GST	Glutathione S-transferase
H_2O_2	Hydrogen peroxide
HIA	γ-H2AX immunofluorescence assay

HO-1	Heme oxygenase 1
HRP	Horseradish peroxidase
HUVECs	Human umbilical vein epithelial cells
JNK	N-terminal kinase
Keap 1	Kelch-like ECH associated protein 1
LPS	Lipopolysaccharide
MAPK	Mitogen-activated protein kinase
MC	Mean fluorescence
Met	Methionine
MTX	Methotrexate
NAD(P)H	Nicotine adenine dinucleotide phosphate
NNAL	4-(Methylnitrosamino)-1-(3-pyridyl)-1-butanol
NNK	4-(Methylnitrosamino)-1-(3-pyridyl)-1-butanone
NNKAc	4-[(Acetoxymethyl)nitrosamino]-1-(3-pyridyl)-1-butanone
NQO-1	NAD(P)H quinone dehydrogenase 1
Nrf2/ARE	Nuclear factor erythroid 2 p45 (NF-E2)-related factor/antioxidant response element
OH	Hydroxyl group
p-Akt	Phospho-Akt
p-Nrf2	Phospho-Nrf2
p62	Sequestosome 1
PALB2	Partner and localizer of BRCA2
PBS	Phosphate-buffered saline

PCA	Protocatechuic acid
PCB2	Procyanidin B2
PGA	Phloroglucinaldehyde
PERK	Protein kinase-like endoplasmic reticulum-resident kinase
PI3K	Phosphatidylinositol 3-kinase
PKC	Protein kinase C
PMS	Phenazine methosulfate
POB-DNA	Pyridyloxobutyl DNA
POD	Anti-BrdU-peroxidase
Q	Quercetin
Ref	References
RIPA	Radio-immunoprecipitation assay
ROS	Reactive oxygen species
SAR	Structure-activity relationship
SDS	Sodium dodecyl sulfate
Ser	Serine residue
SGLT1	Sodium/glucose cotransporter 1
sMaf	Musculoaponeurotic fibrosarcoma
SOD	Superoxide dismutase
SSB	Single strand break
T	Combination of aglycone, conjugates and/or metabolites
t-BHP	Tert-butyl hydroperoxide
T2DM	Type 2 diabetes mellitus

TBE	Tris base/boric acid/ethylenediaminetetraacetic acid
Thre	Threonine
TNF-α	Tumor necrosis factor-α
UD	Unconjugated and free proanthocyanidin dimer in plasma or blood
UG	Unconjugated and free flavonoid glucoside in plasma or blood
UGT	Uridine 5'-diphospho-glucuronosyltransferase
UN	Unconjugated and free flavonoid aglycone in plasma or blood
WHO	World health organization
WTX	Wilms tumor gene on X chromosome

ACKNOWLEDGEMENTS

First and foremost, I wish to express my sincere thanks and gratitude to my supervisor Dr. H.P. Vasantha Rupasinghe and committee members, Dr. Zhaolin Xu, Dr. Graham Dellaire, and Dr. Stephanie Collins for their invaluable contribution and expert guidance throughout the study.

I also wish to express my special gratitude to my lab members, Dr. Jose Merlin, Madumani Amararathna, and Wasitha Thilakarathna for their invaluable support and for providing me with the necessary training for continuing research work. Also, I would like to thank Dr. Wasundara Fernando and my other lab members, Niluni Wijesundara, Surangi Dharmawansa, Cindy Yu, Vandana Tannira, Flávia dos Santos1, Dr. Sajeev Wagle, and Dr. Fagbohun Oladapo for the support given in various ways to complete the research.

I am extremely grateful to the Beatrice Hunter Cancer Research Institute, Halifax, Canada for awarding me the Cancer Research Internship Program Award with funds provided by CIBC and the Discovery Grant of NSERC for financially supporting my thesis project.

I also wish to express my sincere gratitude to the academic and non-academic members of the Department of Plant, Food, and Environmental Sciences, Faculty of Agriculture, Dalhousie University, Canada.

Finally, I would like to thank my parents, my brother, my sister, my fiancée, and my friends for the support they gave me in difficult times during the project.

CHAPTER 1: INTRODUCTION

According to the World Health Organization (WHO), cancer is the second leading cause of death worldwide after deaths caused by heart diseases (1). In 2020, nearly 19.3 million new cancer cases and 10 million cancer-related deaths occurred (2). Among observed cancers, breast, lung, colorectal, and prostate cancers were the most common (2). In 2020, breast and lung cancers were the leading cancers accounted for worldwide higher incidence and mortality rates, respectively (2). In Canada, it is estimated that nearly 23,000 new cases and 85,000 deaths are related to cancers in 2022, and the prevalence of cancer among men is expected to be higher than among women in Canada (3). Even though there are many therapeutic approaches such as chemotherapy, radiation, and surgery to overcome cancers, these treatments are known to cause severe side effects (4–6). Even after therapeutic treatments on cancers, the recurrence and less than five-year net survival rates of several cancers such as lung cancer are common among cancer patients who have undergone treatments (3,7,8).

WHO recommends regular eating of adequate fruits and vegetables to reduce the risk of cancer (1). Phytochemicals present in fruits and vegetables have been shown to reduce the prevalence of cancer in numerous studies (9–11). Therefore, dietary phytochemicals have been gaining attention in the prevention of cancers (12). The reported cancer prevention by dietary phytochemicals, especially (poly)phenols such as flavonoids, stilbenes, curcuminoids, and phenolic acids have been associated with their antioxidant properties (11). These phytochemicals can mitigate oxidative stress caused by the excessive generation of reactive oxygen species (ROS) (9–11). Cellular ROS generation can be induced by both endogenous and endogenous factors (13-17). The mitochondrial

electron transport chain is the primary endogenous source of ROS (13) while ionization radiation, hypoxia, smoking, xenobiotics, air pollutants, and atmospheric pressure plasmas can contribute to cellular ROS production as exogenous stimuli (14–17). ROS has the potential to damage cellular DNA, which can cause cancer if DNA repair is unsatisfactory (18–22). DNA damage can be reduced by dietary antioxidants (i.e., flavonoids) by different mechanisms such as scavenging ROS, metal ion chelating, oxidative enzyme inhibition, and providing antioxidant enzyme cofactors among others (12,23,24). Dietary antioxidants can also activate cellular signaling pathways such as the nuclear factor erythroid 2-related factor 2 (Nrf2)/antioxidant response element (ARE) pathway against oxidative stress (23,25–30).

In general, the Nrf2/ARE pathway is activated by oxidative stress (25,31). The activation of this pathway plays a significant role in the prevention of DNA damage and possible carcinogenesis by managing oxidative stress via the expression of antioxidant defense enzymes and phase 2 detoxifying enzymes (25,31). Phytochemicals such as flavonoids can activate the Nrf2/ARE pathway and upregulate the expression of antioxidant and phase 2 detoxifying enzymes even at a stage devoid of oxidative inducers (32–34). However, limited studies have been carried out on flavonoids in carcinogen-induced experimental models with respect to the reduction of ROS and DNA damage through the activation of the Nrf2/ARE pathway by the physiologically relevant concentrations *in vitro*.

In this study, we employed an in vitro model of carcinogen-induced lung damage, in which we treated the normal bronchial epithelial cell line BEAS-2B with a known carcinogen in cigarette smoke, 4-[(acetoxymethyl)nitrosamino]-1-(3-pyridyl)-1-butanone

(NNKAc) (35). Furthermore, an emphasis was given to studying the activation of the Nrf2/ARE pathway by the most effective flavonoids in reducing carcinogen-induced ROS and DNA damage in bronchial epithelial cells at low concentrations.

1.1 Hypothesis

Flavonoids can reduce carcinogen-induced ROS and DNA damage in cultured normal bronchial epithelial cells through Nrf2/ARE activation.

1.2 Research objectives

Overall objective

To identify dietary flavonoids, which can reduce carcinogen-induced ROS and DNA damage in cultured normal bronchial epithelial cells.

Specific objectives

1 To determines the efficacy of selected flavonoids in the reduction of carcinogen-induced ROS and DNA damage in cultured bronchial epithelial BEAS-2B cells in comparison to flavonoid metabolites, phenolic acids, stilbenes, curcuminoids, and non-phenolics antioxidants.

2 To study whether the reduction of carcinogen-induced ROS and DNA damage by the most effective flavonoids is through the activation of the Nrf2/ARE pathway in BEAS-2B cells.

CHAPTER 2: LITERATURE REVIEW

The first paragraph of Section 2.2, Sections 2.1.1.2, 2.3.1, 2.3.2, 2.3.3, 2.3.3.1, and 2.3.3.2 (except the last two paragraphs), Table 2, and Figure 4 are published in a peer-reviewed open-access review article (Suraweera TL, Rupasinghe HPV, Dellaire G, and Xu Z. Regulation of Nrf2/ARE Pathway by Dietary Flavonoids: A Friend or Foe for Cancer Management? Antioxidants. 2020 Oct;9(10):973 [Impact factor of 6.313]). I wrote the first draft and the three co-authors who are my advisory committee members, have reviewed and provided suggestions and edits.

2.1 Dietary antioxidants: Polyphenols and flavonoids

2.1.1 Polyphenols

Polyphenols are a group of naturally occurring phytochemicals exclusively synthesized in plants (36,37). These compounds are plant secondary metabolites and protect plants against biotic and abiotic stress caused by free radicals, ultraviolet radiation, aggressions from parasites, and pathogens in addition to their role in interactions with the environment such as attracting pollinators (36,38). They are also known to exert potential health benefits to consumers against several chronic diseases (i.e. certain cancers, diabetes, cardiovascular diseases, and neurodegenerative diseases) through different biological activities such as antioxidant, anti-inflammatory, anti-diabetic, and anti-cancer activities (37,39). Polyphenols are an essential part of the human diet and are abundant in most plant-based diets (fruits, vegetables, cereals, wine, tea, coffee, chocolate, etc.) (39). However, the types and the amounts of polyphenols present in different plant sources differ from one to another (40,41).

Polyphenols contain one or multiple hydroxyl groups attached to at least one phenyl ring (42). Phenolic compounds can vary from simple water-soluble simple phenols and their glycosylated forms to condensed, polymerized, or combined high molecular weight, mostly water-insoluble, forms of polyphenols. (43). Based on the chemical structure, polyphenols can be classified into phenolic acids, flavonoids, stilbenes, and lignans (Figure 1) (44).

Phenolic acids are the simplest form of polyphenolic compounds (45,46). The basic structure of phenolic acid contains at least one carboxylic group and one phenolic ring (Figure 1) (45,46). They can be further classified into hydroxycinnamic acids (derivatives of cinnamic acid) and hydroxybenzoate acids (derivatives of benzoic acid) based on the C6-C3 and C6-C1 backbones, respectively (45,46). Phenolic acids are found primarily in commonly consumed fruits and vegetables, and particularly in the bran or hull of grains and seeds (41). Examples of the most common hydroxycinnamates are caffeic acid (sources: coffee, mushroom, and propolis), ferulic acid (sources: cereal grains, spinach, fruits, and mushrooms), sinapic acid (sources: berries, rye, and mustard), and *p*-coumaric acid (sources: coffee, garlic, tomato, carrot, grapes, and spinach) (47). In comparison to hydroxycinnamates, most of the hydroxybenzoate are available in low concentrations in most fruits and vegetables in addition to several exceptions such as gallic acid (sources: tea, wine, and grapes), and ellagic acid (source: berries), and found in considerable amounts (45–47). These acids are mainly found in conjugated form whereas hydroxycinnamates are found as esters of quinic acid (i.e. chlorogenic acid) or glucose and hydroxybenzoate are found as glycosylated products (48,49).

Stilbenes contain a chemical structure characterized by a C6-C2-C6 carbon skeleton, while two benzene rings are linked by a two-carbon methylene bridge (Figure 1) (45,50). Stilbenes are found in most food sources in low amounts (51). Resveratrol is one of the most studied stilbenes and is mostly found in berries, grapes, and peanuts (47).

Lignans are diphenolic compounds characterized by the presence of two combined phenylpropane units (C6-C3) despite having different chemical structures (Figure 1) (39,47,51). Lignans are rich in linseed (i.e. lignanssecoisolariciresinol in high quantities and matairesinol in low quantities) (52). Flaxseeds and sesame are also sources of lignans (47).

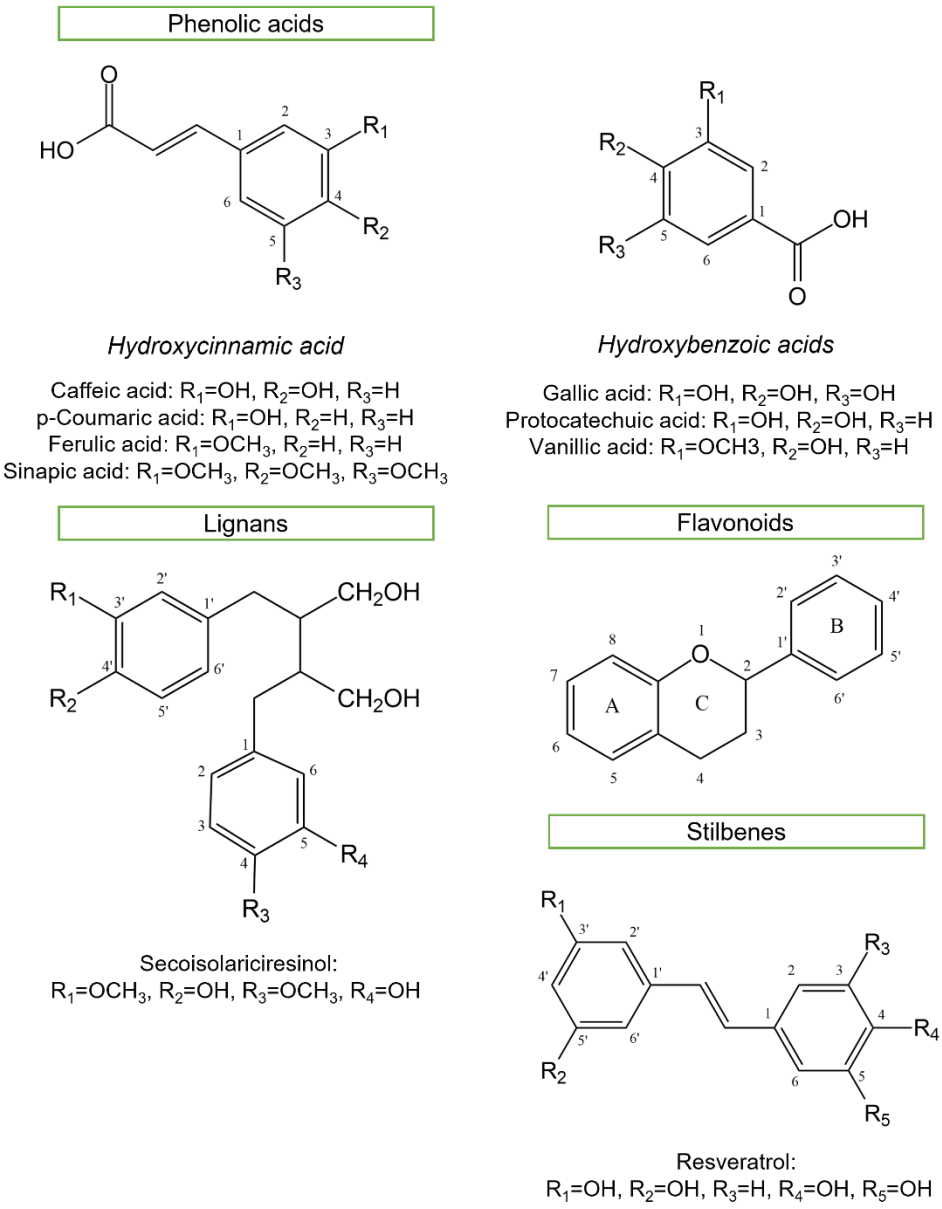

Figure 1: Basic chemical structures of different classes of polyphenols

(Adapted from Grgić *et al*., 2020, Durazzo *et al*., 2018, Gómez-Guzmán *et al*., 2018, Losada-Echeberria *et al*., 2017, and Mojzer *et al*., 2016 (53–57))

2.1.1.1.Flavonoids: classification and dietary sources

Flavonoids are the most abundant group of polyphenols in the plant kingdom and more than 8,000 compounds have been reported to date (47). These compounds are derivatives of benzo-γ-pyrone and are mainly present in plants as major pigments (58,59). Additionally, flavonoids are also found in most fruits (i.e., apples, berries, grapes, citrus fruits, and pears) and vegetables (i.e., onions, cabbage, cauliflower, spinach, and celery), beverages (i.e., red wine, and tea), and legumes (47). The basic structure of flavonoids is universal for each flavonoid characterized by the presence of a C6-C3-C6 carbon structure (Figure 1) (51). Based on the stereochemistry, bond between C and B rings, and substitutions in the C ring, flavonoids can be further classified into subgroups as flavonols, flavones, flavanones, isoflavones, flavanols (flavan-3-ols), anthocyanins, and chalcones (51). The carbon backbone of flavonoids contains two C6 aromatic rings (A and B rings) linked to each other by a C3 ring (C ring) (Figure 2) (51). Except in chalcones, all other flavonoids have a heterocyclic C ring (51). Furthermore, structural differences within a sub-group can be observed due to processes such as hydroxylation, glycosylation, dimerization, methylation, and/or isoprenylation (39,60).

Flavonols are characterized by the configuration of having a double bond between C2 and C3 carbons, a hydroxyl group at C3, and a carboxylic group at the C4 position (Figure 2) (47). This configuration of having three functional groups allows flavonols to react with different reactive substances (47). They are more ubiquitous in the human diet and are generally found as glycosides either with glucose or rhamnose (51). Quercetin and its derivatives (onions, apples, berries, and pear), kaempferol (cauliflower, cabbage, spinach,

and propolis), and myricetin (herbs, berries, and vegetables) are some of the common flavonols found in many dietary sources (47).

Flavones are similar in structure to flavonols despite one main difference. The configuration of flavones consists of a double bond between the C2 and C3 carbons, and a carboxylic group at the C4 position but no hydroxyl group at C3 (Figure 2) (47). The free hydroxyl groups present in the A and B rings of flavones are mainly responsible for their biological activities such as antioxidant activities (47). Although flavones are not widely present in most fruits and vegetables, common flavones such as apigenin (parsley, celery, oregano, and spinach) and luteolin (broccoli, green peppers, and celery) are found in several dietary sources. (47,61).

Flavanones are characterized by the presence of a carboxyl group at the C4 position and the absence of a double bond between the C2 and C3 carbons and the hydroxyl group at the C3 position (Figure 2) (47). These compounds are mainly found in citrus fruits and naringenin and hesperidin are two of the most commonly found flavanones (47).

Isoflavones are the only flavonoid sub-group to have its aromatic B ring linked to the heterocyclic C ring at the C3 carbon position (Figure 2) (47,51). This configuration results in an estrogen-like structure allowing isoflavones to act as agonists or antagonists of estrogen receptor interactions (47). Additionally, a double bond between the C2 and C3 carbons is also present in the isoflavone basic structure (51). Isoflavones are exclusively found in legumes and genistein and daidzein are commonly found in soybean and soybean-based food products (47).

Flavanols, also known as flavan-3-ols, can be found in food sources in monomeric, oligomeric (2-7 monomer), or polymeric forms (51,62). The monomers are called catechins while the oligomers and polymers are called proanthocyanins (51,62). Flavanols are characterized only by the presence of hydroxyl group in position C3 but no double bond at C2-C3 and a carboxyl group at the C4 position (Figure 2) (47). This configuration allows flavanols to have four possible non-identical stereoisomers due to the resulting chiral carbons (asymmetric carbon atoms bonded to 4 different substituents) at the C2 and C3 positions (62). The configuration of monomeric flavanols can be *cis* or *trans* while epicatechins and catechins are the isomers of *cis* and *trans* configurations, respectively. (62). Both epicatechin and catechin can have two stereoisomers for each compound like (-)-epicatechin, (+)-epicatechin, (-)-catechin, and (+)-catechin (62). However, (-)-epicatechins and (+)-catechins and their derivatives such as gallocatechin are mainly found in plant-based foods and are commonly found in tea and cocoa (62).

Proanthocyanidins are also known as condensed tannins and are formed by linking several flavanol monomers through interflavanic bonds between an A ring of one monomer and the pyran ring of another monomer (Figure 2) (45,47,51). Based on these links, procyanidins can be further classified into 2 types of structures: A-type and B-type structures. A-type structures are characterized by C2-*O*-C7 or C2-*O*-C5 bonds and B-type structures are characterized by C4-C6 or C4-C8 bonds (62,63). Procyanidin A2 is an example of an A-type structure, while procyanidins B2 (Figure 2) and B5 are examples of a B-type structure (63). These compounds are commonly found in fruit sources, while grape seeds, plums, and berries (black currants, blueberries, strawberries, and cranberries) are among the top sources (64).

Anthocyanins are the derivatives of flavonols and consist of a hydroxyl group at C3 carbon and two double bonds at C3-C4 position and an oxygen atom and C1 carbon but no carbonyl group at the C4 position (Figure 2) (45,50). This configuration results in a structure of a flavylium ion (45,50). Parts of many fruits and vegetables are colored by the presence of anthocyanins. These compounds can be commonly found as aglycone (i.e., cyanidin, delphinidin, malvidin, and pelargonidin) or glycosylated forms (i.e., cyanidin-3-*O*-glucoside) in plants and are commonly found in berries, grapes, and purple carrot (47,65).

Chalcones, precursors of flavonoids are characterized by the absence of a C ring and hence these compounds are known as open-chain flavonoids (Figure 2) (51,66). These compounds can be commonly found in apples, berries (i.e., bearberries and strawberries), tomatoes, and wheat. Phloretin, phloridzin, arbutin, and chalconaringenin are some of the common examples of chalcones (51).

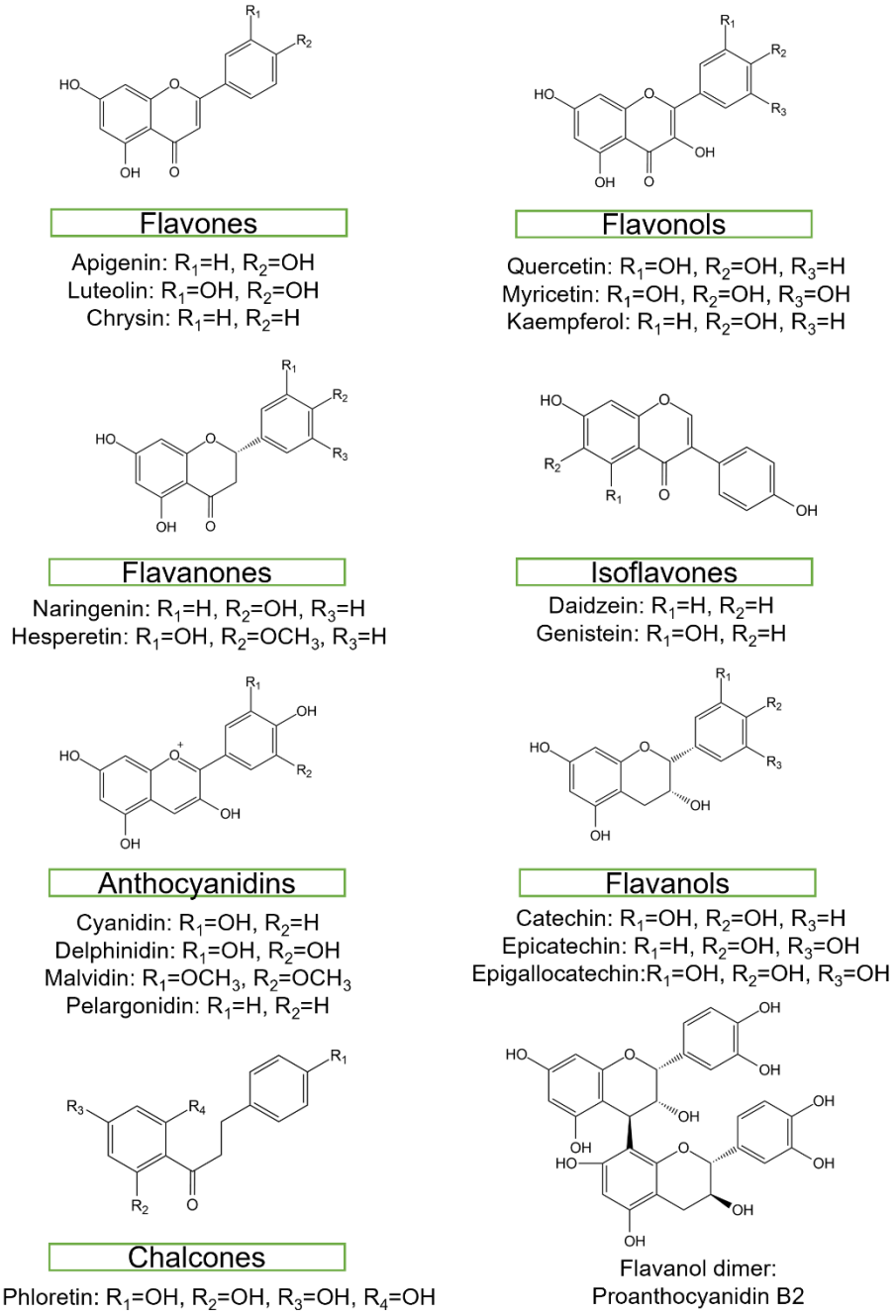

Figure 2: Chemical structures of different sub-classes of flavonoids

(Adapted from Dumitru *et al*., 2021, Nguyen *et al*., 2020, and Semwal *et al*., 2016 (67–69))

2.1.1.2 Hermetic effects of flavonoids

Hormesis is the bi-phasic concentration/dose-response, often depicted as a U-shaped dose-response curve of some dietary antioxidants, drugs, and toxins (70). Accordingly, at low concentrations/doses, biologically active molecules such as flavonoids exert beneficial effects such as stimulation for either adaptation or protection from a stress factor (70–73). At high concentrations/doses, they may exert either detrimental/inhibitory or toxic effects on the cells or tissue microenvironment (70,72–74). Hence, hormetic compounds act as antioxidants at low doses and prooxidants at high doses (9,75–78). For example, apigenin at low concentrations (6.25 μM) exerts stimulatory effects on nuclear factor erythroid 2-related factor 2/antioxidant response element (Nrf2/ARE) pathway in human hepatocellular carcinoma HepG2 cells, significantly increasing mRNA and protein expression of Nrf2 and heme oxygenase 1 (HO-1) with activation of phosphatidylinositol-3-kinase (PI3K)/protein kinase B (Akt) and extracellular signal-regulated protein kinase (ERK) 1/2 signaling (71). However, at high concentrations (50 and 100 μM), apigenin inhibits cancer promotion by reducing mRNA and protein levels of Nrf2, catalase activity, and intracellular glutathione levels in HepG2 cells (74). Similarly, at low concentrations (10 μM), luteolin increases the glutathione (GSH) protein expression in human epithelial colorectal adenocarcinoma Caco-2 cells, and at higher concentrations (above 15 μM) of luteolin decreases GSH expression, showing the hormetic effects (79).

2.1.1.3 Bioavailability and biotransformation of dietary flavonoids

Bioavailability is the proportion of a compound in its active form or active moiety absorbed by the body and available at the specific site of action (80). Despite numerous reported therapeutic effects, flavonoids are known to have low oral bioavailability and vary

between and within classes of flavonoids (Table 1) (81). The absorption and bioavailability of flavonoids depend on factors such as molecular weight, food matrix, glycosylation, metabolic conversion, and interactions between the intestinal microbiota (82,83). Better absorption and distribution to the site of action are necessary for flavonoids to have better therapeutic efficacy (81).

Molecular weight affects the absorption and bioavailability of several flavonoids (82). Due to high molecular weight and structural complexity, polymeric proanthocyanidins are not absorbed from the small intestine but are absorbed from the colon into the bloodstream after colonic microbial degradation (83,84). In contrast, Shoi *et al*., 2006 showed that relatively low molecular weight apple proanthocyanidin oligomers, such as dimers and pentamers, can be absorbed from the male Wister rat intestine and are available in free unconjugated forms (85). The absorption and bioavailability of flavonoids also vary due to the nature of the food matrix in which they are present (82,86). For example, the absorption and bioavailability of anthocyanins can be enhanced by dissolving them in ethanol (i.e. ethanol in red wine) (86). Furthermore, co-administration of flavonoids (i.e., green tea catechins with sucrose and naringenin with sucrose) with carbohydrates increases flavonoid absorption and bioavailability (87,88). Meanwhile, flavonoid intake with fatty matrixes (i.e., pomegranate anthocyanidins with sunflower oil and blueberry anthocyanidins fed with a high-fat diet) increases the clearance time of flavonoids (89–91). In contrast, co-administration of flavonoids with proteins reduces the bioavailability due to interactions of proteins with flavonoids (i.e., proteins bound with rutin and milk proteins bound by tea flavonoids) (89,92).

Dietary flavonoids are mainly available in the glycosylated form in the diet and when ingested they are mainly transformed to their aglycone form in the human small intestine before being absorbed (93). In the human small intestine, near the brush border, lactase phlorizin (LPH) hydrolase hydrolyses the flavonoid glycoside (i.e., quercetin 3-*O*-glucoside, quercetin 4′-*O*-glucoside, and monoglucosides of isoflavones) and results in hydrolyzed sugars and the flavonoid aglycone (86,94). Subsequently, aglycones are taken up into intestinal epithelial cells by passive diffusion (86). Alternatively, polar glycosides (i.e., quercetin 4′-*O*-glucoside, genistein 7-*O*-glucoside, and daidzein 7-*O*-glucoside) can be transported into epithelial cells via sodium-dependent glucose transporters; sodium/glucose cotransporter 1 (SGLT1) and hydrolyzed by the cytosolic β-glucosidase (94,95).

Absorbed flavonoid aglycones are first conjugated after being taken up into epithelial cells of the small intestine by phase 2 enzymes before entering the bloodstream, followed by further conjugation in the liver to facilitate their excretion through urine or bile (96,97). Sulfates, glucuronides, and/or methylated metabolites of flavonoid aglycones are mainly found in the bloodstream due to the actions of sulfotransferases, uridine-5′-diphosphate-glucuronosyltransferases, and catechol-*O*-methyltransferases, respectively (96). Therefore, the levels of flavonoid aglycones or their natural forms present in the bloodstream are very limited, resulting in low physiologically relevant concentrations (Table 1) (97). Flavonoids that were not absorbed in the small intestine undergo structural modifications in the colon through interactions with colonic microflora. For example, non-monoglucosides (quercetin-3-*O*-galactoside and rutin) cannot be hydrolyzed by small intestinal enzymes (98). Their sugar moieties undergo hydrolysis in the cecum and large

intestine by gut microbiota before the resulting aglycone is absorbed into the bloodstream (98). Additionally, flavonoid glucuronides that are being excreted with bile undergo microbial hydrolysis in the colon and re-enter the blood circulation (83,97). Furthermore, aglycones can be further catabolized through colonic microbial interactions into low molecular weight compounds such as phenolic acids that can be easily absorbed and undergo phase 2 metabolism and excreted with urine (99).

Table 1: Bioavailability and physiological concentrations of flavonoids

Group	Compound	Research model	Physiological concentration (μM)	Bioavailability (%)	Ref.
Flavone	Luteolin	Rats	0.35- 26.09 (UN)	4.1-26 (UN)	(100,101)
	Chrysin	Human	0.012-0.064 (T)	0.003-0.02 (T)	(102)
		Rats	1.65-3.89 (Un)		(103)
Flavanone	Naringenin	Human	7.39 (UN)	5.81(UN)	(104)
Isoflavone	Genistein	Mice	0.2 – 1.8 (UN) 0.39-7 (T)	5-23.4 (UN)	(105–107)
		Rats	0.08-2.77 (UN) 0.4-12.3 (T)	6.8-33.5 (UN) 29.14-62.34 (T)	(108–112)
		Human	0.74-6 (UN)		(113–115)
Flavonol	Quercetin	Human	0.026-5 (UN)	0.54 -24 (UN)	(116–119)
		Rats	2.01-3.44 (UN)	16-27.5 (UN)	(120–122)
Anthocyanins	C3G	Mice		1.7 (UG) 3.3 (T)	(123)
		Human	0.00063 (UG)	12.4 (T)	(124,125)
Flavan-3-ols	Epicatechin	Human	0.001-8.9 (UN)	44.3-82.5 (T)	(126,127)
Proanthocyanidin	Procyanidin B2	Rat	0.5-4.49 (UD)	8-11 (T)	(128,129)
		Human	0.016-0.041 (UD)		(130)
Chalcones	Phloretin	Rat	1.14-3.85 (UN)	8.67 (UN)	(131)

Abbreviations; C3G: Cyanidin-3-*O*-glucoside, UN: unconjugated and free flavonoid aglycone in plasma or blood, UG: unconjugated and free flavonoid glucoside in plasma or blood and UD: unconjugated and free proanthocyanidin dimer in plasma or blood and T: combination of aglycone, conjugates and/or metabolites of the flavonoid in plasma or blood.

2.2 Oxidative stress, DNA damage, and carcinogenesis

Several metabolic reactions that occur in the human body generate reactive oxygen species (ROS) (13). Excessive generation of ROS can lead to oxidative stress that causes over 40 non-communicable diseases including certain cancers, diabetes mellitus, neurodegenerative diseases, and accelerated aging (132). In addition to the primary ROS generation in the mitochondrial electron transport chain (13), exogenous stimuli such as air pollutants, cigarette smoke, ionization radiation, xenobiotics, atmospheric pressure plasmas, and hypoxia could induce ROS generation (14–17). Non-communicable diseases and rapid aging induced by oxidative stress are mainly due to unrecoverable damages that occurred to biological macromolecules such as nucleic acids, proteins, and membranes (14,133). For instance, DNA can be damaged in the form of single-strand or double-strand DNA breakage and stable modifications in nitrogen bases of the pentose-phosphate backbone of DNA due to ROS-induced oxidative stress (21,22). If these damages are not repaired, they could lead to epigenetic alterations in proto-oncogenes and tumor suppressor genes, somatic gene mutations, and genomic instability, which could initiate carcinogenesis (18–20,134).

Carcinogenesis is a multi-step process involving several molecular and cellular alterations (135). This process can be classified into three major phases namely, initiation, promotion, and progression (136). Cancers can be initiated due to genomic instability (137,138). Genomic instability is caused by alterations such as mutations, changes in the number of chromosomes, and segments (rearrangements or deletions of segments) that occur in the genome due to processes such as alkylation, oxidation, or exposure to carcinogens (137,138). Among phases of carcinogenesis, initiation is a rapid phase that

could be completed in 1-2 days (139,140). During initiation, the cellular genome can undergo irreversible and/or epigenetic changes, either spontaneously or due to exposure of DNA to a carcinogen (139,141). Epigenetic modifications can include DNA methylation of promoter areas of tumor suppressor genes (135). Tumor suppressor genes are responsible for inhibiting, arresting, or suppressing cell division (142). Epigenetic modifications of tumor suppressor genes, therefore, prevent their transcription and eliminate their functions in tumor-suppressing (135). Moreover, cancer initiation can also be characterized by the conversion of proto-oncogenes into oncogenes by processes such as the formation of DNA adducts by chemical carcinogens (143). Activation of oncogenes disrupts normal cellular functions by deregulation of cell proliferation and suppression of apoptosis and therefore facilitates the process of carcinogenesis (144). Additionally, ROS-induced mutagenic 8-hydroxydeoxyguanosine adducts in genomic DNA lead to conversions of guanosine to thiamine and these changes are common in tumor suppressor genes and oncogenes (135).

Cancer promotion is the longest phase which could last for 10-20 years and may result in abnormal cell replication and the formation of preneoplastic cell foci (139,140). During this phase, tumor promoters can increase cell proliferation and/or inhibit apoptosis through changes in gene expression (135). Tumor promoters are not carcinogenic but can promote the actions of carcinogens and therefore low doses of carcinogens have the ability to generate cancerous cells (135). Moreover, tumor promotion is a reversible phenomenon, and repeated or continuous exposure to tumor promoters is required for an initiated cell to grow clonally into a focal lesion (135).

The final stage of carcinogenesis is the progression which could be completed within less than one year (139,140). This phase is characterized by uncontrolled growth of a tumor, conversion of pre-neoplastic cells into neoplastic cells with an increased level of invasiveness, metastasis (development of secondary tumor growths at a distance organ from a primary organ of cancer), and angiogenesis (formation of new blood vessels) (140).

2.2.2 NNKAC-induced carcinogenesis

4-[(Acetoxymethyl)nitrosamino]-1-(3-pyridyl)-1-butanone (NNKAc) is a commercially available carcinogen commonly used to mimic the carcinogenic effects of 4-(methylnitrosamino)-1-(3-pyridyl)-1-butanone (NNK) mainly in the experimental lung cancer models (35,145,146). NNK is an aromatic chemical compound that is the strongest tobacco-specific nitrosamines-based carcinogen present in tobacco smoke (147). NNK is mainly generated from the nitrosamines that are formed during processes such as curing, fermentation, the storage of tobacco leaves, or during smoking through N-nitrosation (148,149). NNK is a pro-carcinogen and requires to undergo several metabolic reactions to become activated to cause DNA damage (150). Within cells, NNK undergoes three major metabolic reactions, namely carbonyl reduction, hydroxylation, and pyridine nitrogen oxidation (Figure 3) (151). 4-(Methylnitrosamino)-1-(3-pyridyl)-1-butanol (NNAL) is produced by carbonyl reduction of NNK (151,152). NNAL and NNK undergo pyridine nitrogen oxidation which is a detoxification step and generate their respective nitrogen oxides (151,152). NNK and NNAL can also be converted into carcinogenic and mutagenic electrophilic mediators by cytochrome p450 (CYP) enzyme-mediated α-methyl hydroxylation (152–155). The electrophiles resulting from α-methyl hydroxylation could damage DNA by forming bulky pyridyloxobutyl DNA (POB-DNA) adducts (Figure 3)

(152,156). Meanwhile, electrophilic mediators produced by hydroxylated α-methylene NNK induce DNA damage by forming methylated DNA adducts (152).

Several cytochrome P450 enzymes required for NNK activation are not present, and CYP activity is generally low in established cell lines such as bronchial lung epithelial BEAS-2B (157). Therefore, the use of NNK in such cell lines may not demonstrate the actual effects of NNK on DNA damage induction. Hence, NNKAc is commonly used to induce DNA damage in such cell lines (35,145,146). For activation of NNKAc, CYP enzyme activity is not required but esterase enzyme activity is required (158). Once NNKAc is activated, it undergoes α-methyl hydroxylation and generates the intermediate metabolites generated by the α-methyl hydroxylation of NNK (158). Therefore, carcinogenesis caused by NNKAc is mainly explained by the formation of bulky POB-DNA adducts (158). Moreover, NNK-induced carcinogenesis is associated with epigenetic and genetic changes in genes such as *KRAS* oncogenes and tumor suppressor *TP53* (150,159,160). Therefore, the formation of DNA adducts in *TP53* and *KRAS* genes by the electrophilic reactive metabolites generated by NNK or NNKAc can produce cells with cancerous properties (156,161–163).

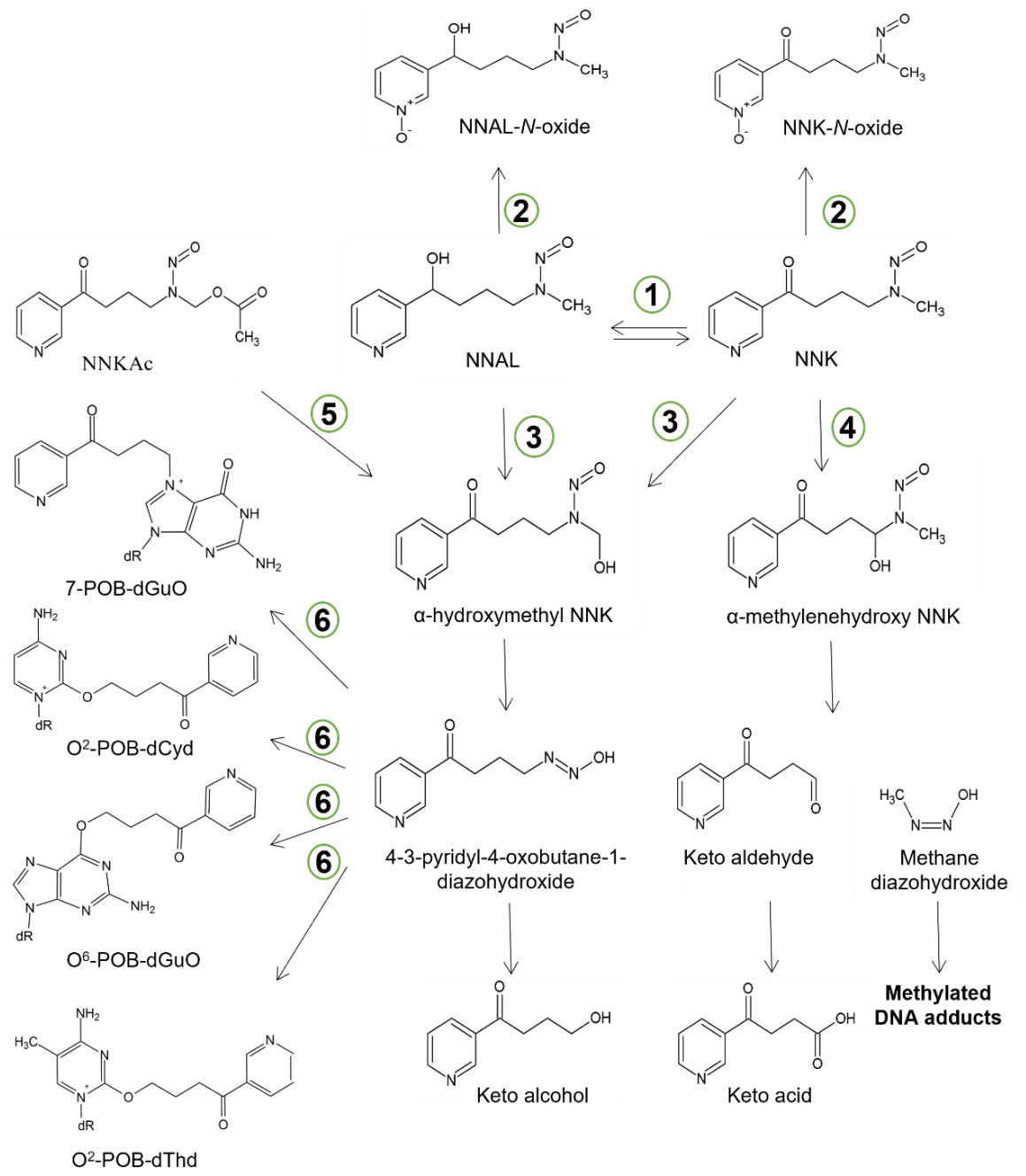

Figure 3: Cellular metabolism of NNK and NNKAc

(1.) Carbonyl reduction, the metabolic reaction that converts NNK to NNAL; (2.) pyridine N oxidation, a detoxification step of both NNK and NNAL to their respective N-oxides. (3.) α-methyl hydroxylation of NNK by CYP enzymes and NNAL results in more reactive electrophilic metabolites. (4.) α-methylene hydroxylation of NNK by CYP 450 enzymes to generate reactive electrophilic metabolites. (5.) Activation of NNKAc by esterase

enzymes. (6.) DNA pyridyloxobutylation, the formation of POB-DNA adducts. (151,164–167)

Abbreviations: NNK: 4-(methylnitrosamino)-1-(3-pyridyl)-1-butanone, NNKAc: 4-[(acetoxymethyl)nitrosamino]-1-(3-pyridyl)-1-butanone, NNAL: 4-(methylnitrosamino)-1-(3-pyridyl)-1-butanol, 7-POB-dGuo: 7-[4-(3-pyridyl)-4-oxobut-1-yl]-2′-deoxyguanosine, O2-POB-dCyd: *O*2-[4- (3-pyridyl)-4-oxobut-1-yl]-2′-deoxycytidine, O6-POB-dGuo: O^6-[4-(3-pyridyl)-4- oxobut-1-yl]-2′-deoxyguanosine, O2-POB-dThd: *O*2-[4-(3- pyridyl)-4-oxobut-1-yl]thymidine, and CYP: cytochrome P450. (Adapted from, Ma *et al*., 2019, Hacht *et al*., 2016 and Peterson, 2010. Figure adapted form Hacht *et al*., 2016 was done under Copyright 2022 American Chemical Society] (151,164,166))

2.3 Dietary antioxidants and cancer prevention

Dietary antioxidants exert cancer-preventive properties at different stages of cancer via different mechanisms (139,140). During cancer initiation, dietary antioxidants such as polyphenols exert cancer-preventive properties mainly through their antioxidant activity (scavenging ROS directly or activating cellular antioxidant defense system), inhibition of phase 1 enzymes, activation of phase 2 drug detoxifying enzyme, and facilitating DNA damage repair (139,140). Furthermore, fruit (poly)phenols are known to exert cancer-preventive properties during the cancer promotion phase through their anti-inflammatory activities, inducing apoptosis and cell cycle arrest and inhibiting cell proliferation (139). During cancer progression, polyphenols exert anti-angiogenesis activities in addition to inhibiting metastasis (139). Therefore, considering the complexity and effectiveness in preventing cancer, it would be vital to prevent or reduce the exposure of DNA to carcinogenic factors.

2.3.1 Antioxidant defense systems in relation to cancer

The cellular antioxidant defense system is the primary mechanism to protect biological macromolecules from oxidative stress (14). The enzymatic and non-enzymatic antioxidants of the antioxidant defense system are capable of neutralizing ROS, such as superoxide anion radical, hydrogen peroxide, and hydroxyl radical, and the secondary reactive species such as peroxyl, and alkoxyl radicals, generated by their further oxidation (14,168,169). In a cellular environment, superoxide anion radical is generated mainly due to the activities of lipoxygenase, nicotine adenine dinucleotide phosphate (NAD(P)H) oxidase, cyclooxygenase, cytochrome P450, and xanthine oxidase (170,171). This free radical is converted to hydrogen peroxide by superoxide dismutase (SOD) (172). Hydrogen peroxide

can also be produced by NAD(P)H oxidase (173), xanthine oxidase (174), and amino acid oxidase enzymes (175) or as a result of oxygen consumption in metabolic reactions happen in peroxisome (176). Hydrogen peroxides are further converted into water and oxygen by catalase (CAT) and glutathione peroxidase (GPx) (172,177). GPx needs secondary enzymes such as glutathione reductase (GR) and co-factors, reduced glutathione and NAD(P)H, to catalyze the conversion of hydrogen peroxide into water (172,177). If hydrogen peroxides are not neutralized by CAT and GPx enzymes, hydrogen peroxides can react with superoxide radical or undergo Fenton reaction or Haber-Weiss reaction in the presence of metal ions such as copper and iron to generate hydroxyl radical (178,179). Fenton reaction and Haber-Weiss reactions are given below.

Fenton reaction: $H_2O_2 + Cu^{+}/Fe^{2+} \rightarrow Cu^{2+}/Fe^{3+} + OH^{-} + \bullet OH$

Haber-Weiss reaction: $H_2O_2 + \bullet O_2^{-} \rightarrow O_2 + OH^{-} + \bullet OH$

Hydroxyl radicals cause severe oxidative damage to DNA, and inefficient repair of DNA can lead to the initiation of carcinogenesis (14,77). Therefore, it is essential to eliminate ROS to prevent oxidative stress-induced DNA damage (168,180). Hence, mechanisms that are activating the expression of proteins related to the antioxidant defense system and other cytoprotective genes are vital in managing oxidative stress-induced DNA damage in the prevention of cancer (168,180).

2.3.2 Mechanisms of activation of the antioxidant defense system and other cytoprotective genes

Activation of the antioxidant defense system and other cytoprotective genes, such as phase 2 detoxification enzymes, is mainly due to the activation of the nuclear factor

erythroid 2-related factor 2 (Nrf2)/antioxidant response element (ARE) pathway in a cellular environment upon oxidative stress (181,182). Briefly, activation of this pathway is initiated by a transcription factor Nrf2, which binds to the promoter region of the ARE, leading to the transcription of genes of antioxidant defense enzymes and phase 2 detoxifying enzymes. Thereby, these proteins restore redox homeostasis by managing oxidative stress (25,32,183–185).

For the initiation of this pathway, Nrf2, a basic leucine-zipper transcription factor, needs to be activated (9,186,187). Under normal cellular physiological conditions, Nrf2 is bound to Kelch-like ECH-associated protein 1 (Keap 1), which is an endogenous inhibitor of Nrf2, bound to actin fibers (9,186,187). Interactions between Keap 1 and Nrf2 via its motifs (Neh2 ETGE and DLG) lead to activating the Nrf2 ubiquitination process, which is mediated by Cullin 3 (Cul3) based E3 ligase complex (188). The degradation of Nrf2 is rapidly undertaken in 26S proteasome leading to low levels of Nrf2 in the cytoplasm (9,189–191). This avoids stabilization, phosphorylation, and nuclear translocation of Nrf2, resulting in 15-40 min of Nrf2 half-life time depending on the type of cell (9,189–191).

However, oxidative stress or the presence of electrophilic compounds induces the activation of the Nrf2 pathway through canonical mechanisms (192–194). Herein, cysteine residues (Cys151, Cys257, Cys273, Cys288, and Cys297) in Keap-1 undergo conformational changes upon oxidation or alkylation and dissociates Nrf2 from Keap 1 (192–194). In addition, non-canonical activation of Nrf2 by the influence of proteins such as p62, p21, dipeptidyl peptidase III (DPP3), Wilms' tumor gene on the X chromosome (WTX), BRCA1 (breast cancer gene 1) and partner and localizer of BRCA2 (PALB2) also leads to the cytoplasmic stabilization of Nrf2 (193). These proteins disrupt the direct

interactions of Keap 1 with Nrf2 either by binding to Keap 1 or Nrf2 (193). Collectively, canonical and non-canonical activation of Nrf2 results in a reduction of Nrf2 ubiquitination and degradation (193). The detached Nrf2 can be negatively regulated by several other proteins, such as glycogen synthase kinase 3 beta (GSK-3β) (187). Herein, GSK-3β-mediated phosphorylation of specific serine residues such as Ser335 and Ser338 (numbers in mouse sequence) in the Neh6 domain of Nrf2 creates a degradation domain, which can be recognized by the ubiquitin ligase adapter E3 ubiquitin-protein ligase (187). Thereafter, proteasomal degradation of Nrf2 is facilitated via the Cul3-based E3 ligase complex (187). However, phosphorylation of serine 558 residue located in the canonical nuclear export signal of Nrf2 protein by 5′ adenosine monophosphate (AMP)-activated protein kinase (AMPK) leads to improved stability of Nrf2 protein facilitating the nuclear translocation (195,196). Once Nrf2 is translocated into the nucleus, it begins heterodimerization with another transcription factor called musculoaponeurotic fibrosarcoma (sMaf) (190,191). The resulted complex binds to ARE and initiates transcription of downstream genes belonging to the antioxidant defense system and phase 2 detoxifying enzymes (182). Once these proteins are expressed, functions such as oxidizing xenobiotics or drugs, conjugation of oxidized metabolites, and transportation of final metabolites out of the intracellular environment will ensure cytoprotection by restoring redox homeostasis (182). Therefore, the identification of endogenous and exogenous molecules that can activate Nrf2/ARE pathway presents potential protection against oxidative stress-mediated diseases.

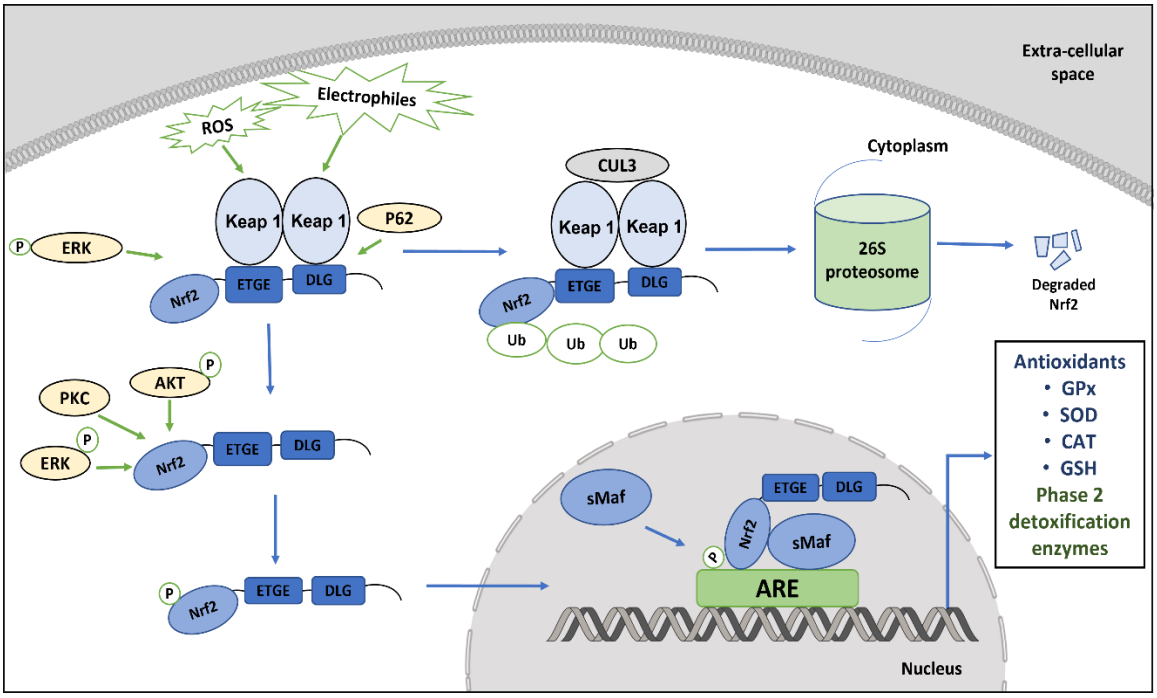

Figure 4: Nrf2/ARE cell signaling pathway

In normal cells, activation of the Nrf2/ARE pathway plays an important role in maintaining redox homeostasis. Under normal physiological conditions, activation of Nrf2 is inhibited by the interactions between Keap 1 and Nrf2 protein which facilitate Nrf2 ubiquitination followed by degradation. In the presence of oxidative stress or electrophilic compounds, Keap 1 protein undergoes conformational changes and releases Nrf2 protein. Detached Nrf2 protein undergoes phosphorylation for stabilization. Phosphorylated Nrf2 translocates to the nucleus and undergoes heterodimerization with sMaf transcription factor before binding to the antioxidant response element (ARE). Then activities of expressed ARE-driven downstream genes such as antioxidant defense and phase 2 detoxifying enzymes will restore normal physiological conditions through mechanisms such as xenobiotic detoxification, drug transportation, and reactive species neutralization (197,198).

Abbreviations: Keap 1: Kelch-like ECH-associated protein 1; Nrf2: Nuclear factor erythroid 2 p45 (NF-E2)-related factor; sMaf: Small musculoaponeurotic fibrosarcoma protein; ARE: Antioxidant response element; GSH: glutathione; SOD: superoxide dismutase; CAT: Catalase; GPx: Glutathione peroxidase; ROS: Reactive oxygen species; ERK: Extracellular signal-regulated protein kinase; PKC: Protein kinase C; Akt: protein

kinase B; p38: Mitogen-activates protein kinase p38; p62: sequestosome 1; JNK: N-terminal kinase (Figure 4 was adapted from Suraweera *et al*., 2020 (198) which was originally adapted from Wu *et al*., 2019 (197))

2.3.3 Role of Nrf2/ARE pathway in cancer chemoprevention

Activation of the Nrf2/ARE pathway in normal cells has been shown to possess cancer chemopreventive effects on non-malignant cells under normal physiological conditions (9,182,199). This can be mainly achieved by controlling redox homeostasis (200), which leads to genomic stability and cell survival that is facilitated by activities of antioxidant defense enzymes (SOD, catalase, GPx, GSH synthase, glutathione S-transferase, thioredoxin, and GSH reductase), phase 2 and 3 detoxifying enzymes (HO-1 and NAD(P)H quinone dehydrogenase 1 (NQO1), aldo-ketoreductase, multidrug resistance-associated proteins, P-glycoprotein, organic anion-transporting polypeptide, ATP-binding cassette, heat shock proteins, glycation defense enzymes, and ferritin) (20,182,185,201,202). These expressed proteins avoid oxidative stress-induced DNA damage by either reducing the exposure of DNA to carcinogens (exogenous or endogenous), inhibiting the activation of pro-carcinogens, or increasing the rate of detoxification of carcinogens (180,203,204). Therefore, the inactivation of the Nrf2/ARE pathway could increase oxidative stress by generating ROS, creating mutagenesis, and initiating carcinogenesis and tumor formation in normal cells (180,203,204). For example, decreased expression of the Nrf2 gene increases the risk of lung cancer among smokers (205). Furthermore, decreased levels of phase 2 enzymes such as HO-1 and Nrf2 proteins in Nrf2-knockout animal models such as female C57BL/6 mice increase the susceptibility towards 7,12-dimethylbenz(a)anthracene-induced skin tumorigenesis (206). Therefore, many investigations propose the activation

of the Nrf2/ARE cell signaling pathway as a potential cellular mechanism of cancer chemoprevention (183).

2.3.3.1 Activators of Nrf2/ARE pathway in non-cancer experimental models

Investigations on the activation of the Nrf2/ARE pathway have shown that some vitamins and a diverse range of dietary phytochemicals, including flavonoids, sulforaphanes, alkaloids, polyphenols activate the pathway by different mechanisms in non-cancer experimental models (9) (Table 2). Further, several endogenous cell signaling molecules, such as PKR-like endoplasmic reticulum-resident kinase (PERK), N-terminal kinase (JNK), extracellular signal-regulated protein kinase (ERK), and p38 under normal conditions known to give similar results (207,208). Activation of Nrf2/ARE pathway mainly occurs through the disruption of Keap1 and Nrf2 interactions (either through canonical or non-canonical mechanisms) (193), Nrf2 phosphorylation (194), and prevention of Nrf2 ubiquitination (209). In addition, some of the activators facilitate Nrf2 nuclear translocation and transcription of cytoprotective genes associated with ARE (209).

Resveratrol, a stilbene derivative, and RTA-408 (omaveloxolone), a synthetic terpenoid activate the Nrf2 pathway through canonical mechanisms (194,210–213). Canonical activators that obstruct the interaction of the Keap1/Nrf2 system possess electrophilic properties and react with cysteine residues (i.e. Cys151, Cys257, Cys273, Cys288, and Cys297) of Keap 1 via either oxidation or alkylation in order to dissociate Nrf2 from Keap 1 (183,192,194,201). For example, in phase 3 clinical trial on chronic subclinical inflammation and redox status, 500 mg of resveratrol in a tablet/day up to 30 days (Table 2) have shown to be interrupting the Nrf2-Keap 1 interactions by conformational changes. These changes occurred due to electrophilic modifications in

Keap 1-Cys151 thiol group (194,213). Cul3-based E3 ligase complex binds and interacts with Keap1 to facilitate Nrf2 polyubiquitination, which promotes Nrf2 degradation at 26S proteasome. Therefore, post-translational modifications in Cys151 lead to the dissociation of Cul3-based E3 ligase complex from Keap 1 and Nrf2 stabilization (189–191,194,210). Thereby, it prevents Nrf2 proteasomal degradation by ubiquitination and facilitates ARE-mediated gene expression (209,214,215). Similar results were observed with RTA-408 (omaveloxolone), a synthetic terpenoid in a clinical trial on inflammation and pain due to ocular surgery (1% ophthalmic suspension of RTA-408 twice a day for 14 days) as well (194,211).

Sequestosome-1, an endogenous signaling molecule, activates the Nrf2 pathway via non-canonical mechanisms by blocking Nrf2 binding to Keap 1 (216) (Table 1). Sequestosome 1, also called p62, not only competes with Nrf2 to bind to Keap 1 and block the formation of Nrf2-Keap 1 complex, but also promotes the autophagic degradation of Keap 1 (193,216). For example, Nrf2 silencing downregulates p62 expression while upregulating Keap 1 expression at mRNA and protein levels in vascular smooth muscle cells (216). Conversely, p62 silencing dramatically upregulates Keap 1 and downregulates Nrf2 at mRNA and protein levels suggesting p62 may be effective in downregulating Keap 1 protein via autophageal degradation (216).

Most of the endogenous activators of Nrf2/ARE pathway act by stimulating the phosphorylation of Nrf2 which leads to the detachment of Nrf2 from Keap 1 (201). For example, PERK-mediated direct phosphorylation of Nrf2 in mouse embryonic fibroblasts results in the dissociation of Nrf2 from Keap 1 (Table 2) (207). Similarly, JNK 1 and 2, ERK2, and p38 phosphorylate Nrf2 at serine (Ser212, Ser400, Ser558, Ser577) and

threonine (Thre559) residues in human embryonic kidney HEK 293T cells (208). It is also suggested that above mentioned endogenous activators of the Nrf2/ARE pathway can be activated by phytochemicals such as diallyl sulfide (217). Diallyl sulfide phosphorylates ERK and p38 in human embryonic lung MRC-5 cells and facilitates dissociation of Nrf2 from Keap 1 and nuclear translocation (217).

Most of the endogenous activators of Nrf2 are protein kinases, which seem to facilitate the nuclear translocation of phosphorylated Nrf2 (195,218,219). Nrf2 phosphorylation mediated by AMPK, casein kinase 2, PERK, ERK, and p38 facilitates Nrf2 nuclear translocation (218). PI3K signaling is also involved in the activation of the Nrf2/ARE pathway through its downstream regulator Akt, which facilitates Nrf2 nuclear translocation and following ARE gene transactivation (220). Therefore, the influence of endogenous signaling molecules, phytochemicals, and synthetic chemicals on activation of Nrf2/ARE at different stages of the pathway will be vital in exerting chemopreventive effects upon activation of Nrf2/ARE pathway (9,194,207,208).

Table 2: Activators of the Nrf2/ARE pathway in non-cancer experimental models: Phytochemicals and other signal molecules

Group	Compound	Effective concentration	Experimental model	Mode of action	Ref.
Phytochemicals: Polyphenols (non-Flavonoids)					
Phenolic acid	Caffeic acid	10 μM	Human kidney epithelial HEK 293T cell line	↑ Nrf2 (S40) phosphorylation. ↑ GPx and HO-1 protein levels.	(221)
	Gallic acid	200 mg/kg of body weight up to 28 days orally	Balb/c mice	↑ total Nrf2 and HO-1 protein levels.	(222)
	Ellagic acid	25-50 μM	Human keratinocyte HaCaT cell line	↑ total Nrf2 nuclear translocation. ↑ SOD enzyme activity.	(223)
	Chlorogenic acid	100 μM	Human retinal pigment epithelial ARPE-19 cell line	↑ mRNA expression of Nrf2 and SOD.	(224)
		500 mg/kg of body weight orally	Sprague-Dawley rats	↑ mRNA expression of Nrf2. ↑ SOD and GSH activities.	(225)
Proanthocyanidin	Procyanidin C 1	5-10 μM	Mouse hippocampal neuronal HT22 cell line	↑ total Nrf2 nuclear translocation. ↑ HO-1 protein levels.	(226)
	Procyanidin B2	20 μM	Normal human colon epithelium NCM460 cells	↑ total Nrf2, NQO1 and HO-1 protein levels.	(227)
		2.5 μM	Human endothelial progenitor cells	↑ Nrf2, NQO1 and CAT mRNA and total protein levels.	(228)

Group	Compound	Effective concentration	Experimental model	Mode of action	Ref.
Proanthocyanidin	Procyanidin B2	8.64 µM	Cerebral cortical neurons of C57BL/6 mice	↑ total Nrf2, and HO-1 protein levels.	(229)
		50 mg/kg of body weight up to 21 days orally	C57BL/6 mice	↑total Nrf2, CAT, SOD, and HO-1 protein levels.	(230)
		10 µM	Human umbilical vein epithelial and primary trophoblasts cells	↑ total Nrf2 nuclear translocation.	(231)
Lignans	Sesamin	100 mg/kg body weight intraperitoneally	C57BL/6 mice	↑ SOD and CAT activities. ↑ GSH and total Nrf2 protein levels.	(232)
		10 µM	Primary chondrocytes	↑ total Nrf2 and HO-1 protein levels.	(233)
Coumarins	Fraxin	50 mg/kg of body weight up to 5 days orally	Sprague–Dawley rats	↑ cellular GSH levels.	(234)
Stilbenes	Resveratrol	5 µM	Primary human coronary artery endothelial cells	↑ mRNA expression of NQO 1.	(235)
		500 mg in a tablet/day up to 30 days in the morning fasting	Phase 3 clinical trial on chronic subclinical inflammation and redox status	↑ electrophilic modification of Keap1-Cys-151	(194,213)

Group	Compound	Effective concentration	Experimental model	Mode of action	Ref.
Stilbenes	Resveratrol	215 mg in a tablet/day up to 52 weeks	Phase 2 clinical trials on Alzheimer's disease	↑ electrophilic modification of Keap1-Cys-151	(194,236)
		0.1 μM	Human umbilical vein epithelial cells	↑ total Nrf2 nuclear translocation. ↑ SOD protein levels.,	(237)
Curcuminoid	Curcumin	5 μM	Human extravillous trophoblast HTR8/Sveo cells	↑ CAT and GSH activities.	(238)
		400 mg/kg body weight/day orally up to 21 days	White Pekin ducklings	↑ CAT, SOD and GPx activities.	(239)
		800 mg/day in two capsules up to 7 days	Phase 3 clinical on diabetic nephropathy	↑ electrophilic modifications of Keap1-Cys-151	(194,210)
Curcuminoid	Curcumin	15 μM	Human retinal pigment epithelial ARPE-19 cell line	↑ total Nrf2 protein levels. ↑ HO-1 activity.	(240)
		15-30 μM	Porcine renal epithelial proximal tubule LLC PK1 cell line	↑ ARE binding activity. ↑ total Nrf2 protein levels. ↑ HO-1 activity.	(241)
		10 μM	Rat kidney epithelial NRK-52E cell line	↑ ARE binding activity.	(241)

Group	Compound	Effective concentration	Experimental model	Mode of action	Ref.
Curcuminoid	Curcumin	200 mg/kg body weight twice a week for 6 weeks orally	Kungming (KM) mice	↑ total Nrf2 nuclear translocation. ↑ HO-1 and NQO-1 protein levels.	(242)
		200 mg/kg body weight for 30 days orally	Balb/c mice	↑ Nrf2 mRNA and total protein levels. ↑ SOD, CAT, NQO1, and HO-1 mRNA levels ↓ Keap 1 protein levels. ↑ SOD, CAT, and GPx activities.	(243)
Phytochemicals: Polyphenols (Flavonoids)					
Flavone	Luteolin	0.1 mg/kg body weight/day for 7 days at two-time points orally.	ICR mice	↑ total Nrf2 nuclear translocation. ↑ HO-1 and NQO-1 protein levels.	(244)
		10 mg/kg body weight intracerebrally injected	Sprague−Dawley rats	↑ total Nrf2 nuclear translocation. ↑ HO-1 and NQO-1 proteins.	(245)
		5-10 μM	Rat myoblast H9c2 cell line	↑ total Nrf2 protein. ↑ mRNA expression of SOD, NQO-1 and HO-1.	(197)
		5 μM	Mouse testis sertoli TM4 cell line	↑ total Nrf2 nuclear translocation.	(246)

Group	Compound	Effective concentration	Experimental model	Mode of action	Ref.
Flavone	3,5-di-O-Methyl Gossypetin	10-25 µg/mL	Human keratinocyte HaCaT cells	↑ total Nrf2 nuclear translocation. ↑ GSH, SOD and HO-1 protein levels	(247)
	Baicalein	160 mg/kg/day for 8 weeks orally	T2DM Kunming mice	↑ total Nrf2 nuclear translocation. ↑ SOD, CAT, GSH protein	(248)
	Baicalin	50 mg/kg body weight twice after 2 and 12 h of subarachnoid hemorrhage intraperitoneally	Sprague-Dawley rats	↑ SOD, GSH, NQO-1 and Nrf2 protein. ↑ mRNA expression of HO-1.	(249)
		75 µM	Rat myoblast H9C2 cell line	↑ total Nrf2 and HO-1 protein levels.	(250)
		450 mg/kg body weight/day up to 7 days orally.	Chicken	↑ total Nrf2 and HO-1 protein levels. ↑ mRNA expression of Nrf2 and HO-1.	(251)
	Apigenin	400 µM	Human retinal pigment epithelial ARPE-19 cell line	↑ mRNA expression of Nrf2. ↑ total Nrf2 protein levels. ↑ total Nrf2 nuclear translocation ↑SOD, CAT, and GPx activities.	(252)

Group	Compound	Effective concentration	Experimental model	Mode of action	Ref.
Flavone	Chrysin	10-25 μM	Rat hepatocytes	↑ total Nrf2 nuclear translocation via ERK2 signaling. ↑cellular GSH protein levels. ↑ ARE binding ability	(253)
		1-5 μM	Bone marrow-derived mesenchymal stem cells of SD rats	↑ total Nrf2 and HO-1 protein levels	(254)
Flavonol	Myricetin	100 mg/kg/day for 6 weeks orally	Kungming mice	↑ total Nrf2 nuclear translocation.	(255)
	Quercetin	30 μM	Human keratinocyte HaCaT and BJ foreskin fibroblast cell lines	↑ total Nrf2 protein levels.	(256)
		200 mg/kg body weight/day for 20 days orally	Broiler chicken	↑ total Nrf2 protein levels. ↑ total Nrf2 nuclear translocation ↑ SOD and CAT protein levels.	(257)
		100 μM	Intestinal epithelial IEC-6 cell line	↑ total Nrf2 nuclear translocation.	(258)
		10 μM	Human umbilical vein epithelial cells	↑ total Nrf2 protein levels.	(259)
		6.25-12.5 μM	Human primary dermal fibroblasts.	↑ total Nrf2 nuclear translocation.	(260)

Group	Compound	Effective concentration	Experimental model	Mode of action	Ref.
Flavonol	Quercetin	6.25-12.5 μM	Human primary epidermal keratinocytes	↑ total Nrf2 nuclear translocation. ↑ HO-1 mRNA levels	(260)
		10-40 μM	Human bronchial epithelial BEAS-2B cells	↑ total Nrf2 and HO-1 protein levels.	(261)
	Rutin	44 μM	Human keratinocyte HaCaT cell line	↑ mRNA expression of HO-1 and NQO-1.	(262)
Flavanone	Naringenin	80 μM	Sprague-Dawley rat neuron cells	↑ total Nrf2, HO-1 and NQO-1 protein levels	(263)
		70 mg/kg body weight/day up to 4 days orally	C57BL/6 mice	↑ total Nrf2 protein levels.	(264)
	Hesperidin	50 mg/kg bodyweight for 28 days orally	Sprague-Dawley rat	↑ total Nrf2 and HO-1 protein levels. ↑ mRNA expression of HO-1.	(265)
Flavan-3-ol	Epicatechin	10-100 μM	Primary astrocytes from WT and Nrf2 deficient KO mice	↑ total Nrf2 nuclear translocation.	(266)
	Epigallocatechin-3-gallate	40 mg/kg body weight/day for 3 days intraperitoneally	Sprague-Dawley rat	↑ total Nrf2 protein levels.	(267)
Isoflavones	Genistein	1 mg/kg body weight intraperitoneally	Sprague-Dawley rat	↑ total Nrf2 nuclear translocation ↑ HO-1 protein levels	(268)

Group	Compound	Effective concentration	Experimental model	Mode of action	Ref.
Isoflavones	Genistein	5 or 15 mg/kg body weight intraperitoneally for 5 days	Sprague-Dawley rat	↑ total Nrf2, HO-1, NQO-1 protein levels. ↓ Keap 1 protein levels.	(269)
		200 mg/kg body weight orally	C57BL/6 mice	↑ total Nrf2, and HO-1 protein and mRNA levels.	(270)
		20 mg/kg body weight for 13 weeks orally	HY-line brown laying hens	↑ total Nrf2, SOD, CAT, GPx, NQO-1and HO-1 mRNA and protein levels. ↓ Keap 1 mRNA and protein levels.	(271)
Anthocyanidin	Cyanidin-3-*O*-glucoside (C3G)	20-40 μM	Human umbilical vein epithelial cells	↑ total Nrf2 nuclear translocation. ↑mRNA expression of NQO-1 and HO-1	(272)
Chalcone	Buteine	20 μM	Human dental pulp cell line	↑ total Nrf2 nuclear translocation.	(273)
	Phloretin	50 mg/kg body weight for 2 weeks orally	*Swiss albino* mice	↑ Nrf2 mRNA levels	(274)
Other phytochemicals (non-Polyphenols)					
Sulfur-containing	Sulforaphane	5 μM	Mouse skin JB6 P+ cells	↑ total Nrf2 nuclear translocation. ↑ HO-1 and NQO-1 protein levels	(275)

Group	Compound	Effective concentration	Experimental model	Mode of action	Ref.
Sulfur-containing	Sulforaphane	6.25 μM	Human primary dermal fibroblasts and epidermal keratinocytes.	↑ total Nrf2 nuclear translocation. ↑ NQO1 mRNA levels	(260)
	Diallyl sulfide	15 μM	Human embryonic lung MRC-5 cell line	Dissociates Nrf2 from Keap 1 through phosphorylated ERK and p38 interactions. ↑ total Nrf2 nuclear translocation.	(217)
		150 mg/kg body weight/day intraperitoneally for 6 days	Wistar rats	↑ total Nrf2 protein levels. ↑SOD, CAT, GPx, GR, GST and quinone reductase activities.	(276)
Alkaloids	Berberine	200 mg/kg body weight/day orally for 16 weeks	Wistar rats	↑ mRNA expression of Nrf2.	(277)
Vitamins					
Fat-soluble vitamins	Vitamin D	40 000 U/kg/week of bodyweight intratracheally for 8 weeks	C57BL/6 mice	↑ mRNA expression Aldo-keto reductase family 1 member C1 (AKR1C1) and GCLM.	(278)
	Vitamin E	100 mg/kg body weight/day intraperitoneally for 6 days	Balb/c mice	↑ total Nrf2 and HO-1 protein levels.	(279)

Group	Compound	Effective concentration	Experimental model	Mode of action	Ref.
Fat-soluble vitamins	Vitamin A	100,000 U/kg body weight/day subcutaneously for 14 days	Wistar rats	↑ total Nrf2 nuclear translocation. ↑ HO-1 and NQO 1 protein levels.	(280)
Water-soluble vitamins	Vitamin C	27-65 mg/kg body feed twice a day for 8 weeks	Juvenile *Sillago sihama*	↑ mRNA expression of Nrf2, CAT, SOD, GPx, GR and GST in intestine and liver cells.	(281)
	Vitamin B2	30 mg/kg body weight/day intra-gastrically	APP/PS1 double transgenic mice	↑ SOD, CAT, GSH and GPx activities. ↑ total Nrf2 expression. ↓ Keap 1 expression.	(282,283)
Endogenous signaling molecules					
Protein kinases	PI3K	N/A	Human retinal pigment epithelial RPE-19 cell line	↑ total Nrf2 nuclear translocation.	(220)
	JNK 1 & 2	N/A	Human embryonic kidney HEK 293T cell line	Phosphorylates Nrf2 at S212, S408, S558, S577 and T559.	(208)
	p38	N/A	Human embryonic kidney HEK 293T cell line	Phosphorylates Nrf2 at Ser212, Ser408, Ser558, Ser577 and Thre559.	(208)
	AMPK	N/A	Human embryonic kidney HEK 293T cell line	Phosphorylates Nrf2 at the Ser558 residue. ↑ total Nrf2 nuclear translocation	(195)

Group	Compound	Effective concentration	Experimental model	Mode of action	Ref.
Protein kinases	ERK2	N/A	Human embryonic kidney HEK 293T cell line	Phosphorylates Nrf2 at Ser212, Ser408, Ser558, Ser577 and Thre559.	(208)
	Casein kinase 2	N/A	Human embryonic kidney HEK 293T cell line	↑ Nrf2 phosphorylation. ↑ total Nrf2 nuclear translocation.	(218)
	PKC	N/A	New Zealand white rabbits	↑ total Nrf2 nuclear translocation.	(219)
	PERK	N/A	Mouse embryonic fibroblasts	Dissociates Nrf2 from Keap 1 by phosphorylation of Nrf2	(207)
Autophagy-substrate proteins	Sequestosome 1 (p62)	N/A	Human aortic smooth muscle cells	Competes with Nrf2 to bind with Keap 1.	(216)
Synthetic compounds					
Synthetic triterpenoids	Bradoxolone-methyl (CDDO-Me)	25 -150 mg/day for 52 weeks	Phase 2 clinical on diabetic nephropathy	↑ electrophilic modification of Keap1-Cys-151	(194,212)
	RTA-408 (omaveloxolone)	1% ophthalmic suspension for twice a day for 14 days	Phase 2 clinical trial on inflammation and pain following ocular surgery	↑ electrophilic modification of Keap1-Cys-151	(194,211)
Synthetic lignans	LGM2605 (Secoisolariciresinol diglucoside)	50 µM	Murine peritoneal macrophages derived from C57BL/6J mice	↑ mRNA expression of GST and redoxin reductase 1.	(284)

Abbreviations: HaCaT: human skin keratinocytes; ARPE-19: human retinal pigment epithelial cell line; BEAS-2B: human bronchial epithelial cell line; HT22: mouse hippocampal neuronal cell line; LLC $PK_{1:}$ porcine renal epithelial proximal tubule cell line; NCM460: normal human colon epithelial cell line; NRK-52E: rat kidney epithelial cell line; IEC-6: intestinal epithelial cell line; MRC5: human embryonic lung cell line; HTR8/Sveo: extravillous trophoblast cell line ; HEK 293T: human embryonic kidney 293T cell line; HT22: mouse neuronal cell line; H9C2: rat myoblast cell line: TM4: mouse Sertoli cell line; T2DM mice: type 2 diabetes mellitus mice; BJ: human foreskin fibroblast cell line; WT: wild type; KO: knock-out; JB6 P+: mouse skin cells; APP/PSI: ARTE1; GCLM: glutamate-cysteine ligase modifier; GSH: glutathione; CAT: catalase; SOD; superoxide dismutase; Gpx: glutathione peroxidase; ARE: antioxidant response element; ERK: extracellular signal-regulated protein kinase; GSK-3β: glycogen synthase kinase 3; Akt: protein kinase B; GR: glutathione reductase; NQO-1: NAD(P)H quinone dehydrogenase 1; HO-1: heme oxygenase 1; GST- glutathione S-transferase; Ser212: serine residue 212; Ser408: serine residue; Ser558: serine residue 558; Ser577: serine residue 577; Thre559: threonine residue 559; PI3K: phosphorylation of phosphatidylinositol 3-kinase; JNK: N-terminal kinase; AMPK: 5′ adenosine monophosphate-activated protein kinase; PKC: protein kinase C; PERK: PKR-like endoplasmic reticulum-resident kinase; p62: sequestosome 1; Keap 1: Kelch-like ECH-associated protein 1; Nrf2: Nuclear factor erythroid 2 p45 (NF-E2)-related factor; Ref: reference. (Table 2 was reproduced from Suraweera, *et al*., 2020 (198) with minor changes and updated with Lee, *et al*., 2011, Fan, *et al*., 2021, Gao, *et al*., 2021, Hu, *et al*., 2021, Liu, *et al*., 2022, Ma, *et al*. , 2021, Singh, *et al*., 2021, Singla, *et al*., 2021, Zhou, *et al*., 2021, Zhu, *et al*., 2021, Wu, *et al*., 2021, Bhullar, *et al*., 2022, Li, *et al*., 2022, Rajnochova, *et al*., 2022, and Wang, *et al*., 2022 (222,227–231,237,243,260,261)).

2.3.3.2 Flavonoids: Nrf2/ARE activation in non-cancer experimental models

Flavonoids are among the most noticeable dietary phytochemicals which activate the Nrf2/ARE pathway under normal physiological and induced conditions (Table 2). The sub-class flavones (luteolin, baicalin, and apigenin) are more prominent in upregulating Nrf2 protein expression in both *in vitro* and pre-clinical studies (197,249,252). For example, luteolin upregulates Nrf2 protein expression in relieving high glucose-induced cell injury in rat myoblast H9C2 cells at rat physiological concentrations (100,197). Baicalin also increases Nrf2 protein expression against hypoxia-induced apoptosis in rat myoblast H9C2 cells, although the required concentration was higher than rat physiological concentrations (250,285). Furthermore, intraperitoneal administration of baicalin demonstrates a similar effect in male Sprague-Dawley rats after inducing subarachnoid hemorrhage by endovascular perforation (249,286). A study conducted by Xu and colleagues shows that apigenin increases Nrf2 protein level as a response to *tert*-butyl hydroperoxide (t-BHP)-induced oxidative cell injury in human retinal pigment epithelial ARPE-19 cells at much higher concentrations compared to other flavones (252). However, the tested concentrations were much higher than the bioavailable apigenin levels in human plasma (287).

Further, the upregulation of Nrf2 protein was observed in flavonols (quercetin), flavanones (naringenin, hesperidin), and flavan-3-ols (epigallocatechin-3-gallate) (256,263,265,267). Naringenin, a flavanone found in citrus fruits upregulates Nrf2 protein in hypoxia-induced neuron cells derived from neonatal Sprague-Dawley rats (263). However, comparatively at higher concentrations that may not be achievable in pre-clinical studies considering the limited bioavailability of naringenin in rats (263,288,289).

Quercetin upregulates Nrf2 protein expression in different human cell lines such as human skin keratinocytes HaCaT, BJ foreskin fibroblast, and human umbilical vein endothelial cells (HUVECs) but at concentrations higher than physiologically relevant concentrations considering the low bioavailability of quercetin through human diet (256,259,290,291). Also, oral administration of quercetin upregulates Nrf2 protein levels against lipopolysaccharide-induced intestinal oxidative stress in broiler chicken (257). Furthermore, pre-clinical studies on oral administration of naringenin show upregulation of Nrf2 protein in male C57BL/6 mice with 6-hydroxydopamine (6-OHDA)-induced neurotoxicity at a concentration that is not toxic (264,292). Also, both hesperidin (oral) and epigallocatechin-3-gallate (intraperitoneal) have shown that similar upregulations can be achievable at non-toxic concentrations in male Sprague-Dawley rats with methotrexate (MTX)-induced hepatotoxicity and cerebral ischemia-induced oxidative stress, respectively (265,267,293,294). In contrast, mRNA levels of Nrf2 were upregulated only in flavones such as baicalin (chicken with *Mycoplasma gallisepticum* infection-induced oxidative stress) and apigenin (human retinal pigment epithelial ARPE-19 cells with *t*-BHP-induced oxidative cell injury) in pre-clinical and *in vitro* models (251,252). However, the molecular mechanisms of flavonoid-mediated increase of cellular Nrf2 mRNA and protein levels remain unclear.

Nuclear translocation of phosphorylated Nrf2 is a necessity in order to proceed with ARE-driven gene transcription (195,196). Many subclasses of flavonoids including flavones (luteolin, baicalein, chrysin, and apigenin), flavonols (myricetin and quercetin), flavanones (eriodyctiol), flavan-3-ols (epicatechin), isoflavones (genistein), anthocyanidins (cyanidin-3-*O*-glucoside [C3G]), and chalcones (buteine) promote Nrf2

nuclear translocation (Table 2). Luteolin and epicatechin upregulate the Nrf2 nuclear translocation in mice cells; mouse testis Sertoli TM4 (triptolide-induced apoptosis) and hemoglobin toxicity induced primary astrocytes of mice, respectively (246,266). Similarly, chrysin and quercetin upregulate the Nrf2 nuclear translocation in rat hepatocytes (*t*-BHP-induced oxidative stress) and rat intestinal epithelial IEC-6 cells (253,295). Also, in rat hepatocytes, chrysin-mediated upregulation of the phosphorylated ERK1 increases the Nrf2 nuclear translocation (253). Therefore, ERK1-mediated influences may be due to the improved stability of Nrf2 upon Nrf2 phosphorylation, which prevents Nrf2 ubiquitination and degradation (296). However, the tested concentrations of luteolin (mouse testis Sertoli TM4 cells), epicatechin (primary astrocytes from mice), quercetin (rat hepatocytes), and chrysin (IEC-6 cells) in above murine cells are higher than the achievable physiological concentrations in murine models upon oral administration (244,297–299). Also, cyanidin-*O*-glucoside (C3G) upregulates Nrf2 nuclear translocation in HUVECs challenged with tumor necrosis factor-α (272). However, tested concentrations of C3G on HUVECs are much higher than the serum levels that can be achieved in humans upon oral uptake (300). Apigenin also facilitates nuclear translocation in human retinal epithelial ARPE-19 cells at concentrations higher than physiological in humans (252,287). Similarly, butein upregulates Nrf2 nuclear translocation against hydrogen peroxide-induced oxidative stress in human dental pulp cells (247,273). Further, due to the lack of availability of clinical data on the bioavailability of butein, the physiological relevance of tested concentrations of butein is mostly unknown.

Furthermore, promising results on upregulation of Nrf2 nuclear translocation were observed in several pre-clinical studies (ICR mice, Sprague-Dawley rats, Kunming mice,

and broiler chicken) (244,245,248,255,257). Luteolin, baicalein, myricetin, quercetin, and genistein demonstrates their ability in upregulating Nrf2 nuclear translocation (244,245,248,255,257). Luteolin increases Nrf2 nuclear translocation in male Sprague-Dawley rats with intracerebral hemorrhage-induced secondary brain damage (intraperitoneal administration) and male ICR mice (oral administration) at concentrations that are not toxic (244,245,301–303). Similarly, oral administration of baicalein facilitates Nrf2 nuclear translocation in male type 2 diabetes mellitus (T2DM) Kunming mice with high glucose-induced oxidative stress at a concentration much lesser than the maximum toleratable levels for mice (248,304). Further, myricetin (oral administration) was effective in upregulating Nrf2 nuclear translocation against cuprizone-induced demyelination in male Kunming mice (255). The concentration of myricetin tested on Kunming mice are much lesser than sub-lethal concentrations of myricetin in mice (255,305). Also, both quercetin (oral administration) and genistein (intraperitoneal administration) upregulate Nrf2 nuclear translocation in broiler chickens (lipopolysaccharide-induced intestinal oxidative stress) and male Sprague-Dawley rats (cerebral ischemia-induced oxidative stress) (257,268). Further, tested concentrations of genistein on Sprague-Dawley rats are much lesser than concentrations that show toxic effects in mice (306).

Downstream activation of Nrf2/ARE pathway at Nrf2 nuclear translocation by flavonoids has been demonstrated. Overexpression of antioxidant defense genes (GSH, SOD, GPx, and CAT) and phase 2 detoxifying genes (HO-1 and NQO-1) was observed due to flavones (luteolin, apigenin, baicalin, baicalein, chrysin), flavanones (naringenin, and hesperidin), flavonols (quercetin, rutin), anthocyanidins (C3G) and isoflavones (genistein) (Table 1). Chrysin upregulates cellular GSH proteins (antioxidant defense gene)

in relieving *t*-BHP-induced oxidative stress of rat hepatocytes (253). Baicalin and naringenin upregulate phase 2 detoxifying enzymes at the protein level against hypoxia-induced oxidative stress or apoptosis in H9C2 (HO-1) and Sprague-Dawley neuronal cells (HO-1 and NQO-1), respectively (250,263). Although the concentrations tested were higher than the physiologically relevant range, rutin and C3G upregulate the expression of HO-1 and NQO-1 at mRNA levels in HaCaT and HUVECs, respectively (262,272,291,300). Further, apigenin enhances the activity of SOD, CAT, and GPx in human retinal epithelial ARPE-19 cells, but at much higher concentrations than can be achieved physiologically in humans (252,287).

In preclinical studies, oral administration of baicalein and quercetin upregulates proteins related to antioxidant defense genes against relieving oxidative stress in high glucose-induced male T2DM Kunming mice (SOD, CAT, and GSH) and lipopolysaccharide-induced broiler chicken (SOD and CAT), respectively (248,257). In contrast, upregulation of both antioxidant defense (SOD and GSH) and phase 2 detoxifying genes (NQO-1 and mRNA HO-1) was observed with intraperitoneal administration of baicalin in male Sprague-Dawley rats after inducing subarachnoid hemorrhage (249). Luteolin upregulates phase 2 detoxifying enzymes (HO-1 and NQO-1) in male Sprague-Dawley rats with intracerebral hemorrhage-induced secondary brain damage (intraperitoneal administration) and male ICR mice (oral administration) (244,245). In contrast, the upregulation of HO-1 was observed at the protein level against cerebral ischemia-induced oxidative stress in Sprague-Dawley rats with intraperitoneal administration of genistein (268). Also, oral administration of baicalin and hesperidin has upregulated HO-1 at both protein and mRNA levels against *Mycoplasma gallisepticum*

infection-induced oxidative stress in chicken and MTX-induced hepatotoxicity in male Sprague-Dawley rats, respectively (251,265). More importantly, the above upregulations of either or both antioxidant and phase 2 detoxifying enzymes by luteolin (ICR mice and Sprague-Dawley rats), baicalein (T2DM Kunming mice), baicalin (Sprague-Dawley rats), hesperidin (Sprague-Dawley rats) and genistein (Sprague-Dawley rats) were observed in concentration lesser than toxic or lethal in *in vivo* studies (286,293,301,302,304,306).

Moreover, studies on activators of Nrf2/ARE pathway since the literature review by Suraweera *et al*., 2020 (198) further demonstrate the ability of compounds such as quercetin, genistein, and procyanidin B2 in activating Nrf2/ARE pathway in different non-cancer experimental models (Table 2). Genistein upregulated the Nrf2, antioxidant and/or, phase 2 detoxifying enzymes at transcriptional and/or translational levels in pre-clinical experimental models such as male C57BL/6 mice (oral administration; Nrf2, HO-l mRNA, and proteins), and HY-line brown laying hens (oral administration; Nrf2, SOD, CAT, GPx, HO-1) in physiological conditions, and pentylenetetrazol-induced male Sprague-Dawley rats (intraperitoneal administration; Nrf2, HO-1, and NQO-1 proteins) (269–271). Furthermore, downregulation of Keap 1 at mRNA and/or protein levels was observed with genistein treated HY-line brown laying hens and pentylenetetrazol-induced male Sprague-Dawley rats (269,271). The tested concentrations of genistein in C57BL/6 mice and Sprague-Dawley rats were lesser than the toxic concentrations tested in mice (269,270,306). Furthermore, Rajnochova and colleagues (2022) (260) showed that quercetin can upregulate the Nrf2 nuclear translocation in both human primary dermal fibroblasts and epidermal keratinocytes under physiological conditions but at concentrations higher than human physiological concentrations. In addition to that, the

same study demonstrated the ability of quercetin treatments in upregulating HO-1 mRNA levels in human primary epidermal keratinocytes (116–119,260). Additionally, procyanidin B2 demonstrated the ability to upregulate Nrf2, antioxidant and/or phase 2 detoxifying protein and/or mRNA levels in preclinical (male C57BL/6 mice under physiological conditions; Nrf2, CAT, SOD, HO-1 proteins) and *in vitro* experimental models such as cerebral cortical neurons of C57BL/6 mice (against cypermethrin induced neuronal injury; Nrf2 and HO-1), normal human colon epithelium NCM460 cells (against irradiation-induced oxidative stress; Nrf2, CAT, SOD, and HO-1 protein), and human endothelial progenitor cells (against high glucose-induced oxidative stress; Nrf2, NQO-1, and HO-1 mRNA and proteins) (227,229,230). Upregulation of the Nrf2/ARE pathway in pre-clinical experimental models with procyanidin B2 was observed at non-toxic concentrations in rats (307). Furthermore, procyanidin B2 was effective in facilitating Nrf2 nuclear translocation in HUVECs and trophoblasts cells at physiological conditions at rat physiological concentrations (128,129,231).

Even though numerous studies have demonstrated the ability of flavonoids to activate the Nrf2/ARE pathway in exerting cancer prevention, comprehensive studies carried out with respect to the concentrations similar or closer to physiological concentrations are mostly limited. Additionally, it is important to identify the lowest effective concentrations that may have a positive effect on exerting cancer prevention considering the diet-related health benefits of flavonoids. Therefore, studies designed to determine the effects of flavonoids with respect to the activation of Nrf2/ARE pathway at physiological concentrations are a necessity considering the dietary intake of flavonoids through fruits, vegetables, and supplementation.

CHAPTER 3: MATERIALS AND METHODS

3.1 Antibodies, chemicals, and reagents.

Anti-Nrf2 rabbit (Catalogue number [Cat]: ab62352) and anti-phospho-Nrf2 (Ser40) rabbit (Cat: ab76026) primary antibodies were purchased from Abcam Inc., (Toronto, ON, Canada). Anti-phospho-histone H2AX (ser139) mouse (Cat: 05-636) primary antibody was purchased from Sigma-Millipore (Etobicoke, ON, Canada). Anti-Akt rabbit (Cat: 92725), anti-phospho-Akt rabbit (Ser473) (Cat: 4060T) primary antibodies, horseradish peroxidase (HRP)-linked anti-rabbit secondary antibody (Cat: 7074P2) and HRP conjugated anti-β-actin rabbit (Cat: 12620S) antibody were purchased from Cell Signalling Technology, Inc., (Danvers, MA, USA). Alexa Fluor® 594 donkey anti-mouse (Cat: A-21203) and Alexa FlourTM 488 goat anti-rabbit (Cat: A11034) secondary antibodies were purchased from Thermo Fisher Scientific (Chelmsford, MA, USA).

Test compounds ascorbic acid (Cat: A5960), beta carotene (Cat: 22040), caffeic acid (Cat: C0625), catechol (Cat: 135011), chlorogenic acid (Cat: C3878), chrysin (Cat: 95082), curcumin (Cat: C1386), cyanidin-3-*O*-glucoside (Cat: PHL89616), cyanidin chloride (Cat: 528-58-5), dimethyl fumarate (DMF) (Cat: 242926), epicatechin (Cat: E1753), genistein (Cat: 4478-93-7), isorhamnetin (Cat: 17794), luteolin (Cat: 491-70-3), methyl 4-hydroxybenzoate (Cat: H5501), naringenin (Cat: 52186), phloretin (Cat: 60-82-2), phloridzin dihydrate (Cat: P3449), phloroglucinaldehyde (Cat: T65404), protocatechuic acid (Cat: 08992), quercetin (Cat: Q4951-109), quercetin-3-*O*-glucuronic acid (Cat: 22688-79-5), resveratrol (Cat: R5010), and sulforaphane (Cat: 4478-93-7) were purchased from Sgma-Aldrich (Oakville, ON, Canada). Procyanidin B2 (Cat: 29106-49-8) was purchased from Chengdu Alfa Biotechnology Co., Ltd (Pixian, Chengdu, China). 4-

[(Acetoxymethyl) nitrosamino]-1-(3-pyridyl)-1-butanone (NNKAc) (Cat: 167550) was purchased from Toronto Research Chemicals (Toronto, ON, Canada).

2-Mercaptoethanol (Cat: 21985-023), Dulbecco's modified eagle medium (DMEM) with no phenol red (Cat: 21063029), fetal bovine serum (FBS)(Cat: 12483-020), LHC-8 growth medium (Cat: 12678017), phenylmethylsulfonyl fluoride protease inhibitor (Cat: 329-98-6), Tris base (Cat: 77-86-1), Tris base/boric acid/ethylenediaminetetraacetic acid (EDTA) (TBE) buffer (Cat: B52), TrypLETM Express solution (Cat: 12604021), and Tween 20 (Cat: 9005-64-5) were purchased from Thermo Fisher Scientific (Chelmsford, MA, USA). 2' 7'-Dichlorofluorescein diacetate (DCFDA) (Cat: D6883), 0.25% trypsin – EDTA (Cat: T3924), bovine collagen type 1 (Cat: C4243), bovine serum albumin (BSA) (Cat: A8022), dimethyl sulfoxide (DMSO) (Cat: 276855), fibronectin human plasma (Cat: F2006), glycine (Cat: G8898), paraformaldehyde (Cat: P6148), penicillin-streptomycin (Cat: P0781), phenazine methosulfate (PMS) (Cat: P9625), polyvinylepyriilodone (Cat: P0930), protease inhibitor cocktail (Cat: P8340), sodium dodecyl sulfate (SDS) (Cat: D6750), and triton X-100 (Cat: T8787) were purchased from Sigma-Aldrich (Oakville, ON, Canada). Cell Titer 96® AQueous MTS reagent powder (Cat: G1111) was purchased from Promega (Madison, WI, USA). Vectashield® containing 4′,6-diamidino-2-phenylindol (DAPI) (Cat: H-1200) was purchased from Vector Laboratories Inc. (Burlingame, CA, USA). Dulbecco’s phosphate-buffered saline (PBS) (Cat: 02-0119-1000) was purchased from VWR Life Sciences (Edmonton, AB, Canada). Precision Plus Protein™ Dual Color Marker (Cat: 161-0374) was purchased from Bio-Rad Laboratories Inc., Hercules, CA, USA). All the chemicals used in this study were of analytical grade and suitable for cell based-experiments.

3.2 Cell line and cell culture conditions

The normal bronchial epithelial cell line, BEAS-2B (ATCC® CRL-9609TM) was purchased from the American Tissue Type Culture Collection (Manassas, VA, USA). The BEAS-2B cells were cultured in the LHC-8 medium supplemented with 5% FBS, 100 U/mL penicillin, and 100 μg/mL streptomycin in T-75 polystyrene culture flasks (75 cm^2) at 37 ºC and 5% CO_2 in an incubator (VWR 3074, VWR International, LLC, Hampton, NH, USA) maintained at 100% humidity. Prior to use, culture flasks were coated with a mixture of fibronectin (0.01 mg/mL), BSA (0.01 mg/mL) and bovine collagen type 1 (0.03 mg/mL) in PBS overnight. Sub-culturing was performed before reaching 80% confluence. A cell culture flask with a monolayer of BEAS-2B cells was rinsed with PBS after aspirating the medium. Trypsin-EDTA solution consisting of 0.5% polyvinylpyrrolidone was added to the culture flask and incubated for 5 min at 37 ºC, 5% CO_2 until cells were detached from the flask. Detached cells were aspirated and transferred into a centrifuge tube after mixing cells with an additional volume of fresh LHC-8 medium in the flask. Then, a centrifuge tube containing cells was centrifuged at 1,000 × *g* for 5 min. The resultant cell pellet was resuspended in a fresh LHC-8 medium and cultured in a newly coated T-75 flask. Cells grown up to 80% confluence and cell passages between five and 25 were used in the experiments.

3.3 Evaluation of the protective effects of dietary antioxidants in the reduction of carcinogen-induced ROS generation in BEAS-2B cells

In this study, for the initial screening, we evaluated the dose-dependent efficacy of 8 subclasses of flavonoids (quercetin, epicatechin, naringenin, cyanidin chloride, cyanidin-3-*O*-glucoside, genistein, chrysin, luteolin, phloridzin dihydrate, phloretin, and

procyanidin B2) and metabolites of flavonoids (isorhamnetin, quercetin-3-*O*-glucuronic acid, protocatechuic acid, and phloroglucinaldehyde) in reducing NNKAc-induced ROS in BEAS-2B cells. In addition, dose-dependent effects of vitamins (ascorbic acid), The US Food and Drug Administration approved Nrf2 activator (DMF), curcuminoids (curcumin), stilbene (resveratrol), sulfur-containing compounds (sulforaphane), simple phenolics (catechol), phenolic acids (caffeic acid, chlorogenic acid, and methyl 4-hydroxybenzoate) and carotenoids (beta-carotene) on NNKAc-induced ROS were also studied.

3.3.1 Measurement of intracellular ROS

The ROS levels in the BEAS-2B cells were determined following treatments according to the method described by Wang and Joseph (1999) (308). Cells were seeded in black 96-well microplates at a density of 1×10^4 per well and incubated for 24 h at 37 ºC and 5% CO_2 in a humidified incubator (VWR 3074, VWR International, LLC, Hampton, NH, USA). Cells were pre-treated with six concentrations (0.1, 1, 5, 10, 25, and 50 µM) of selected compounds for 3 h. Pre-treated cells were exposed to 100 µM NNKAc for another 3 h to induce ROS generation. DMSO (0.1% or 0.4%) was used as the vehicle control. Subsequently, treatments were discarded, and cells were washed with PBS (× 1). Then, 100 µL of 5 µM 2' 7'-dichlorofluorescein diacetate (DCFDA) dissolved in DMEM media with no phenol red supplemented with 1% FBS and 100 U/mL penicillin, and 100 µg/mL streptomycin was added to each well and incubated for 30 min at 37 ºC and 5% CO_2 in a humidified incubator (VWR 3074, VWR International, LLC, Hampton, NH, USA). Following the treatments, the medium was discarded and washed three times with PBS (×1). After discarding PBS, fresh DMEM media with no phenol red was added to the wells, and the fluorescence intensity was measured at an excitation wavelength of 485 nm and an

emission wavelength of 535 nm using a microplate reader (Infinite® 200 PRO, Tecan Trading AG, Mannedorf, Switzerland).

3.4 Evaluation of the protective effects of selected dietary antioxidants in the reduction of carcinogen-induced DNA damage in cultured lung epithelial cells

The most effective tested compounds in section 3.3 for the reduction of NNKAc-induced ROS at concentrations equal to or lesser than 25 μM were selected to evaluate further their cytoprotective ability against NNKAc-induced DNA damage. The effects of seven flavonoids (quercetin, naringenin, cyanidin chloride, genistein, chrysin, luteolin, and procyanidin B2), DMF, curcumin, resveratrol, catechol, and sulforaphane were tested for BEAS-2B cell viability using MTS assay and DNA protective effects using *γ*-H2AX immunofluorescence assay, comet assay, and DNA fragmentation enzyme-linked immunosorbent assay (ELISA).

3.4.1 Cell viability by Cell Titer 96^{TM} cell viability assay

The cell viability of BEAS-2B was determined using the Cell Titer 96^{TM} cell viability assay (MTS), as described by Wang *et al.,* 2010. (309). Cells were seeded in a clear flat-bottom 96-well microplate at a density of 1×10^4 cells per well and incubated for 24 h overnight at 37 ºC and 5% CO_2 in a humidified incubator (VWR 3074, VWR International, LLC, Hampton, NH, USA). After 24 h, cells were pre-treated with 5 concentrations (0.1, 1, 5, 10, and 25 μM) of selected compounds for 3 h. To induce ROS generation, pre-treated cells were exposed to 100 μm NNKAc for another 3 hours. DMSO (0.1% or 0.4%) was used as the vehicle control. Blanks for the experiment were conducted without cells but with tested treatment. Following treatments, the MTS reagent with PMS (20:1) was added

to each well (15 µL/well) and incubated for 3 hours in the dark. Absorbance was measured at 490 nm using a microplate reader (Infinite® 200 PRO, Tecan Trading AG, Mannedorf, Switzerland). Results were expressed in terms of percentage cell viability using the following formula, A is the absorbance of the treated cells, B is the absorbance of medium control with cells, C is the absorbance of the blank of treated compounds, and D is the absorbance of medium without cells.

$$\text{Percentage reduction of cell number} = \left(\frac{A-C}{B-D}\right) \times 100$$

3.4.2 *γ*-H2AX immunofluorescence assay

DNA damage at histone levels was measured using the immunofluorescence assay previously described by Ivashkevich *et al*., 2012 (310) by quantifying *γ*-H2AX foci in BEAS-2B cells. Initially, 1×10^5 cells per well were seeded on a sterilized coated coverslip placed in a clear flat-bottom 6-well plate followed by a 24-hour incubation. After 24 h, cells were treated with selected test compounds and NNKAc as explained before (section 3.4.1). Following treatments, cells were thoroughly washed (3 times) with PBS (×1) and fixed with 3.7% paraformaldehyde for 20 min in the dark. Then, cells were washed three times with PBS (×1) for 5 min on a shaker and permeabilized with 0.5% Triton X-100 in PBS (×1) for another 15 min at room temperature. Then, Triton X-100 was removed, and cells were washed three times with PBS for 5 min. A filter paper wetted with distilled water was placed at the bottom of a 15 cm petri-dish to set up a humidifying chamber. After setting up the chamber, a parafilm sheet was placed on the wet filter paper inside the humidifying chamber. Blocking was performed by transferring coverslips with cells onto drops of 4% BSA (50 µL) on the parafilm sheet for 20 min at room temperature. After

blocking, coverslips were placed on 50 µL of anti-phospho-histone H2AX, the primary antibody dissolved in 4% BSA (1:250 ratio) and incubated for 1 h at room temperature. Subsequently, coverslips were transferred back to 6-well plates and washed three times with PBS for 5 min. Coverslips were then placed on 50 µL of secondary antibody (Alexa fluorophore® 594 donkey anti-mouse) dissolved in 4% BSA (1: 500 ratio) and incubated for another 45 min at room temperature in the dark. Once excessive secondary antibodies on coverslips were washed three times with PBS (×1) for 5 min, excessive PBS was blotted thoroughly from the coverslips. Then, wet mounting of coverslips onto glass slides was performed using Vectashield® containing 4′,6-diamidino-2-phenylindol (DAPI), the wet-mounting medium. Coverslips were sealed with clear nail polish and dried in the dark at room temperature. Images of slides were taken using a fluorescence microscope (EVOSTM FLoid Imaging System, Bothell, WA, USA) at 100× magnification. The number of phosphorylated histone-H2AX foci was quantified for at least 50 nuclei per treatment using "Find maxima" option at prominence greater than 7 available in ImageJ software (Version 1.53k, National Institute of Mental Health, Bethesda, MD, USA).

3.4.3 Comet assay

The DNA damage in BEAS-2B cells was determined by single-cell gel electrophoresis assay using the Comet SCGE assay kit (Cat: ADI-900-166, Enzo, New York, NY, USA). Initially, 1×10^5 cells per well were seeded in a clear flat-bottom 6-well plate followed by a 24 h incubation. After 24 h, cells were treated with selected compounds and NNKAc as explained before (section 3.4.1). Following treatments, cells were harvested and centrifuged at 1000 × *g* for 5 min. The cell pellet was suspended in 1 mL of ice-cold PBS (×1) after carefully washing it with ice-cold PBS (×1). Low melting point agarose (LMA)

were melted using boiling water and cooled down to 37 ºC in a water bath. The molten LMA agarose was mixed with 1×10^5 cells in 1 mL PBS at a ratio of 10: 1 by volume. Thirty microliters of each sample were inserted into a well in a 20-well comet slide (Cat: 4252-500-01, R & D Systems, Minneapolis, MN, USA) immediately. The sample was spread to form a thin layer on the comet slide and was kept at 4 ºC under dark conditions for 20 min to solidify. The cold lysis buffer was used to immerse the slides for 45 min at 4 ºC. The slides were then subjected to an alkaline treatment (pH> 13) consisting of 300 mM NaOH and 1 mM EDTA and incubated for 45 min in the dark at room temperature. The slides were washed once with 1× TBE buffer for 5 min and subjected to horizontal electrophoresis conditions of 1 V/cm for 11 min in 1× TBE buffer. Following electrophoresis, slides were immersed in ethanol (70%) for 5 min and air-dried. Slides were stained with CYGREEN® dye in a ratio of 1: 1000 and imaged using fluorescence microscopy (EVOSTM FLoid Imaging System; Bothell, WA, USA) at 100× magnification. The OpenComet plugin in ImageJ software (Version 1.53k, National Institute of Mental Health, Bethesda, MD, USA) was used to calculate the tail moment of the DNA. A minimum of 30 cells were quantified for each treatment.

3.4.4 DNA fragmentation analysis

Cellular DNA fragmentation ELISA kit (Ref # 11585045001, Roche Diagnostics, Mannheim, Berlin, Germany) (311) was used to determine the DNA fragmentation in BEAS-2B cells. Initially, 1×10^5 cells/mL were labeled with bromodeoxyuridine (BrdU) (10 μM) in the culture medium for 2 h in a humidified incubator (VWR 3074, VWR International, LLC, Hampton, NH, USA) at 37 ºC and 5% CO_2. BrdU labeled cells in the culture medium were centrifuged at 1000 × *g* for 5 min, and the cell pellet was suspended

in a fresh culture medium. The cells were seeded in a clear flat-bottom 96-well microplate at a density of 1×10^4 cells per well and incubated for 24 h. After 24 h, cells were treated as mentioned before (section 3.4.1). Treated cells were centrifuged at 1000 × *g* for 5 min, and supernatants were carefully and thoroughly removed. The cells were treated with incubation buffer (200 µL/well) and incubated for 30 min at room temperature. Then, the microplate containing cells was centrifuged at 1000 × *g* for 5 min, and 100 µL of supernatants from each treatment were collected. A clear flat-bottom 96-well microplate was coated with the coating solution containing anti-DNA (100 µL/well) and incubated for 1 h in an incubator (VWR 3074, VWR International, LLC, Hampton, NH, USA) at 37 ºC. After 1 h, the anti-DNA coating solution was removed, and the microplate was incubated for another 30 min at room temperature with the incubation buffer. The incubation buffer was then removed, and the anti-DNA coated plate was washed three times with the washing solution (200 µL/well) for 3 min using a shaker. Then, 100 µL of supernatants from each treatment were transferred to anti-DNA coated microplates and incubated overnight at 4 ºC. The supernatants were then removed, and wells were washed thrice for 3 min using washing buffer. Next, the microplate with 200 µL of washing buffer per well was subjected to microwave irradiation at 500 W for 5 min. Once the microplate was cooled down to room temperature, the anti-BrdU-peroxidase (POD) conjugate solution (100 µL/well) was added and incubated for 90 min at room temperature. Then, the microplate was washed thrice using washing buffer for 3 min followed by the addition of 100 µL substrate solution. The microplate was incubated for 5 min in the dark on a shaker for color development, and the stop solution (concentrated sulfuric acid) (25 µL/well) was added. After that, the microplate was incubated for another 1 min on the shaker, and the absorbance was recorded

using a microplate reader (Infinite® 200 PRO, Tecan Trading AG, Mannedorf, Switzerland) at a wavelength of 450 nm.

3.5 Effects of quercetin, genistein, and procyanidin B2 on Nrf2/ARE pathway in BEAS-2B cells

Among tested compounds in section 3.3, three flavonoids (quercetin, genistein, and procyanidin B2) were effective at low concentrations (0.1-1 μM) in reducing NNKAc-induced DNA damage and were further studied for their potential mechanisms of activation of Nrf2/ARE pathway.

3.4.2 Effect of quercetin, genistein, and procyanidin B2 on Akt and Nrf2 phosphorylation in BEAS-2B cells

Western blot analysis was performed to study the effect of quercetin, genistein, and procyanidin B2 on phosphorylation of Akt and Nrf2 as described by George and Rupasinghe, 2017 (1). The expression of phospho-Akt (p-Akt), total Akt, phospho-Nrf2 (p-Nrf2), and total Nrf2 proteins at cellular levels were measured, and β-actin was used to normalize the protein expressions.

Initially, 1×10^6 BEAS-2B cells were seeded in T-75 polystyrene culture flasks (75 cm^2) and incubated for 24 h in an incubator (VWR 3074, VWR International, LLC, Hampton, NH, USA). After 24 h, cells were pre-treated with two concentrations (1 and 25 μM) of quercetin, genistein, and procyanidin B2 for 3 h. Pre-treated cells were then challenged with 100 μM NNKAc for another 3 h. The cells treated with 25 μM DMF, and 10 μM hydrogen peroxide for 3 h were used as positive controls, and 0.1% DMSO was used as the vehicle control. Following the treatments, TrypLE^{TM} Express solution was used to harvest cells and centrifuged at $1000 \times g$ for 5 min to obtain the cell pellet. One milliliter

of cold PBS (×1) was used to wash the cell pellet and centrifuged in a micro-centrifuge (Legend MICRO 21R, Cat: 75002446, Thermo Fisher Scientific, Osterode, Germany) at 4 ºC for 5 min at 1000 × *g* followed by careful and thorough removal of PBS from the cell pellet. For cell lysis, 50 µL of a mixture of radio-immunoprecipitation assay (RIPA) buffer (0.1% sodium dodecyl sulfate [SDS], 5 mM EDTA, 25 mM Tris-HCl [pH-7.6], 1% Triton X-100, 1 % sodium deoxycholate, and 150 mM NaCl) and protease inhibitor cocktail mixed at a ratio of 10:1 was added to the cell pellet. The cell pellet was incubated for 30 min on ice followed by centrifugation at 12,000 × *g* for 20 min at 4 ºC using a micro-centrifuge (Legend MICRO 21R, Cat: 75002446, Thermo Fisher Scientific, Osterode, Germany). After centrifugation, supernatants were carefully collected without disturbing the pellets of cell debris.

Pierce™ Coomassie (Bradford) protein assay kit (Cat: 23200, Thermo Fisher Scientific, Rockford, IL, USA) was used to estimate the protein content in extracted proteins samples. BSA was used as the standard compound for protein estimation in cell extracts. A stock solution of 5 mg/mL BSA was used to prepare a solution of 0, 0.078125, 0.15625, 0.3125, 0.625, 1.25, and 2.5 mg/mL to generate the standard solution series. A volume of 10 µL from BSA solutions and protein extracts (5× diluted) was mixed with 2 mL of Coomassie blue solution and incubated for 30 min at room temperature. A volume of 200 µL from each sample was pipetted to a clear flat-bottom 96-well plate, and the absorbance was recorded at 595 nm in a microplate reader (Infinite® 200 PRO, Tecan Trading AG, Mannedorf, Switzerland). Protein content was estimated using the BSA standard curve.

Blue protein loading dye kit (Cat: B7703S, New England BioLabs™ Inc., Ipswich, MA, USA) was used to denature the extracted proteins as suggested by the manufacturer. Briefly, fresh 3× reducing blue protein loading dye was prepared by mixing 3× blue protein loading dye and 30× reducing agent at a 1:10 ratio. Protein extracts were then mixed with freshly prepared 3× reducing blue protein loading dye at a ratio of 2:1 and heated for 5 min at 96 ºC in a heat block. Denatured protein samples were further diluted with a mixture of RIPA buffer and 3× reducing blue protein loading dye (2:1 ratio) to obtain a similar protein concentration in each sample.

SDS-PAGE gel electrophoresis was performed using BIO-RAD Mini PROTEAN® Tetra Cell and Bio-Rad PowerPac™ Universal Power Supply (Cat: 1658026, Bio-Rad Laboratories, Inc. Hercules, CA, USA). Polyacrylamide gels containing 10% polyacrylamide in the separating component (375 mM Tris (pH 8.8), 0.1 % SDS, 0.05% ammonium persulfate, and 0.05% tetramethyl ethylenediamine) and 4% polyacrylamide in the stacking component (125 mM Tris [pH 6.8], 0.1% SDS, 0.05% ammonium persulfate, and 0.05% tetramethyl ethylenediamine) were set with the running module of BIO-RAD Mini PROTEAN® Tetra Cell unit. The running module was then filled with 1× SDS running buffer (25 mM tris base. 192 mM glycine, and 0.1 % SDS) before loading 7 µL of Precision Plus Protein™ Dual Color Marker and protein extracts containing 20 µg of proteins. SDS-PAGE gel electrophoresis was performed for 1.5 h at 80 V. Proteins separated in SDS-PAGE gels were electro-transferred onto a polyvinylidene difluoride (PVDF) membrane (Cat: 88518, Thermo Fisher Scientific, Rockford, IL, USA) using a Trans-Blot® Turbo™ Transfer System (Cat: 1704150, Bio-Rad Laboratories, Inc. Hercules, CA, USA). PVDF membranes were immersed in 100% methanol for 5-10

seconds for activation. Then, both PVDF membranes and thick blotting papers (Cat: 1703966, Bio-Rad Laboratories Inc., Hercules, CA, USA) were equilibrated in transfer buffer (pH-8.3, 25 mM tris, 192 mM glycine, and 20% methanol) by immersing and gently rocking membranes for 20 min in the transfer buffer. The trans-blot sandwich was set in the Trans-Blot® Turbo™ Transfer System by placing an SDS-PAGE gel on a PVDF membrane placed on a thick blotting paper followed by placing another thick blotting paper on the polyacrylamide gel. Electro-transfer of proteins from gels to PVDF membrane was carried out at 1 A and 20 V for 30 min.

Electro-transferred PVDF membranes were then blocked with commercially available 5% non-fat milk in 1× Tris-buffered saline (20 mM Tris-HCl, pH 7.6, 200 mM NaCl) containing 0.1% tween 20 (TBST) for 1 h at room temperature with gentle shaking on a rocker. Blocked PVDF membrane was probed overnight with gentle shaking at 4 ºC with specific primary antibodies dissolved in 5% BSA in TBST. Anti-phospho-Akt (Ser473), anti-Akt, and anti-Nrf2 rabbit primary antibodies were dissolved in 5% BSA in TBST at a ratio of 1:1000, and anti-phospo-Nrf2 (Ser40) rabbit antibody was dissolved in 5% BSA in TBST at a ratio of 1:5000. Following probing for primary antibodies, membranes were washed three times with TBST for 5 min and re-probed with the HRP-linked anti-rabbit secondary antibodies (1:2000) for 1 h with gentle shaking on a rocker. For β-actin, HRP conjugated anti-β-actin rabbit antibody was probed overnight. Probed PVDF membranes were then washed three times with TBST for 5 min.

Clarity™ and Clarity Max™ Western ECL Substrates Kit (Cat: 1705060, Bio-Rad Laboratories Inc., Hercules, CA, USA) was used to develop the membranes for imaging using BIO-RAD Chemidoc MP™ imaging system (Universal hood III, Bio-Rad

Laboratories Inc., Hercules, CA, USA). Clarity™ Western ECL substrate solutions, peroxide solution, and luminol/enhancer solution were mixed at a ratio of 1:1 before adding to the membranes. After incubating the membrane for 5 min, membranes were imaged in signal accumulation mode. The membranes probed to study p-Akt and p-Nrf2 were used to probe their respective total protein antibodies after stripping off the anti-bodies from the membrane. The membrane was washed three times for 20 min with TBST after imaging and incubated with stripping buffer (pH-2.2) containing 1.5% glycine, 0.1% SDS, 1% Tween 20 for 10 min. After incubation, stripping buffer was discarded, and the membrane was washed twice with TBST solution for 10 min. Incubation with stripping buffer was continued for another two more rounds, followed by the washing with TBST two times for 10 min. The stripped membranes were re-probed for the total protein contents, as mentioned before. Images were analyzed for band intensity using Image Lab™ software (Version 6.0.1, Bio-Rad Laboratories Inc., Hercules, CA, USA). Protein expression of each band was normalized to their respective β-actin band intensity. Results were expressed as the phosphorylated protein expression: total protein expression relative to the control.

3.5.2 Effect of quercetin, genistein, and procyanidin B2 on nuclear translocation of p-Nrf2 in BEAS-2B cells

The effect of quercetin, genistein, and procyanidin B2 on p-Nrf2 nuclear translocation was evaluated using an immunofluorescence assay. The immunofluorescence assay protocol identified in section 3.3.5 was followed to study the level of p-Nrf2 nuclear translocation with minor modifications. Cells were treated as mentioned in the 3.4.1 section. Anti-phospho-Nrf2 (Ser40) was used as the primary antibody at a ratio of 1:200 in 4% BSA, and Alexa Flour™ 488 goat anti-rabbit secondary antibody was used at a ratio

of 1:500 in 4% BSA. Images of slides were taken using a fluorescence microscope (EVOSTM FLoid Imaging System, Bothell, WA, USA) at 100× magnification. The corrected total nuclear fluorescence (CTNF) values of at least 30 nuclei per treatment were measured using ImageJ software (Version 1.53k, National Institute of Mental Health, Bethesda, MD, USA). CTNF values were calculated using the following formula, A is the area of the selected nucleus while MC is the mean fluorescence value of the cell, and MB is the mean fluorescence value of the background.

Corrected total nuclear fluorescence value (CTNF) $= (\mathrm{A} \times \mathrm{MC}) - (\mathrm{A} * \mathrm{MB})$

3.5.3 Effect of quercetin, genistein, and procyanidin B2 on antioxidant enzyme activity in BEAS-2B cells

Antioxidant enzyme activities were evaluated in terms of superoxide dismutase (SOD), catalase, and glutathione peroxidase (GPx) activities in BEAS-2B cells. Initially, 1 × 10^6 and 2 × 10^6 BEAS-2B cells were seeded in T-75 polystyrene culture flasks (75 cm^2) and incubated for 24 h in an incubator (VWR 3074, VWR International, LLC, Hampton, NH, USA) for catalase and SOD activity assays, respectively. For the GPx assay, 2 × 10^5 cells were seeded in clear flat bottom 6-well plates. After 24 h, cells were treated as described earlier (Section 3.4.1). TrypLE^{TM} Express solution was used to harvest cells and centrifuged at 1000 × *g* for 5 min to obtain the cell pellet. One milliliter of cold PBS (1 ×) was used to wash the cell pellet and centrifuged in a micro-centrifuge (Legend MICRO 21R, Cat: 75002446, Thermo Fisher Scientific, Osterode, Germany) for 5 min at 1000 × *g* at 4 ºC followed by careful and thorough removal of PBS from the cell pellet. The cell pellets were kept on ice.

3.5.3.1 Superoxide dismutase activity

Superoxide dismutase (SOD) activity assay kit (Cat: ab65354, Abcam Inc, Toronto, ON, Canada) was used to determine the SOD activity in BEAS-2B cells. After harvesting cells, the cells pellet was resuspended and homogenized in ice-cold 0.1 M Tris-HCL lysis buffer (pH 7.4, 0.5% Triton X-100, 5 mM 2-mercaptoethanol, and 0.1 mg/mL phenylmethylsulfonyl fluoride protease inhibitor). The lysis buffer containing cells was then centrifuged for 5 min at 4 ºC in a micro-centrifuge (Legend MICRO 21R, Cat: 75002446, Thermo Fisher Scientific, Osterode, Germany) at 14,000 × *g*. After micro-centrifugation, supernatants containing proteins in lysis buffer were carefully collected without disturbing the pellets of cell debris and kept on ice while using. A clear flat-bottom 96-well plate was used to perform the assay. Reaction wells consisted of three types of blanks in addition to the sample wells. Blank 1 and blank 3 were loaded with 20 µL of deionized water, whereas both blank 2 and sample wells were loaded with 20 µL of extracted proteins in lysis buffer. Then, 200 µL of WST solution provided with the kit was added to each well, followed by the addition of 20 µL of dilution buffer to blanks 2 and 3. Twenty microliters of SOD enzyme solution were then added to sample wells and blank 1 well. The reaction mixtures were incubated for 20 min at 37 ºC. The absorbance was recorded at 450 nm using a microplate reader Infinite® 200 PRO, Tecan Trading AG, Mannedorf, Switzerland). SOD activity in terms of percentage inhibition rate was calculated using the following formulae, whereas Ab1, Ab2, Ab3, and As are the absorbance values of blank 1, blank 2, blank 3, and samples, respectively.

$$\text{SOD activity (\% inhibition rate)} = \left(\frac{(Ab1 - Ab3) - (As - Ab2)}{(Ab1 - Ab3)}\right) \times 100$$

3.5.3.2 Catalase activity

The catalase activity assay kit (Cat: ab83464, Abcam Inc, Toronto, ON, Canada) was used to determine the catalase activity in BEAS-2B cells. After harvesting cells, the cell pellet was resuspended and homogenized in the ice-cold catalase assay buffer provided with the kit. The mixture was then centrifuged for 15 min at 4 ºC in a micro-centrifuge (Legend MICRO 21R, Cat: 75002446, Thermo Fisher Scientific, Osterode, Germany) at 10,000 × *g.* After centrifugation, supernatants containing proteins in catalase assay buffer were carefully collected without disturbing the pellets of cell debris and kept on ice while using. Hydrogen peroxide was used as the standard compound to determine the catalase activity. A stock solution of 20 mM hydrogen peroxide was used to prepare solutions of 0, 2, 4, 6, 8, and 10 nmol/well to generate the standard solution series. A clear flat-bottom 96-well plate was used to load the samples, whereas 90 µL/well of standard solutions and 5 µL/well of protein extracts were loaded to sample wells (catalases active sample wells) and sample high control wells (samples that were inhibited for catalase activity). The volumes of sample wells and sample high control wells were then adjusted to 78 µL/well with catalase assay buffer. The stop solution (10 µL/well) was added to both hydrogen peroxide standard wells and sample high control wells and incubated at room temperature for 5 min to inhibit the catalase activity. Fresh 1 mM hydrogen peroxide (12 µL/well) was added to sample wells and sample high control wells and incubated for 30 min at room temperature. After incubation, 10 µL/well of stop solution was added to each sample well. Then, a volume of 50 µL/well of the developer mix containing HRP solution, OxiRed probe, and catalase assay buffer at a ratio of 1:1:23 was added to each well and incubated for 10 min at room temperature. The absorbance was recorded at 570 nm using a microplate reader

(Infinite® 200 PRO, Tecan Trading AG, Mannedorf, Switzerland). The standard curve was used to calculate the reacted hydrogen peroxide amount in the sample using the absorbance values obtained by subtracting the absorbance of sample wells from the sample high control wells. One unit of catalase activity represents the amount of catalases that decomposes 1 µM of hydrogen peroxide per min at room temperature at pH 4.5. The catalase activity (mU/mL) of samples was calculated using the following formula, whereas B is the amount of hydrogen peroxide in the sample well calculated from the standard curve (nmol), 30 is the catalase reaction time (min), V is the sample volume added into the reaction volume (mL), and D is the dilution factor.

$$\text{Catalase activity} = \left(\frac{\text{B}}{30 \times \text{V}}\right) \times \text{D}$$

3.5.3.3 Glutathione peroxidase activity

Glutathione peroxidase (GPx) activity assay kit (Cat: ab219926, Abcam Inc, Toronto, ON, Canada) was used to determine the GPx activity in BEAS-2B cells. After harvesting cells, the cell pellet was resuspended and homogenized in ice-cold 0.1 M Tris-HCL lysis buffer (pH 7.4, 0.5% Triton X-100, 5 mM 2-mercaptoethanol, and 0.1 mg/mL phenylmethylsulfonyl fluoride protease inhibitor). The lysis buffer containing cells was then centrifuged for 5 min at 4 ºC in a micro-centrifuge (Legend MICRO 21R, Cat: 75002446, Thermo Fisher Scientific, Osterode, Germany) at 13,000 × *g*. After centrifugation, supernatants containing proteins in lysis buffer were carefully collected without disturbing the pellets of cell debris and kept on ice while using.

GPx enzyme was used as the standard compound to determine the GPx activity. A stock solution of 10 U/mL GPx was used to prepare solutions of 0, 0.625, 1.25, 2.5, 5, 10,

20, and 40 mU/mL to generate the standard solution series. A black clear flat-bottom 96-well plate was used to perform the assay, and 50 µL of PBS and 50 µL standard solutions were added to blank control wells and standard wells, respectively. The sample wells were loaded with 2 µL of extracted protein samples and adjusted the volumes of sample wells with PBS up to 50 µL. Then, 50 µL of GPx assay mixture containing 100× GSH stock solution and enzyme mix solution at a ratio of 1:1 was added to each well. The reaction mixture was then incubated for 30 min in the dark at room temperature. After incubation, 20 µL of NADP sensor probe in PBS (1:20 ratio) and 20 µL of NADP assay solution were added to each well. The reaction mixture was incubated for 10 min in the dark at room temperature. After 10 min, 15 µL of enhancer solution was added to the reaction volume, and fluorescence increase was measured at an excitation wavelength of 420 nm and an emission wavelength of 480 nm using a microplate reader (Infinite® 200 PRO, Tecan Trading AG, Mannedorf, Switzerland) in kinetic mode for every 2 min, for at least 30 min. The reaction rate (ΔRFU) was calculated as follows, whereas T1 and T2 are the chosen time points in minutes in the linear phase of the reaction progress curve. RFU1 and RFU2 values are fluorescence values of the sample at T1 and T2 time points, and RFUb1 and RFUb2 are the fluorescence values of blanks at T1 and T2 time points.

$$\Delta\mathrm{RFU} = [\frac{(\mathrm{RFU2} - \mathrm{RFUb2}) - (\mathrm{RFU1} - \mathrm{RFUb1})}{(\mathrm{T2} - \mathrm{T1})}]$$

GPx activity (mU/mL) of the original samples was then calculated using the following equation, whereas B is the GPx activity in sample wells calculated using ΔRFU and GPx standard curve, Vw is the total volume of the well after reaction, Vs is the original sample volume added to the reaction mixture, and D is the dilution factor.

$$\text{GPx activity} = \text{B} \times (\frac{\text{Vw}}{\text{Vs}}) \times \text{D}$$

3.6 Experimental design and statistical analysis

A complete randomized design was used for all experiments. Results were presented as mean values with standard deviation (± SD) relative to medium control. Analysis of variance was performed using one-way analysis of variance (ANOVA), and mean comparison was performed using Tukey's multiple mean comparisons at $p < 0.05$ using Minitab 19 statistical software. Screening of polyphenols for the effects on NNKAc-induced ROS was performed in triplicates and independently, two times. MTS assay, DNA fragmentation ELISA, catalase activity, GPx activity, and SOD activity assays were performed in duplicates and independently three times. All other experiments were performed in triplicates and independently, at least three times.

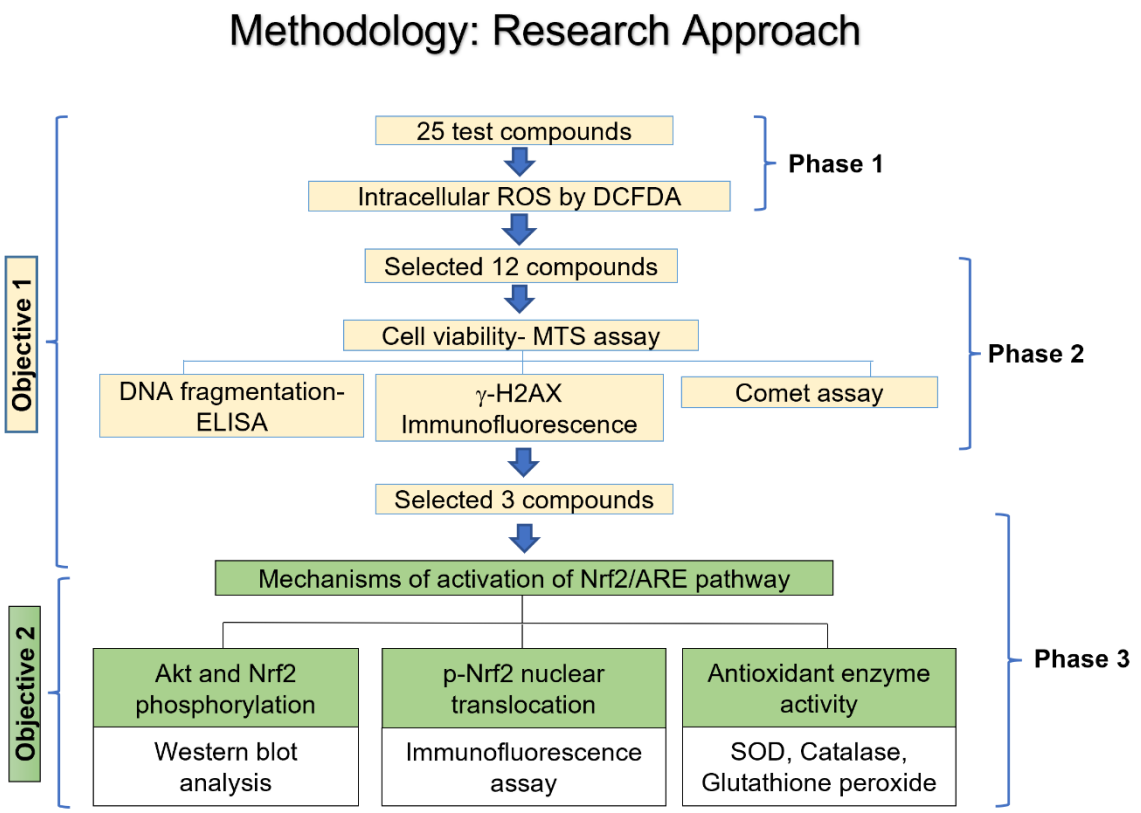

Figure 5: Research methodology that was followed in this thesis

This investigation was carried out in three major phases. In phase 1, 25 dietary antioxidants representing selected flavonoids, flavonoid metabolites, phenolic acids, simple polyphenols, stilbenes, curcuminoids, and non-phenolics were investigated for their efficacy against NNKAc-induced ROS generation in cultured BEAS-2B cells. Among these 25 compounds, compounds that reduced NNKAc-induced ROS in BEAS-2B cells at concentrations equal to or less than 25 µM were selected for phase 2. In phase 2, 12 most efficacious antioxidant compounds were further investigated for their cytotoxicity and prevention of DNA damage induced by the NNKAc challenge. In phase 3, the three most efficacious antioxidant compounds at low concentrations that reduced NNKAc-induced ROS and DNA damage in BEAS-2B cells were further investigated for their possible mechanisms of activation of the Nrf2/ARE pathway.

Abbreviations: Akt: protein kinase B, DCFDA: 2' 7'-dichlorofluorescein diacetate, ELISA: enzyme-linked immunosorbent assay), Nrf2/ARE: Nuclear factor erythroid 2 p45 (NF-E2)-related factor/ antioxidant response element, SOD: superoxide dismutase

CHAPTER 4: RESULTS

4.1 Effects of dietary antioxidants in the reduction of NNKAc-induced ROS generation in BEAS-2B cells

The dose-dependent effects (0.1, 1, 5, 10, 25, and 50 μM) of selected 25 dietary antioxidants on NNKAc-induced intracellular ROS generation in BEAS-2B cells were studied using the DCFDA assay. NNKAc-treated BEAS-2B cells showed significantly increased ($p < 0.05$) ROS levels by 20-30% compared to DMSO control. BEAS-2B cells treated with different concentrations (0.1-50 μM) of dietary antioxidants alone did not influence ROS level ($p > 0.05$) when compared to the DMSO control. Among tested flavonoids, pre-exposure of BEAS-2B cells to 3-hydroxy flavonoids (Figure 6) such as quercetin (5-50 μM), cyanidin (25-50 μM), and procyanidin B2 (0.1-50 μM) and 3-deoxy flavonoids (Figure 7) such as luteolin (5-50 μM), chrysin (10-50 μM), naringenin (25-50 μM), and genistein (1-50 μM) depicted significant reductions ($p < 0.05$) in NNKAc-induced ROS levels. However, epicatechin, C3G, phloretin, and phloridzin did not prevent NNKAc-induced ROS generation. Among the tested flavonoid metabolites, isorhamnetin at 50 μM, significantly reduced ($p < 0.05$) ROS levels induced by NNKAc in BEAS-2B cells (Figure 8). BEAS-2B cells pretreated with curcumin (5-50 μM), resveratrol (10-50 μM), and catechol (25-50 μM) showed significantly reduced ($p < 0.05$) ROS levels in NNKAc-treated cells (Figure 9). However, BEAS-2B cells pretreated with phenolic acids (i.e., caffeic acid, chlorogenic acid, and methyl 4-hydroxybenzoate) did not reduce ($p > 0.05$) NNKAc-induced ROS levels (Figure 9). Furthermore, pretreated BEAS-2B cells with non-phenolic compounds (Figure 10) such as ascorbic acid (50 μM), sulforaphane (5-50 μM), and dimethyl fumarate (25-50 μM) also showed significant reductions ($p < 0.05$)

in NNKAc-induced ROS levels at different concentrations. However, pre-exposure with beta-carotene was not effective in the reduction ($p > 0.05$) of NNKAc-induced ROS in BEAS-2B cells (Figure 5).

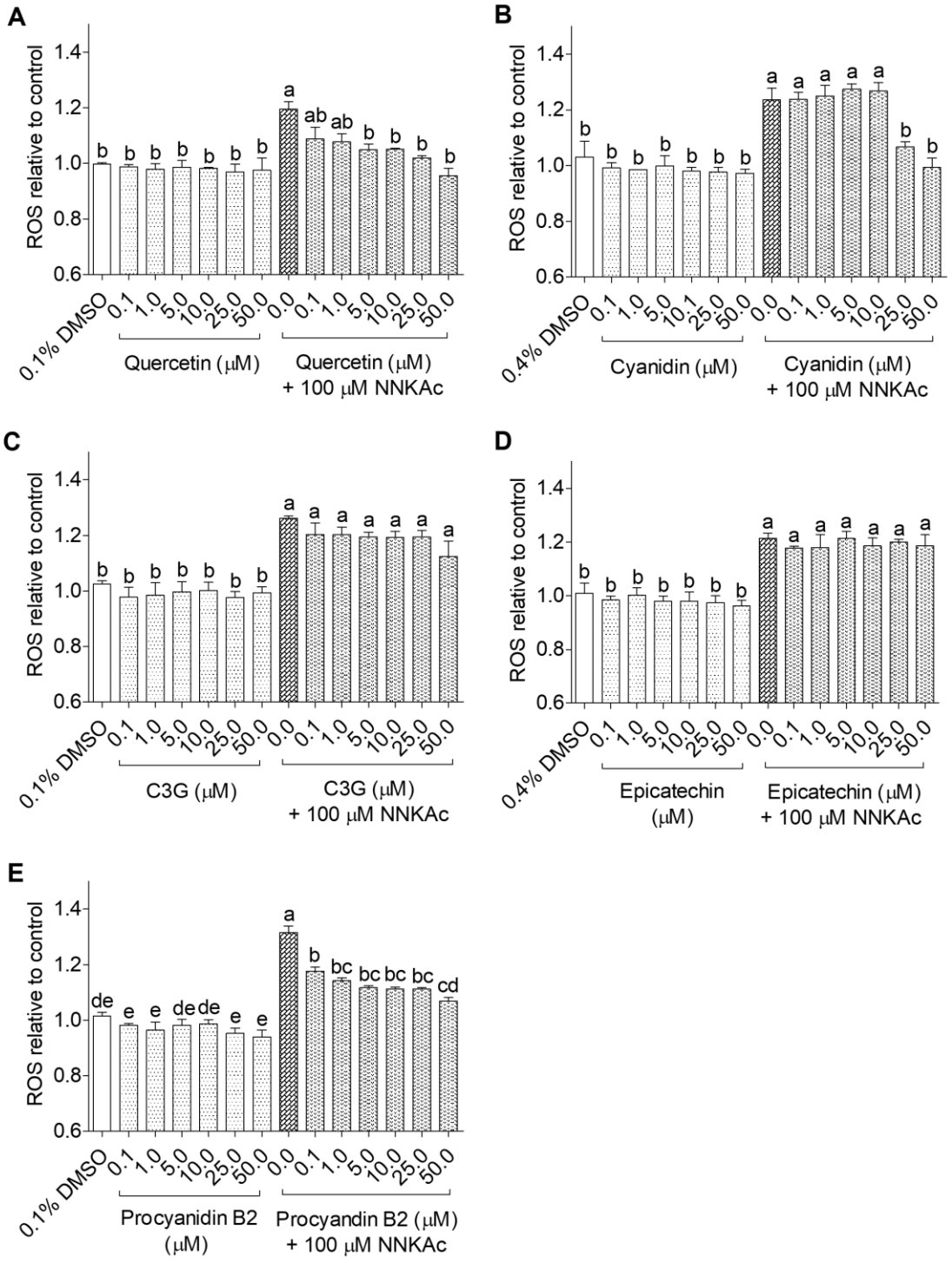

Figure 6: Effect of quercetin (A), cyanidin (B), cyanidin-3-*O*-glucoside (C), epicatechin (D), and procyanidin B2 (E) on reducing NNKAc-induced ROS in BEAS-2B cells

Cells were pre-treated with concentrations ranging from 0.1- 50 µM of 3-hydroxy flavonoids for 3 h. Pre-treated cells were exposed to 100 µM NNKAc for another 3 h to induce ROS generation. DMSO (0.1 or 0.4%) was used as the vehicle control. Effects on ROS levels were quantified using DCFDA fluorescence assay. Two independent studies (each done in triplicates) were performed, and results were expressed as mean ± standard deviation. Statistical analysis of data was performed by one-way ANOVA and mean comparison was done by Tukey's mean comparison method (α=0.05) using Minitab 19 statistical software. Mean values that do not share similar letters (i.e., a-e) in bar graphs are significantly different ($p<0.05$). Abbreviations: NNKAc: 4-[(acetoxymethyl)nitrosamino]-1-(3-pyridyl)-1-butanone, ROS: reactive oxygen species, DCFDA: 2' 7'-dichlorofluorescein diacetate, DMSO: dimethylsulfoxide, C3G: cyanidin-3-O-glucoside.

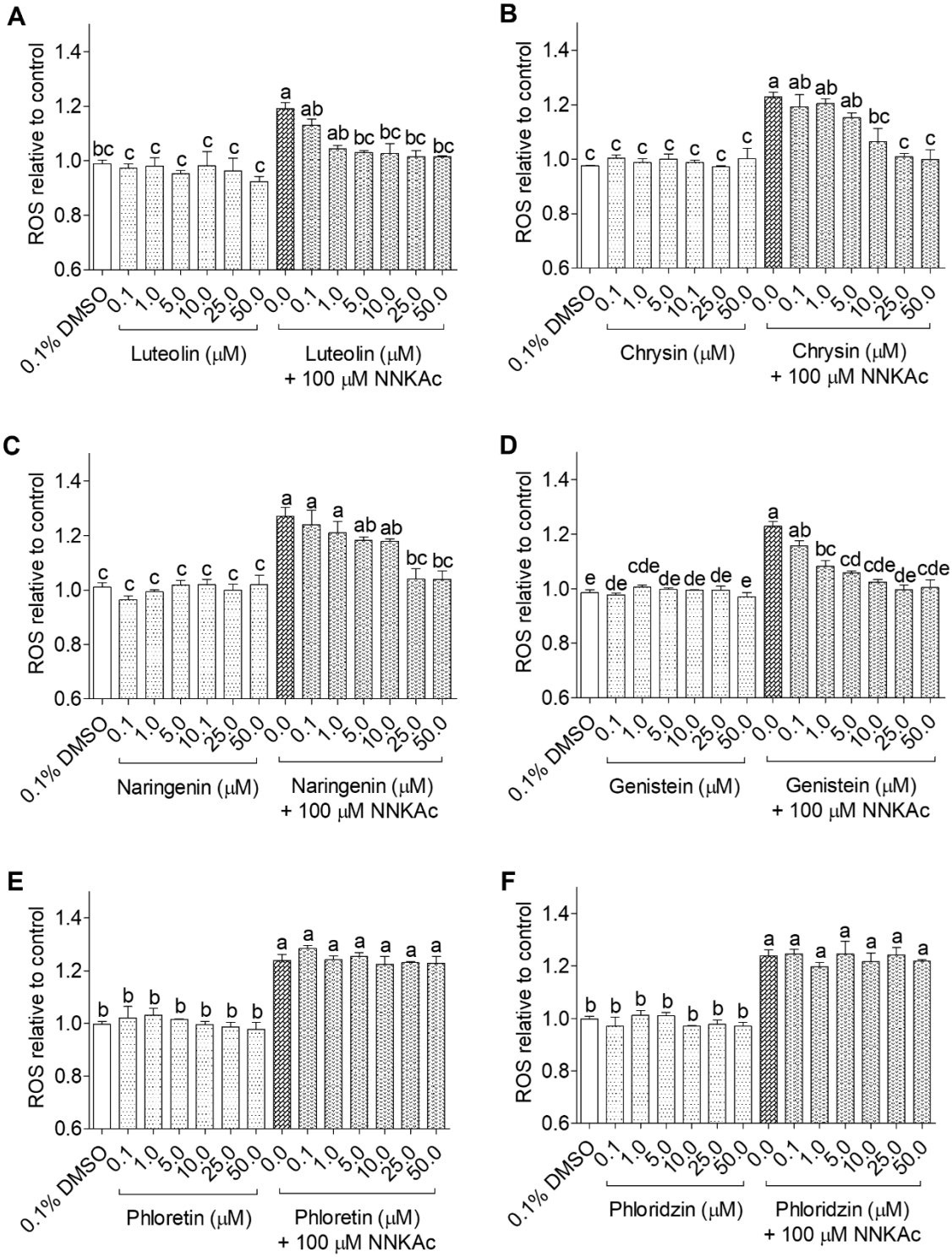

Figure 7: Effect of luteolin (A), chrysin (B), naringenin (C), genistein (D), phloretin (E), and phloridzin on reducing NNKAc-induced ROS in BEAS-2B cells

Cells were pre-treated with concentrations ranging from 0.1- 50 µM of selected 3-deoxy flavonoids and chalcones for 3 h. Pre-treated cells were exposed to 100 µM NNKAc for another 3 h to induce ROS generation. DMSO (0.1%) was used as the vehicle control. Effects on ROS levels were quantified using DCFDA fluorescence assay. Two independent studies (each done in triplicates) were performed, and results were expressed as mean ± standard deviation. Statistical analysis of data was performed by one-way ANOVA and mean comparison was done by Tukey's mean comparison method (α=0.05) using Minitab 19 statistical software. Mean values letters that do not share similar letters (i.e., a-e) in bar graphs are significantly different ($p<0.05$). Abbreviations: NNKAc: 4-[(acetoxymethyl)nitrosamino]-1-(3-pyridyl)-1-butanone, DCFDA: 2' 7'-dichlorofluorescein diacetate, ROS: reactive oxygen species, DMSO: dimethylsulfoxide.

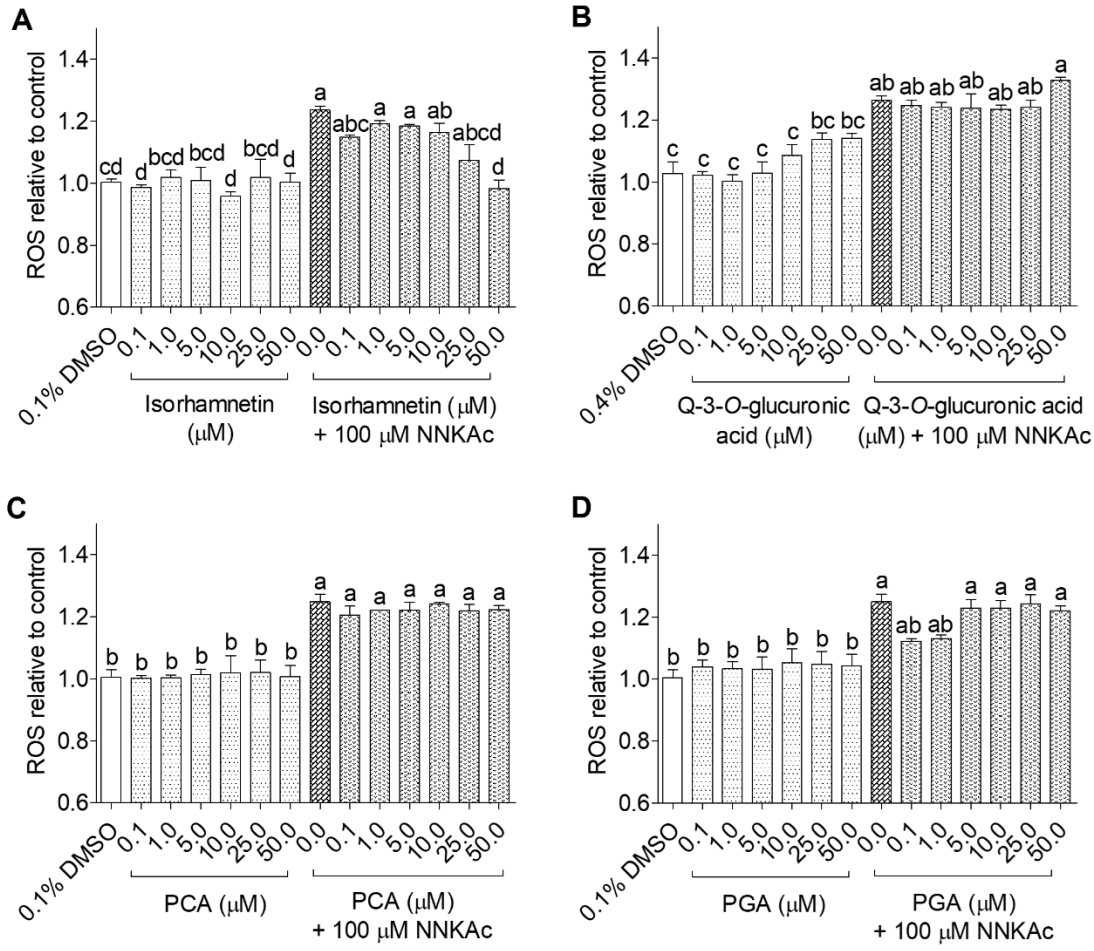

Figure 8: Effect of isorhamnetin (A), quercetin-3-*O*-glucuronic acid (B), protocatechuic acid (C), and phloroglucinaldehyde (D) on reducing NNKAc-induced ROS in BEAS-2B cells

Cells were pre-treated with concentrations ranging from 0.1- 50 μM of selected polyphenol metabolites for 3 h. Pre-treated cells were exposed to 100 μM NNKAc for another 3 h to induce ROS generation. DMSO (0.1% or 0.4%) was used as the vehicle control. Effects on ROS levels were quantified using DCFDA fluorescence assay. Two independent studies (each done in triplicates) were performed, and results were expressed as mean ± standard deviation. Statistical analysis of data was performed by one-way ANOVA and mean comparison was done by Tukey's mean comparison method (α=0.05) using Minitab 19 statistical software. Mean values that do not share similar letters (i.e., a- e) in bar graphs are significantly different ($p<0.05$). Abbreviations: NNKAc: 4-

[(Acetoxymethyl)nitrosamino]-1-(3-pyridyl)-1-butanone, DCFDA: 2' 7'-dichlorofluorescein diacetate, ROS: reactive oxygen species, DMSO: dimethylsulfoxide, Q: quercetin, PCA: protocatechuic acid, PGA: phloroglucinaldehyde.

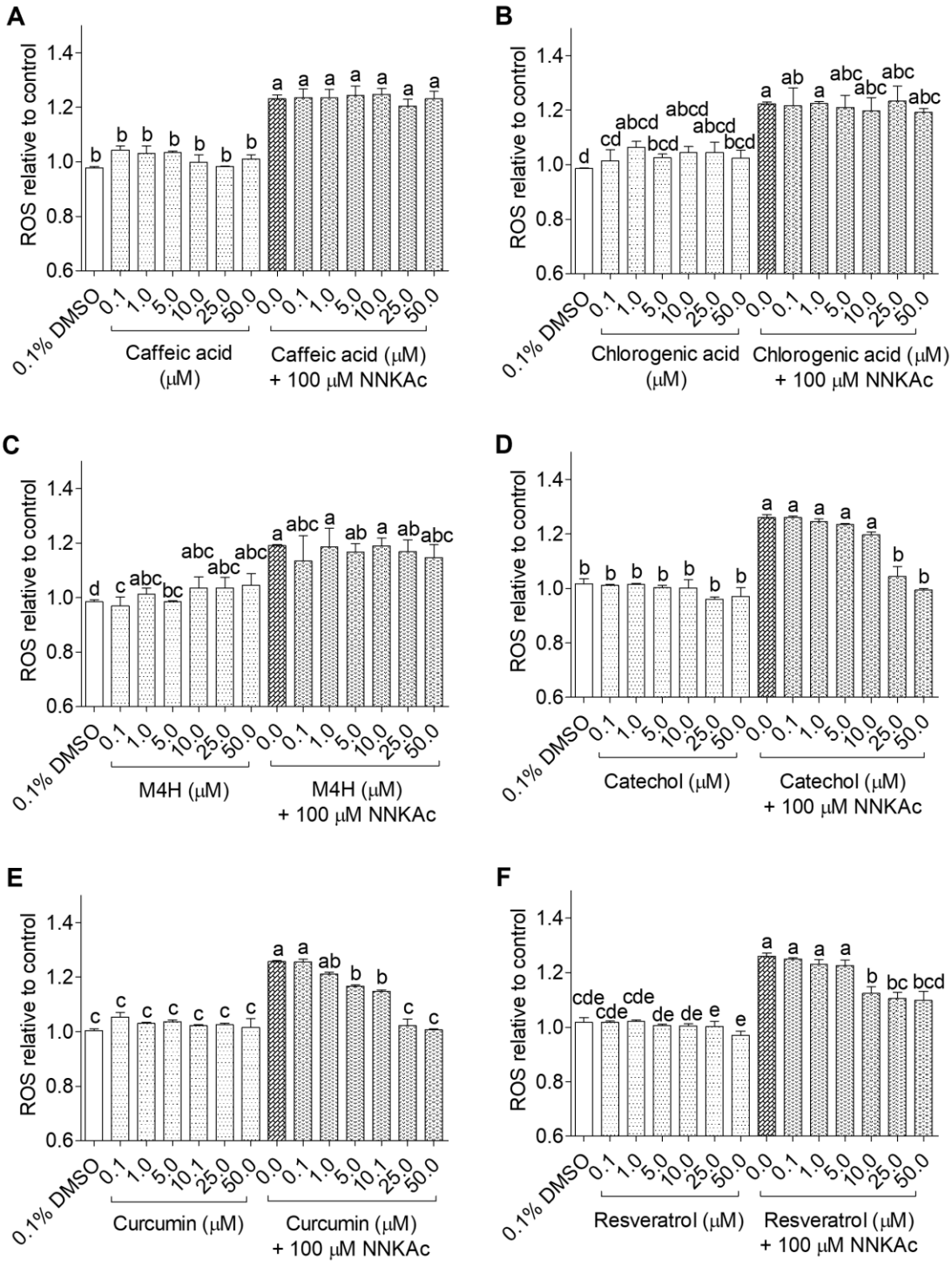

Figure 9: Effect of caffeic acid (A), chlorogenic acid (B), methyl 4-hydroxybenzoate (C), catechol (D), curcumin (E), and resveratrol (F) on reducing NNKAc-induced ROS in BEAS-2B cells

Cells were pre-treated with concentrations ranging from 0.1- 50 µM of selected phenolic acids and other polyphenols for 3 h. Pre-treated cells were exposed to 100 µM NNKAc for another 3 h to induce ROS generation. DMSO (0.1%) was used as the vehicle control. Effects on ROS levels were quantified using DCFDA fluorescence assay. Two independent studies (each done in triplicates) were performed, and results were expressed as mean ± standard deviation. Statistical analysis of data was performed by one-way ANOVA and mean comparison was done by Tukey's mean comparison method (α=0.05) using Minitab 19 statistical software. Mean values that do not share similar letters (i.e., a-e) in bar graphs are significantly different ($p<0.05$). Abbreviations: M4H: methyl 4-hydroxybenzoate NNKAc: 4-[(acetoxymethyl)nitrosamino]-1-(3-pyridyl)-1-butanone, DCFDA: 2' 7'-dichlorofluorescein diacetate, ROS: reactive oxygen species, DMSO: dimethylsulfoxide.

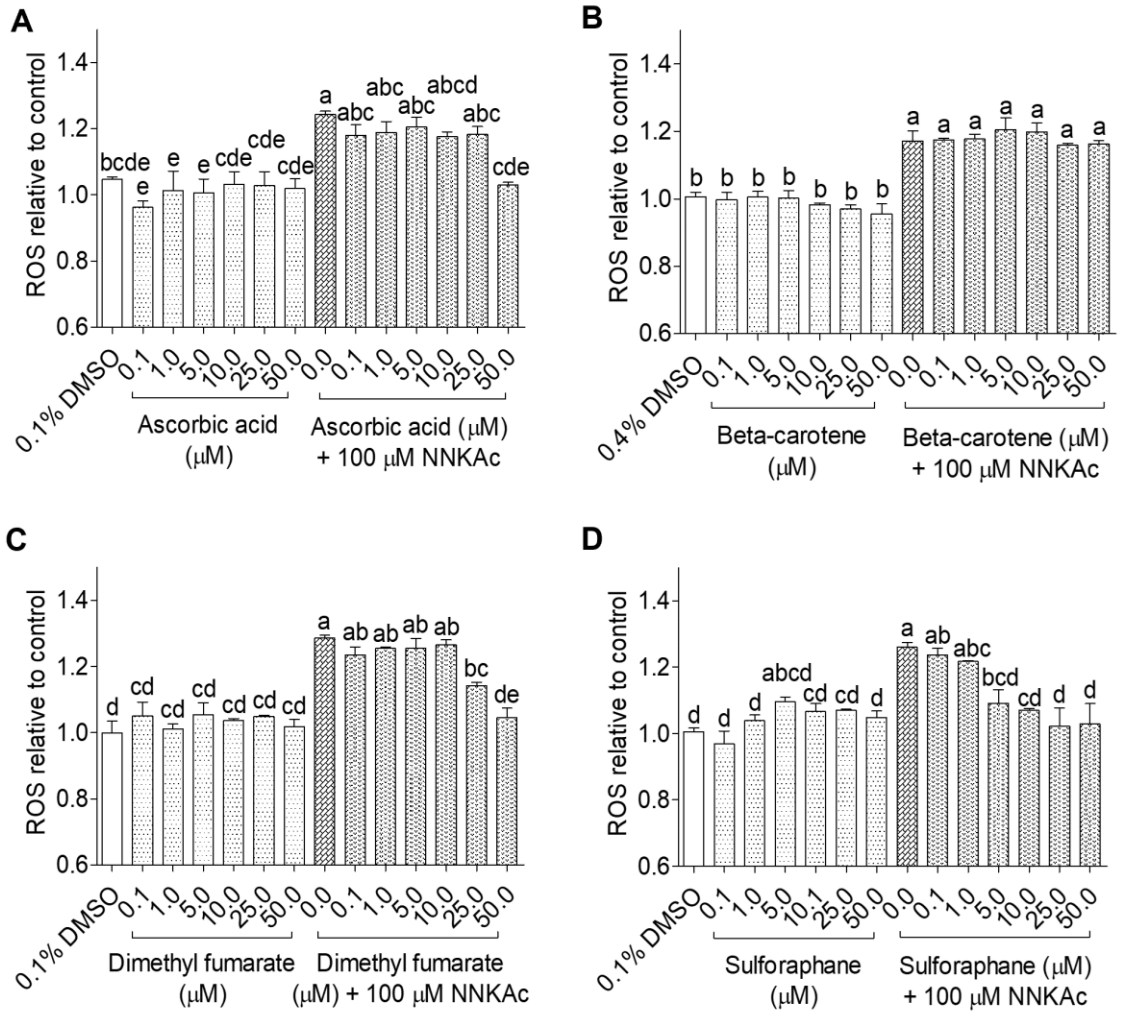

Figure 10: Effect of ascorbic acid (A), beta-carotene (B), dimethyl fumarate (C), and sulforaphane (D) on reducing NNKAc-induced ROS in BEAS-2B cells

Cells were pre-treated with concentrations ranging from 0.1- 50 μM of selected non-phenolic compounds for 3 h. Pre-treated cells were exposed to 100 μM NNKAc for another 3 h to induce ROS generation. DMSO (0.1% or 0.4%) was used as the vehicle control. Effects on ROS levels were quantified using DCFDA fluorescence assay. Two independent studies (each done in triplicates) were performed, and results were expressed as mean ± standard deviation. Statistical analysis of data was performed by one-way ANOVA and mean comparison was done by Tukey's mean comparison method (α=0.05) using Minitab 19 statistical software. Mean values that do not share similar letters (i.e., a-e) in bar graphs are significantly different ($p<0.05$).

Abbreviations: NNKAc: 4-[(Acetoxymethyl)nitrosamino]-1-(3-pyridyl)-1-butanone, DCFDA: 2' 7'-dichlorofluorescein diacetate, ROS: reactive oxygen species, DMSO: dimethyl sulfoxide.

4.2 Effects of dietary antioxidants in the reduction of NNKAc-induced DNA damage in BEAS-2B cells

To assess cytoprotective and genoprotective effects against NNKAc-challenged BEAS-2B cells, the dose-dependent effects of 12 selected compounds were assessed using 5 different concentrations (0.1, 1, 5, 10, and 25 μM). The 12 compounds were selected based on their ability to reduce the NNKAc-induced ROS generation in BEAS-2B cells at concentrations equals or less than 25 μM. The selected compounds include: 3-hydroxy (quercetin, cyanidin, and procyanidin B2) and 3-deoxy (luteolin, chrysin, naringenin, and genistein) flavonoids, simple polyphenols (catechol), stilbenes (resveratrol), curcuminoids (curcumin) and non-phenolic compounds (DMF and sulforaphane) that reduced NNKAc-induced ROS in BEAS-2B cells at concentrations equal to or less than 25 μM were selected.

4.2.1 Effects of dietary antioxidants on BEAS-2B cell viability.

The effects of test compounds on cell viability under experimental conditions were studied using the MTS assay (Appendix 1 and 2). The viability of BEAS-2B cells was reduced by 10-20% due to the exposure of 100 μM NNKAc but the reduction was not significant ($p > 0.05$) when compared to the DMSO control. The test compounds at concentrations of 0.1–25 μM did not impact ($p > 0.05$) on the viability of BEAS-2B cells when compared to the DMSO control.

4.2.2 Effects of dietary antioxidants on NNKAc-induced DNA damage in BEAS-2B cells

The protective effects of selected test compounds on NNKAc-induced DNA damage in BEAS-2B cells were studied using *γ*-H2AX immunofluorescence assay (HIA; Figure 11-13 and Table 3), comet assay (CA; Figure 14-16 and Table 3), and DNA fragmentation-ELISA assay (DFEA; Figures 17 and 18 and Table 3). Effects on DNA double-strand breaks (DSBs) induced by NNKAc in BEAS-2B cells were evaluated by quantifying γ-H2AX foci per nucleus using the immunofluorescence assay. Percentage tail moment of single BEAS-2B cells from comet assay was used to study the protective effects of tested compounds on both DNA single-strand breaks (SSBs) and DNA DSBs induced by NNKAc in BEAS-2B cells. For DNA fragmentation by ELISA assay, absorbance at 450 nm was recorded to measure the level of DNA fragmentation by spectrophotometry.

BEAS-2B cells-treated with NNKAc showed significantly higher *γ*-H2AX foci per nucleus, percentage DNA tail moment, and DNA fragmentation levels ($p<0.05$) compared to DMSO control. BEAS-2B cells treated with different concentrations (0.1–25 μM) of all 12 selected dietary antioxidants without NNKAc challenge showed no significant DNA damage ($p > 0.05$) in all three experiments compared to DMSO control. BEAS-2B cells pre-treated with 3-hydroxy flavonoids such as quercetin (1-25 μM) and procyanidin B2 (0.1-25 μM) and 3-deoxy flavonoid genistein (0.1-25 μM) showed significant ($p < 0.05$) reductions in γ-H2AX foci per nucleus, percentage DNA tail moment, and DNA fragmentation levels in BEAS-2B cells against NNKAc challenge at both low and high concentrations. Meanwhile, significantly reduced ($p < 0.05$) NNKAc-induced DNA damage in BEAS-2B cells with pre-treatment with luteolin (HIA: 10-25 μM, CA:5-25 μM,

and DFEA: 5-25 μM), chrysin (HIA: 25 μM, CA: 10-25 μM and DFEA: 10-25 μM), naringenin (HIA: 25 μM, CA: 25 μM and DFEA: 25 μM) and cyanidin (CA: 25 μM and DFEA: 25 μM) was observed at comparatively higher concentrations than genistein, procyanidin B2, and quercetin. Interestingly, despite a dose-dependent reduction in NNKAc-induced DNA DSBs in BEAS-2B in terms of reduction of γ-H2AX foci per nucleus by cyanidin pretreatment, the observed reductions were not significant ($p > 0.05$). Meanwhile, non-flavonoids such as curcumin (DFEA: 5-25 μM, HIA: 10-25 μM, and CA:5-25 μM), catechol (DFEA: 25 μM, HIA: 25 μM, and CA: 25 μM), resveratrol (DFEA: 10-25 μM, HIA: 10-25 μM, and CA: 10-25 μM), sulforaphane (DFEA: 10-25 μM, HIA: 5-25 μM, and CA-5-25 μM), and dimethyl fumarate (DFEA: 25 μM, HIA: 25 μM, and CA: 25 μM) also significantly ($p < 0.05$) reduced NNKAc-induced DNA damage in BEAS-2B cells compared to BEAS-2B cells treated with NNKAc at relatively higher concentrations.

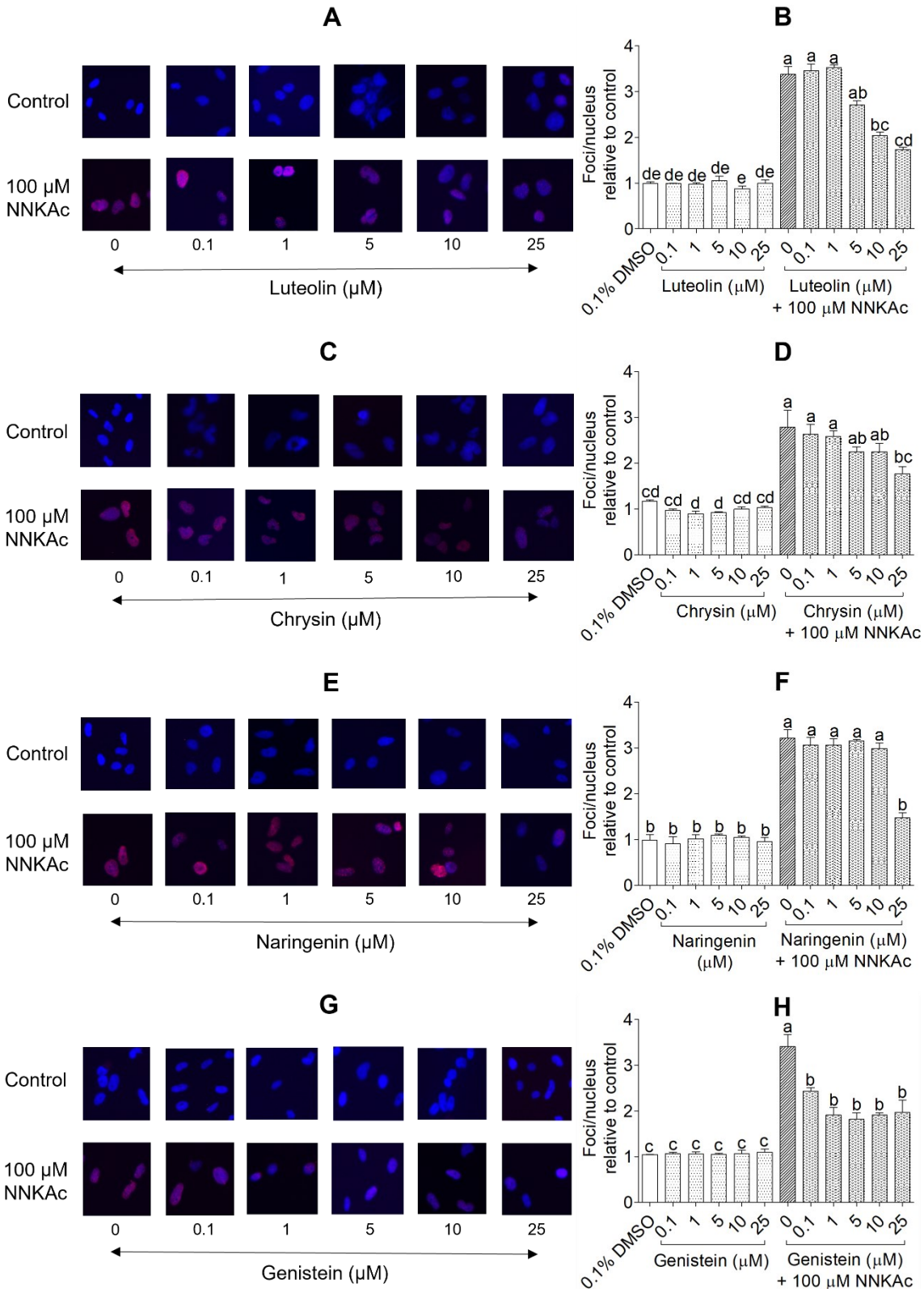

Figure 11: Effect of luteolin (A-B), chrysin (C-D), naringenin (E-F), and genistein (G-H) on NNKAc-induced DNA damage in BEAS-2B cells measured by γ-H2AX immunofluorescence assay

Cells were pre-treated with concentrations ranging from 0.1- 25 µM of selected compounds for 3 h. Pre-treated cells were exposed to 100 µM NNKAc for another 3 h. DMSO (0.1%) was used as the vehicle control. Specific antibodies were used to label the phosphorylated histone γ-H2AX foci (Ser139) and DAPI was used to stain the nucleus. The foci/nucleus ratio was quantified using at least 50 nuclei per treatment. Nuclei were imaged by fluorescence microscopy (×100 magnification). The number of foci per nuclei was counted by ImageJ software. Three independent studies were performed, and results were expressed as mean ± standard deviation. Statistical analysis of data was performed by one-way ANOVA and mean comparison was done by Tukey's mean comparison method (α=0.05) using Minitab 19 statistical software. Mean values that do not share similar letters (i.e., a-e) in bar graphs are significantly different ($p<0.05$). Abbreviations: NNKAc: 4-[(Acetoxymethyl)nitrosamino]-1-(3-pyridyl)-1-butanone, DMSO: dimethyl sulfoxide.

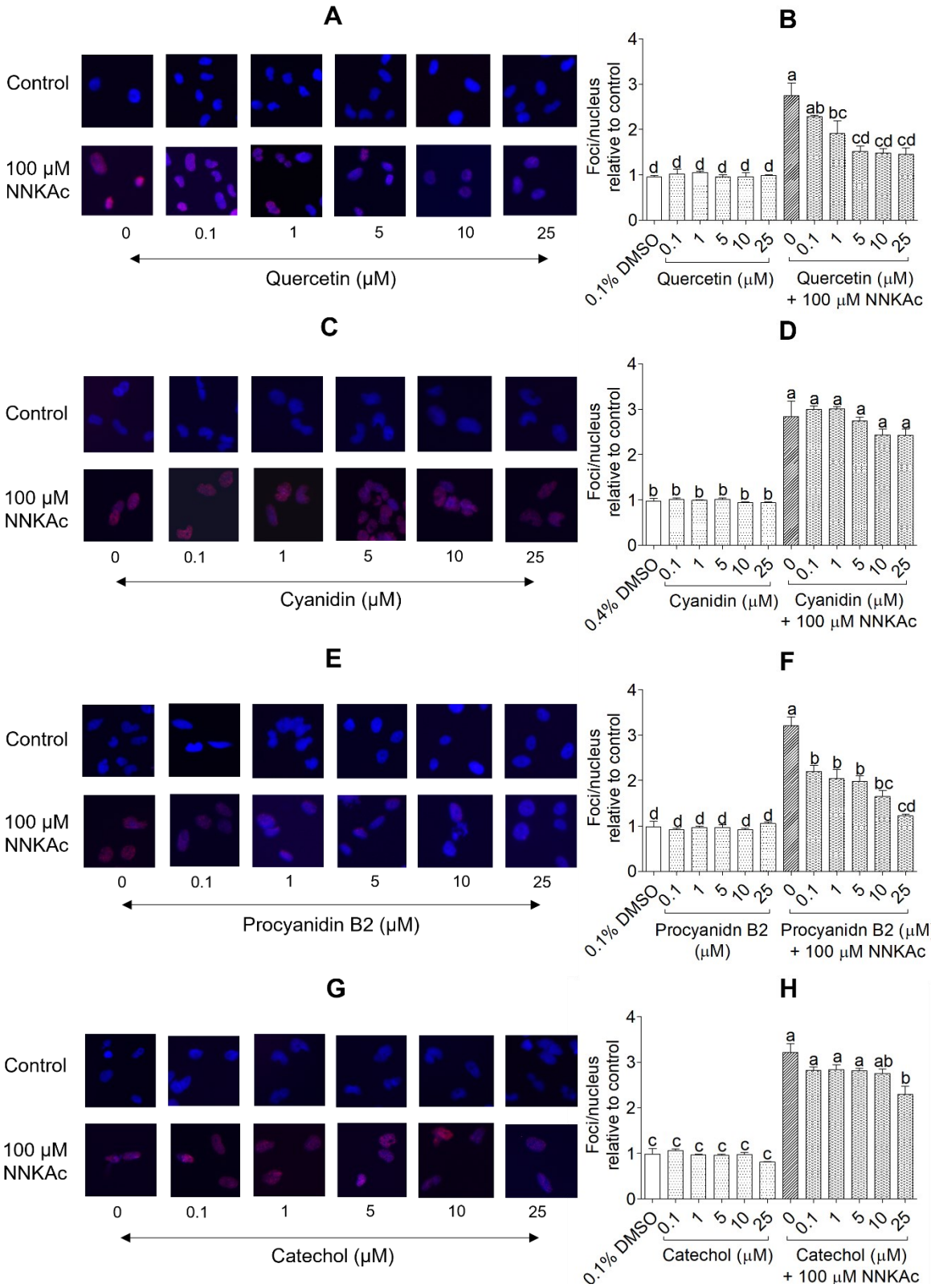

Figure 12: Effect of quercetin (A-B), cyanidin (C-D), procyanidin B2 (E-F), and catechol (G-H) on NNKAc-induced DNA damage in BEAS-2B cells measured by γ-H2AX immunofluorescence assay

Cells were pre-treated with concentrations ranging from 0.1- 25 µM of selected compounds for 3 h. Pre-treated cells were exposed to 100 µM NNKAc for another 3 h. DMSO (0.1% or 0.4%) was used as the vehicle control. Specific antibodies were used to label the phosphorylated histone γ-H2AX foci (Ser139) and DAPI was used to stain the nucleus. The foci/nucleus ratio was quantified using at least 50 nuclei per treatment. Nuclei were imaged by fluorescence microscopy (×100 magnification). The number of foci per nuclei was counted by ImageJ software. Three independent studies were performed, and results were expressed as mean ± standard deviation. Statistical analysis of data was performed by one-way ANOVA and mean comparison was done by Tukey's mean comparison method (α=0.05) using Minitab 19 statistical software. Mean values that do not share similar letters (i.e., a-e) in bar graphs are significantly different ($p<0.05$). Abbreviations: NNKAc: 4-[(acetoxymethyl)nitrosamino]-1-(3-pyridyl)-1-butanone, DMSO: dimethyl sulfoxide.

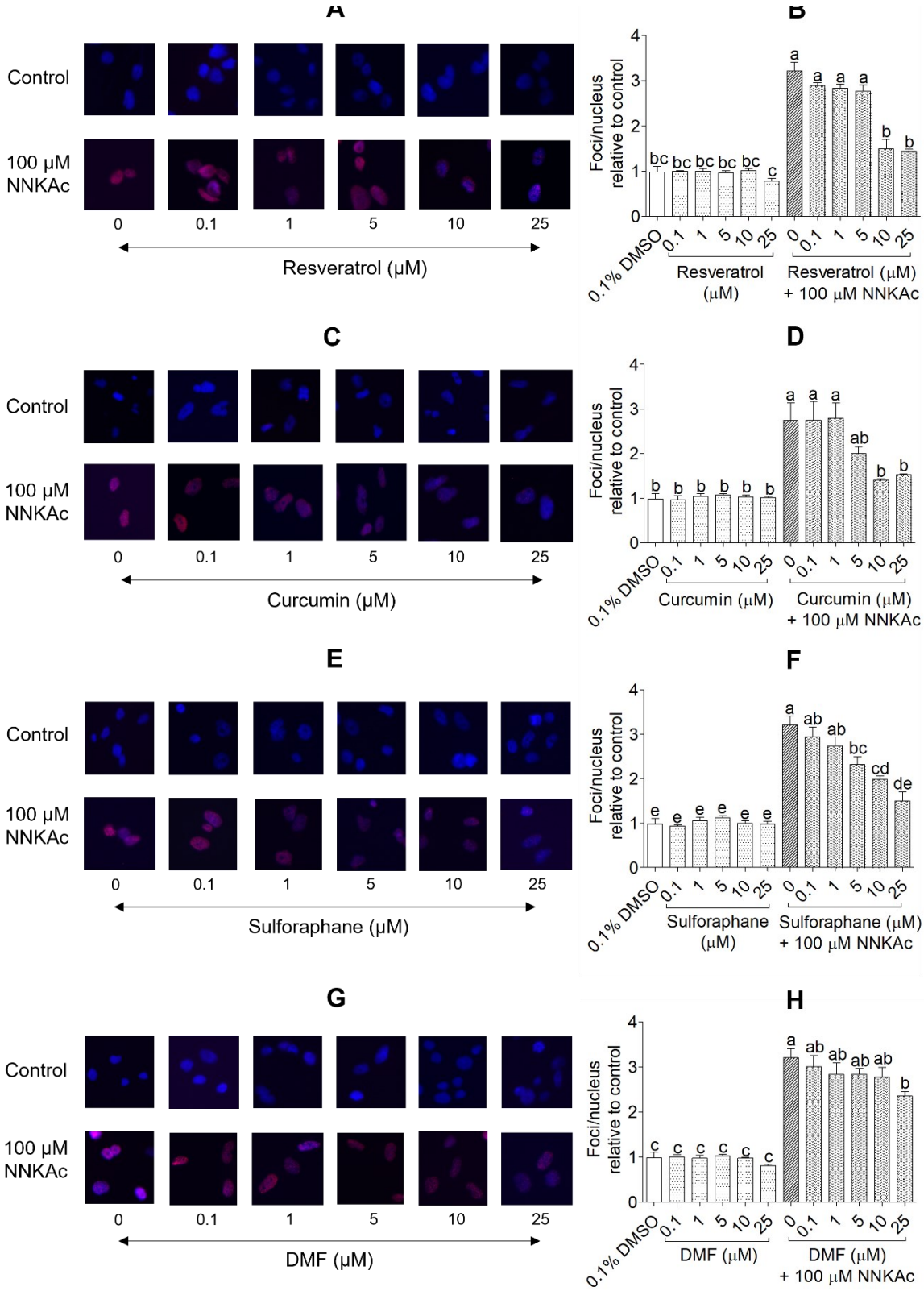

Figure 13: Effect of resveratrol (A-B), catechol (C-D), and dimethyl fumarate (E-F) on NNKAc-induced DNA damage in BEAS-2B cells measured by γ-H2AX immunofluorescence assay

Cells were pre-treated with concentrations ranging from 0.1- 25 µM of selected compounds for 3 h. Pre-treated cells were exposed to 100 µM NNKAc for another 3 h. DMSO (0.1%) was used as the vehicle control. Specific antibodies were used to label the phosphorylated histone γ-H2AX foci (Ser139) and DAPI was used to stain the nucleus. The foci/nucleus ratio was quantified using at least 50 nuclei per treatment. Nuclei were imaged by fluorescence microscopy (×100 magnification). The number of foci per nuclei was counted by ImageJ software. Three independent studies were performed, and results were expressed as mean ± standard deviation. Statistical analysis of data was performed by one-way ANOVA and mean comparison was done by Tukey's mean comparison method (α=0.05) using Minitab 19 statistical software. Mean values that do not share similar letters (i.e., a-e) in bar graphs are significantly different ($p<0.05$). Abbreviations: NNKAc: 4-[(acetoxymethyl)nitrosamino]-1-(3-pyridyl)-1-butanone, DMF: dimethyl fumarate, DMSO: dimethyl sulfoxide.

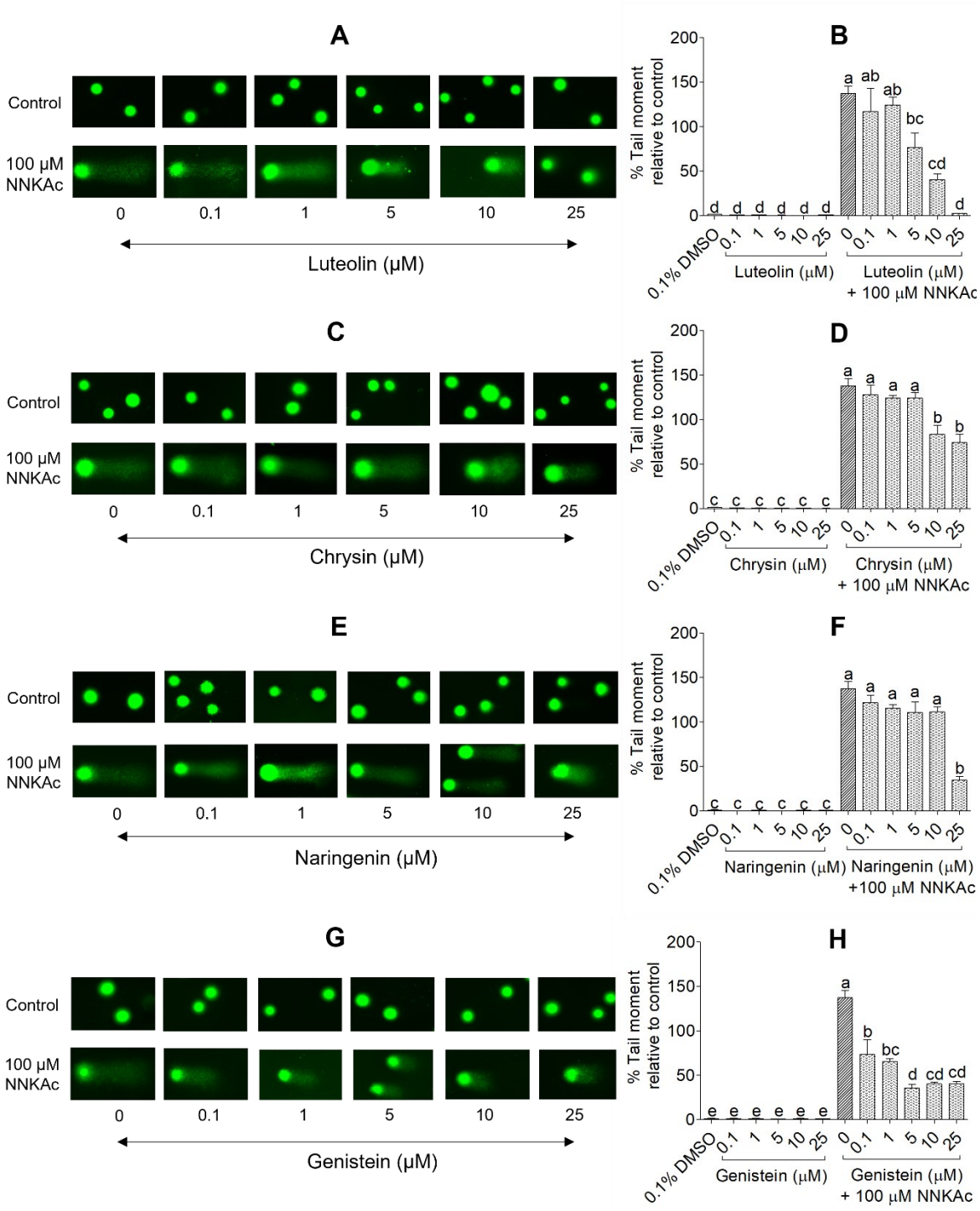

Figure 14: Effect of luteolin (A-B), chrysin (C-D), naringenin (E-F), and genistein (G-H) on NNKAc-induced DNA damage in BEAS-2B cells measured by comet assay

Cells were pre-treated with concentrations ranging from 0.1- 25 µM of selected compounds for 3 h. Pre-treated cells were exposed to 100 µM NNKAc for another 3 h. DMSO (0.1%) was used as the vehicle control. Comets were imaged by fluorescence microscopy (×100 magnification). Percentage tail moment using at least 30 comets per treatment was calculated by using the OpenComet plugin in ImageJ software. Three independent studies were performed, and results were expressed as mean ± standard deviation. Statistical analysis of data was performed by one-way ANOVA and mean comparison was done by Tukey's mean comparison method (α=0.05) using Minitab 19 statistical software. Mean values that do not share similar letters (i.e., a-e) in bar graphs are significantly different ($p<0.05$). Abbreviations: NNKAc: 4-[(acetoxymethyl)nitrosamino]-1-(3-pyridyl)-1-butanone, DMSO: dimethyl sulfoxide.

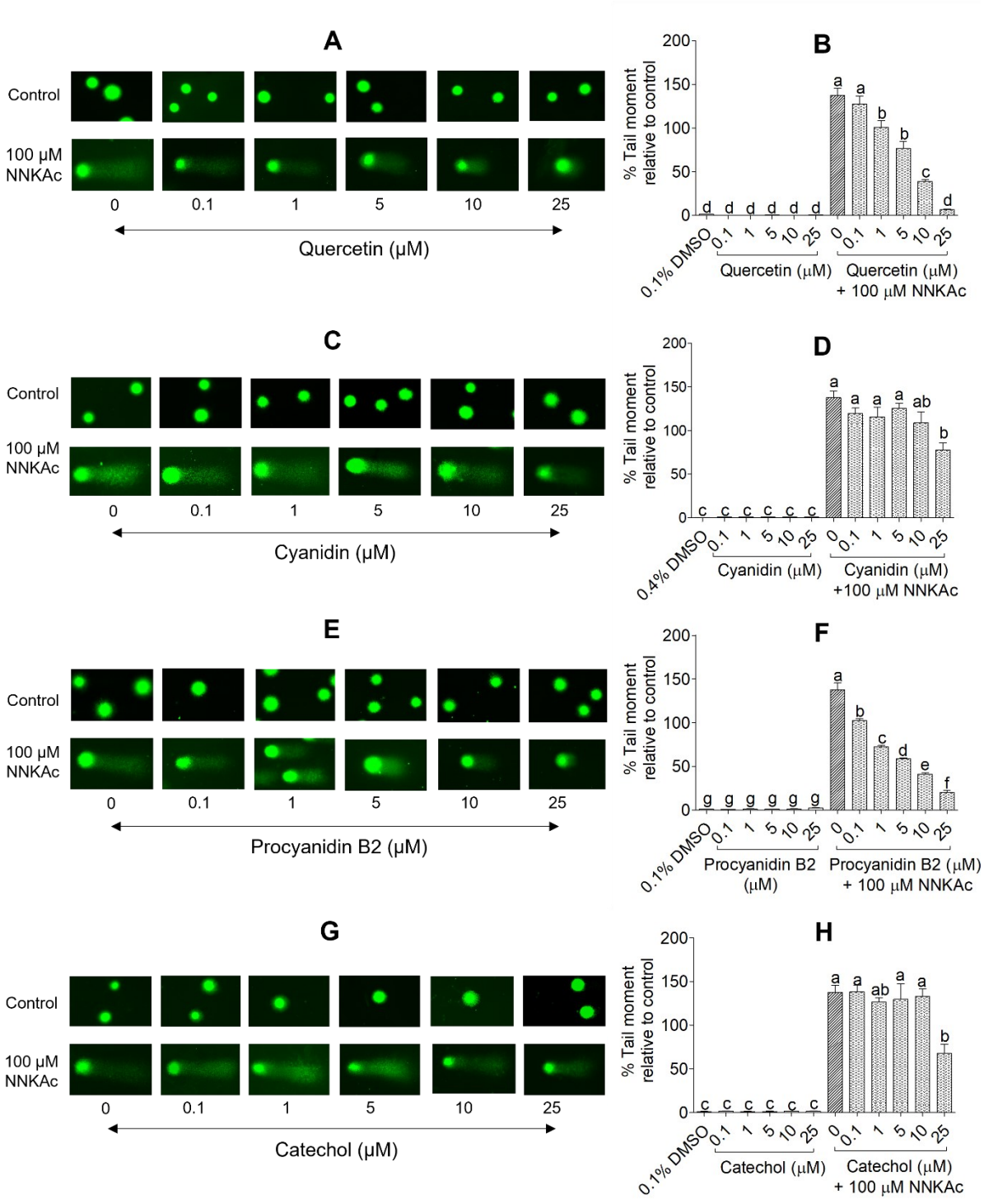

Figure 15: Effect of quercetin (A-B), cyanidin (C-D), procyanidin B2 (E-F), and catechol (G-H) on NNKAc-induced DNA damage in BEAS-2B cells measured by comet assay

Cells were pre-treated with concentrations ranging from 0.1- 25 µM of selected compounds for 3 h. Pre-treated cells were exposed to 100 µM NNKAc for another 3 h. DMSO was used as the vehicle control (0.1%). Comets were imaged by fluorescence microscopy (×100 magnification). Percentage tail moment using at least 30 comets per treatment was calculated by using the OpenComet plugin in ImageJ software. Three independent studies were performed, and results were expressed as mean ± standard deviation. Statistical analysis of data was performed by one-way ANOVA and mean comparison was done by Tukey's mean comparison method (α=0.05) using Minitab 19 statistical software. Mean values that do not share similar letters (i.e., a-e) in bar graphs are significantly different ($p<0.05$). Abbreviations: NNKAc: 4-[(acetoxymethyl)nitrosamino]-1-(3-pyridyl)-1-butanone, DMSO: dimethyl sulfoxide.

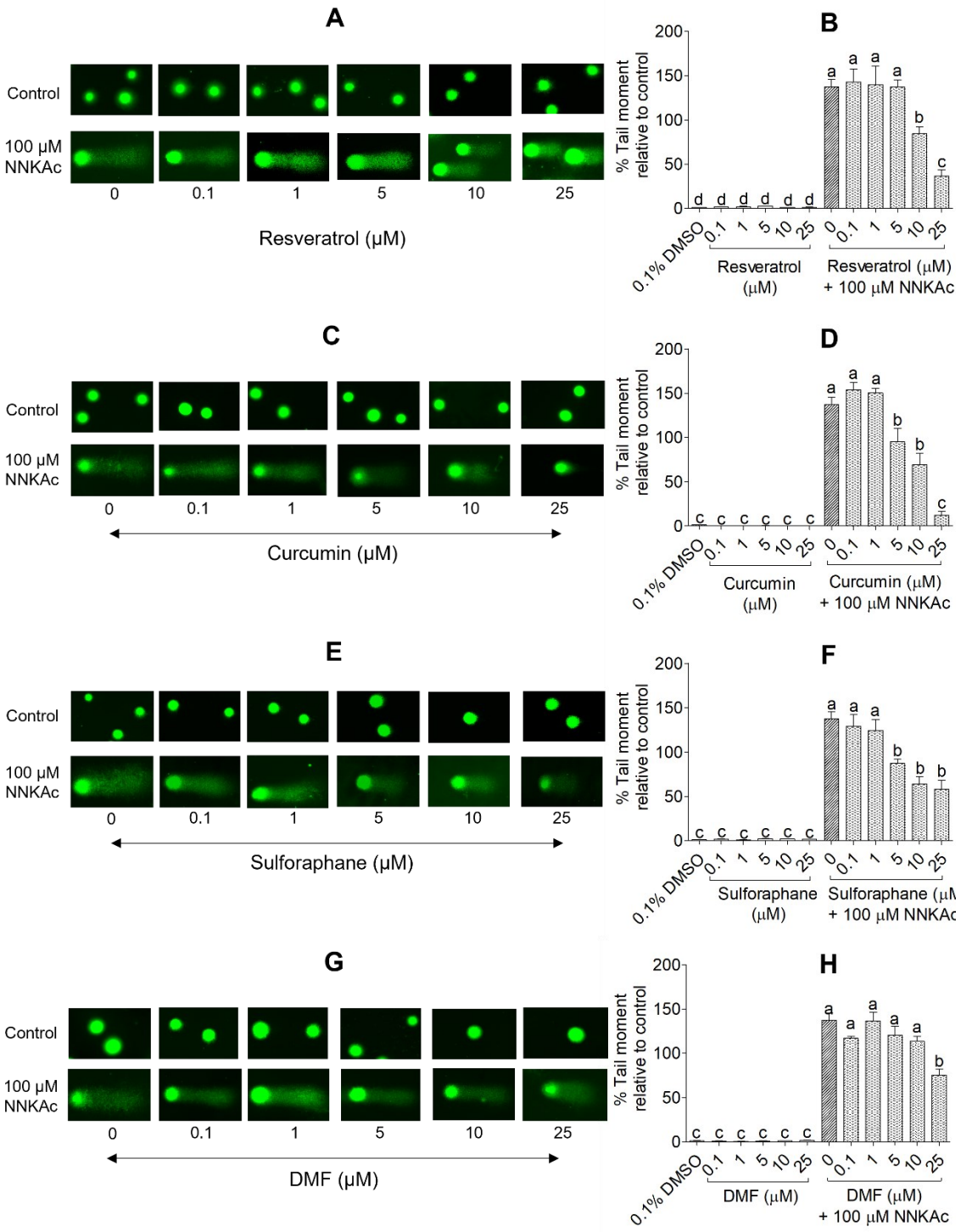

Figure 16: Effect of resveratrol (A-B), curcumin (C-D), sulforaphane (E-F), and dimethyl fumarate (G-H) on NNKAc-induced DNA damage in BEAS-2B cells measured by comet assay

Cells were pre-treated with concentrations ranging from 0.1- 25 µM of selected compounds for 3 h. Pre-treated cells were exposed to 100 µM NNKAc for another 3 h. DMSO (0.1%) was used as the vehicle control. Comets were imaged by fluorescence microscopy (×100 magnification). Percentage tail moment using at least 30 comets per treatment was calculated by using the OpenComet plugin in ImageJ software. Three independent studies were performed, and results were expressed as mean ± standard deviation. Statistical analysis of data was performed by one-way ANOVA and mean comparison was done by Tukey's mean comparison method (α=0.05) using Minitab 19 statistical software. Mean values that do not share similar letters (i.e., a-e) in bar graphs are significantly different ($p<0.05$). Abbreviations: NNKAc: 4-[(acetoxymethyl)nitrosamino]-1-(3-pyridyl)-1-butanone, DMF: dimethyl fumarate, DMSO: dimethyl sulfoxide.

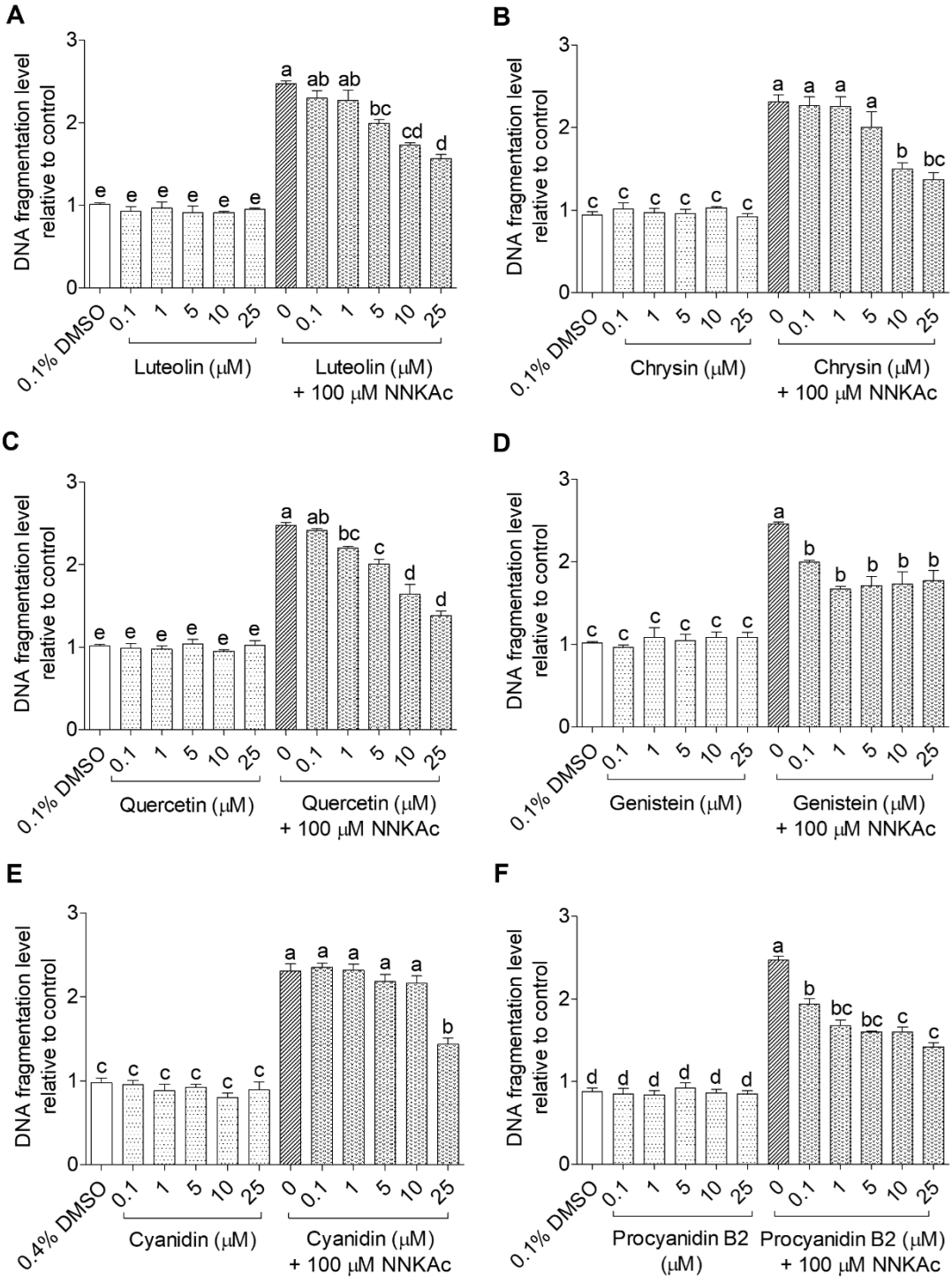

Figure 17: Effect of luteolin (A), chrysin (B), quercetin (C), genistein (D), cyanidin (E), and procyanidin B2 (F) on DNA fragmentation level against NNKAc-induced DNA damage in BEAS-2B cells

Cells were pre-treated with concentrations ranging from 0.1- 25 μM of selected compounds for 3 h. Pre-treated cells were exposed to 100 μM NNKAc for another 3 h. DMSO (0.1% or 0.4%) was used as the vehicle control. Effects on the level of DNA fragmentation were quantified using DNA fragmentation ELISA assay. Three independent studies (each done in duplicates) were performed, and results were expressed as mean ± standard deviation. Statistical analysis of data was performed by one-way ANOVA and mean comparison was done by Tukey's mean comparison method (α=0.05) using Minitab 19 statistical software. Mean values that do not share similar letters (i.e., a-e) in bar graphs are significantly different ($p<0.05$). Abbreviations: NNKAc: 4-[(acetoxymethyl)nitrosamino]-1-(3-pyridyl)-1-butanone, DMSO: dimethyl sulfoxide.

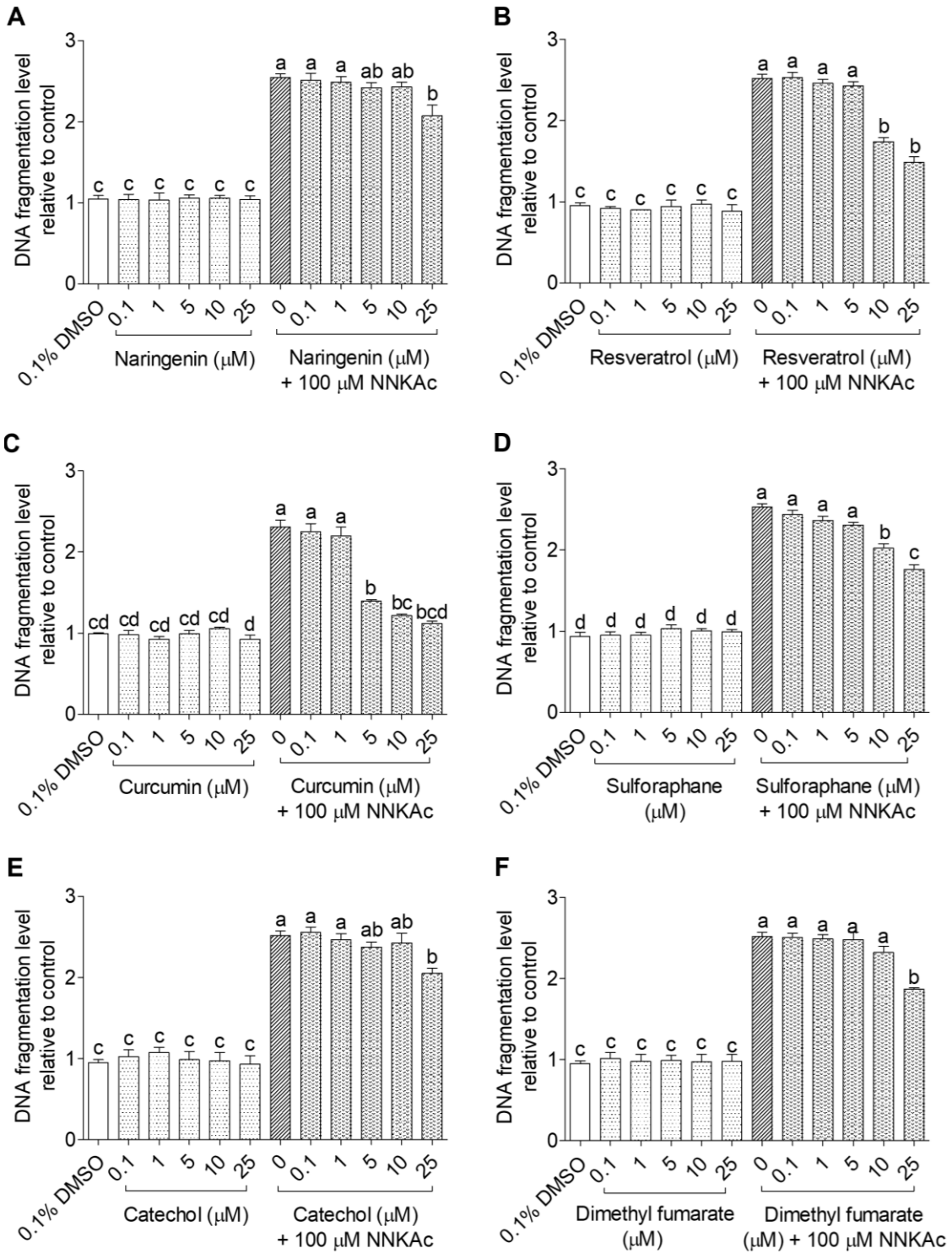

Figure 18: Effect of naringenin (A), resveratrol (B), curcumin (C), sulforaphane (D), catechol (E), and dimethyl fumarate (F) on DNA fragmentation level against NNKAc-induced DNA damage in BEAS-2B cells

Cells were pre-treated with concentrations ranging from 0.1- 25 µM of selected compounds for 3 h. Pre-treated cells were exposed to 100 µM NNKAc for another 3 h. DMSO (0.1%) was used as the vehicle control. Effects on the level of DNA fragmentation were quantified using DNA fragmentation ELISA assay. Three independent studies (each done in duplicates) were performed, and results were expressed as mean ± standard deviation. Statistical analysis of data was performed by one-way ANOVA and mean comparison was done by Tukey's mean comparison method (α=0.05) using Minitab 19 statistical software. Mean values that do not share similar letters (i.e., a-e) in bar graphs are significantly different ($p<0.05$). Abbreviations: NNKAc: 4-[(acetoxymethyl)nitrosamino]-1-(3-pyridyl)-1-butanone, DMSO: dimethyl sulfoxide.

4.3 Effects of quercetin, genistein, and procyanidin B2 on Nrf2/ARE signaling pathway in BEAS-2B cells

To assess the effects on Nrf2/ARE pathway in NNKAc challenged and normal BEAS-2B cells, the dose-dependent (1 and 25 μM) effects of the most effective flavonoids (quercetin, genistein, and procyanidin B2) in reducing NNKAc-induced ROS and DNA damage in BEAS-2B cells were studied.

4.3.1 Effect of quercetin, genistein, and procyanidin B2 on the phosphorylation of Akt and Nrf2 in BEAS-2B cells

Western blot analysis was used to assess the effects of quercetin, genistein, and procyanidin B2 on the activation of Nrf2 and its upstream kinase Akt through phosphorylation in BEAS-2B cells (Figure 19). BEAS-2B cells treated with NNKAc showed significantly ($p < 0.05$) higher p-Akt/Akt and p-Nrf2/Nrf2 ratios compared to DMSO control. In addition, two positive controls, namely DMF and hydrogen peroxide, were tested for their effects on Akt and Nrf2 phosphorylation in BEAS-2B cells. However, a significant increase ($p < 0.05$) compared to the DMSO control was observed only with the p-Nrf2/Nrf2 ratio but not with the p-Akt/Akt ratio after treatment of BEAS-2B cells with DMF or hydrogen peroxide.

BEAS-2B cells were treated with quercetin or procyanidin B2, but genistein, showed a dose-dependent increase in the p-Akt/Akt ratio. Genistein treatment showed an increase in the p-Akt/Akt ratio in BEAS-2B cells at the lowest concentration (1 μM) tested, but the observed levels were not significantly different ($p > 0.05$) from the DMSO control. Exposure of BEAS-2B cells only to procyanidin B2 but not quercetin and genistein significantly increased ($p < 0.05$) the p-Nrf2/Nrf2 ratio in BEAS-2B. However, a

significant increase ($p < 0.05$) in the p-Nrf2/Nrf2 ratio compared to the DMSO control was only observed with procyanidin B2 treatment at its highest concentration tested (25 μM). A dose dependent reduction in the p-Akt/Akt and p-Nrf2/Nrf2 ratios was also observed in BEAS-2B cells pretreated with 1 and 25 μM quercetin, genistein, or procyanidin B2 followed by NNKAc treatment. However, these observed reductions in the p-Akt/Akt and p-Nrf2/Nrf2 ratio were not significantly different ($p > 0.05$) from BEAS-2B cells treated with NNKAc alone.

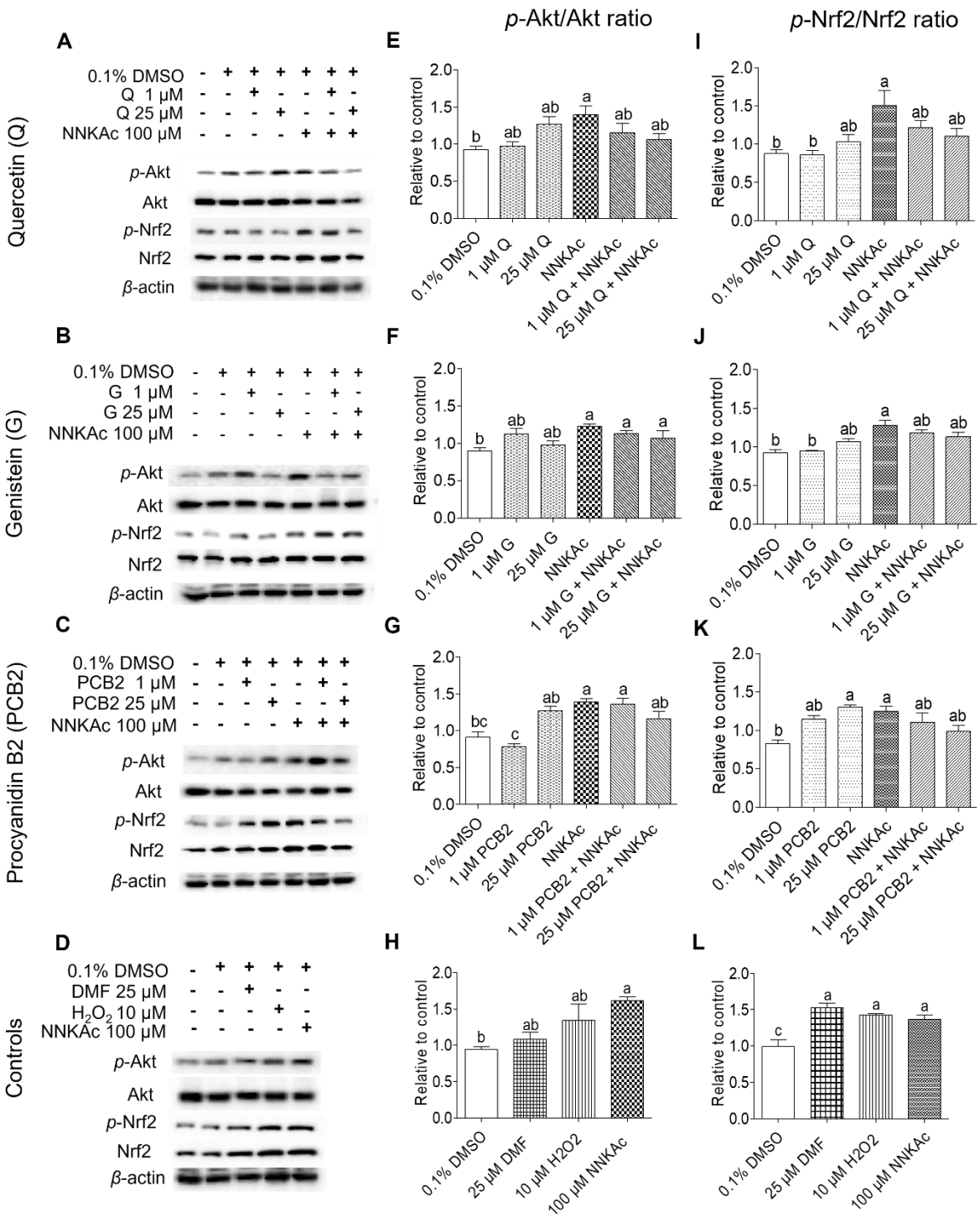

Figure 19: Effect of quercetin (A), genistein (B), procyanidin B2 (C), and controls (D) on phosphorylation of Nrf2 and Akt proteins in BEAS-2B cells

Cells were pre-treated with 1 μM and 25 μM of quercetin, genistein, or procyanidin B2 for 3 h. Pre-treated cells were exposed to 100 μM NNKAc for another 3 h to induce DNA damage. DMF (25 μM) and H_2O_2 (10 μM) were used as the positive controls and 0.1% DMSO was used as the vehicle control. The relative expression of p-Akt (Ser473) (E-H) and p-Nrf2 (Ser40) (I-L) protein levels to their respective total protein expressions were quantified using western blot analysis. At least 3 independent studies were performed, and results were expressed as mean ± standard deviation. Statistical analysis of data was performed by one-way ANOVA and mean comparison was done by Tukey's mean comparison method (α=0.05) using Minitab 19 statistical software. Mean values that do not share similar letters (i.e., a-e) in bar graphs are significantly different ($p<0.05$). Abbreviations: NNKAc: 4-[(acetoxymethyl)nitrosamino]-1-(3-pyridyl)-1-butanone, DMF: dimethyl fumarate DMSO: dimethyl sulfoxide, H_2O_2: hydrogen peroxide, G: genistein, Q: quercetin, PCB2: procyanidin B2.

4.3.2 Effect of quercetin, genistein, and procyanidin B2 on p-Nrf2 nuclear translocation in BEAS-2B cells.

The immunofluorescence assay was used to assess the effects of quercetin, genistein, and procyanidin B2 on the nuclear translocation of p-Nrf2 in BEAS-2B cells (Figure 20). BEAS-2B cells treated with NNKAc, DMF, or hydrogen peroxide showed significantly ($p < 0.05$) higher levels of p-Nrf2 nuclear translocation compared to DMSO control. BEAS-2B cells treated quercetin, genistein, or procyanidin B2 showed a dose-dependent increase in nuclear p-Nrf2 levels. However, a significant ($p < 0.05$) increase in nuclear p-Nrf2 levels was observed only with genistein and procyanidin B2 treatments at all tested concentrations. Moreover, a dose-dependent reduction ($p > 0.05$) in nuclear p-Nrf2 levels was observed with pretreatment of BEAS-2B cells with quercetin, genistein, or procyanidin B2 followed by the NNKAc treatment in comparison to cells treated with NNKAc alone.

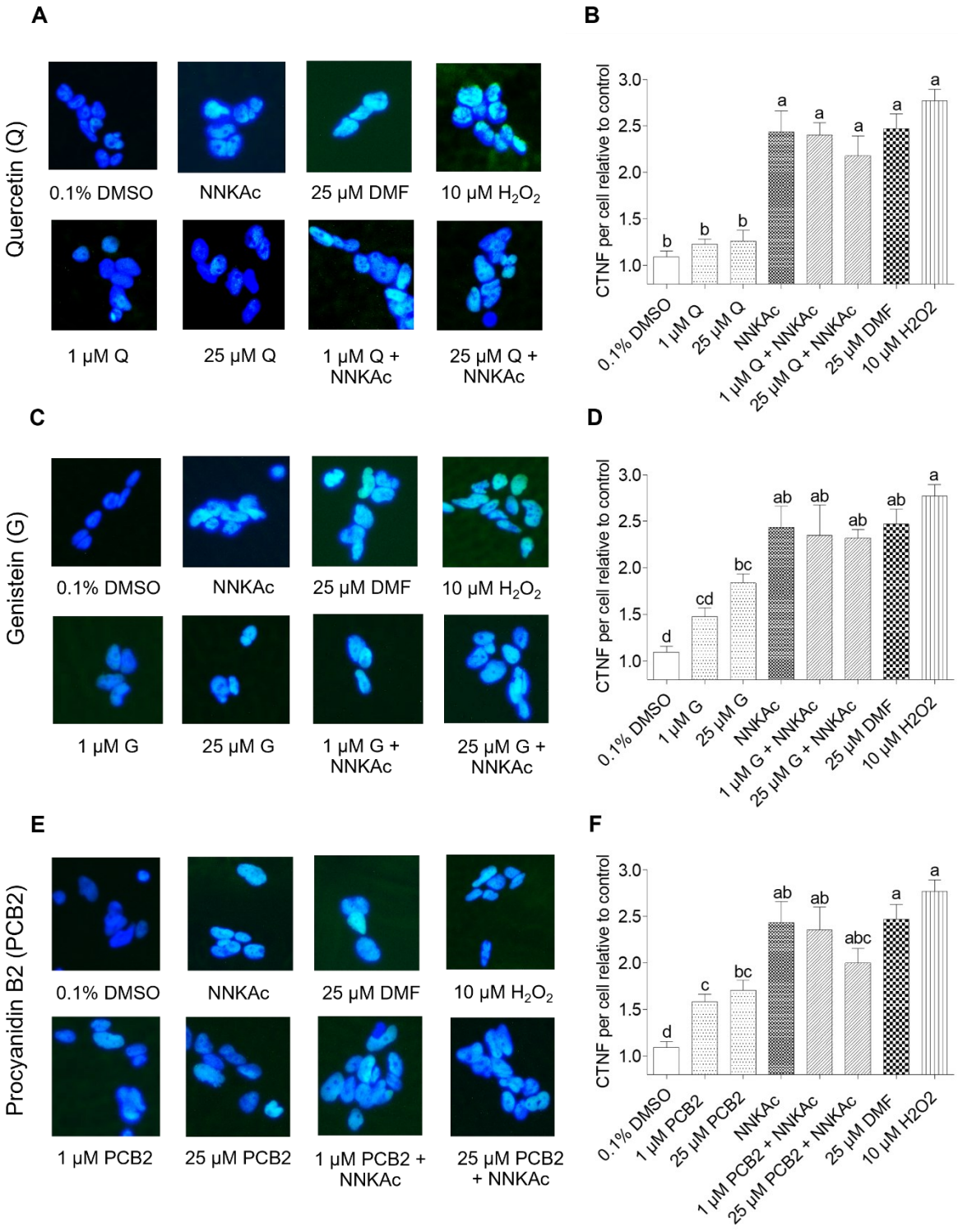

Figure 20: Effect of quercetin (A, B), genistein (C, D), and procyanidin B2 (E, F) on p-Nrf2 nuclear translocation in BEAS-2B cells measured by immunofluorescence assay

Cells were pre-treated with 1 μM and 25 μM of quercetin, genistein, or procyanidin B2 for 3 h. Pre-treated cells were exposed to 100 μM NNKAc for another 3 h to induce DNA damage. DMF (25 μM) and H_2O_2 (10 μM) were used as the positive controls and 0.1% DMSO was used as the vehicle control. Phosphorylated Nrf2 (Ser40) (p-Nrf2) was labeled with specific antibodies and nuclei were stained with DAPI. Nuclei were imaged by fluorescence microscopy (×100 magnification). The corrected nuclear fluorescence (CTNF) levels per nucleus were quantified using at least 30 nuclei per treatment to measure the level of p-Nrf2 nuclear translocation by immunofluorescence analysis. CTNF per nucleus was measured by ImageJ software. Three independent studies were performed, and results were expressed as mean ± standard deviation. Statistical analysis of data was performed by one-way ANOVA and mean comparison was done by Tukey's mean comparison method (α=0.05) using Minitab 19 statistical software. Mean values that do not share similar letters (i.e., a-e) in bar graphs are significantly different ($p<0.05$). Abbreviations: NNKAc: 4-[(acetoxymethyl)nitrosamino]-1-(3-pyridyl)-1-butanone, DMF: dimethyl fumarate DMSO: dimethyl sulfoxide, H_2O_2: hydrogen peroxide, Q: quercetin, G: genistein, PCB2: procyanidin B2.

4.3.3 Effect of quercetin, genistein, and procyanidin B2 on antioxidant enzyme activities in BEAS-2B cells.

Effects of quercetin, genistein, or procyanidin B2 on antioxidant enzyme activities in BEAS-2B cells were evaluated in terms of SOD (percentage inhibition of superoxide radical), catalase (mU/mL), and GPx (mU/mL) activities (Figure 21). BEAS-2B cells treated with NNKAc showed decreased SOD and catalase activities but slightly increased GPx activity compared to DMSO control. The reduction in catalase activity in NNKAc-treated BEAS-2B cells was significantly ($p < 0.05$) different from DMSO control. However, the observed changes in SOD and GPx activities in NNKAc-treated cells were not significantly ($p > 0.05$) different from the DMSO control. In addition to that BEAS-2B cells treated with hydrogen peroxide showed a significant ($p<0.05$) increase in both catalase and GPx activities but not SOD activity compared to DMSO control. Furthermore, no significant changes ($p > 0.05$) were observed in the antioxidant enzyme activities of BEAS-2B cells treated with DMF compared to the DMSO control.

BEAS-2B cells treated with 25 μM genistein or 25 μM procyanidin B2 showed a significant increase ($p < 0.05$) in the activity of catalase when compared with DMSO control. Also, no significant changes ($p > 0.05$) were observed in the SOD and GPx activities of BEAS-2B cells treated with quercetin, genistein, or procyanidin B2, even though the GPx activities were lower than those of the DMSO control.

BEAS-2B cells pretreated with quercetin, genistein, or procyanidin B2 did not increase ($p > 0.05$) in SOD activity against NNKAc challenge. The observed increase in SOD activity by flavonoids against NNKAc treatment was similar to the levels of DMSO control but not significantly different ($p > 0.05$). Furthermore, quercetin, genistein, and

procyanidin B2 did not significantly increase ($p > 0.05$) the NNKAc-reduced catalase activity. However, a slight increase in NNKAc-reduced catalase activity was observed with pretreatment of BEAS-2B cells with quercetin (1 μM), genistein (1 and 25 μM), and procyanidin B2 (1 and 25 μM) which was not significantly different ($p > 0.05$) from DMSO control. Meanwhile, a dose-dependent reduction in GPx activity was observed in BEAS-2B cells pretreated with quercetin, genistein, or procyanidin B2 against the NNKAc challenge. However, these observed reductions in GPx activity were not significantly different ($p > 0.05$) from BEAS-2B cells only treated with NNKAc or DMSO.

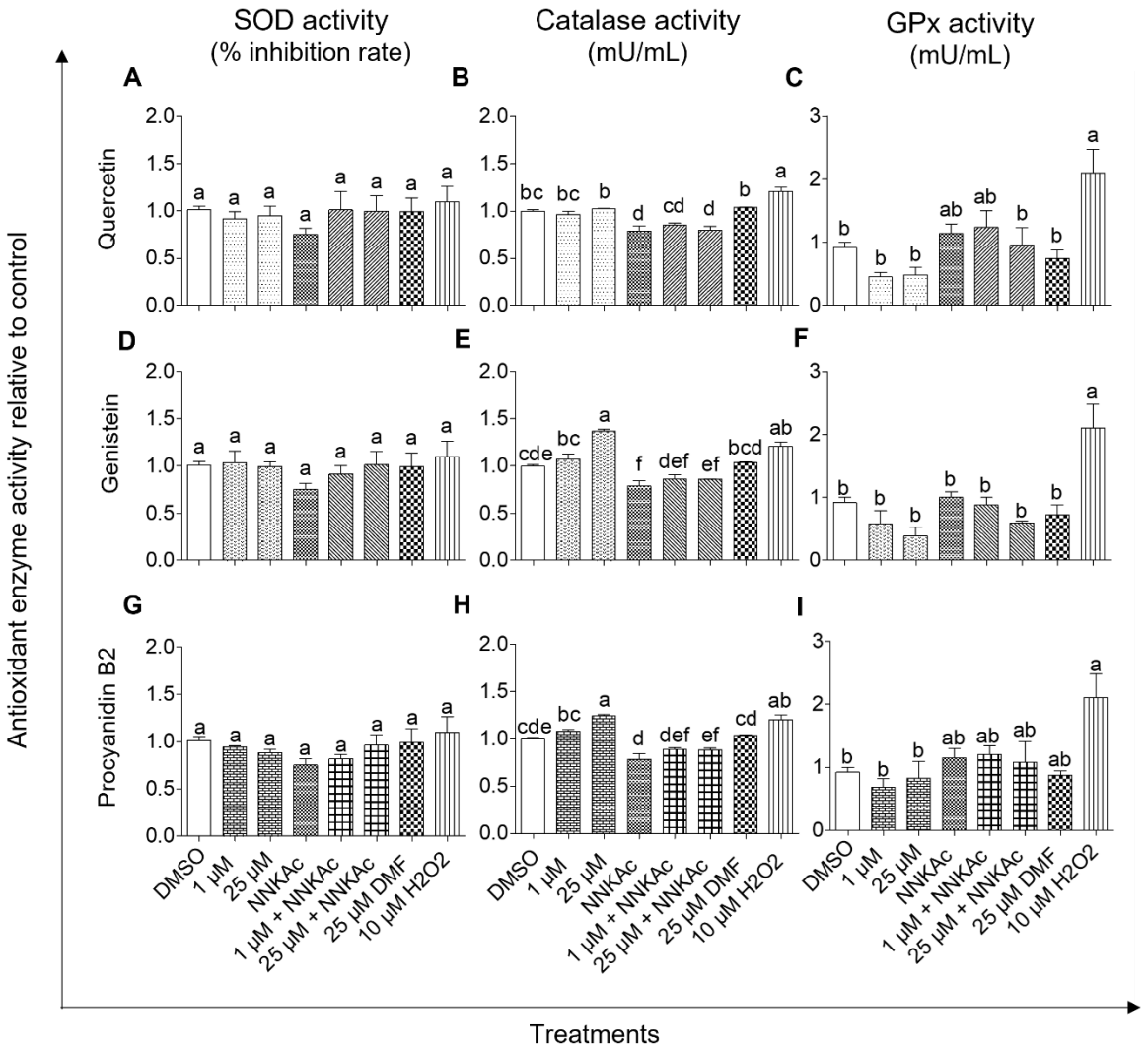

Figure 21: Effect of quercetin (A-C), genistein (D-F), and procyanidin B2 (G-I) on antioxidant enzyme (superoxide dismutase, catalase, and glutathione peroxidase) activities in BEAS-2B cells

Cells were pre-treated with 1 µM or 25 µM of quercetin, genistein, or procyanidin B2 for 3 h. Pre-treated cells were exposed to 100 µM NNKAc for another 3 h to induce DNA damage. DMF (25 µM) and H_2O_2 (10 µM) were used as the positive controls and 0.1% DMSO was used as the vehicle control. Effects of tested compounds on the activity of SOD, catalase, and GPx were assessed. Three independent studies (each done in duplicates) were performed, and results were expressed as mean ± standard deviation. Statistical analysis of data was performed by one-way ANOVA and mean comparison was done by Tukey's mean comparison method (α=0.05) using Minitab 19 statistical software. Mean values that do not share similar letters (i.e., a-e) in bar graphs are significantly different

($p<0.05$). Abbreviations: NNKAc: 4-[(acetoxymethyl)nitrosamino]-1-(3-pyridyl)-1-butanone, DMF: dimethyl fumarate DMSO: dimethyl sulfoxide, H_2O_2: hydrogen peroxide, GPx: glutathione peroxidase, SOD: superoxide dismutase.

Table 3: Summary of tested compounds on reduction of NNKAc-induced ROS and DNA damage in BEAS-2B cells

Group	Compound	ROS-DCFDA assay						*γ*-H2AX immunofluorescence assay					Comet assay					DNA fragmentation-ELISA assay				
		Test compound concentration (μM) + 100 μM NNKAc																				
		0.1	1	5	10	25	50	0.1	1	5	10	25	0.1	1	5	10	25	0.1	1	5	10	25
Flavone	Luteolin	N	N	*	*	*	*	N	N	N	*	*	N	N	*	*	*	N	N	*	*	*
	Chrysin	N	N	N	*	*	*	N	N	N	N	*	N	N	N	*	*	N	N	N	*	*
Flavanone	Naringenin	N	N	N	N	*	*	N	N	N	N	*	N	N	N	N	*	N	N	N	N	*
Isoflavone	Genistein	N	*	*	*	*	*	*	*	*	*	*	*	*	*	*	*	*	*	*	*	*
Flavonol	Quercetin	N	N	*	*	*	*	N	*	*	*	*	N	*	*	*	*	N	*	*	*	*
Anthocyanin	Cyanidin	N	N	N	N	*	*	N	N	N	N	N	N	N	N	N	*	N	N	N	N	*
	C3G	N	N	N	N	N	N															
Flavan-3-ols	Epicatechin	N	N	N	N	N	N															
Proanthocyanidin	Procyanidin B2	*	*	*	*	*	*	*	*	*	*	*	*	*	*	*	*	*	*	*	*	*
Chalcones	Phloretin	N	N	N	N	N	N															
	Phloridzin	N	N	N	N	N	N															
Flavonoid metabolites	PCA	N	N	N	N	N	N															
	PGA	N	N	N	N	N	N															
	Isorhamnetin	N	N	N	N	N	*															
	Quercetin-3-*O*-glucuronic acid	N	N	N	N	N	N															
Simple phenols	Catechol	N	N	N	N	*	*	N	N	N	N	*	N	N	N	N	*	N	N	N	N	*
Phenolic acids	Caffeic acid	N	N	N	N	N	N															
	Chlorogenic acid	N	N	N	N	N	N															

Group	Compound	ROS-DCFDA assay						γ-H2AX immunofluorescence assay					Comet assay					DNA fragmentation-ELISA assay				
		Test compound concentration (μM) + 100 μM NNKAc																				
		0.1	1	5	10	25	50	0.1	1	5	10	25	0.1	1	5	10	25	0.1	1	5	10	25
Phenolic acids	Methyl 4-hydroxy benzoate	N	N	N	N	N	N															
Curcuminoid	Curcumin	N	N	*	*	*	*	N	N	N	*	*	N	N	*	*	*	N	N	*	*	*
Stilbenes	Resveratrol	N	N	N	*	*	*	N	N	N	*	*	N	N	N	*	*	N	N	N	*	*
Sulfur-containing compounds	Sulforaphane	N	N	*	*	*	*	N	N	*	*	*	N	N	*	*	*	N	N	N	*	*
Vitamins	Ascorbic acid	N	N	N	N	N	*															
Carotenoids	Beta-carotene	N	N	N	N	N	N															
FDA approved Nrf2 activator	Dimethyl fumarate	N	N	N	N	*	*	N	N	N	N	*	N	N	N	N	*	N	N	N	N	*

N and * represent non-significant ($p > 0.05$) and significant ($p < 0.05$) effects of tested compounds at selected concentrations on reducing NNKAc-induced ROS or DNA damage in BEAS-2B cells, respectively. The gray area in the table indicates that the parameters have not been determined. Abbreviations: C3G: cyanidin-3-*O*-glucoside, PCA: protocatechuic acid, PGA: phloroglucinaldehyde, NNKAc: 4-[(acetoxymethyl)nitrosamino]-1-(3-pyridyl)-1-butanone, DMSO: dimethyl sulfoxide.

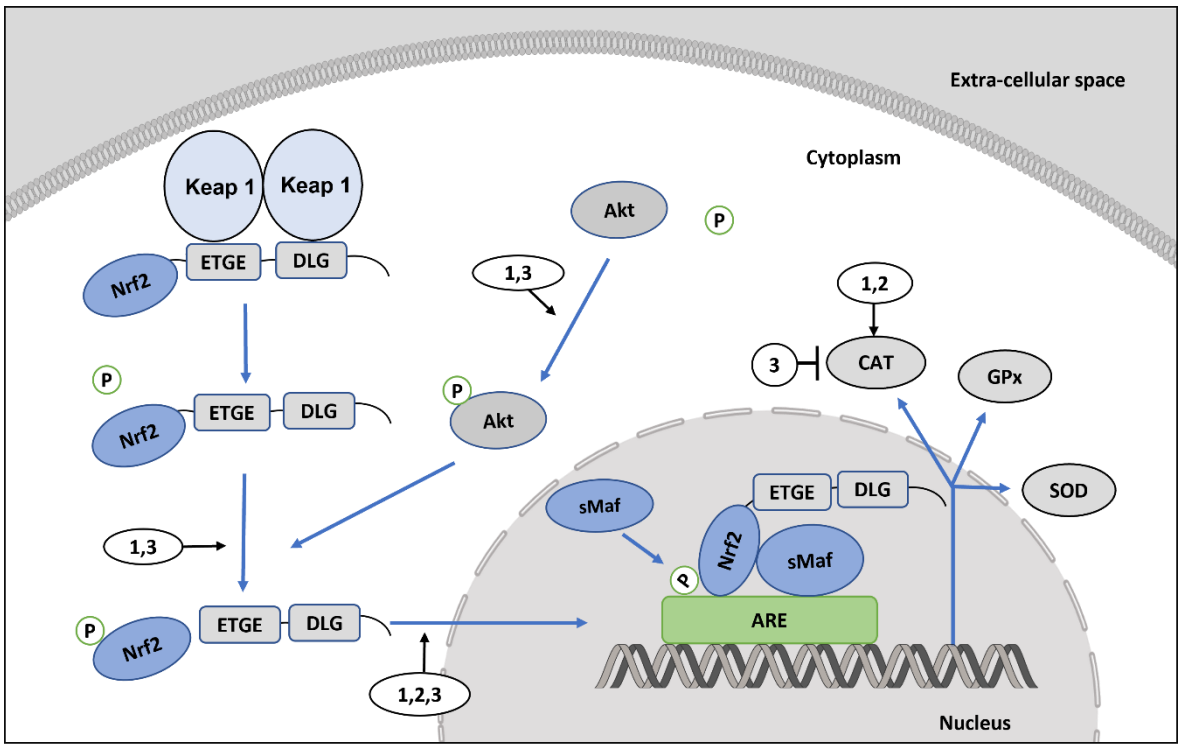

Figure 22: Summary of tested flavonoids on the regulation of Nrf2/ARE pathway in BEAS-2B cells

In BEAS-2B cells, the activation of Nrf2 in terms of Nrf2 phosphorylation (Ser40 residue) and phosphorylation of its upstream kinase Akt at Ser473 residue (non-canonical activator of Nrf2) was promoted by procyanidin B2 (1) treatment alone. Further, BEAS-2B cells treated only with procyanidin B2 (1) or genistein (2) facilitated the phospho-Nrf2 nuclear translocation followed by the increase of catalase activity. Meanwhile, BEAS-2B cells treated with quercetin was not effective in activation of Nrf2/ARE pathway. We tested the potential of flavonoids to activate Nrf2/ARE pathway in a carcinogen (NNKAc) induced BEAS-2B cell model. Interestingly, NNKAc (3) upregulated the Nrf2 phosphorylation, Akt phosphorylation and phosphor-Nrf2 nuclear translocation but reduced the catalase activity in BEAS-2B cells. Pre-treatment of BEAS-2B cells with procyanidin B2 (1), genistein (2), or quercetin prior to carcinogen insult did not significantly effect ($p>0.05$) the Nrf2/ARE pathway activation compared to the BEAS-2B cells treated with NNKAc (3) alone.

Abbreviations: 1: Procyanidin B2, 2: Genistein, 3: NNKAc (4-[(acetoxymethyl)nitrosamino]-1-(3-pyridyl)-1-butanone);, Keap 1: Kelch-like ECH-associated protein 1; Nrf2: Nuclear factor erythroid 2 p45 (NF-E2)-related factor; sMaf: Small musculoaponeurotic fibrosarcoma protein; ARE: Antioxidant response element; GSH: glutathione; SOD: superoxide dismutase; CAT: Catalase; GPx: Glutathione peroxidase; Akt: protein kinase B. (Figure 22 was adapted from Suraweera *et al*., 2020 (198) which was originally adapted from Wu *et al*., 2019 (197))

CHAPTER 5: DISCUSSION

Dietary antioxidants have received increasing interest among scientists, manufacturers, and consumers due to their potential health benefits against many non-communicable diseases. Over the years, dietary polyphenols, particularly flavonoids, have been widely studied and reviewed for their physiological benefits, including their role as antioxidants in cancer chemoprevention (35,198,312–317). In this study, we investigated the efficacy of selected flavonoids in comparison to flavonoid metabolites, phenolic acids, simple polyphenols, stilbenes, curcuminoids, and non-phenolic antioxidants in reducing carcinogen-induced DNA damage in normal lung epithelial BEAS-2B cells. In addition, we also investigated whether the DNA damage reductions observed by the three most effective flavonoids are due to the activation of the antioxidant defense system via the Nrf2/ARE pathway.

5.1 NNKAc-induced normal bronchial epithelial BEAS-2B cell model

The *in vitro* carcinogen-induced normal bronchial epithelial BEAS-2B cell model developed by Amararathna, *et al*., 2020 (35) was used in this study. This carcinogen-induced DNA damage experimental model has been developed taking into account the positive correlation between tobacco smoke and lung cancer (35). Cultured human bronchial epithelial BEAS-2B cells pre-treated with dietary antioxidants were exposed to NNKAc to induce DNA damage. NNKAc mimics the carcinogenic effects of NNK, the strongest nicotine-derived carcinogen present in tobacco smoke (147). For the activation and metabolism of NNK, the activities of CYP enzymes are required but the CYP activity in BEAS-2B cells is low (157). Therefore, the carcinogenic effects of NNK may not be expressed effectively in BEAS-2B cells (157). However, NNKAc is activated in a cellular

environment by esterase enzymes and CYP activities are not required (158). Therefore, to induce cyto- and geno-toxicity in BEAS-2B cells, NNKAc has been successfully used in numerous studies (35,145,146).

5.2 Effects of dietary antioxidants in the reduction of NNKAc-induced ROS in BEAS-2B cells

ROS generation is one of the factors contributing to DNA damage (21,134). In this study, NNKAc treatment generated ROS in BEAS-2B cells. Similarly, ROS generation in BEAS-2B cells upon NNKAc insult under similar experimental conditions has been demonstrated before (35,145). Even though the ROS levels induced by the NNKAc treatment in BEAS-2B cells are significantly higher ($p < 0.05$) than the vehicle control, the observed increase in this study is approximately 20-30%. Intracellular ROS levels in BEAS-2B cells were studied using DCFDA assay. The DCFDA assay detects ROS and reactive nitrogen species (RNS) such as hydroxyl radical, hydrogen peroxide, and nitrogen peroxides but not superoxide radicals (318). NNK generates higher levels of superoxide radicals in BEAS-2B cells (318). Therefore, if NNKAc had generated significant levels of superoxide radicals in BEAS-2B cells, determining levels of ROS are an understatement.

Among the many functional properties of polyphenols, antioxidant activities are widely studied to date (319,320). Mechanisms of antioxidant actions of polyphenols include ROS scavenging, metal ion chelation, inhibition of ROS-generating enzymes, and upregulation of antioxidant defense systems (319,320). The antioxidant activities of flavonoids involve most of the above-mentioned mechanisms including their combinations (321). The arrangement of functional groups in the carbon skeleton of the flavonoids is responsible for the different antioxidant activities of flavonoids (322,323). The number of

hydroxyl groups, configuration, and substitution pattern determines the antioxidant activities (i.e., ROS scavenging and chelating metal ions) of different classes of flavonoids (322,323).

Pretreatment of BEAS-2B cells with flavonoids such as quercetin, cyanidin, procyanidin B2, luteolin, chrysin, naringenin, or genistein except for epicatechin, C3G, phloretin, and phloridzin effectively reduced the NNKAc-induced ROS in BEAS-2B cells in a dose-dependent manner. The employed concentrations of the tested antioxidants were determined based on literature that showed more than 80% cell viability (145,324–344). Among tested antioxidants, only quercetin, luteolin, genistein, or procyanidin B2 were able to reduce the NNKAc-induced ROS at physiologically relevant concentrations (Table 1 and 3) (100,101,113–119,128,129). The ability of flavonoids such as quercetin, luteolin, chrysin, genistein, cyanidin, naringenin, and procyanidin B2 to reduce chemically induced ROS in different experimental models has been very well demonstrated (145,263,345–351). The ability to reduce chemically induced ROS by quercetin, especially in BEAS-2B cells has been also previously demonstrated (145,345). Pratheeshkumar, and colleagues (2016) have demonstrated that pretreatment of quercetin reduces the chromium (VI)-induced hydrogen peroxide in BEAS-2B cells by upregulating the catalase enzyme at physiologically relevant concentrations tested in the current study (116–119,345). Similarly, Merlin, *et al*., 2021 (145) showed that quercetin can reduce NNKAc- and methotrexate-induced ROS levels in BEAS-2B cells at 50 μM (the highest effective concentration tested in the current study). Quercetin is one of the most studied flavonoids, especially with respect to its ability to scavenge ROS, chelate metal ions, and induce signal transduction pathways (i.e., Nrf2/ARE, PI3K/Akt, and mitogen-activated protein kinase

(MAPK)/ Nuclear factor kappa B (NF-κB) signaling pathways, etc.) to exert antioxidant activities in numerous studies (352–355). The structural characteristics such as 3-hydroxyl group (OH) and 2-3 double bond in the C ring conjugated with the 4-oxo group are mainly contributing to the radical scavenging activities of quercetin as evident in numerous quantitative structure-activity relationship studies (352,353,356). The presence of the 4-oxo group and 5-OH group in quercetin are also important for the metal ion chelation (356). Furthermore, blocking or removal of the 3-OH group from the quercetin structure is associated with reduced antioxidant activities (352,353,356). In this study, we also evaluated the effectiveness of two quercetin metabolites (isorhamnetin and quercetin-3-*O*-glucuronic acid), only isorhamnetin was effective at its tested highest concentration. If the scavenging activities of quercetin have been contributing to the reduction of NNKAc-induced ROS in BEAS-2B cells, the inability of quercetin-3-*O*-glucuronic acid to reduce ROS levels may be due to the blocking of the 3-OH group by glucuronide group. Meanwhile, isorhamnetin, the 3′ methylated metabolite of quercetin was able to reduce NNKAc-induced ROS levels at higher concentrations compared to quercetin aglycone. The number and position of OH groups in the B ring are also contributing factors to the antioxidant activity of a flavonoid (353). Quercetin aglycone's 3′ and 4′ hydroxyl groups are associated with higher cellular antioxidant activity demonstrated in hepatocellular carcinoma HepG2 cells (356). The requirement of a higher concentration of isorhamnetin compared to quercetin to reduce NNKAc-induced ROS could be due to blocking the 3′ -OH group of quercetin aglycone by methylation.

In comparison to flavonols such as quercetin, flavones are expected to exert low antioxidant activities in terms of radical scavenging activities (356). In the current study,

chrysin was effective in reducing NNKAc-induced ROS in BEAS-2B cells at comparatively higher concentrations than quercetin. This could be explained by the reduction of cellular antioxidant activity of chrysin due to the lack of hydroxyl groups in the B ring (3′ and 4′ hydroxyl groups) and 3-OH group in the C ring in comparison to quercetin (356). Furthermore, chrysin has also demonstrated its ability to attenuate high glucose-induced ROS levels in bone marrow mesenchymal cells through activation of PI3K/Akt/Nrf2 signaling (254). However, luteolin was able to reduce NNKAc-induced ROS levels at concentrations similar to quercetin. Pratheeshkumar, and colleagues (2014) have also demonstrated that pretreatment of luteolin reduces the chromium (VI)-induced hydrogen peroxide in BEAS-2B cells at effective concentrations tested in the current study (347). Also, the study conducted by Wolfe and Liu, (2008) showed that the ORAC of luteolin and quercetin are approximately similar to each other (356). Therefore, the effectiveness of luteolin at concentrations similar to quercetin may be due to their structural similarities despite not having a 3-OH group in luteolin (356).

As per the quantitative structure-activity relationship (QSAR) studies, both isoflavones and flavanones are known to exert lesser antioxidant activities in comparison to flavonols (352,353,356). Naringenin, a flavanone was effective at higher concentrations compared to quercetin against NNKAc-induced ROS in BEAS-2B cells. This may be due to the comparatively reduced radical scavenging ability of naringenin due to the lack of 2-3 double bond of C-ring, 3-OH, and 3′-OH groups in comparison to quercetin structure (356). Furthermore, naringenin has also demonstrated its ability to attenuate LPS-induced ROS levels in neuron cells isolated from Sprague-Dawley rats through activation of the Nrf2/ARE pathway at concentrations similar to the current study (263). Interestingly,

genistein, an isoflavone tested in this study was found to be much more effective at comparatively low concentrations than quercetin. The ability to scavenge radicals by genistein is largely affected by the attachment of B-ring at 3-position of C ring (357). In general, the radical scavenging capacity of genistein is comparatively lesser than quercetin (357,358). However, the single 4′ -OH in the B ring and 5,7-dihydroxy groups in the A ring of genistein can contribute to the radical scavenging activity (357). Grossini and colleagues (2018) showed that genistein-mediated reduction of hydrogen peroxide-induced ROS levels in human visceral adipocytes was associated with Akt and AMPK activation at concentrations similar to the present study (346). Therefore, the effectiveness of genistein at low concentration in the current study could be due to indirect mechanisms of genistein such as effects on signal transduction pathways in addition to their ability to scavenge ROS.

Cyanidin and C3G (glucoside of cyanidin) are two anthocyanidins tested to study the effects on NNKAc-induced ROS levels in BEAS-2B cells. Anthocyanidins such as cyanidin are as effective as flavonols (i.e. quercetin) in exerting *in vitro* antioxidant activities, mainly through radical scavenging activities as suggested by numerous QSAR studies (352,353,356). The radical scavenging activities of cyanidin are mainly due to the presence of the 3-OH group in the C-ring and 3′, 4′ -dihydroxy group in the B ring in addition to having a central anthocyanidin C-ring in cyanidin which allows conjugation (352). However, in this study, cyanidin was effective in reducing NNKAc-induced ROS in BEAS-2B cells at comparatively higher concentrations. Furthermore, C3G was not effective as its aglycone in reducing NNKAc-induced ROS levels in BEAS-2B cells at tested concentrations. Similarly, a study conducted by Gan, *et al*., 2020 (350) has

demonstrated that cyanidin aglycone is more effective than C3G in reducing myeloperoxidase (an enzyme that catalyzes the ROS generation) and nitric oxide levels against 2,4,6-trinitrobenzene sulfonic acid-induced mice colitis and LPS-induced inflammation in human epithelial colorectal adenocarcinoma Caco-2 cells, respectively. Furthermore, as previously reported the 2,2-diphenyl-1-picrylhydrazyl (DPPH) radical scavenging activity of cyanidin *in vitro* is slightly higher than those of its glucoside at similar concentrations (359). However, in a cellular environment, cell uptake of flavonoid aglycones is generally higher than its glycosides (360). Cyanidin uptake is higher than C3G in human epithelial colorectal adenocarcinoma Caco-2 BBe1 cells (360). The same study further revealed that increased cyanidin uptake is associated with passive diffusion and that C3G uptake was dependent on active transport by hexose transporters sodium/glucose cotransporter 1 and glucose transporter 2 (360). Therefore, the differences in the effectiveness of cyanidin aglycone and its glucoside against NNKAc-induced ROS in BEAS-2B may be due to differences in cellular uptake.

Relative to flavonols such as quercetin, flavanol epicatechin shows lesser antioxidant activities (356,358). In the current study, epicatechin was not effective against NNKAc-induced ROS at tested concentrations. Epicatechin does not contain a 2-3 double bond in the C-ring and 4-oxo group which is important to radical scavenging but contains a 3-OH group and 3′, 4′ -dihydroxy groups in the B-ring (356). Furthermore, epicatechin was associated with weak cellular antioxidant activity in HepG2 cells while flavanols with galloyl group (epicatechin gallate, epigallocatechin gallate) exhibited greater cellular antioxidant activities (356). Among monomeric and dimeric flavanols tested, only procyanidin B2 was effective in reducing NNKAc-induced ROS in BEAS-2B cells. The

study conducted by Zheng, *et al*., 2020 (351) showed that *in vitro* radical scavenging activities of procyanidin B2 in terms of DPPH and 2,2′-azino-bis-(3-ethylbenzothiazoline-6-sulfonic acid (ABTS) radical scavenging activities are greater than epicatechin. The same study further revealed that procyanidin B2 is greatly effective in alleviating oxidative stress induced by D-galactose in Kunming mice (female and male) through expressing antioxidant defense enzymes (SOD, CAT, and GPx) (351). The protective role of procyanidin B2 over epicatechin was further demonstrated in reducing acrylamide-induced ROS in the Caco-2 cell model (361). Furthermore, studies by Steffen and colleagues in 2007 (362) and 2008 (363) suggest that epicatechin metabolites ((−)-epicatechin glucuronide, 3′-*O*-methyl epicatechin, and 4′-*O*-methyl epicatechin) and procyanidin B2 except unconjugated epicatechin prevent the generation of superoxide radical by nicotinamide adenine dinucleotide phosphate (NAD(P)H)-oxidase enzyme inhibition in HUVECs (362,363). These studies further revealed that epicatechin primarily scavenged superoxide radical while procyanidin B2 scavenged superoxide radical in addition to inhibiting NAD(P)H-oxidase activity (362,363). The ability to increase NAD(P)H-oxidase activity and thereby increase superoxide radical levels by cigarette smoke extracts and NNK has previously been demonstrated in human pancreatic ductal HPDE6-c7 cells (364). However, the effects of NNKAc on NAD(P)H-oxidase remain to be explored. The effects of epicatechin and procyanidin B2 on superoxide radicals in the current study may have not been demonstrated as the DCFDA assay cannot measure the superoxide radicals (318). The observed difference between epicatechin and procyanidin B2 in the present study might be due to the strong scavenging activities and ability to upregulate antioxidant defense proteins by procyanidin B2 compared to epicatechin.

Phloretin and phloridzin (glucoside of phloretin) are two chalcones commonly found in apples tested to study the effects on NNKAc-induced ROS levels in BEAS-2B cells. Chalcones containing 3-4 hydroxyl groups such as phloretin and phloridzin are known to exert better antioxidant activities in terms of radical scavenging activities but are less effective than flavanols (i.e., quercetin) (353). Protective effects of phloridzin (i.e., phorbol 12-myristate 13-acetate-induced ROS in bone marrow-derived macrophages isolated C57BL/6JOlaHsd mice and hydrogen peroxide-induced oxidative damage in HepG2 cells) and phloretin (i.e., palmitic acid-induced ROS levels in human umbilical vein endothelial cells and tumor necrosis factor-α (TNF-α)-stimulated ROS levels in BEAS-2B) in reducing chemically induced ROS in different experimental models has been demonstrated previously (333,365–367). In addition to that phloridzin, the glycoside of phloretin, exhibits lower antioxidant activities due to the glycosylation at the 2′-OH group (in the A ring) compared to phloretin and requires a higher concentration to exert a similar effect to phloretin (368). However, both phloretin and phloridzin were not effective in reducing NNKAc-induced ROS in BEAS-2B cells at tested concentrations.

In this study, tested phenolic acids (caffeic acid, chlorogenic acid, methyl-4-hydroxybenzoate, and protocatechuic acid [PCA]) and phloroglucinaldehyde (PGA), aldehyde of PCA, were not effective in reducing NNKAc induced ROS levels in BEAS-2B cells. In comparison to flavonoids, phenolic acids are weak radical scavengers (353). The lower efficiency of phenolic acids compared to flavonoids in scavenging free radicals is mainly due to the lower number of hydroxyl groups present in their structures (1-3 hydroxyl groups) (353). In addition to scavenging ROS, phenolic acids such as caffeic acid, chlorogenic acid, and PCA has demonstrated their ability in exerting antioxidant effects

through indirect mechanisms such as activating antioxidant defense systems, and inhibiting ROS generating enzymes (i.e., caffeic acid and chlorogenic acid inhibit xanthine oxidase) (221,369–374). For example, caffeic acid reduced the hydrogen peroxide-induced ROS levels in human liver L-02 cells through activation of the ERK signaling pathway (369). Bhullar *et al*., 2022 also demonstrated the ability to activate Nrf2 through interactions of caffeic acid and ERK amino acid residues, aspartate (Asp) 106, and methionine (Met) 108 (221). Furthermore, both caffeic acid and chlorogenic acid reduced the hydrogen peroxide-induced ROS generation in Caco-2 cells through hydroxyl groups present in their catechol groups (373). Additionally, Pahlke, *et al*., 2021 (375) demonstrated that PCA was only effective in reducing hydrogen peroxide-induced oxidative stress in human epithelial colorectal adenocarcinoma Caco-2 2BBe1 cells at concentrations greater than 200 μM. In contrast, PGA exhibited a slight reduction in ROS levels at concentrations between 0.01 and 0.1 μM but increased ROS levels at concentrations greater than 5 μM (375). Furthermore, the same study revealed that there were no effects from PCA and PGA on activation of the Nrf2/ARE pathway in hydrogen peroxide-induced Caco-2 2BBe1 cells (375). A similar trend was observed with PGA pretreatment in BEAS-2B cells against NNKAc-induced ROS in the current study, although the results were not significant ($p > 0.05$) (Figure 8). Most *in vitro* studies related to caffeic acid, chlorogenic acid, and PCA have demonstrated their protective effects against chemical-induced ROS production at relatively high concentrations compared to the concentrations tested in the current study (370,373,375). Therefore, to reduce NNKAc-induced ROS in BEAS-2B cells, higher concentrations may be required.

The protective effects of methyl-4-hydroxybenzoate and catechol against cellular ROS stress are generally unclear in the literature. However, methyl-4-hydroxy benzoate is known to exert pro-oxidant effects due to the generation of ROS by autooxidation (376). Methyl-4-hydroxybenzoate exposed to sunlight induces oxidative DNA damage in calf thymus DNA due to ROS generated as a result of catechol autooxidation (376). In contrast, methyl-4-hydroxybenzoate increased ROS levels in male Nile tilapia (*Oreochromis niloticus*) fish (377). The long-term gavage of methyl-4-hydroxybenzoate to Nile tilapia fish has also facilitated adaptive responses through upregulating the expression of antioxidant defense enzymes (catalase, GPx, SOD, and GR) (377). In this study, methyl-4-hydroxybenzoate did not reduce the NNKAc-induced ROS in BEAS-2B cells. Meanwhile, catechol reduced the NNKAc-induced ROS levels in BEAS-2B cells at tested high concentrations (25-50 μM). *In vitro* hydrogen peroxide scavenging activity and DPPH radical scavenging activity of catechol have been demonstrated in QSAR studies (378). Catechol exerts antioxidant activity through two hydroxyl groups present in its ortho positions which allows it to trap ROS such as peroxyl radicals (378,379). Observed reductions in NNKAc-induced ROS levels could be due to the direct antioxidant activities of catechol. However, catechol has also known to generate superoxide radicals because of autooxidation (380).

Curcumin, resveratrol, and sulforaphane showed comparable effectiveness in reducing NNKAc-induced ROS levels in BEAS-2B cells to most of the tested flavonoids despite having different structures. These results were observed at concentrations higher than physiologically relevant concentrations of curcumin, resveratrol, and sulforaphane in humans (381–384). Curcumin, and resveratrol act as antioxidants through different

mechanisms including ROS scavenging, metal ion chelation, and activation of antioxidant defense systems (194,385,385). Curcumin chelates ferrous ions through its hydroxyl and methoxyl or oxo groups similar to the flavonoids with 4-oxo and 5-OH groups (385). Resveratrol chelates ferrous ions through its adjacent two OH groups (386). Radical scavenging activities of curcumin and resveratrol have been further demonstrated in terms of DPPH, hydrogen peroxide, superoxide anion, and ABTS radical scavenging activities (385,385). Curcumin mainly exerted scavenging activities from the active carbon positioned in the methandienone link between two methoxy phenol rings (385). The radical scavenging activities of resveratrol are mainly exerted through the 4′ -OH group (386). Even though sulforaphane has demonstrated weak radical scavenging activities (i.e. DPPH and ABTS), sulforaphane acts as an antioxidant mainly through activation of the Nrf2/ARE pathway (387–390). Curcumin, resveratrol, and sulforaphane have demonstrated their abilities in activating Nrf2 via Keap-1 cysteine (Cys-151) modifications in several clinical trials (Table 2) (194). Kin *et al*., 2020 (263) have demonstrated the ability of curcumin in reducing urban particulate matter-induced ROS levels in human nasal fibroblast cells through upregulation of HO-1 and SOD2 enzymes at concentrations similar to the current study. Similarly, curcumin reduced the benzo[a] pyrene-induced ROS levels in BEAS-2B cells at similar concentrations to the current study (391). Meanwhile, resveratrol also upregulated the HO-1 and downregulated the Keap-1 protein levels against hydrogen peroxide-induced ROS in human rheumatoid arthritis fibroblast-like synoviocytes at concentrations that were effective in the current study (392). Furthermore, sulforaphane activated the Nrf2/ARE pathway in human and rat lens epithelial cells in reducing UV B-induced ROS levels through upregulating peroxiredoxin 6 (Prdx6), catalase and GST

enzymes in a dose-dependent manner at similar concentrations tested in BEAS-2B cells (393). The observed efficacy of curcumin, resveratrol, and sulforaphane in reducing NNKAc-induced ROS levels in BEAS-2B cells could be due to one or more of the above-mentioned direct and/or indirect antioxidant mechanisms.

Beta-carotene is a singlet oxygen quenching carotenoid due to its triplet lysing energy levels near singlet oxygen (394,395). In addition to that beta-carotene has demonstrated its ability to activate the Nrf2/ARE pathway in male, C57BL/6 mice against traumatic brain injury (upregulates mRNA levels of NQO-1 and HO-1 in addition to increasing SOD activity) (396). Furthermore, low concentrations (0.5-1 μM) of beta carotene reduced the *Helicobacter pylori* bacteria-induced ROS in gastric adenocarcinoma cells by suppressing NAD(P)H oxidase activity (397). However, beta-carotene was not effective in reducing NNKAc-induced ROS levels in BEAS-2B cells. The observed result with beta-carotene in NNKAc-induced BEAS-2B cells could be due to the inability of beta-carotene to act on the type of ROS generated by NNKAc during the experiment duration. For a better understanding, the type of ROS generated by NNKAc and the effects of beta-carotene on NNKAc-induced ROS in a time-dependent manner need to be further studied.

DMF is an Nrf2 activator approved by the US-FDA to treat relapsing forms of multiple sclerosis (398). DMF significantly reduced ($p < 0.05$) the NNKAc-induced ROS levels in BEAS-2B cells but at concentrations higher than the physiological concentration in mice (399). The activation of Nrf2 protein is demonstrated in BEAS-2B cells with DMF treatment alone in terms of p-Nrf2/Nrf2 ratio using western blot analysis (Figure 19). DMF exerts its antioxidant effects mainly through activation of the Nrf2/ARE pathway (400). DMF activates Nrf2 protein through modification of Keap 1 cysteine residues such as Cys-

151, Cys-257, and Cys-273 and thereby inhibits the interactions between Keap-1 and Nrf2 protein resulting release of Nrf2 from Keap 1 protein (401). The ability of DMF to induce SOD, HO-1, GST, and catalase enzymes against heme-induced oxidative stress in murine models (NY1DD and HbSS-Townes sickle cell disease mice) of sickle cell disease has been demonstrated before (400). Additionally, DMF upregulated the gene expression of GST, NQO-1, SOD2, sulfiredoxin 1 (Srxn1), and ferritin (Fth1) to alleviate hydrogen peroxide-induced oxidative DNA damage in neural stem/progenitor cells derived from rat embryonic E15-18 pups (402). However, BEAS-2B cells treated with DMF did not show any significant changes ($p > 0.05$) in SOD, CAT, and GPx activities compared to DMSO control (Figure 21). Therefore, reductions of ROS levels and DNA damage in NNKAc-induced BEAS-2B cells need further studies in terms of upregulation of phase 2 detoxification enzyme expression by DMF.

Vitamin C (L-ascorbic acid) is an antioxidant well known to exert cytoprotective effects against oxidative stress through different mechanisms such as ROS scavenging, vitamin E-mediated neutralization of lipid hydroxyperoxyl radicals, and prevention of protein alkylation from electrophilic lipid peroxidation products in addition to Nrf2/ARE pathway activation (281,403). Vitamin C reduced the NNKAc-induced ROS levels in BEAS-2B cells at a physiologically relevant concentration in humans (404–406). Similarly, Merlin, *et al*., 2021 showed that vitamin C reduced the NNKAc-induced ROS levels in BEAS-2B cells at similar concentrations tested in the current study (145). However, most of the tested flavonoids (quercetin, chrysin, luteolin, procyanidin B2, naringenin, cyanidin, and genistein) were much more effective at lower concentrations compared to vitamin C. Similarly, superior antioxidant activities of flavonoids (quercetin,

luteolin, apigenin, and kaempferol) over vitamin C has been previously demonstrated in human lymphocytes in terms of reduction of oxidative DNA damage (407). The protective effects of vitamin C have been previously demonstrated in human pulmonary fibroblast by reducing arsenic trioxide-induced ROS (408). Additionally, vitamin C reduced the UV-B-induced ROS in HaCaT cells through upregulation of catalase and GSH protein levels (409). However, these studies required more vitamin C concentrations than the current study to exert a protective effect against ROS (408,409). The protective effects observed in this study by vitamin C could be due to its ability to scavenge ROS or indirect mechanisms such as upregulation of antioxidant defense enzymes. To assess the effects of vitamin C on the antioxidant defense system in NNKAc-induced BEAS-2B cells, further studies are required.

5.3 Effects of dietary antioxidants on BEAS-2B cell viability

Following the screening of 25 antioxidant compounds for ROS assay, the compounds that reduced NNKAc-induced ROS levels at concentrations equal to or lesser than 25 μM were selected for further studies. The studies of cell viability of selected test compounds from ROS assay and NNKAc revealed that tested concentrations were not cytotoxic to BEAS-2B cells. Test compounds maintained more than 80% cell viability in BEAS-2B up to 25 μM concentration under the experimental conditions (Appendix 1 and 2).

5.4 Effects of dietary antioxidants in the reduction of NNKAc-induced DNA damage in BEAS-2B cells

The protective effects of selected flavonoids (quercetin, luteolin, chrysin, naringenin, genistein, cyanidin, and procyanidin B2), DMF, curcumin, sulforaphane,

resveratrol, and catechol in reducing NNKAc-induced DNA damage in BEAS-2B cells was studied. DNA damage was assessed using γ-H2AX immunofluorescence, alkaline comet, and DNA fragmentation ELISA assays since altered genetic stability is considered an early event in carcinogenesis (139,141). NNKAc cellular metabolism causes DNA damage, which can be characterized by DNA adduct formation and strand breaks (35,145,146,158). In this study, DNA damage in BEAS-2B cells was induced by NNKAc (100 μM) as observed by γ-H2AX immunofluorescence, comet and, and DNA fragmentations-ELISA assays (35,145,146). Post-translational modifications of histone H2AX are an early event of DNA DSBs (410). γ-H2AX foci in the nucleus are a measurement of DNA DSBs (411). Pre-treatment of BEAS-2B cells with test compounds reduced the NNKAc-mediated histone variant reorganization which regulates the DNA methylation (310). This could have resulted in the observed similarities between reduced levels of NNKAc-induced γ-H2AX foci and DNA fragmentation levels with pre-treatment of test compounds (146). DNA fragmentation is an irreversible phenomenon that leads to cell death (310). The levels of DNA fragmentation seen in untreated BEAS-2B cells could be due to normal cellular homeostatic mechanisms to remove large DNA fragments from dying cells (412). The alkaline comet assay is used to measure the effects of carcinogenic substances such as NNKAc on both DNA DSBs and SSBs (413). NNKAc can damage all DNA bases (DNA base damage potential: guanine > adenine > cytosine > thymine) by forming bulky POB-DNA adducts and causes both SSBs and DSBs (145,414). Additionally, NNK induces oxidative DNA lesions (415). The study by Xu, *et al*., 1992 showed increased levels of 8-oxodeoxyguanosine in female A/J mice and male F344 rat models with NNK treatment (415). However, there is no sufficient evidence of NNKAc-

induced oxidative DNA damage in the literature. Therefore, levels of oxidative DNA damage markers such as 8-oxodeoxyguanosine with NNKAc treatment in BEAS-2B cells need to be explored.

Polyphenols exert cancer chemoprevention through mechanisms such as modulation of phase 1/2 enzymes, inhibition of DNA damaging proteins, and activation of DNA damage repair pathways in addition to their direct and indirect antioxidant activities (20). The effects of phenolic compounds, including flavonoids on DNA damage response (DDR) mechanisms, have been demonstrated in numerous studies (20,416–418). Activation of proteins such as *γ*-H2AX, ataxia-telangiectasia mutated protein (ATM), ataxia telangiectasia and rad 3-related protein (ATR), checkpoint kinase 1 (Chk1), checkpoint kinase 2 (Chk2), breast cancer gene 1 (BRACA1) and tumor protein p53 are observed with cells showing DNA damage and replication stress (418). Merlin *et al*., 2021 (145) have previously demonstrated that NNKAc treatment in BEAS-2B cells activated ATR/ Chk1 signaling and initiates the DNA damage repair through p53/ BRACA1/ *γ*-H2AX signaling which facilitates DNA repair via homologous recombination. Furthermore, the same study revealed that quercetin together with a vitamin-containing antioxidant formula consisting of ascorbic acid, lipoic acid, beta-carotene, folate, and N-acetyl cysteine significantly reduced ($p < 0.05$) the activation of ATR/Chk1 signaling and phosphorylation of DDR proteins (145). Similarly, George and Rupasinghe, 2017 showed that pretreatment of apple flavonoid fraction 4 rich with phloridzin, epicatechin, chlorogenic acid, cyanidin-3-*O*-galactoside, and quercetin glycosides with BEAS-2B cells reduced the NNKAc-induced DNA damage through downregulation of ATR/Chk1 signaling and initiating DNA repair mechanisms (146). Therefore, to better understand the

cancer preventive effects of test compounds in addition to studying their antioxidant mechanisms, studying their effects on DDR mechanisms against NNKAc-induced DNA damage is also important.

Luteolin, chrysin, cyanidin, and non-flavonoid compounds curcumin in the current study were able to reduce the NNKAc-induced DNA damage in terms of both DNA DSBs and SSBs (alkaline comet assay) and DNA fragmentation levels at concentrations that reduced the NNKAc-induced ROS levels. However, for the significant reduction ($p < 0.05$) of NNKAc-induced phosphorylated γ-H2AX foci in BEAS-2B, comparatively higher concentrations of luteolin, chrysin, and curcumin were required. Furthermore, a significant reduction ($p > 0.05$) in NNKAc-induced phosphorylated γ-H2AX foci was not observed with cyanidin at the tested concentrations ($p > 0.05$). The observed differences between the comet and γ-H2AX immunofluorescence assays could be due to the effectiveness of chrysin, luteolin, cyanidin, and curcumin in reducing NNKAc-induced DNA SSBs at comparatively low concentrations. Since, the alkaline comet assay quantifies both SSBs and DSBs, to study the effects of chrysin, luteolin, cyanidin, and curcumin, the neutral comet assay that quantifies the DSBs should be further studied (419). Furthermore, DNA protective effects of compounds such as luteolin, chrysin, cyanidin, and curcumin against numerous carcinogenic factors via different mechanisms have been previously reported in numerous studies (420–423). For example, luteolin reduced UV B-induced DNA damage and ROS generation in human keratinocyte HaCaT cells through UV absorbent, and antioxidant activities (radical scavenging activities) (420). Chrysin (oral administration) is effective in reducing doxorubicin-induced oxidative DNA damage in male Wistar albino rat testes through upregulating catalase and GSH levels (423). Cyanidin demonstrated its

ability to reduce the lysine/methylglyoxal-induced oxidative DNA damage with or without the presence of copper ions in pUC19 plasmid derived from *Escherichia coli* through methylglyoxal trapping and radical scavenging activities (superoxide and hydroxyl radicals) (422). Meanwhile, oral intake of 500 mg twice/ day of curcumin reduced the oxidative DNA damage caused by chronic exposure to arsenic through DNA damage repair mechanisms (non-homologous end joining and base excision repair pathways) in a clinical study carried out with 116 human subjects who live in West Bengal in India (421).

Furthermore, naringenin, procyanidin B2, and non-flavonoids such as DMF, resveratrol, catechol, and sulforaphane demonstrated reduced DNA damage determined by γ-H2AX, comet, and DNA fragmentation ELISA assays at concentrations similar to the concentrations that reduced NNKAc-induced ROS levels significantly ($p < 0.05$). Similarly, pre-treatment of naringenin to splenocytes derived from Swiss albino mice reduced the ionization radiation-induced ROS generation through ROS scavenging (424). Furthermore, the same study showed that reduction of ionization-induced oxidative DNA damage was associated with the reduction of DNA-dependent protein kinases (DNA-PK) and phosphorylated-γ-H2AX (424). Procyanidin B2 reduced the oxidative DNA damage induced by hydrogen peroxide in terms of reduction of 8-oxo-7,8-dihydro-2′-deoxyguanosine in human leukemia HL-60 cells (425). Co-treatment of resveratrol with house dust mites reduced the house dust mites induced-ROS generation and oxidative DNA damage in human bronchial epithelial 16HBE cells (426). However, the underlying mechanism of ROS and DNA damage reduction in this study is not studied (426). The study conducted by Ding, *et al*., 2010 showed that sulforaphane reduced the 4-aminobiphenyl-induced DNA damage in human bladder RT4 cells through activation of

the Nrf2 signaling pathway (427). The protective effects of sulforaphane were observed due to the transactivation of ARE-driven phases 2 detoxifying proteins such as NQO-1 and glutamate cysteine ligase (427). Furthermore, in the current study, both genistein and quercetin were able to reduce the NNKAc-induced DNA damage at concentrations lesser than the concentrations that reduced ROS levels in NNKAc-induced BEAS-2B cells significantly ($p < 0.05$). Quercetin has previously demonstrated its ability to repair oxidative DNA damage induced by hydrogen peroxide in terms of reducing human 8-oxoguanine DNA glycosylase mRNA levels in Caco-2 cells at physiologically relevant concentrations tested in the current study. The same study further suggested that the time-dependent reduction in DNA damage was independent of the direct antioxidant activities of quercetin on hydrogen peroxide (428). Therefore, the effectiveness of both quercetin and genistein in reducing the DNA damage at concentrations lesser than the concentrations reduced ROS levels could be due to the effects of quercetin and genistein on mechanisms such as activation of DNA damage repair pathways.

Inhibition of esterase enzyme and detoxification of NNKAc and/or its electrophilic metabolites could play a pivotal role in reducing NNKAc-induced ROS generation and DNA damage (158,161,429,430). Activation of NNKAc into its carcinogenic forms is catalyzed by esterase enzymes (158). Chieli *et al*., 2009 previously demonstrated the *in vitro* inhibitory effects of polyphenols from mango bark extract, quercetin, mangiferin, gallic acid, and catechin on pure rabbit liver esterase enzymes (431). However, effects on esterase enzymes by polyphenols are limited to date. Therefore, the effects of the dietary antioxidants on esterase enzymes should be further investigated to better understand the reduction of NNKAc-induced ROS and DNA damage in BEAS-2B cells. Upregulation of

phase 2 detoxifying enzymes by flavonoids could play a pivotal role in reducing the ROS and DNA damage caused by NNKAc and/or its electrophilic metabolites (161,429,430). NNKAc generates similar electrophilic metabolites to the metabolites generated from α-methyl hydroxylation of NNK by CYP enzymes (152–155). Phase 2 enzymes are involved in the detoxification of NNK and/or its electrophilic metabolites (161). For example, glucuronidation of NNAL which is produced from carbonyl reduction of NNK is catalyzed by uridine 5′-diphospho-glucuronosyltransferase (UGT) (432). Glutathione-S-transferases (GST) are involved in the removal of electrophilic metabolites by conjugating to glutathione (433). Polyphenols have demonstrated the ability to upregulate phase 2 enzymes such as UGT and GST before (429,430). Quercetin has previously demonstrated its ability to upregulate UGT expression in Caco-2 cells (protein levels) and human intestinal tissues (mRNA levels) (434,435). Oral gavage of Cranberry extracts enriched with proanthocyanins and anthocyanins increased the UGT enzyme activity in hepatic tissues of male Wistar rats (429). Non-flavonoids such as resveratrol increased the UGT mRNA levels in Caco-2 cells (430). Furthermore, dietary intake of curcumin or quercetin increased the UGT activity in male Wistar rats (436). Meanwhile, anthocyanins such as cyanidin, peonidin, and delphinidin induce GST activity in rat hepatic Clone 9 cells (437). Chrysin (intraperitoneal administration), a flavone upregulates the GST activity in streptozotocin-induced diabetic Wistar albino rats (male) (438). Furthermore, flavanols such as epigallocatechin gallate, epicatechin gallate, and epigallocatechin upregulated the GST activity against benzo[*a*]pyrene-diol epoxide-induced DNA damage in BEAS-2B cells (439). However, the mechanisms involved in detoxification of NNKAc and its

metabolites are yet to be explored and the effects of test compounds on phase 2 enzymes such as UGT and GST against NNKAc insult in BEAS-2B need to be further studied.

5.5 Effects of quercetin, genistein, and procyanidin B2 on regulation of Nrf2/ARE pathway

The activation of Nrf2/ARE pathway plays a significant role in the prevention of DNA damage and possible carcinogenesis by managing oxidative stress via the expression of antioxidant defense enzymes and phase 2 detoxifying enzymes (25,184). The effects of quercetin, genistein, and procyanidin B2 on Nrf2/ARE signaling was further investigated to determine if the observed ROS and DNA damage reductions are due to activation of the Nrf2/ARE pathway. From the studies on reductions in NNKAc-induced DNA damage in BEAS-2B cells, quercetin, genistein, and procyanidin B2 were effective in reducing NNKAc-induced ROS and DNA damage in lower concentrations compared to other tested compounds. Therefore, the effects of selected compounds on Nrf2 and its upstream kinase Akt phosphorylation, p-Nrf2 nuclear translocation, and antioxidant defense enzyme activities (SOD, catalase, and GPx) were studied.

In general, the Nrf2/ARE pathway is activated by oxidative stress (25,31). However, Nrf2 protein can be activated from both canonical and non-canonical mechanisms (Table 2) (192,193,193,194). Akt is an upstream regulatory protein (non-canonical activator) that plays an important role in cell survival, cell proliferation, cell growth, cell metabolism, and angiogenesis in a cellular environment (440,441). Phosphorylated Akt (p-Akt) activates Nrf2 protein by phosphorylating Nrf2 (p-Nrf2) at Ser40 residue (440,442–444). Phosphorylation of Ser473 residue is facilitated by either mammalian target of rapamycin (mTOR) 2 or DNA-PKs while Threonine (Thre) 308 is

phosphorylated by upstream kinases such as PI3K (441,445,446). Zheng *et al*., 2018 demonstrated that activation of Akt-Nrf2 signalling protects rat embryonic ventricular H9c2 cells from oxygen glucose deprivation/re-oxygenation exposure (444). The same study demonstrated that protective effects were associated with Akt phosphorylation at Ser473 and Nrf2 phosphorylation at Ser40 and the blockage of Akt phosphorylation at Ser473 blocked the Nrf2 phosphorylation at Ser40 and the expression of HO-1 (444). Furthermore, Gong *et al*., 2016 showed that Akt-Nrf2 signaling is important for retinal pigment epithelial cell survival against UV-induced oxidative stress and apoptosis (440). The same study showed that cytoprotective effects of activation of the Nrf2/ARE pathway and upregulation of cytoprotective enzymes such as NQO-1 and HO-1 were associated with p-Akt (Ser473) mediated phosphorylation of Nrf2 protein at Ser40 (440). Li and colleagues (2016) also demonstrated the UV protective effects in human retinal pigment epithelial cells through upregulated levels of p-Akt (Ser473), which facilitated the Akt/mTORC1/Nrf2/HO-1 signaling (442). However, both Gong *et al*., 2016 and Li *et al*., 2016 have used Ser40 to threonine mutation of Nrf2 to demonstrate that Ser40 phosphorylation of Nrf2 is required for the expression of its downstream target proteins (440,442). However, there is no evidence on Ser40 to threonine mutation to be considered as a dominant negative mutation as it is a synonymous mutation to Ser40, which is still a substrate for Akt (447).

DMF and hydrogen peroxide were used as positive controls to study their effects on activation of Nrf2/ARE pathway in BEAS-2B cells. BEAS-2B cells treated only with positive controls, DMF, or hydrogen peroxide did not exhibit a significant ($p > 0.05$) increase ($p < 0.05$) of p-Akt/Akt ratio despite hydrogen peroxide treatment showing higher

levels of p-Akt/Akt ratio compared to DMSO control. In contrast, the p-Nrf2/Nrf2 ratio of cells treated with DMF, or hydrogen peroxide showed an increase compared DMSO control but not NNKAc-treated cells. As discussed previously, DMF activates Nrf2 protein through canonical mechanisms such as modification of Keap 1 Cys residues (401). Therefore, the DMF-mediated Nrf2 activation could be independent of Akt phosphorylation. However, Nrf2 phosphorylation at Ser40 can also be mediated by PKC (448). Moreover, the hydrogen peroxide-mediated phosphorylation of Nrf2 protein could be dependent on Akt phosphorylation. Zhuang, *et al*., 2019 have previously demonstrated the upregulation of p-Akt (Ser473), nuclear Nrf2 levels, and cellular HO-1 protein levels against hydrogen peroxide treatment in intestinal epithelial IEC-6 cells (449). However, the Akt phosphorylation can be bi-phasic with time which depends on the type of cell and the activator as demonstrated previously (450,451). Furthermore, increased levels of nuclear-translocated p-Nrf2 were observed with hydrogen peroxide and DMF similar to the NNKAc. The increased levels of nuclear p-Nrf2 could be due to the Nrf2 phosphorylation followed by stabilization which suppresses the Nrf2 ubiquitination mediated degradation (187,194). Interestingly, exogenous hydrogen peroxide substantially upregulated the catalase and GPx activities but SOD activity in BEAS-2B cells. Antioxidant defense enzymes such as catalase and GPx are known to neutralize cellular hydrogen peroxide levels by converting them into water (172,177). However, to maintain the catalytic activity of GPx, several cofactors (reduced glutathione, and NAD(P)H) and glutathione reductase are required (172,177). The ability of hydrogen peroxide to upregulate antioxidant defense enzymes (i.e. catalase) has been previously demonstrated at comparatively low concentrations (< 50 μM) (452,453). However, at higher

concentrations, reduced levels of antioxidant defense enzyme levels have been reported in numerous studies (449,454,455). Meanwhile, DMF treatment maintained the SOD, catalase, and GPx activities in BEAS-2B cells at basal levels which indicates that DMF does not affect the redox balance under normal physiological conditions.

In this study, the effects of quercetin, genistein, and procyanidin B2 on phosphorylation of Akt at Ser473 were studied. BEAS-2B cells treated only with quercetin or procyanidin B2 at the tested highest concentration (25 μM) exhibited a higher level of p-Akt/Akt ratio. However, higher levels of p-Akt/Akt ratio observed with quercetin were not significantly different ($p > 0.05$) from the DMSO control. Lee and colleagues (2011) demonstrated that quercetin decreased cell viability (even at concentrations less than 20 μM) and p-Akt levels in BEAS-2B cells compared to the control cells (261). However, this result was based on visual observations using western blot bands consisting of inconsistent bandwidths and intensities (261). Furthermore, reduced cell viabilities are associated with downregulation of Akt mediated cell survival (261). However, the findings of the study conducted by Lee and colleagues in 2011 (261) are contradictory to the current study since BEAS-2B cell viability was not affected at tested concentrations in addition to the observed no difference ($p > 0.05$) in p-Akt/Akt ratio. Supporting the findings of our study, Merlin, *et al*., 2021 have demonstrated that BEAS-2B cells treated with quercetin up to 100 μM (> 95% cell viability) do not affect the cell viability (145). Furthermore, quercetin does not affect the human oral keratinocyte cell viability up to 100 μM and upregulates the PI3K/Akt pathway to attenuate the LPS-induced cell injury (456).

However, the inhibitory effects of flavonoids such as quercetin on Akt protein have been demonstrated in numerous studies at different concentrations, experimental models

(cell and preclinical models), and treatment times which are mostly associated with reduced cell viabilities (261,457–459). Furthermore, the Akt inhibitory activities of flavonoids can be varied due to their structural differences (460). For example, the downregulation of Akt (Ser473) phosphorylation in human endothelial EA.hy926 cells is associated with the presence of the C2=C3 double bond in the C-ring, hydroxylation at 5, 6, and 7 positions in the A-ring, hydroxylation at 3′ and 4′ positions in B-ring in flavones and flavonols (460). However, the presence of a hydroxyl group at 3 positions in the C-ring (i.e. quercetin) and glycosylation of flavonoids suppress the inhibitory effects on Akt phosphorylation (460). Therefore, inhibitory effects that were not observed with quercetin in the current study could be due to the presence of the 3-OH group in the C-ring (460). Similarly, the monomer of procyanidin B2 (epicatechin) contains a 3-OH group, and it lacks a C2=C3 double bond but contains 4′ OH and 5-OH groups. In the current study, inhibitory effects on Akt phosphorylation with procyanidin B2 treatment were not observed but the p-Akt/Akt ratio was increased at the tested highest concentration. Similarly, upregulation of p-Akt (Ser473 and Thre308) with procyanidin B2 treatment in human umbilical vein endothelial cells at physiological conditions has been reported previously (461). In comparison, genistein also has functional groups similar to flavones and flavonols which exert down regulatory effects on Akt phosphorylation (i.e., C2=C3 double bond, 4′ OH and 5-OH group). However, Dirimanov and Högger, 2019 did not find any inhibitory effects on p-Akt (Ser473) with genistein treatment in human endothelial EA.hy926 cells (460). This could be due to the presence of the B ring at the 3 position of the C-ring which requires further studies. In our study, even though genistein showed a non-significant ($p > 0.05$) increase in the p-Akt/Akt ratio at the tested lowest concentration, it was found to be reducing the increased levels

back to basal levels at tested highest concentration. The observed dose-dependent reductions of p-Akt/Akt levels with genistein treatment can be explained by the homeostatic effects of genistein reported previously (331).

The ability of quercetin, genistein, and procyanidin B2 to activate the Nrf2/ARE pathway has been previously demonstrated in numerous experimental models (Table 2) (229,259,269–271). In this study, both quercetin and genistein treatments alone did not increase the p-Nrf2/Nrf2 ratio in BEAS-2B cells significantly ($p > 0.05$). In contrast, procyanidin B2 treatment alone was effective in increasing the p-Nrf2/Nrf2 ratio. Similar to the current study, procyanidin B2 has previously demonstrated its ability to upregulate Nrf2 proteins through upregulation of p-Akt levels in alleviating cypermethrin-induced oxidative stress in cerebral cortical neurons of C57BL/6 mice (229). Similar upregulation of Nrf2 at translational and/or transcriptional levels has been previously demonstrated by genistein in different experimental models (oral administration: male C57BL/6 mice and HY-line brown laying hens, and intraperitoneal administration: pentylenetetrazol-induced male Sprague-Dawley rats (Table 2) (269–271). Furthermore, the up regulatory effects of quercetin on Nrf2 protein expression (time-dependent), Nrf2 nuclear translocation, and HO-1 protein expression in BEAS-2B cells have been previously demonstrated (261). In our experimental model, BEAS-2B cells treated with quercetin were not effective in p-Nrf2 nuclear translocation and antioxidant defense enzyme activities. Therefore, the inability of quercetin to activate the Nrf2/ARE pathway effectively in BEAS-2B cells could be due to the time-dependent effects of quercetin. However, in the literature, reported effects on Nrf2 activation by quercetin, genistein, and procyanidin B2 were mostly limited to studying the total Nrf2 protein and/or mRNA levels (229,259,269–271).

In comparison to quercetin, both genistein and procyanidin B2 were able to upregulate the Nrf2 nuclear translocation and catalase activity in BEAS-2B cells. Since genistein and procyanidin B2 facilitated the p-Nrf2 nuclear translocation, the mechanisms of genistein and procyanidin B2 that facilitate Nrf2 nuclear translocation should be further investigated. GSK3β is a serine/threonine kinase that phosphorylates Nrf2 at Ser335 and Ser338 (mouse sequence) in the Neh6 domain which facilitates Nrf2 nuclear export in addition to the Nrf2 degradation (187). In contrast, AMPK facilitates Nrf2 nuclear translocation through phosphorylation of Nrf2 at Ser558 which improves the Nrf2 stability (195,196). As previously discussed, genistein-mediated reduction of hydrogen peroxide-induced ROS levels in human visceral adipocytes was associated with activation of Akt and AMPK (346). Therefore, the effects of genistein and procyanidin B2 on inhibition of GSK3β and upregulation of AMPK should be further studied. As described previously, Nrf2 activation can be facilitated by PKC (448). Li, *et al*., 2018 showed that a methyl derivative of genistein (7-*O*-methylbiochanin A) mediated Nrf2 activation and upregulation of NQO-1 protein levels are associated with the activation of PI3K, MAPK, PKC, and PERK pathways (462). Joo, *et al*., 2016 also suggested that PKC and AMPK could have a complementary effect on Nrf2 activation and nuclear translocation *in vitro* (195). Since a substantial effect on p-Akt level in genistein-treated BEAS-2B cells was not observed, the effects of genistein on PKC should be further investigated in a time-dependent manner.

The presence of a catechol group and higher oxidation potential of flavonoids are associated with the activation of Nrf2/ARE pathway and expression of phase 2 detoxifying enzymes such as HO-1 (463). Oxidation of catechol-containing flavonoids generates

quinones that can act as electrophilic compounds (463). Thereby, generated quinones can activate Nrf2 protein via Keap 1 cysteine residue modification (463). Quercetin and procyanidin B2 (and its monomer) contain catechol groups (463). Both quercetin and epicatechin, the monomer of procyanidin B2 have higher oxidation potential (463). Procyanidin B2 has demonstrated its ability to undergo autooxidation via conversion of catechol into quinone in primary cerebellar granule neurons harvested from 7-day-old Sprague-Dawley rat pups (both males and females) (464). Catechol groups can generate superoxide radicals through autooxidation (380). Later generated superoxide radicals can be converted to hydrogen peroxide by endogenous SOD (465,466). Furthermore, as reported previously, pyrogallol and pyrocatechol, two catechol-containing metabolites of proanthocyanidins generate hydrogen peroxide in cell-free culture media such as bronchial epithelial growth medium and minimum essential medium Eagle in a dose-dependent manner (467). Therefore, increased catalase enzyme activity in BEAS-2B cells could be due to the accumulated hydrogen peroxide in cell culture media induced activation of Nrf2 or the canonical activation of Nrf2 by electrophilic compounds generated from procyanidin B2 autooxidation. In comparison to procyanidin B2, genistein does not contain a catechol moiety in its structure. Compared to catechins, the oxidation potential of isoflavones is comparatively low (463). However, to better understand the effects of genistein and procyanidin B2 in upregulating the Nrf2/ARE pathway with special emphasis on catalase activity increase, the time-dependent effects of genistein and procyanidin B2 on hydrogen peroxide production in BEAS-2B cells and cell-free culture media should be further studied. Additionally, the effects of procyanidin B2, genistein, and their metabolites on

Keap-1-Nrf2 interactions should be further studied using molecular docking techniques to unveil other possible mechanisms of Nrf2/ARE activation.

BEAS-2B cells treated with NNKAc upregulated the Nrf2/ARE pathway by increasing p-Akt /Akt and p-Nrf2/Nrf2 ratios and p-Nrf2 nuclear translocation. However, NNKAc treatment significantly reduced ($p < 0.05$) the activities of antioxidant defense enzymes (SOD, catalase, and GPx). The higher percentage of cell viability (> 80%) observed with NNKAc-treated BEAS-2B in this study could be due to the increased cell survival due to p-Akt mediated mechanisms such as suppression of cell apoptosis (440). Meanwhile, a dose-dependent non-significant reduction ($p > 0.05$) of NNKAc-induced p-Akt/Akt and p-Nrf2/Nrf2 ratios and subsequent p-Nrf2 nuclear translocation was observed in BEAS-2B cells pretreated with quercetin, genistein, or procyanidin B2. Furthermore, George and Rupasinghe, 2017 demonstrated that NNKAc can upregulate DNA-PK levels in BEAS-2B cells under similar experimental conditions (146). Therefore, the phosphorylation of Akt at the Ser473 position could be mediated by NNKAc-induced DNA-PK expression due to the activation of DDR mechanisms (445). The same study further revealed that the reduction of NNKAc-induced DNA damage is associated with reduced expression of DNA-PK and other DDR proteins (146). Therefore, the observed reduction of p-Akt/Akt ratio with quercetin, genistein, and procyanidin B2 pre-treatment against NNKAc insult in BEAS-2B cells could be due to the reduction of DNA damage or facilitation of DNA damage repair by tested flavonoids. However, the mechanisms of NNKAc-dependent activation of Akt are yet to be explored even though NNK upregulates PI3K/Akt mediated cell survival, cell proliferation, and suppression of cell apoptosis in lung epithelial cells through inhibiting caspase 9 expression (161).

In addition to activation of Nrf2 by effects of NNKAc on Akt protein or its upstream kinases, Nrf2 can be activated through NNKAc-mediated canonical mechanisms as electrophilic compounds and ROS can activate the Nrf2 through modifying Keap 1 cysteine residues either by alkylation or oxidation (192–194). Therefore, NNKAc-induced ROS and the electrophilic metabolites generated during NNKAc cellular metabolism could influence the Nrf2 activation (156,161–163). Furthermore, increased levels of ROS observed with NNKAc-induced BEAS-2B cells could be due to the reduced SOD, catalase, and GPx enzyme activities observed in the current study. Agreeing with our results, George and Rupasinghe, 2017 have also demonstrated the inhibitory effects of NNKAc on SOD, catalase, and GPx at protein levels in BEAS-2B cells (146). Therefore, observed non-significant ($p > 0.05$) dose-dependent reductions of p-Nrf2/Nrf2 ratios and subsequent p-Nrf2 nuclear translocation with pre-treating BEAS-2B cells with quercetin, genistein, or procyanidin B2 could be due to mechanisms involved in the reduction of ROS levels (ROS scavenging), reduction of Akt phosphorylation (via reducing the expression of DNA-PK), expression of phase 2 detoxification enzymes, and inhibiting esterase enzyme. However, to confirm these predictions, further studies are required.

Pre-treatment of quercetin, genistein, or procyanidin B2 was not effective in upregulating the NNKAc-reduced catalase activity but increased the NNKAc-reduced SOD activity ($p > 0.05$). Also, cells pre-treated with quercetin, genistein or procyanidin B2 dose-dependently reduced GPx activity with the presence of NNKAc treated cells but not significantly ($p > 0.05$). However, BEAS-2B cells treated only with genistein or procyanidin B2 demonstrated a higher catalase activity at 25 μM. Additionally, a slight increase of NNKAc-reduced catalase activity in BEAS-2B cells pre-treated with quercetin

(only at 1 μM), genistein, and procyanidin B2 was observed which is significantly not different ($p > 0.05$) from the DMSO control. In comparison, NNKAc-reduced SOD activities were also found to be increased up to levels of DMSO with quercetin, genistein, or procyanidin B2 pre-treatment despite not having a significant difference ($p > 0.05$) among any treatment group. Similarly, Manna and colleagues (2015) demonstrated the ability of naringenin to partially restore the antioxidant defense proteins (SOD, catalase, and GSH) to basal levels against gamma radiation-induced oxidative DNA damage in murine splenocytes (424). The same study demonstrated that murine splenocytes treated with naringenin alone depicted a non-significant dose-dependent increase of SOD, catalase, and GSH protein levels as observed with procyanidin B2 and genistein in increasing catalase activity in BEAS-2B cells (424). Furthermore, Manna, *et al*., 2015 further revealed that gamma-irradiation-induced ROS levels and oxidative DNA damage were attenuated through scavenging ROS, DDR mechanisms, suppressing gamma-irradiation-induced cell cycle arrest and inflammation, and so forth (424). Therefore, the reduction of NNKAc-induced ROS and DNA damage in BEAS-2B cells by tested polyphenols including quercetin, genistein, and procyanidin B2 could involve multiple cellular mechanisms. Furthermore, in this study, the protective effects of dietary flavonoids in reducing NNKAc-induced ROS and DNA damage in terms of activation of Nrf2/ARE pathway is not clear which requires further studies.

CHAPTER 6: CONCLUSION

The investigated flavonoids, genistein, quercetin, luteolin, chrysin, cyanidin, naringenin, and procyanidin B2, flavonoid metabolites (isorhamnetin), simple polyphenols (catechol), stilbenes (resveratrol), curcuminoids (curcumin), and non-phenolics (sulforaphane and DMF) protected normal lung epithelial BEAS-2B cells from *in vitro* carcinogen insult. Evaluation of the most effective flavonoids (quercetin, genistein, and procyanidin B2) on the mechanisms involved in protecting BEAS-2B cells revealed that genistein and procyanidin B2 but not quercetin activated the Nrf2/ARE pathway. The procyanidin B2 mediated activation of the Nrf2/ARE pathway in terms of Nrf2 phosphorylation could be associated with the phosphorylation of Akt. Both genistein and procyanidin B2 upregulated p-Nrf2 nuclear translocation and catalase activity in BEAS-2B cells. However, pre-treatment of BEAS-2B cells with tested flavonoids showed that inhibitory effects of carcinogen insult on antioxidant defense enzyme activities cannot be restored. However, further studies are required to confirm the role of the Nrf2/ARE pathway in exerting protective effects on NNKAc-induced BEAS-2B cells.

Future studies should be designed to study the mechanisms involved in protecting BEAS-2B cells against carcinogen insult while addressing the limitations of this research. The safe doses of tested compounds were determined using reported values in the scientific literature due to the higher number of compounds screened in this study and the time-dependent effects of dietary antioxidants were not studied. The present experimental model should be improved to study the time-dependent effects of flavonoids in exerting their protective effects. The interactions between test compounds and cell-free culture media should be also studied with respect to the generation of ROS. Even though NNKAc mimics

the carcinogenic effects of NNK, a tobacco smoke carcinogen, it does not reflect the full spectrum of NNK-mediated carcinogenic effects on lung epithelial cells. Therefore, an NNK-induced animal experimental model can be suggested to study the effects of dietary flavonoids in exerting protective effects against the tobacco carcinogen. To study the protective effects of flavonoids on reducing carcinogen-induced ROS generation through activation of the Nrf2/ARE pathway, NNKAc is not suitable to be used as NNKAc was found to be an activator of Nrf2. Furthermore, the effects of NNKAc on oxidative DNA damage markers such as 8-oxodeoxyguanosine should be further studied to understand the role of NNKAc in causing oxidative DNA damage. Additionally, further studies are required to assess the role of the Nrf2/ARE pathway in exerting protective effects by flavonoids on carcinogen-induced BEAS-2B cells in terms of effects on phase 2 detoxifying enzymes. In addition to that, the protective effects of flavonoids should be further studied with respect to the DDR mechanisms, effects on inhibiting cellular esterase enzyme, and Akt activation. More importantly, these effects should be studied time-dependently. Furthermore, the effects of flavonoids on activation of Nrf2 through canonical (i.e., inhibition of Keap-1-Nrf2 interactions) and non-canonical (i.e., Nrf2 activation by PKC) mechanisms and mechanisms that facilitate Nrf2 nuclear translocations (i.e., effects on AMPK and GSK3β) need to be further studied to unveil the other possible mechanisms of Nrf2/ARE pathway activation in BEAS-2B cells. Moreover, consumption of diets rich in quercetin (i.e., onions, apples, and parsley), genistein (i.e., soy-based food), and procyanidin B2 (i.e., cocoa-based food, grape seeds, plums, and berries) could provide a protective effect against carcinogen-induced cancer. Since the protective effects of genistein, quercetin, and procyanidin B2 in BEAS-2B cells were also observed at

physiologically relevant concentrations, a flavonoid-inspired functional food and/or a nutraceutical using the effective physiologically relevant concentrations of quercetin, genistein, and procyanidin B2 can be developed and assessed to reduce the risk of cancer. Additionally, the ability of dietary flavonoids to activate Nrf2/ARE pathway in exerting protective effects against other chronic disorders such as neurodegenerative diseases and diabetes mellitus that are associated with oxidative stress should be further studied.

REFERENCES

1. Global health estimates: Leading causes of death [Internet]. [cited 2022 May 10]. Available from: https://www.who.int/data/gho/data/themes/mortality-and-global-health-estimates/ghe-leading-causes-of-death

2. Sung H, Ferlay J, Siegel RL, Laversanne M, Soerjomataram I, Jemal A, et al. Global Cancer Statistics 2020: GLOBOCAN Estimates of Incidence and Mortality Worldwide for 36 Cancers in 185 Countries. CA Cancer J Clin. 2021;71(3):209–49.

3. Lee S. Cancer statistics at a glance [Internet]. Canadian Cancer Society. [cited 2022 May 10]. Available from: https://cancer.ca/en/research/cancer-statistics/cancer-statistics-at-a-glance

4. Side effects of cancer treatment [Internet]. National Cancer Institute. 2015 [cited 2019 Nov 15]. Available from: https://www.cancer.gov/about-cancer/treatment/side-effects

5. MacDonald V. Chemotherapy: Managing side effects and safe handling. Can Vet J. 2009 Jun;50(6):665–8.

6. Zhang H, Jiang H, Hu X, Jia Z. Aidi injection combined with radiation in the treatment of non-small cell lung cancer: A meta-analysis evaluation the efficacy and side effects. J Cancer Res Ther. 2015 Aug 1;11(5):118.

7. Uramoto H, Tanaka F. Recurrence after surgery in patients with NSCLC. Transl Lung Cancer Res. 2014 Aug;3(4):242–9.

8. Hung JJ, Hsu WH, Hsieh CC, Huang BS, Huang MH, Liu JS, et al. Post-recurrence survival in completely resected stage I non-small cell lung cancer with local recurrence. Thorax. 2009 Mar 1;64(3):192–6.

9. Fernando W, Rupasinghe HPV, Hoskin DW. Dietary phytochemicals with anti-oxidant and pro-oxidant activities: A double-edged sword in relation to adjuvant chemotherapy and radiotherapy? Cancer Lett. 2019 Jun 28;452:168–77.

10. Fike LT, Munro H, Yu D, Dai Q, Shrubsole MJ. Dietary polyphenols and the risk of colorectal cancer in the prospective Southern Community Cohort Study. Am J Clin Nutr. 2022 Apr 1;115(4):1155–65.

11. Briguglio G, Costa C, Pollicino M, Giambò F, Catania S, Fenga C. Polyphenols in cancer prevention: New insights (Review). Int J Funct Nutr. 2020 Nov 1;1(2):1–1.

12. Amararathna M, Johnston MR, Rupasinghe HPV. Plant polyphenols as chemopreventive agents for lung cancer. Int J Mol Sci. 2016 Aug 19;17(8).

13. Hancock JT, Desikan R, Neill SJ. Role of reactive oxygen species in cell signalling pathways. Biochem Soc Trans. 2001 May;29(Pt 2):345–50.

14. Birben E, Sahiner UM, Sackesen C, Erzurum S, Kalayci O. Oxidative stress and antioxidant defense. World Allergy Organ J. 2012 Jan;5(1):9–19.

15. Nimse SB, Pal D. Free radicals, natural antioxidants, and their reaction mechanisms. RSC Adv. 2015 Mar 16;5(35):27986–8006.

16. Bae YS, Oh H, Rhee SG, Yoo YD. Regulation of reactive oxygen species generation in cell signaling. Mol Cells. 2011 Dec 31;32(6):491–509.

17. Mitra S, Nguyen LN, Akter M, Park G, Choi EH, Kaushik NK. Impact of ROS generated by chemical, physical, and plasma techniques on cancer attenuation. Cancers. 2019 Jul;11(7):1030.

18. Wajed SA, Laird PW, DeMeester TR. DNA methylation: an alternative pathway to cancer. Ann Surg. 2001 Jul;234(1):10–20.

19. Broustas CG, Lieberman HB. DNA damage response genes and the development of cancer metastasis. Radiat Res. 2014 Jan 7;181(2):111–30.

20. George VC, Dellaire G, Rupasinghe HPV. Plant flavonoids in cancer chemoprevention: role in genome stability. J Nutr Biochem. 2017 Jul 1;45:1–14.

21. Sipowicz MA, Amin S, Desai D, Kasprzak KS, Anderson LM. Oxidative DNA damage in tissues of pregnant female mice and fetuses caused by the tobacco-specific nitrosamine, 4-(methylnitrosamino)-1-(3-pyridyl)-1-butanone (NNK). Cancer Lett. 1997 Jul 15;117(1):87–91.

22. Barnes JL, Zubair M, John K, Poirier MC, Martin FL. Carcinogens and DNA damage. Biochem Soc Trans. 2018 Oct 19;46(5):1213–24.

23. Karadag A, Ozcelik B, Saner S. Review of methods to determine antioxidant capacities. Food Anal Methods. 2(1):41–60.

24. Lobo V, Patil A, Phatak A, Chandra N. Free radicals, antioxidants and functional foods: Impact on human health. Pharmacogn Rev. 2010 Jul;4(8):118–26.

25. Rojo de la Vega M, Chapman E, Zhang DD. NRF2 and the hallmarks of cancer. Cancer Cell. 2018 09;34(1):21–43.

26. Solis LM, Behrens C, Dong W, Suraokar M, Ozburn NC, Moran CA, et al. Nrf2 and Keap1 abnormalities in non-small cell lung carcinoma and association with clinicopathologic features. Clin Cancer Res Off J Am Assoc Cancer Res. 2010 Jul 15;16(14):3743–53.

27. Liang F, Fang Y, Cao W, Zhang Z, Pan S, Xu X. Attenuation of tert-butyl hydroperoxide (t-BHP)-induced oxidative damage in HepG2 cells by tangeretin: Relevance of the Nrf2–ARE and MAPK signaling pathways. J Agric Food Chem. 2018 Jun 27;66(25):6317–25.

28. Lee B, Shim I, Lee H, Hahm DH. The polymethoxylated flavone, Tangeretin improves cognitive memory in rats experiencing a single episode of prolonged post-traumatic stress. Anim Cells Syst. 2018 Jan 2;22(1):54–62.

29. Qin S, Chen J, Tanigawa S, Hou DX. Microarray and pathway analysis highlight Nrf2/ARE-mediated expression profiling by polyphenolic myricetin. Mol Nutr Food Res. 2013;57(3):435–46.

30. Lobo V, Patil A, Phatak A, Chandra N. Free radicals, antioxidants and functional foods: Impact on human health. Pharmacogn Rev. 2010;4(8):118–26.

31. Tsushima M, Liu J, Hirao W, Yamazaki H, Tomita H, Itoh K. Emerging evidence for crosstalk between Nrf2 and mitochondria in physiological homeostasis and in heart disease. Arch Pharm Res. 2020 Mar 1;43(3):286–96.

32. Stefanson AL, Bakovic M. Dietary regulation of Keap1/Nrf2/ARE pathway: Focus on plant-derived compounds and trace minerals. Nutrients. 2014 Sep 19;6(9):3777–801.

33. Nakai K, Fujii H, Kono K, Goto S, Kitazawa R, Kitazawa S, et al. Vitamin D activates the Nrf2-Keap1 antioxidant pathway and ameliorates nephropathy in diabetic rats. Am J Hypertens. 2014 Apr 1;27(4):586–95.

34. Mostafavi-Pour Z, Ramezani F, Keshavarzi F, Samadi N. The role of quercetin and vitamin C in Nrf2-dependent oxidative stress production in breast cancer cells. Oncol Lett. 2017 Mar;13(3):1965–73.

35. Amararathna M, Hoskin WD, Rupasinghe HPV. Anthocyanin-rich haskap (Lonicera caerulea L.) berry extracts reduce nitrosamine-induced DNA damage in human normal lung epithelial cells in vitro. J Food Chem Toxicol. 2020;

36. Naczk M, Shahidi F. Extraction and analysis of phenolics in food. J Chromatogr A. 2004 Oct 29;1054(1–2):95–111.

37. Bertelli A, Biagi M, Corsini M, Baini G, Cappellucci G, Miraldi E. Polyphenols: From theory to practice. Foods. 2021 Oct 27;10(11):2595.

38. Corso M, Perreau F, Mouille G, Lepiniec L. Specialized phenolic compounds in seeds: structures, functions, and regulations. Plant Sci. 2020 Jul 1;296:110471.

39. Pandey KB, Rizvi SI. Plant polyphenols as dietary antioxidants in human health and disease. Oxid Med Cell Longev. 2009;2(5):270–8.

40. Vidal-Casanella O, Moreno-Merchan J, Granados M, Nuñez O, Saurina J, Sentellas S. Total polyphenol content in food samples and nutraceuticals: Antioxidant indices versus high performance liquid chromatography. Antioxidants. 2022 Feb;11(2):324.

41. Tsao R. Chemistry and biochemistry of dietary polyphenols. Nutrients. 2010 Dec 10;2(12):1231–46.

42. Singla RK, Dubey AK, Garg A, Sharma RK, Fiorino M, Ameen SM, et al. Natural polyphenols: Chemical classification, definition of classes, subcategories, and structures. J AOAC Int. 2019 Sep 1;102(5):1397–400.

43. Ziaullah, Rupasinghe HPV. Application of NMR spectroscopy in plant polyphenols associated with human health. In: Application of NMR Spectroscopy in Food Sciences (Eds). Oak Park, IL, USA: Bentham Science Publishers; p. 3–92.

44. Mitra S, Tareq AM, Das R, Emran TB, Nainu F, Chakraborty AJ, et al. Polyphenols: A first evidence in the synergism and bioactivities. Food Rev Int. 2022 Jan 24;0(0):1–23.

45. Durazzo A, Lucarini M, Souto EB, Cicala C, Caiazzo E, Izzo AA, et al. Polyphenols: A concise overview on the chemistry, occurrence, and human health. Phytother Res. 2019;33(9):2221–43.

46. Pereira Souza AC, Deyse Gurak P, Damasceno Ferreira Marczak L. Maltodextrin, pectin and soy protein isolate as carrier agents in the encapsulation of anthocyanins-rich extract from jaboticaba pomace. Food Bioprod Process. 2017 Mar 1;102:186–94.

47. Albuquerque BR, Heleno SA, Oliveira MBPP, Barros L, Ferreira ICFR. Phenolic compounds: current industrial applications, limitations and future challenges. Food Funct. 2021 Jan 18;12(1):14–29.

48. Mattila P, Hellström J, Törrönen R. Phenolic acids in berries, fruits, and beverages. J Agric Food Chem. 2006 Sep 1;54(19):7193–9.

49. Liang N, Kitts DD. Role of chlorogenic acids in controlling oxidative and inflammatory stress conditions. Nutrients. 2015 Dec 28;8(1):16.

50. Mark R, Lyu X, Lee JJL, Parra-Saldívar R, Chen WN. Sustainable production of natural phenolics for functional food applications. J Funct Foods. 2019 Jun 1;57:233–54.

51. Garg SK, Shukla A, Choudhury S. Polyphenols and flavonoids. In: Gupta RC, Srivastava A, Lall R, editors. Nutraceuticals in Veterinary Medicine. Cham: Springer International Publishing; 2019. p. 187–204.

52. Adlercreutz H, Mazur W. Phyto-oestrogens and Western diseases. Ann Med. 1997 Apr;29(2):95–120.

53. Gómez-Guzmán M, Rodríguez-Nogales A, Algieri F, Gálvez J. Potential role of seaweed polyphenols in cardiovascular-associated disorders. Mar Drugs. 2018 Aug;16(8):250.

54. Losada-Echeberría M, Herranz-López M, Micol V, Barrajón-Catalán E. Polyphenols as promising drugs against main breast cancer signatures. Antioxidants. 2017 Dec;6(4):88.

55. Brglez Mojzer E, Knez Hrnčič M, Škerget M, Knez Ž, Bren U. Polyphenols: Extraction methods, antioxidative action, bioavailability and anticarcinogenic effects. Molecules. 2016 Jul;21(7):901.

56. Durazzo A, Lucarini M, Camilli E, Marconi S, Gabrielli P, Lisciani S, et al. Dietary lignans: Definition, description and research trends in databases development. Molecules. 2018 Dec;23(12):3251.

57. Grgić J, Šelo G, Planinić M, Tišma M, Bucić-Kojić A. Role of the encapsulation in bioavailability of phenolic compounds. Antioxidants. 2020 Oct;9(10):923.

58. Kumar S, Pandey AK. Chemistry and biological activities of flavonoids: An overview. Sci World J. 2013 Dec 29;2013:e162750.

59. Havsteen BH. The biochemistry and medical significance of the flavonoids. Pharmacol Ther. 2002 Dec;96(2–3):67–202.

60. Alseekh S, Perez de Souza L, Benina M, Fernie AR. The style and substance of plant flavonoid decoration; towards defining both structure and function. Phytochemistry. 2020 Jun;174:112347.

61. Shukla S, Gupta S. Apigenin: a promising molecule for cancer prevention. Pharm Res. 2010 Jun;27(6):962–78.

62. Tsao R, Yang R, Young JC, Zhu H. Polyphenolic profiles in eight apple cultivars using high-performance liquid chromatography (HPLC). J Agric Food Chem. 2003 Oct 8;51(21):6347–53.

63. Ou K, Gu L. Absorption and metabolism of proanthocyanidins. J Funct Foods. 2014 Mar 1;7:43–53.

64. Gu L, Kelm MA, Hammerstone JF, Beecher G, Holden J, Haytowitz D, et al. Concentrations of proanthocyanidins in common foods and sstimations of normal consumption. J Nutr. 2004 Mar 1;134(3):613–7.

65. Carocho M, Morales P, Ferreira ICFR. Natural food additives: Quo vadis? Trends Food Sci Technol. 2015 Oct 1;45(2):284–95.

66. Doan KV, Ko CM, Kinyua AW, Yang DJ, Choi YH, Oh IY, et al. Gallic acid regulates body weight and glucose homeostasis through AMPK activation. Endocrinology. 2015 Jan 1;156(1):157–68.

67. Nguyen NA, Cao NT, Nguyen THH, Le TK, Cha GS, Choi SK, et al. Regioselective hydroxylation of phloretin, a bioactive compound from apples, by human cytochrome P450 enzymes. Pharmaceuticals. 2020 Nov;13(11):330.

68. Semwal DK, Semwal RB, Combrinck S, Viljoen A. Myricetin: A dietary molecule with diverse biological activities. Nutrients. 2016 Feb;8(2):90.

69. Dumitru C, Dinica RM, Bahrim GE, Vizireanu C, Baroiu L, Iancu AV, et al. New insights into the antioxidant compounds of achenes and sprouted buckwheat cultivated in the Republic of Moldova. Appl Sci. 2021 Jan;11(21):10230.

70. Calabrese V, Cornelius C, Trovato A, Cavallaro M, Mancuso C, Di Rienzo L, et al. The hormetic role of dietary antioxidants in free radical-related diseases. Curr Pharm Des. 2010;16(7):877–83.

71. Paredes-Gonzalez X, Fuentes F, Jeffery S, Saw CLL, Shu L, Su ZY, et al. Induction of NRF2-mediated gene expression by dietary phytochemical flavones apigenin and luteolin. Biopharm Drug Dispos. 2015 Oct 1;36(7):440–51.

72. Rattan SIS. Hormesis in aging. Ageing Res Rev. 2008 Jan 1;7(1):63–78.

73. Calabrese EJ. Astrocytes: Adaptive responses to lowdosesof neurotoxins. Crit Rev Toxicol. 2008 Jan 1;38(5):463–71.

74. Valdameri G, Trombetta-Lima M, Worfel PR, Pires ARA, Martinez GR, Noleto GR, et al. Involvement of catalase in the apoptotic mechanism induced by apigenin in HepG2 human hepatoma cells. Chem Biol Interact. 2011 Sep 5;193(2):180–9.

75. Rahal A, Kumar A, Singh V, Yadav B, Tiwari R, Chakraborty S, et al. Oxidative stress, prooxidants, and antioxidants: The interplay. BioMed Res Int. 2014;2014:e761264.

76. Martins LAM, Coelho BP, Behr G, Pettenuzzo LF, Souza ICC, Moreira JCF, et al. Resveratrol induces pro-oxidant effects and time-dependent resistance to cytotoxicity in activated hepatic stellate cells. Cell Biochem Biophys. 2014 Mar;68(2):247–57.

77. Trachootham D, Lu W, Ogasawara MA, Valle NRD, Huang P. Redox regulation of cell survival. Antioxid Redox Signal. 2008 Aug;10(8):1343–74.

78. Franco R, Navarro G, Martínez-Pinilla E. Hormetic and mitochondria-related mechanisms of antioxidant action of phytochemicals. Antioxidants. 2019 Sep 4;8(9).

79. Yang Y, Cai X, Yang J, Sun X, Hu C, Yan Z, et al. Chemoprevention of dietary digitoflavone on colitis-associated colon tumorigenesis through inducing Nrf2 signaling pathway and inhibition of inflammation. Mol Cancer. 2014 Mar 6;13(1):48.

80. CFR - Code of federal regulations title 21 [Internet]. [cited 2020 Feb 13]. Available from: https://www.accessdata.fda.gov/scripts/cdrh/cfdocs/cfcfr/CFRSearch.cfm?CFRPart=172&showFR=1&subpartNode=21:3.0.1.1.3.5

81. Khan J, Deb PK, Priya S, Medina KD, Devi R, Walode SG, et al. Dietary flavonoids: Cardioprotective potential with antioxidant effects and their pharmacokinetic, toxicological and therapeutic concerns. Molecules. 2021 Jan;26(13):4021.

82. Thilakarathna SH, Rupasinghe HPV. Flavonoid bioavailability and attempts for bioavailability enhancement. Nutrients. 2013 Sep;5(9):3367–87.

83. Scalbert A, Morand C, Manach C, Rémésy C. Absorption and metabolism of polyphenols in the gut and impact on health. Biomed Pharmacother Biomedecine Pharmacother. 2002 Aug;56(6):276–82.

84. Williamson G, Clifford MN. Colonic metabolites of berry polyphenols: the missing link to biological activity? Br J Nutr. 2010 Oct;104(S3):S48–66.

85. Shoji T, Masumoto S, Moriichi N, Akiyama H, Kanda T, Ohtake Y, et al. Apple procyanidin oligomers absorption in rats after oral administration: Analysis of procyanidins in plasma using the porter method and high-performance liquid chromatography/tandem mass spectrometry. J Agric Food Chem. 2006 Feb 1;54(3):884–92.

86. Williamson G, Kay CD, Crozier A. The bioavailability, transport, and bioactivity of dietary flavonoids: A review from a historical perspective. Compr Rev Food Sci Food Saf. 2018;17(5):1054–112.

87. Kruger J, Sus N, Frank J. Ascorbic acid, sucrose and olive oil lipids mitigate the inhibitory effects of pectin on the bioaccessibility and Caco-2 cellular uptake of ferulic acid and naringenin. Food Funct. 2020;11(5):4138–45.

88. Peters CM, Green RJ, Janle EM, Ferruzzi MG. Formulation with ascorbic acid and sucrose modulates catechin bioavailability from green tea. Food Res Int. 2010 Jan 1;43(1):95–102.

89. Kamiloglu S, Tomas M, Ozdal T, Capanoglu E. Effect of food matrix on the content and bioavailability of flavonoids. Trends Food Sci Technol. 2021 Nov 1;117:15–33.

90. Ribnicky DM, Roopchand DE, Oren A, Grace M, Poulev A, Lila MA, et al. Effects of a high fat meal matrix and protein complexation on the bioaccessibility of blueberry anthocyanins using the TNO gastrointestinal model (TIM-1). Food Chem. 2014 Jan 1;142:349–57.

91. Sengul H, Surek E, Nilufer-Erdil D. Investigating the effects of food matrix and food components on bioaccessibility of pomegranate (Punica granatum) phenolics and anthocyanins using an in-vitro gastrointestinal digestion model. Food Res Int. 2014 Aug 1;62:1069–79.

92. Nizamova AM, Ziyatdinova GK, Budnikov GK. Electrogenerated bromine as a coulometric reagent for the estimation of the bioavailability of polyphenols. J Anal Chem. 2011 Mar 1;66(3):301–9.

93. Day AJ, Gee JM, DuPont MS, Johnson IT, Williamson G. Absorption of quercetin-3-glucoside and quercetin-4′-glucoside in the rat small intestine: the role of lactase phlorizin hydrolase and the sodium-dependent glucose transporter. Biochem Pharmacol. 2003 Apr 1;65(7):1199–206.

94. Day AJ, DuPont MS, Ridley S, Rhodes M, Rhodes MJC, Morgan MRA, et al. Deglycosylation of flavonoid and isoflavonoid glycosides by human small intestine and liver β-glucosidase activity. FEBS Lett. 1998;436(1):71–5.

95. Gee JM, DuPont MS, Day AJ, Plumb GW, Williamson G, Johnson IT. Intestinal transport of quercetin glycosides in rats involves both deglycosylation and interaction with the hexose transport pathway. J Nutr. 2000 Nov 1;130(11):2765–71.

96. Chen Z, Zheng S, Li L, Jiang H. Metabolism of flavonoids in human: A comprehensive review. Curr Drug Metab. 15(1):48–61.

97. Landete JM. Updated knowledge about polyphenols: functions, bioavailability, metabolism, and health. Crit Rev Food Sci Nutr. 2012 Oct 1;52(10):936–48.

98. Erlund I, Kosonen T, Alfthan G, Mäenpää J, Perttunen K, Kenraali J, et al. Pharmacokinetics of quercetin from quercetin aglycone and rutin in healthy volunteers. Eur J Clin Pharmacol. 2000 Nov 1;56(8):545–53.

99. Kawabata K, Yoshioka Y, Terao J. Role of intestinal microbiota in the bioavailability and physiological functions of dietary polyphenols. Molecules. 2019 Jan;24(2):370.

100. Sarawek S, Derendorf H, Butterweck V. Pharmacokinetics of luteolin and metabolites in rats. Nat Prod Commun. 2008 Dec 1;3(12):1934578X0800301218.

101. Lin LC, Pai YF, Tsai TH. Isolation of luteolin and luteolin-7-O-glucoside from Dendranthema morifolium ramat tzvel and their pharmacokinetics in rats. J Agric Food Chem. 2015 Sep 9;63(35):7700–6.

102. Walle T, Otake Y, Brubaker JA, Walle UK, Halushka PV. Disposition and metabolism of the flavonoid chrysin in normal volunteers. Br J Clin Pharmacol. 2001 Feb;51(2):143–6.

103. Baidya D, Kushwaha J, Mahadik K, Patil S. Chrysin-loaded folate conjugated PF127-F68 mixed micelles with enhanced oral bioavailability and anticancer activity against human breast cancer cells. Drug Dev Ind Pharm. 2019 May 4;45(5):852–60.

104. Kanaze FI, Bounartzi MI, Georgarakis M, Niopas I. Pharmacokinetics of the citrus flavanone aglycones hesperetin and naringenin after single oral administration in human subjects. Eur J Clin Nutr. 2007 Apr;61(4):472–7.

105. Ju YH, Allred CD, Allred KF, Karko KL, Doerge DR, Helferich WG. Physiological concentrations of dietary genistein dose-dependently stimulate growth of estrogen-dependent human breast cancer (MCF-7) tumors implanted in athymic nude mice. J Nutr. 2001 Nov 1;131(11):2957–62.

106. Yang Z, Zhu W, Gao S, Xu H, Wu B, Kulkarni K, et al. Simultaneous determination of genistein and its four phase II metabolites in blood by a sensitive and robust UPLC-MS/MS method: application to an oral bioavailability study of genistein in mice. J Pharm Biomed Anal. 2010 Sep 21;53(1):81–9.

107. Santell RC, Kieu N, Helferich WG. Genistein inhibits growth of estrogen-independent human breast cancer cells in culture but not in athymic mice. J Nutr. 2000 Jul 1;130(7):1665–9.

108. Sepehr E, Cooke G, Robertson P, Gilani GS. Bioavailability of soy isoflavones in rats Part I: application of accurate methodology for studying the effects of gender and source of isoflavones. Mol Nutr Food Res. 2007 Jul;51(7):799–812.

109. Coldham NG, Zhang AQ, Key P, Sauer MJ. Absolute bioavailability of [14C] genistein in the rat; plasma pharmacokinetics of parent compound, genistein glucuronide and total radioactivity. Eur J Drug Metab Pharmacokinet. 2002 Dec;27(4):249–58.

110. Zhou S, Hu Y, Zhang B, Teng Z, Gan H, Yang Z, et al. Dose-dependent absorption, metabolism, and excretion of genistein in rats. J Agric Food Chem. 2008 Sep 24;56(18):8354–9.

111. Kwon SH, Kang MJ, Huh JS, Ha KW, Lee JR, Lee SK, et al. Comparison of oral bioavailability of genistein and genistin in rats. Int J Pharm. 2007 Jun 7;337(1–2):148–54.

112. Gu L, House SE, Prior RL, Fang N, Ronis MJJ, Clarkson TB, et al. Metabolic phenotype of isoflavones differ among female rats, pigs, monkeys, and women. J Nutr. 2006 May;136(5):1215–21.

113. Morton MS, Wilcox G, Wahlqvist ML, Griffiths K. Determination of lignans and isoflavonoids in human female plasma following dietary supplementation. J Endocrinol. 1994 Aug 1;142(2):251–9.

114. Setchell KDR, Cassidy A. Dietary Isoflavones: Biological Effects and Relevance to Human Health. J Nutr. 1999 Mar 1;129(3):758S-767S.

115. Xu X, Wang HJ, Murphy PA, Cook L, Hendrich S. Daidzein is a more bioavailable soymilk isoflavone than is genistein in adult women. J Nutr. 1994 Jun 1;124(6):825–32.

116. Ader P, Wessmann A, Wolffram S. Bioavailability and metabolism of the flavonol quercetin in the pig. Free Radic Biol Med. 2000 Apr 1;28(7):1056–67.

117. Hollman PCH, van Trijp JMP, Buysman MNCP, v.d. Gaag MS, Mengelers MJB, de Vries JHM, et al. Relative bioavailability of the antioxidant flavonoid quercetin from various foods in man. FEBS Lett. 1997 Nov 24;418(1):152–6.

118. de Vries JHM, Hollman PCH, van Amersfoort I, Olthof MR, Katan MB. Red wine is a poor source of bioavailable flavonols in men. J Nutr. 2001 Apr 1;131(3):745–8.

119. Olthof MR, Hollman PCH, Vree TB, Katan MB. Bioavailabilities of quercetin-3-glucoside and quercetin-4′-glucoside do not differ in humans. J Nutr. 2000 May 1;130(5):1200–3.

120. Kaşıkcı MB, Bağdatlıoğlu N. Bioavailability of quercetin. Curr Res Nutr Food Sci J. 2016 Oct 25;4(Special Issue Nutrition in Conference October 2016):146–51.

121. Khaled KA, El-Sayed YM, Al-Hadiya BM. Disposition of the flavonoid quercetin in rats after single intravenous and oral doses. Drug Dev Ind Pharm. 2003 Apr;29(4):397–403.

122. Pool H, Mendoza S, Xiao H, McClements DJ. Encapsulation and release of hydrophobic bioactive components in nanoemulsion-based delivery systems: impact of physical form on quercetin bioaccessibility. Food Funct. 2013 Jan;4(1):162–74.

123. Marczylo TH, Cooke D, Brown K, Steward WP, Gescher AJ. Pharmacokinetics and metabolism of the putative cancer chemopreventive agent cyanidin-3-glucoside in mice. Cancer Chemother Pharmacol. 2009 Nov;64(6):1261–8.

124. Giordano L, Coletta W, Tamburrelli C, D'Imperio M, Crescente M, Silvestri C, et al. Four-week ingestion of blood orange juice results in measurable anthocyanin urinary levels but does not affect cellular markers related to cardiovascular risk: a randomized cross-over study in healthy volunteers. Eur J Nutr. 2012 Aug 1;51(5):541–8.

125. Olivas-Aguirre FJ, Rodrigo-García J, Martínez-Ruiz NDR, Cárdenas-Robles AI, Mendoza-Díaz SO, Álvarez-Parrilla E, et al. Cyanidin-3-O-glucoside: Physical-chemistry, foodomics and health Effects. Molecules. 2016 Sep;21(9):1264.

126. Rein D, Lotito S, Holt RR, Keen CL, Schmitz HH, Fraga CG. Epicatechin in human plasma: In vivo determination and effect of chocolate consumption on plasma oxidation status. J Nutr. 2000 Aug 1;130(8):2109S-2114S.

127. Hollands WJ, Hart DJ, Dainty JR, Hasselwander O, Tiihonen K, Wood R, et al. Bioavailability of epicatechin and effects on nitric oxide metabolites of an apple flavanol-rich extract supplemented beverage compared to a whole apple puree: a randomized, placebo-controlled, crossover trial. Mol Nutr Food Res. 2013;57(7):1209–17.

128. Baba S, Osakabe N, Natsume M, Terao J. Absorption and urinary excretion of procyanidin B2 [epicatechin-(4β-8)-epicatechin] in rats. Free Radic Biol Med. 2002 Jul 1;33(1):142–8.

129. Stoupi S, Williamson G, Viton F, Barron D, King LJ, Brown JE, et al. In vivo bioavailability, absorption, excretion, and pharmacokinetics of [14C]procyanidin B2 in male rats. Drug Metab Dispos Biol Fate Chem. 2010 Feb;38(2):287–91.

130. Holt RR, Lazarus SA, Sullards MC, Zhu QY, Schramm DD, Hammerstone JF, et al. Procyanidin dimer B2 [epicatechin-(4β-8)-epicatechin] in human plasma after the consumption of a flavanol-rich cocoa. Am J Clin Nutr. 2002 Oct 1;76(4):798–804.

131. Zhao Y yuan, Fan Y, Wang M, Wang J, Cheng J xue, Zou J bo, et al. Studies on pharmacokinetic properties and absorption mechanism of phloretin: In vivo and in vitro. Biomed Pharmacother. 2020 Dec 1;132:110809.

132. Liguori I, Russo G, Curcio F, Bulli G, Aran L, Della-Morte D, et al. Oxidative stress, aging, and diseases. Clin Interv Aging. 2018 Apr 26;13:757–72.

133. Apak R, Gorinstein S, Böhm V, Schaich KM, Özyürek M, Güçlü K. Methods of measurement and evaluation of natural antioxidant capacity/activity (IUPAC Technical Report). Pure Appl Chem. 2013;85(5):957–98.

134. Lodish H, Berk A, Zipursky SL, Matsudaira P, Baltimore D, Darnell J. DNA damage and repair and their role in carcinogenesis. Mol Cell Biol 4th Ed. 2000;

135. Klaunig JE. Chapter 8 - Carcinogenesis. In: Pope CN, Liu J, editors. An Introduction to Interdisciplinary Toxicology. Academic Press; 2020. p. 97–110.

136. Malarkey DE, Hoenerhoff MJ, Maronpot RR. Chapter 6 - Carcinogenesis: Manifestation and mechanisms. In: Wallig MA, Haschek WM, Rousseaux CG, Bolon B, editors. Fundamentals of Toxicologic Pathology (Third Edition). Academic Press; 2018. p. 83–104.

137. Shen Z. Genomic instability and cancer: an introduction. J Mol Cell Biol. 2011 Feb;3(1):1–3.

138. Jia P, Her C, Chai W. DNA excision repair at telomeres. DNA Repair. 2015 Dec;36:137–45.

139. Rupasinghe HPV, Nair SVG, Robinson RA. Chapter 8 - Chemopreventive properties of fruit phenolic compounds and their possible mode of actions. In: Atta-ur-Rahman, editor. Studies in Natural Products Chemistry. Elsevier; 2014. p. 229–66.

140. Ramos S. Polyphenols and health: New and recent advances. N. Vassallo. New York: Nova Science Publishers, Inc; 2008. 507–526 p.

141. Siddiqui IA, Sanna V, Ahmad N, Sechi M, Mukhtar H. Resveratrol nanoformulation for cancer prevention and therapy. Ann N Y Acad Sci. 2015;1348(1):20–31.

142. Watson, Joni L. Your guide to cancer prevention. 1st ed. Pittsburg, PA, USA: The Oncology Nursing Society; 2018.

143. Weston A, Harris CC. Multistage carcinogenesis. Holl-Frei Cancer Med 6th Ed. 2003;

144. Brown G. Oncogenes, proto-oncogenes, and lineage restriction of cancer stem cells. Int J Mol Sci. 2021 Sep 7;22(18):9667.

145. Merlin JPJ, Dellaire G, Murphy K, Rupasinghe HPV. Vitamin-containing antioxidant formulation reduces carcinogen-induced DNA damage through

ATR/Chk1 signaling in bronchial epithelial cells In vitro. Biomedicines. 2021 Nov 11;9(11):1665.

146. George VC, Rupasinghe HPV. Apple flavonoids suppress carcinogen-induced DNA damage in normal human bronchial epithelial cells. Oxid Med Cell Longev. 2017;2017:1767198.

147. Gankhuyag N, Lee KH, Cho JY. The role of nitrosamine (NNK) in breast cancer carcinogenesis. J Mammary Gland Biol Neoplasia. 2017 Sep 1;22(3):159–70.

148. Hoffmann D, Hoffmann I, El-Bayoumy K. The less harmful cigarette: a controversial issue. a tribute to Ernst L. Wynder. Chem Res Toxicol. 2001 Jul;14(7):767–90.

149. Hoffmann D, Brunnemann KD, Prokopczyk B, Djordjevic MV. Tobacco-specific N-nitrosamines and Areca-derived N-nitrosamines: chemistry, biochemistry, carcinogenicity, and relevance to humans. J Toxicol Environ Health. 1994 Jan;41(1):1–52.

150. Xue J, Yang S, Seng S. Mechanisms of cancer induction by tobacco-specific NNK and NNN. Cancers. 2014 May 14;6(2):1138–56.

151. Hecht SS, Stepanov I, Carmella SG. Exposure and metabolis activation biomakers of carcinogenic tobacco-specific nitrosamines. Acc Chem Res. 2016 Jan 19;49(1):106–14.

152. Hecht SS, Trushin N, Reid-Quinn CA, Burak ES, Jones AB, Southers JL, et al. Metabolism of the tobacco-specific nitrosamine 4-(methylnitrosamino)-1-(3-pyridyl)-1-butanone in the patas monkey: pharmacokinetics and characterization of glucuronide metabolites. Carcinogenesis. 1993 Feb 1;14(2):229–36.

153. Hodgson E. A Textbook of Modern Toxicology, 4th Edition | Wiley. 648 p.

154. Ioannides C, Lewis DFV. Cytochromes P450 in the bioactivation of chemicals. Curr Top Med Chem. 2004;4(16):1767–88.

155. Guengerich FP. Cytochrome p450 and chemical toxicology. Chem Res Toxicol. 2008 Jan;21(1):70–83.

156. Peterson LA. Context matters: Contribution of specific DNA adducts to the genotoxic properties of the tobacco specific nitrosamine NNK. Chem Res Toxicol. 2017 Jan 17;30(1):420–33.

157. Garcia-Canton C, Minet E, Anadon A, Meredith C. Metabolic characterization of cell systems used in in vitro toxicology testing: Lung cell system BEAS-2B as a working example. Toxicol In Vitro. 2013 Sep 1;27(6):1719–27.

158. Ma B, Villalta PW, Zarth AT, Kotandeniya D, Upadhyaya P, Stepanov I, et al. Comprehensive high-resolution mass spectrometric analysis of DNA phosphate adducts formed by the tobacco-specific lung carcinogen 4-(methylnitrosamino)-1-(3-pyridyl)-1-butanone. Chem Res Toxicol. 2015 Nov 16;28(11):2151–9.

159. Cooper D. The molecular genetics of lung cancer. Berlin Heidelberg: Springer-Verlag; 2005.

160. Chen RJ, Chang LW, Lin P, Wang YJ. Epigenetic effects and molecular mechanisms of tumorigenesis induced by cigarette smoke: An overview. J Oncol. 2011 Mar 22;2011:e654931.

161. Amararathna DIM. Chemopreventive effect of Haskap berry polyphenols against tobacco specific nitrosamine-induced DNA damage in normal lung epithelial cells in vitro [Thesis]. 2017.

162. Wen J, Fu J, Zhang W, Guo M. Genetic and epigenetic changes in lung carcinoma and their clinical implications. Mod Pathol. 2011 Jul;24(7):932–43.

163. Ding L, Getz G, Wheeler DA, Mardis ER, McLellan MD, Cibulskis K, et al. Somatic mutations affect key pathways in lung adenocarcinoma. Nature. 2008 Oct 23;455(7216):1069–75.

164. Peterson LA. Formation, repair, and genotoxic properties of bulky DNA adducts formed from tobacco-specific nitrosamines. J Nucleic Acids. 2010 Sep 5;2010:e284935.

165. Yalcin E, de la Monte S. Tobacco nitrosamines as culprits in disease: mechanisms reviewed. J Physiol Biochem. 2016 Mar 1;72(1):107–20.

166. Ma B, Stepanov I, Hecht SS. Recent studies on DNA adducts resulting from human exposure to tobacco smoke. Toxics. 2019 Mar;7(1):16.

167. Carmella SG, Borukhova A, Akerkar SA, Hecht SS. Analysis of human urine for pyridine-N-oxide metabolites of 4-(methylnitrosamino)-1-(3-pyridyl)-1-butanone, a tobacco-specific lung carcinogen. Cancer Epidemiol Biomark Prev Publ Am Assoc Cancer Res Cosponsored Am Soc Prev Oncol. 1997 Feb;6(2):113–20.

168. Ighodaro OM, Akinloye OA. First line defence antioxidants-superoxide dismutase (SOD), catalase (CAT) and glutathione peroxidase (GPX): Their fundamental role in the entire antioxidant defence grid. Alex J Med. 2018 Dec 1;54(4):287–93.

169. Kalam S, Singh R, Mani A, Patel J, Khan FN, Pandey A. Antioxidants: Elixir of life. Int Multidiscip Res J. 2012 Jan 21;2(1):1540.

170. Finkel T. Redox-dependent signal transduction. FEBS Lett. 2000 Jun 30;476(1–2):52–4.

171. Vignais PV. The superoxide-generating NADPH oxidase: structural aspects and activation mechanism. Cell Mol Life Sci CMLS. 2002 Sep;59(9):1428–59.

172. Arteaga O, Álvarez A, Revuelta M, Santaolalla F, Urtasun A, Hilario E. Role of antioxidants in neonatal hypoxic-ischemic brain injury: New therapeutic approaches. Int J Mol Sci. 2017 Jan 28;18(2).

173. Sirokmány G, Geiszt M. The relationship of NADPH oxidases and heme peroxidases: Fallin' in and out. Front Immunol. 2019;10.

174. Kelley EE, Khoo NKH, Hundley NJ, Malik UZ, Freeman BA, Tarpey MM. Hydrogen peroxide is the major oxidant product of xanthine oxidase. Free Radic Biol Med. 2010 Feb 15;48(4):493–8.

175. Zhang H, Yang Q, Sun M, Teng M, Niu L. Hydrogen peroxide produced by two amino acid oxidases mediates antibacterial actions. J Microbiol Seoul Korea. 2004 Dec;42(4):336–9.

176. Elsner M, Gehrmann W, Lenzen S. Peroxisome-generated hydrogen peroxide as important mediator of lipotoxicity in insulin-producing cells. Diabetes. 2011 Jan;60(1):200–8.

177. Liu J, Hinkhouse MM, Sun W, Weydert CJ, Ritchie JM, Oberley LW, et al. Redox regulation of pancreatic cancer cell growth: role of glutathione peroxidase in the suppression of the malignant phenotype. Hum Gene Ther. 2004 Mar;15(3):239–50.

178. Lyngsie G, Krumina L, Tunlid A, Persson P. Generation of hydroxyl radicals from reactions between a dimethoxyhydroquinone and iron oxide nanoparticles. Sci Rep. 2018 Jul 17;8(1):1–9.

179. Kehrer JP. The Haber-Weiss reaction and mechanisms of toxicity. Toxicology. 2000 Aug 14;149(1):43–50.

180. Jeeva JS, Sunitha J, Ananthalakshmi R, Rajkumari S, Ramesh M, Krishnan R. Enzymatic antioxidants and its role in oral diseases. J Pharm Bioallied Sci. 2015 Aug;7(Suppl 2):S331-333.

181. Otsuki A, Yamamoto M. Cis-element architecture of Nrf2–sMaf heterodimer binding sites and its relation to diseases. Arch Pharm Res. 2020 Mar 1;43(3):275–85.

182. Wu S, Lu H, Bai Y. Nrf2 in cancers: A double-edged sword. Cancer Med. 2019 Mar 30;8(5):2252–67.

183. Krajka-Kuźniak V, Paluszczak J, Baer-Dubowska W. The Nrf2-ARE signaling pathway: An update on its regulation and possible role in cancer prevention and treatment. Pharmacol Rep. 2017 Jun 1;69(3):393–402.

184. Tsushima M, Liu J, Hirao W, Yamazaki H, Tomita H, Itoh K. Emerging evidence for crosstalk between Nrf2 and mitochondria in physiological homeostasis and in heart disease. Arch Pharm Res. 2019 Nov 11;

185. Furfaro AL, Traverso N, Domenicotti C, Piras S, Moretta L, Marinari UM, et al. The Nrf2/HO-1 axis in cancer cell growth and chemoresistance. Oxid Med Cell Longev. 2016;2016:1958174.

186. Zhang H, Liu H, Davies KJA, Sioutas C, Finch CE, Morgan TE, et al. Nrf2-regulated phase II enzymes are induced by chronic ambient nanoparticle exposure in young mice with age-related impairments. Free Radic Biol Med. 2012 May 1;52(9):2038–46.

187. Cuadrado A. Structural and functional characterization of Nrf2 degradation by glycogen synthase kinase 3/β-TrCP. Free Radic Biol Med. 2015 Nov;88(Pt B):147–57.

188. Tong KI, Katoh Y, Kusunoki H, Itoh K, Tanaka T, Yamamoto M. Keap1 recruits Neh2 through binding to ETGE and DLG motifs: characterization of the two-site molecular recognition model. Mol Cell Biol. 2006 Apr;26(8):2887–900.

189. Kobayashi A, Kang MI, Okawa H, Ohtsuji M, Zenke Y, Chiba T, et al. Oxidative stress sensor Keap1 functions as an adaptor for Cul3-based E3 ligase to regulate proteasomal degradation of Nrf2. Mol Cell Biol. 2004 Aug;24(16):7130–9.

190. Cuadrado A, Manda G, Hassan A, Alcaraz MJ, Barbas C, Daiber A, et al. Transcription factor NRF2 as a therapeutic target for chronic diseases: A systems medicine approach. Pharmacol Rev. 2018;70(2):348–83.

191. Yamamoto M, Kensler TW, Motohashi H. The KEAP1-NRF2 system: A thiol-based sensor-effector apparatus for maintaining redox homeostasis. Physiol Rev. 2018 01;98(3):1169–203.

192. Dinkova-Kostova AT, Holtzclaw WD, Cole RN, Itoh K, Wakabayashi N, Katoh Y, et al. Direct evidence that sulfhydryl groups of Keap1 are the sensors regulating induction of phase 2 enzymes that protect against carcinogens and oxidants. Proc Natl Acad Sci U S A. 2002 Sep 3;99(18):11908–13.

193. Hayes JD, Dinkova-Kostova AT. The Nrf2 regulatory network provides an interface between redox and intermediary metabolism. Trends Biochem Sci. 2014 Apr;39(4):199–218.

194. Robledinos-Antón N, Fernández-Ginés R, Manda G, Cuadrado A. Activators and Inhibitors of NRF2: A Review of Their Potential for Clinical Development. Oxid Med Cell Longev. 2019 Jul 14;2019:e9372182.

195. Joo MS, Kim WD, Lee KY, Kim JH, Koo JH, Kim SG. AMPK facilitates nuclear accumulation of Nrf2 by phosphorylating at Serine 550. Mol Cell Biol. 2016 15;36(14):1931–42.

196. Zimmermann K, Baldinger J, Mayerhofer B, Atanasov AG, Dirsch VM, Heiss EH. Activated AMPK boosts the Nrf2/HO-1 signaling axis--A role for the unfolded protein response. Free Radic Biol Med. 2015 Nov;88(Pt B):417–26.

197. Li L, Luo W, Qian Y, Zhu W, Qian J, Li J, et al. Luteolin protects against diabetic cardiomyopathy by inhibiting NF-κB-mediated inflammation and activating the Nrf2-mediated antioxidant responses. Phytomedicine. 2019 Jun 1;59:152774.

198. L. Suraweera T, Rupasinghe HPV, Dellaire G, Xu Z. Regulation of Nrf2/ARE pathway by dietary flavonoids: A friend or foe for cancer management? Antioxidants. 2020 Oct;9(10):973.

199. Kwak MK, Kensler TW. Targeting NRF2 signaling for cancer chemoprevention. Toxicol Appl Pharmacol. 2010 Apr 1;244(1):66–76.

200. Basak P, Sadhukhan P, Sarkar P, Sil PC. Perspectives of the Nrf-2 signaling pathway in cancer progression and therapy. Toxicol Rep. 2017 Jan 1;4:306–18.

201. Abed DA, Goldstein M, Albanyan H, Jin H, Hu L. Discovery of direct inhibitors of Keap1–Nrf2 protein–protein interaction as potential therapeutic and preventive agents. Acta Pharm Sin B. 2015 Jul 1;5(4):285–99.

202. Jung KA, Kwak MK. The Nrf2 system as a potential target for the development of indirect antioxidants. Mol Basel Switz. 2010 Oct 20;15(10):7266–91.

203. Vogelstein B, Kinzler KW. Cancer genes and the pathways they control. Nat Med. 2004 Aug;10(8):789–99.

204. Kensler TW, Wakabayashi N, Biswal S. Cell survival responses to environmental stresses via the Keap1-Nrf2-ARE pathway. Annu Rev Pharmacol Toxicol. 2007;47:89–116.

205. Suzuki T, Shibata T, Takaya K, Shiraishi K, Kohno T, Kunitoh H, et al. Regulatory nexus of synthesis and degradation deciphers cellular Nrf2 expression levels. Mol Cell Biol. 2013 Jun;33(12):2402–12.

206. Xu C, Huang MT, Shen G, Yuan X, Lin W, Khor TO, et al. Inhibition of 7,12-dimethylbenz(a)anthracene-induced skin tumorigenesis in C57BL/6 mice by sulforaphane is mediated by nuclear factor E2–related factor 2. Cancer Res. 2006 Aug 15;66(16):8293–6.

207. Cullinan SB, Zhang D, Hannink M, Arvisais E, Kaufman RJ, Diehl JA. Nrf2 is a direct PERK substrate and effector of PERK-dependent cell survival. Mol Cell Biol. 2003 Oct;23(20):7198–209.

208. Sun Z, Huang Z, Zhang DD. Phosphorylation of Nrf2 at multiple sites by MAP kinases has a limited contribution in modulating the Nrf2-dependent antioxidant response. PLoS ONE. 2009 Aug 11;4(8).

209. Giudice A, Arra C, Turco MC. Review of molecular mechanisms involved in the activation of the Nrf2-ARE signaling pathway by chemopreventive agents. Methods Mol Biol Clifton NJ. 2010;647:37–74.

210. Interaction of polymorphism rs35652124 with curcumin supplementation on NFE2L2 gene expression, antioxidant capacity and renal function in patients with early diabetic nephropathy [Internet]. clinicaltrials.gov; 2018 May. Report No.: NCT03262363. Available from: https://clinicaltrials.gov/ct2/show/NCT03262363

211. RTA 408 ophthalmic suspension for the treatment of ocular inflammation and pain following ocular surgery [Internet]. clinicaltrials.gov; 2014 Feb. Report No.: NCT02065375. Available from: https://clinicaltrials.gov/ct2/show/NCT02065375

212. A 52-week, multi-center, double-blind, randomized, placebo-controlled phase IIb trial to determine the effects of bardoxolone methyl (RTA 402) on eGFR in patients with type 2 diabetes and chronic kidney disease with an eGFR of 20 - 45 mL/Min/1.73m2 [Internet]. clinicaltrials.gov; 2012 Jun. Report No.: study/NCT00811889. Available from: https://clinicaltrials.gov/ct2/show/study/NCT00811889

213. Anti-inflammatory and antioxidant effects of resveratrol on healthy adults [Internet]. ClinicalTrials.gov; 2011 Dec [cited 2020 Jun 11]. Report No.: NCT01492114. Available from: https://clinicaltrials.gov/ct2/show/record/NCT01492114

214. Zhang DD, Hannink M. Distinct cysteine residues in Keap1 are required for Keap1-dependent ubiquitination of Nrf2 and for stabilization of Nrf2 by chemopreventive agents and oxidative stress. Mol Cell Biol. 2003 Nov;23(22):8137–51.

215. Zhang DD, Lo SC, Cross JV, Templeton DJ, Hannink M. Keap1 is a redox-regulated substrate adaptor protein for a Cul3-dependent ubiquitin ligase complex. Mol Cell Biol. 2004 Dec;24(24):10941–53.

216. Wei R, Enaka M, Muragaki Y. Activation of KEAP1/NRF2/P62 signaling alleviates high phosphate-induced calcification of vascular smooth muscle cells by suppressing reactive oxygen species production. Sci Rep. 2019 Jul 17;9(1):1–13.

217. Ho CY, Cheng YT, Chau CF, Yen GC. Effect of diallyl sulfide on in vitro and in vivo Nrf2-mediated pulmonic antioxidant enzyme expression via activation ERK/p38 signaling pathway. J Agric Food Chem. 2012 Jan 11;60(1):100–7.

218. Apopa PL, He X, Ma Q. Phosphorylation of Nrf2 in the transcription activation domain by casein kinase 2 (CK2) is critical for the nuclear translocation and transcription activation function of Nrf2 in IMR-32 neuroblastoma cells. J Biochem Mol Toxicol. 2008;22(1):63–76.

219. Zhang X, Xiao Z, Yao J, Zhao G, Fa X, Niu J. Participation of protein kinase C in the activation of Nrf2 signaling by ischemic preconditioning in the isolated rabbit heart. Mol Cell Biochem. 2013 Jan;372(1–2):169–79.

220. Wang L, Chen Y, Sternberg P, Cai J. Essential roles of the PI3 kinase/Akt pathway in regulating Nrf2-dependent antioxidant functions in the RPE. Invest Ophthalmol Vis Sci. 2008 Apr 1;49(4):1671–8.

221. Bhullar KS, Nael MA, Elokely KM, Doiron JA, LeBlanc LM, Lassalle-Claux G, et al. Ketone analog of caffeic acid phenethyl ester exhibits antioxidant activity via activation of ERK-dependent Nrf2 pathway. Appl Sci. 2022 Jan;12(6):3062.

222. Singla E, Puri G, Dharwal V, Naura AS. Gallic acid ameliorates COPD-associated exacerbation in mice. Mol Cell Biochem. 2021 Jan 1;476(1):293–302.

223. Hseu YC, Chou CW, Senthil Kumar KJ, Fu KT, Wang HM, Hsu LS, et al. Ellagic acid protects human keratinocyte (HaCaT) cells against UVA-induced oxidative stress and apoptosis through the upregulation of the HO-1 and Nrf-2 antioxidant genes. Food Chem Toxicol. 2012 May 1;50(5):1245–55.

224. Tate PS, Marazita MC, Marquioni-Ramella MD, Suburo AM. Ilex paraguariensis extracts and its polyphenols prevent oxidative damage and senescence of human retinal pigment epithelium cells. J Funct Foods. 2020 Apr 1;67:103833.

225. Liu D, Wang H, Zhang Y, Zhang Z. Protective effects of chlorogenic acid on cerebral ischemia/reperfusion injury rats by regulating oxidative stress-related Nrf2 pathway. Drug Des Dev Ther Macclesfield. 2020;14:51–60.

226. Song JH, Lee HJ, Kang KS. Procyanidin C1 activates the Nrf2/HO-1 signaling pathway to prevent glutamate-induced apoptotic HT22 cell death. Int J Mol Sci. 2019 Jan 2;20(1).

227. Zhu X, Tian X, Yang M, Yu Y, Zhou Y, Gao Y, et al. Procyanidin B2 promotes intestinal injury repair and attenuates colitis-associated tumorigenesis via suppression of oxidative stress in mice. Antioxid Redox Signal. 2021 Jul 10;35(2):75–92.

228. Fan J, Liu H, Wang J, Zeng J, Tan Y, Wang Y, et al. Procyanidin B2 improves endothelial progenitor cell function and promotes wound healing in diabetic mice via activating Nrf2. J Cell Mol Med. 2021;25(2):652–65.

229. Zhou L, Chang J, Gao Y, Wang C. Procyanidin B2 attenuates cypermethrin-induced neuronal injury by regulating P13K/Akt/Nrf2 signaling pathway. J South Med Univ. 2021 Aug 20;41(8):1158–64.

230. Ma L, Li C, Lian S, Xu B, Lv H, Liu Y, et al. Procyanidin B2 alleviates liver injury caused by cold stimulation through Sonic hedgehog signalling and autophagy. J Cell Mol Med. 2021;25(16):8015–27.

231. Liu L, Wang R, Xu R, Chu Y, Gu W. Procyanidin B2 ameliorates endothelial dysfunction and impaired angiogenesis via the Nrf2/PPARγ/sFlt-1 axis in preeclampsia. Pharmacol Res. 2022 Mar 1;177:106127.

232. Rousta AM, Mirahmadi SMS, Shahmohammadi A, Nourabadi D, Khajevand-Khazaei MR, Baluchnejadmojarad T, et al. Protective effect of sesamin in

lipopolysaccharide-induced mouse model of acute kidney injury via attenuation of oxidative stress, inflammation, and apoptosis. Immunopharmacol Immunotoxicol. 2018 Sep 3;40(5):423–9.

233. Kong P, Chen G, Jiang A, Wang Y, Song C, Zhuang J, et al. Sesamin inhibits IL-1β-stimulated inflammatory response in human osteoarthritis chondrocytes by activating Nrf2 signaling pathway. Oncotarget. 2016 Nov 15;7(50):83720–6.

234. Chang BY, Jung YS, Yoon CS, Oh JS, Hong JH, Kim YC, et al. Fraxin prevents chemically induced hepatotoxicity by reducing oxidative stress. Molecules. 2017 Apr;22(4):587.

235. Ungvari Z, Bagi Z, Feher A, Recchia FA, Sonntag WE, Pearson K, et al. Resveratrol confers endothelial protection via activation of the antioxidant transcription factor Nrf2. Am J Physiol - Heart Circ Physiol. 2010 Jul;299(1):H18–24.

236. Medical College of Wisconsin. Randomized, placebo-controlled clinical trial of resveratrol supplement effects on cognition, function and behavior in patients with mild-to-moderate Alzheimer's disease [Internet]. clinicaltrials.gov; 2015 Aug [cited 2020 Jun 8]. Report No.: NCT00743743. Available from: https://clinicaltrials.gov/ct2/show/study/NCT00743743

237. Zhou X, Ruan Q, Ye Z, Chu Z, Xi M, Li M, et al. Resveratrol accelerates wound healing by attenuating oxidative stress-induced impairment of cell proliferation and migration. Burns. 2021 Feb 1;47(1):133–9.

238. Qi L, Jiang J, Zhang J, Zhang L, Wang T. Curcumin protects human trophoblast HTR8/SVneo cells from H2O2-induced oxidative stress by activating Nrf2 signaling pathway. Antioxidants. 2020 Feb 1;9(2).

239. Zhai SS, Ruan D, Zhu YW, Li MC, Ye H, Wang WC, et al. Protective effect of curcumin on ochratoxin A–induced liver oxidative injury in duck is mediated by

modulating lipid metabolism and the intestinal microbiota. Poult Sci. 2020 Feb 1;99(2):1124–34.

240. Bucolo C, Drago F, Maisto R, Romano GL, D'Agata V, Maugeri G, et al. Curcumin prevents high glucose damage in retinal pigment epithelial cells through ERK1/2-mediated activation of the Nrf2/HO-1 pathway. J Cell Physiol. 2019;234(10):17295–304.

241. Balogun E, Hoque M, Gong P, Killeen E, Green CJ, Foresti R, et al. Curcumin activates the haem oxygenase-1 gene via regulation of Nrf2 and the antioxidant-responsive element. Biochem J. 2003 May 1;371(3):887–95.

242. Gao S, Duan X, Wang X, Dong D, Liu D, Li X, et al. Curcumin attenuates arsenic-induced hepatic injuries and oxidative stress in experimental mice through activation of Nrf2 pathway, promotion of arsenic methylation and urinary excretion. Food Chem Toxicol. 2013 Sep 1;59:739–47.

243. Wang Y, Liu F, Liu M, Zhou X, Wang M, Cao K, et al. Curcumin mitigates aflatoxin B1-induced liver injury via regulating the NLRP3 inflammasome and Nrf2 signaling pathway. Food Chem Toxicol. 2022 Mar 1;161:112823.

244. Kitakaze T, Makiyama A, Yamashita Y, Ashida H. Low dose of luteolin activates Nrf2 in the liver of mice at start of the active phase but not that of the inactive phase. PLoS One San Franc. 2020 Apr;15(4):e0231403.

245. Tan X, Yang Y, Xu J, Zhang P, Deng R, Mao Y, et al. Luteolin exerts neuroprotection via modulation of the p62/Keap1/Nrf2 pathway in intracerebral hemorrhage. Front Pharmacol. 2020;10.

246. Ma B, Zhang J, Zhu Z, Zhao A, Zhou Y, Ying H, et al. Luteolin ameliorates testis injury and blood–testis barrier disruption through the Nrf2 signaling pathway and by upregulating Cx43. Mol Nutr Food Res. 2019;63(10):1800843.

247. Sobeh M, Petruk G, Osman S, El Raey MA, Imbimbo P, Monti DM, et al. Isolation of myricitrin and 3,5-di-O-methyl gossypetin from Syzygium samarangense and

evaluation of their involvement in protecting keratinocytes against oxidative stress via activation of the Nrf-2 pathway. Molecules. 2019 May 13;24(9).

248. Dong Y, Xing Y, Sun J, Sun W, Xu Y, Quan C. Baicalein alleviates liver oxidative stress and apoptosis induced by high-level glucose through the activation of the PERK/Nrf2 signaling pathway. Molecules. 2020 Jan 30;25(3).

249. Zhang H bin, Tu X kun, Song S wei, Liang R sheng, Shi S sheng. Baicalin reduces early brain injury after subarachnoid hemorrhage in rats. Chin J Integr Med. 2020 Jan 23;26(7):510–8.

250. Yu H, Chen B, Ren Q. Baicalin relieves hypoxia-aroused H9c2 cell apoptosis by activating Nrf2/HO-1-mediated HIF1α/BNIP3 pathway. Artif Cells Nanomedicine Biotechnol. 2019 Dec 4;47(1):3657–63.

251. Ishfaq M, Chen C, Bao J, Zhang W, Wu Z, Wang J, et al. Baicalin ameliorates oxidative stress and apoptosis by restoring mitochondrial dynamics in the spleen of chickens via the opposite modulation of NF-κB and Nrf2/HO-1 signaling pathway during Mycoplasma gallisepticum infection. Poult Sci. 2019 Dec 1;98(12):6296–310.

252. Xu X, Li M, Chen W, Yu H, Yang Y, Hang L. Apigenin attenuates oxidative injury in ARPE-19 cells thorough activation of Nrf2 pathway. Oxid Med Cell Longev. 2016;2016:e4378461.

253. Huang CS, Lii CK, Lin AH, Yeh YW, Yao HT, Li CC, et al. Protection by chrysin, apigenin, and luteolin against oxidative stress is mediated by the Nrf2-dependent up-regulation of heme oxygenase 1 and glutamate cysteine ligase in rat primary hepatocytes. Arch Toxicol. 2013 Jan 1;87(1):167–78.

254. Li Y, Wang X. Chrysin attenuates high glucose-induced BMSC dysfunction via the activation of the PI3K/AKT/Nrf2 signaling pathway. Drug Des Devel Ther. 2022 Jan 13;16:165–82.

255. Zhang Q, Li Z, Wu S, Li X, Sang Y, Li J, et al. Myricetin alleviates cuprizone-induced behavioral dysfunction and demyelination in mice by Nrf2 pathway. Food Funct. 2016 Oct 12;7(10):4332–42.

256. Schadich E, Hlaváč J, Volná T, Varanasi L, Hajdúch M, Džubák P. Effects of ginger phenylpropanoids and quercetin on Nrf2-ARE pathway in human BJ fibroblasts and HaCaT keratinocytes. BioMed Res Int. 2016;2016:e2173275.

257. Sun L, Xu G, Dong Y, Li M, Yang L, Lu W. Quercetin protects against lipopolysaccharide-induced intestinal oxidative stress in broiler chickens through activation of Nrf2 pathway. Molecules. 2020 Feb 26;25(5).

258. Barraza-Garza G, Pérez-León JA, Castillo-Michel H, de la Rosa LA, Martinez-Martinez A, Cotte M, et al. Antioxidant effect of phenolic compounds (PC) at different concentrations in IEC-6 cells: A spectroscopic analysis. Spectrochim Acta A Mol Biomol Spectrosc. 2020 Feb 15;227:117570.

259. Tian R, Yang Z, Lu N, Peng YY. Quercetin, but not rutin, attenuated hydrogen peroxide-induced cell damage via heme oxygenase-1 induction in endothelial cells. Arch Biochem Biophys. 2019 Nov 15;676:108157.

260. Rajnochová Svobodová A, Ryšavá A, Čížková K, Roubalová L, Ulrichová J, Vrba J, et al. Effect of the flavonoids quercetin and taxifolin on UVA-induced damage to human primary skin keratinocytes and fibroblasts. Photochem Photobiol Sci. 2022 Jan 1;21(1):59–75.

261. Lee YJ, Song J, Oh MH, Lee YJ, Kim YB, Im JH, et al. ERK1/2 activation in quercetin-treated BEAS-2B cell plays a role in Nrf2-driven HO-1 expression. Mol Cell Toxicol. 2011;

262. Ebabe Elle R, Rahmani S, Lauret C, Morena M, Bidel LPR, Boulahtouf A, et al. Functionalized mesoporous silica nanoparticle with antioxidants as a new carrier that generates lower oxidative stress impact on cells. Mol Pharm. 2016 Aug 1;13(8):2647–60.

263. Wang K, Chen Z, Huang L, Meng B, Zhou X, Wen X, et al. Naringenin reduces oxidative stress and improves mitochondrial dysfunction via activation of the Nrf2/ARE signaling pathway in neurons. Int J Mol Med. 2017 Nov 1;40(5):1582–90.

264. Lou H, Jing X, Wei X, Shi H, Ren D, Zhang X. Naringenin protects against 6-OHDA-induced neurotoxicity via activation of the Nrf2/ARE signaling pathway. Neuropharmacology. 2014 Apr 1;79:380–8.

265. Abdelaziz RM, Abdelazem AZ, Hashem KS, Attia YA. Protective effects of hesperidin against MTX-induced hepatotoxicity in male albino rats. Naunyn Schmiedebergs Arch Pharmacol. 2020 Feb 26;393(8):1405–17.

266. Lan X, Han X, Li Q, Wang J. (−)-Epicatechin, a natural flavonoid compound, protects astrocytes against hemoglobin toxicity via Nrf2 and AP-1 signaling pathways. Mol Neurobiol. 2017 Dec;54(10):7898–907.

267. Han J, Wang M, Jing X, Shi H, Ren M, Lou H. (−)-Epigallocatechin gallate protects against cerebral ischemia-induced oxidative stress via Nrf2/ARE signaling. Neurochem Res. 2014 Jul 1;39(7):1292–9.

268. Wang R, Tu J, Zhang Q, Zhang X, Zhu Y, Ma W, et al. Genistein attenuates ischemic oxidative damage and behavioral deficits via eNOS/Nrf2/HO-1 signaling. Hippocampus. 2013;23(7):634–47.

269. Hu Q peng, Yan H xia, Peng F, Feng W, Chen F fang, Huang X yi, et al. Genistein protects epilepsy-induced brain injury through regulating the JAK2/STAT3 and Keap1/Nrf2 signaling pathways in the developing rats. Eur J Pharmacol. 2021 Dec 5;912:174620.

270. Wu C, Zhou S, Ma S, Suzuki K. Effect of genistein supplementation on exercise-induced inflammation and oxidative stress in mice liver and skeletal muscle. Medicina (Mex). 2021 Oct;57(10):1028.

271. Gao Z, Gao X, Fan W, Liu S, Li M, Miao Y, et al. Bisphenol A and genistein have opposite effects on adult chicken ovary by acting on ERα/Nrf2-Keap1-signaling pathway. Chem Biol Interact. 2021 Sep 25;347:109616.

272. Speciale A, Anwar S, Canali R, Chirafisi J, Saija A, Virgili F, et al. Cyanidin-3-O-glucoside counters the response to TNF-alpha of endothelial cells by activating Nrf2 pathway. Mol Nutr Food Res. 2013;57(11):1979–87.

273. Lee DS, Li B, Kim KS, Jeong GS, Kim EC, Kim YC. Butein protects human dental pulp cells from hydrogen peroxide-induced oxidative toxicity via Nrf2 pathway-dependent heme oxygenase-1 expressions. Toxicol In Vitro. 2013 Mar 1;27(2):874–81.

274. Singh G, Thaker R, Sharma A, Parmar D. Therapeutic effects of biochanin A, phloretin, and epigallocatechin-3-gallate in reducing oxidative stress in arsenic-intoxicated mice. Environ Sci Pollut Res. 2021 Apr 1;28(16):20517–36.

275. Su ZY, Zhang C, Lee JH, Shu L, Wu TY, Khor TO, et al. Requirement and epigenetics reprogramming of Nrf2 in suppression of tumor promoter TPA-induced mouse skin cell transformation by sulforaphane. Cancer Prev Res Phila Pa. 2014 Mar;7(3):319–29.

276. Kalayarasan S, Prabhu PN, Sriram N, Manikandan R, Arumugam M, Sudhandiran G. Diallyl sulfide enhances antioxidants and inhibits inflammation through the activation of Nrf2 against gentamicin-induced nephrotoxicity in Wistar rats. Eur J Pharmacol. 2009 Mar 15;606(1–3):162–71.

277. Yuan X, Wang J, Tang X, Li Y, Xia P, Gao X. Berberine ameliorates nonalcoholic fatty liver disease by a global modulation of hepatic mRNA and lncRNA expression profiles. J Transl Med. 2015 Jan 27;13:24.

278. Tao S, Zhang H, Xue L, Jiang X, Wang H, Li B, et al. Vitamin D protects against particles-caused lung injury through induction of autophagy in an Nrf2-dependent manner. Environ Toxicol. 2019;34(5):594–609.

279. Duan L, Li J, Ma P, Yang X, Xu S. Vitamin E antagonizes ozone-induced asthma exacerbation in Balb/c mice through the Nrf2 pathway. Food Chem Toxicol. 2017 Sep 1;107:47–56.

280. Wang G, Xiu P, Li F, Xin C, Li K. Vitamin A supplementation alleviates extrahepatic cholestasis liver injury through Nrf2 activation. Oxid Med Cell Longev. 2014;2014.

281. Huang Q, Zhang S, Du T, Yang Q, Chi S, Liu H, et al. Modulation of growth, immunity and antioxidant-related gene expressions in the liver and intestine of juvenile Sillago sihama by dietary vitamin C. Aquac Nutr. 2020;26(2):338–50.

282. Zhao R, Wang H, Qiao C, Zhao K. Vitamin B2 blocks development of Alzheimer's disease in APP/PS1 transgenic mice via anti-oxidative mechanism. Trop J Pharm Res. 2018 Jan 1;17(6):1049-1054–1054.

283. Said HM. Intestinal absorption of water-soluble vitamins in health and disease. Biochem J. 2011 Aug 1;437(3):357–72.

284. Pietrofesa RA, Chatterjee S, Park K, Arguiri E, Albelda SM, Christofidou-Solomidou M. Synthetic lignan secoisolariciresinol diglucoside (LGM2605) reduces asbestos-induced cytotoxicity in an Nrf2-dependent and -independent manner. Antioxid Basel. 2018;7(3):38.

285. Zhao L, Wei Y, Huang Y, He B, Zhou Y, Fu J. Nanoemulsion improves the oral bioavailability of baicalin in rats: in vitro and in vivo evaluation. Int J Nanomedicine. 2013;8:3769–79.

286. Chang HM, But PPH. Pharmacology and applications of Chinese materia medica. Vol. 1. World Scientific; 2014.

287. Meyer H, Bolarinwa A, Wolfram G, Linseisen J. Bioavailability of apigenin from apiin-rich parsley in humans. Ann Nutr Metab. 2006;50(3):167–72.

288. Li SQ, Dong S, Su ZH, Zhang HW, Peng JB, Yu CY, et al. Comparative pharmacokinetics of naringin in rat after oral administration of Chaihu-Shu-Gan-San aqueous extract and naringin alone. Metabolites. 2013 Sep 30;3(4):867–80.

289. Salehi B, Fokou PVT, Sharifi-Rad M, Zucca P, Pezzani R, Martins N, et al. The therapeutic potential of naringenin: A review of clinical trials. Pharmaceuticals. 2019 Jan 10;12(1):11.

290. Egert S, Wolffram S, Bosy-Westphal A, Boesch-Saadatmandi C, Wagner AE, Frank J, et al. Daily quercetin supplementation dose-dependently increases plasma quercetin concentrations in healthy humans. J Nutr. 2008 Sep 1;138(9):1615–21.

291. Erlund I, Kosonen T, Alfthan G, Mäenpää J, Perttunen K, Kenraali J, et al. Pharmacokinetics of quercetin from quercetin aglycone and rutin in healthy volunteers. Eur J Clin Pharmacol. 2000 Nov;56(8):545–53.

292. Ortiz-Andrade RR, Sánchez-Salgado JC, Navarrete-Vázquez G, Webster SP, Binnie M, García-Jiménez S, et al. Antidiabetic and toxicological evaluations of naringenin in normoglycaemic and NIDDM rat models and its implications on extra-pancreatic glucose regulation. Diabetes Obes Metab. 2008 Nov 1;10(11):1097–104.

293. Li Y, Kandhare AD, Mukherjee AA, Bodhankar SL. Acute and sub-chronic oral toxicity studies of hesperidin isolated from orange peel extract in Sprague Dawley rats. Regul Toxicol Pharmacol RTP. 2019 Jul;105:77–85.

294. Chen JH, Tipoe GL, Liong EC, So HSH, Leung KM, Tom WM, et al. Green tea polyphenols prevent toxin-induced hepatotoxicity in mice by down-regulating inducible nitric oxide-derived prooxidants. Am J Clin Nutr. 2004 Sep;80(3):742–51.

295. Liu YW, Liu XL, Kong L, Zhang MY, Chen YJ, Zhu X, et al. Neuroprotection of quercetin on central neurons against chronic high glucose through enhancement of

Nrf2/ARE/glyoxalase-1 pathway mediated by phosphorylation regulation. Biomed Pharmacother. 2019 Jan 1;109:2145–54.

296. Shi L, Hao Z, Zhang S, Wei M, Lu B, Wang Z, et al. Baicalein and baicalin alleviate acetaminophen-induced liver injury by activating Nrf2 antioxidative pathway: The involvement of ERK1/2 and PKC. Biochem Pharmacol. 2018 Apr 1;150:9–23.

297. Noh K, Oh DG, Nepal MR, Jeong KS, Choi Y, Kang MJ, et al. Pharmacokinetic interaction of chrysin with caffeine in rats. Biomol Ther. 2016 Jul;24(4):446–52.

298. Manach C, Morand C, Demigné C, Texier O, Régérat F, Rémésy C. Bioavailability of rutin and quercetin in rats. FEBS Lett. 1997 Jun 2;409(1):12–6.

299. Ishii S, Kitazawa H, Mori T, Kirino A, Nakamura S, Osaki N, et al. Identification of the catechin uptake transporter responsible for intestinal absorption of epigallocatechin gallate in mice. Sci Rep. 2019 Jul 29;9(1):11014.

300. Czank C, Cassidy A, Zhang Q, Morrison DJ, Preston T, Kroon PA, et al. Human metabolism and elimination of the anthocyanin, cyanidin-3-glucoside: a 13C-tracer study. Am J Clin Nutr. 2013 May 1;97(5):995–1003.

301. Yang D, Tan X, Lv Z, Liu B, Baiyun R, Lu J, et al. Regulation of Sirt1/Nrf2/TNF-α signaling pathway by luteolin is critical to attenuate acute mercuric chloride exposure induced hepatotoxicity. Sci Rep. 2016 17;6:37157.

302. Zhang H, Tan X, Yang D, Lu J, Liu B, Baiyun R, et al. Dietary luteolin attenuates chronic liver injury induced by mercuric chloride via the Nrf2/NF-κB/P53 signaling pathway in rats. Oncotarget. 2017 Apr 21;8(25):40982–93.

303. Dai LM, Cheng H, Li WP, Liu SQ, Chen MZ, Xu SY. The influence of luteolin on experimental inflammatory models in rats. Acta Anhui Med Univ. 1985;20:1–3.

304. Chen L, Dou J, Su Z, Zhou H, Wang H, Zhou W, et al. Synergistic activity of baicalein with ribavirin against influenza A (H1N1) virus infections in cell culture and in mice. Antiviral Res. 2011 Sep 1;91(3):314–20.

305. Yang Y, Choi JK, Jung CH, Koh HJ, Heo P, Shin JY, et al. SNARE-wedging polyphenols as small molecular botox. Planta Med. 2012 Feb;78(3):233–6.

306. Singh P, Sharma S, Kumar Rath S. Genistein induces deleterious effects during its acute exposure in Swiss mice. BioMed Res Int. 2014 May 22;2014:e619617.

307. Takahashi T, Yokoo Y, Inoue T, Ishii A. Toxicological studies on procyanidin B-2 for external application as a hair growing agent. Food Chem Toxicol. 1999 May 1;37(5):545–52.

308. Wang H, Joseph JA. Quantifying cellular oxidative stress by dichlorofluorescein assay using microplate reader. Free Radic Biol Med. 1999 Sep;27(5–6):612–6.

309. Wang P, Henning SM, Heber D. Limitations of MTT and MTS-based assays for measurement of antiproliferative activity of green tea polyphenols. PLOS ONE. 2010 Apr 16;5(4):e10202.

310. Ivashkevich A, Redon CE, Nakamura AJ, Martin RF, Martin OA. Use of the γ-H2AX assay to monitor DNA damage and repair in translational cancer research. Cancer Lett. 2012 Dec 31;327(1–2):123–33.

311. George VC, Naveen Kumar DR, Suresh PK, Kumar S, Kumar RA. Comparative studies to evaluate relative in vitro potency of luteolin in inducing cell cycle arrest and apoptosis in HaCaT and A375 cells. Asian Pac J Cancer Prev APJCP. 2013;14(2):631–7.

312. Shen N, Wang T, Gan Q, Liu S, Wang L, Jin B. Plant flavonoids: Classification, distribution, biosynthesis, and antioxidant activity. Food Chem. 2022 Jul 30;383:132531.

313. Caruso G, Torrisi SA, Mogavero MP, Currenti W, Castellano S, Godos J, et al. Polyphenols and neuroprotection: Therapeutic implications for cognitive decline. Pharmacol Ther. 2022 Apr 1;232:108013.

314. Adefegha SA, Oboh G, Oluokun OO. Chapter 11 - Food bioactives: the food image behind the curtain of health promotion and prevention against several degenerative diseases. In: Atta-ur-Rahman, editor. Studies in Natural Products Chemistry. Elsevier; 2022. p. 391–421. (Studies in Natural Products Chemistry; vol. 72).

315. Montenegro-Landívar MF, Tapia-Quirós P, Vecino X, Reig M, Valderrama C, Granados M, et al. Polyphenols and their potential role to fight viral diseases: An overview. Sci Total Environ. 2021 Dec 20;801:149719.

316. Csekes E, Račková L. Skin aging, cellular senescence and natural polyphenols. Int J Mol Sci. 2021 Jan;22(23):12641.

317. Elejalde E, Villarán MC, Alonso RM. Grape polyphenols supplementation for exercise-induced oxidative stress. J Int Soc Sports Nutr. 2021 Jan 7;18(1):3.

318. Demizu Y, Sasaki R, Trachootham D, Pelicano H, Colacino JA, Liu J, et al. Alterations of cellular redox state during NNK-induced malignant transformation and resistance to radiation. Antioxid Redox Signal. 2008 May;10(5):951–61.

319. Halliwell B, Gutteridge JMC. Free radicals in biology and medicine. 5th ed. Oxford: Oxford University Press; 2015. 944 p.

320. Mishra A, Kumar S, Pandey AK. Scientific validation of the medicinal efficacy of Tinospora cordifolia. Sci World J. 2013 Dec 23;2013:e292934.

321. Brown EJ, Khpdr H, Hider CR, Rice-Evans CA. Structural dependence of flavonoid interactions with Cu2+ ions: implications for their antioxidant properties. Biochem J. 1998 Mar 15;330(3):1173–8.

322. Heim KE, Tagliaferro AR, Bobilya DJ. Flavonoid antioxidants: chemistry, metabolism and structure-activity relationships. J Nutr Biochem. 2002 Oct 1;13(10):572–84.

323. Pandey AK, Mishra AK, Mishra A. Antifungal and antioxidative potential of oil and extracts derived from leaves of Indian spice plant Cinnamomum tamala. Cell Mol Biol Noisy--Gd Fr. 2012 Dec 22;58(1):142–7.

324. Liu B, Ranji-Burachaloo H, Gurr PA, Goudeli E, Qiao GG. A nontoxic reversible thermochromic binary system via π–π stacking of sulfonephthaleins. J Mater Chem C. 2019 Aug 1;7(30):9335–45.

325. Yu L, Zhang S dong, Zhao X lian, Ni H yan, Song X rui, Wang W, et al. Cyanidin-3-glucoside protects liver from oxidative damage through AMPK/Nrf2 mediated signaling pathway in vivo and in vitro. J Funct Foods. 2020 Oct 1;73:104148.

326. Silva Santos LF, Stolfo A, Calloni C, Salvador M. Catechin and epicatechin reduce mitochondrial dysfunction and oxidative stress induced by amiodarone in human lung fibroblasts. J Arrhythmia. 2017;33(3):220–5.

327. Lee KW, Kang NJ, Oak MH, Hwang MK, Kim JH, Schini-Kerth VB, et al. Cocoa procyanidins inhibit expression and activation of MMP-2 in vascular smooth muscle cells by direct inhibition of MEK and MT1-MMP activities. Cardiovasc Res. 2008 Jul 1;79(1):34–41.

328. Guo DJ, Li F, Yu PHF, Chan SW. Neuroprotective effects of luteolin against apoptosis induced by 6-hydroxydopamine on rat pheochromocytoma PC12 cells. Pharm Biol. 2013 Feb 1;51(2):190–6.

329. Xue C, Chen Y, Hu DN, Iacob C, Lu C, Huang Z. Chrysin induces cell apoptosis in human uveal melanoma cells via intrinsic apoptosis. Oncol Lett. 2016 Dec 1;12(6):4813–20.

330. Chen P, Xiao Z, Wu H, Wang Y, Fan W, Su W, et al. Beneficial Effects of Naringenin in Cigarette Smoke-Induced Damage to the Lung Based on Bioinformatic Prediction and In Vitro Analysis. Molecules. 2020 Jan;25(20):4704.

331. Choi YR, Shim J, Kim MJ. Genistin: A novel potent anti-adipogenic and anti-lipogenic agent. Molecules. 2020 Jan;25(9):2042.

332. Li J, Yang Q, Han L, Pan C, Lei C, Chen H, et al. C2C12 Mouse Myoblasts Damage Induced by Oxidative Stress Is Alleviated by the Antioxidant Capacity of the Active Substance Phloretin. Front Cell Dev Biol. 2020;8.

333. Wang H, Cheng J, Wang H, Wang M, Zhao J, Wu Z. Protective effect of apple phlorizin on hydrogen peroxide-induced cell damage in HepG2 cells. J Food Biochem. 2019;43(12):e13052.

334. Lee MS, Kim Y. Effects of Isorhamnetin on Adipocyte Mitochondrial Biogenesis and AMPK Activation. Molecules. 2018 Aug;23(8):1853.

335. Lee S, Oh DG, Singh D, Lee HJ, Kim GR, Lee S, et al. Untargeted Metabolomics Toward Systematic Characterization of Antioxidant Compounds in Betulaceae Family Plant Extracts. Metabolites. 2019 Sep;9(9):186.

336. Son JH, Kim SY, Jang HH, Lee SN, Ahn KJ. Protective effect of protocatechuic acid against inflammatory stress induced in human dermal fibroblasts. Biomed Dermatol. 2018 Feb 10;2(1):9.

337. Hong YJ, Yang SY, Nam MH, Koo Y chang, Lee KW. Caffeic Acid Inhibits the Uptake of 2-Amino-1-methyl-6-phenylimidazo[4,5-*b*]pyridine (PhIP) by Inducing the Efflux Transporters Expression in Caco-2 Cells. Biol Pharm Bull. 2015;38(2):201–7.

338. Rebai O, Belkhir M, Sanchez-Gomez MV, Matute C, Fattouch S, Amri M. Differential Molecular Targets for Neuroprotective Effect of Chlorogenic Acid and its Related Compounds Against Glutamate Induced Excitotoxicity and Oxidative Stress in Rat Cortical Neurons. Neurochem Res. 2017 Dec 1;42(12):3559–72.

339. Lim WC, Kim H, Kim YJ, Jeon BN, Kang HB, Ko H. Catechol inhibits epidermal growth factor-induced epithelial-to-mesenchymal transition and stem cell-like properties in hepatocellular carcinoma cells. Sci Rep. 2020 May 6;10(1):7620.

340. Chang YC, Chang WC, Hung KH, Yang DM, Cheng YH, Liao YW, et al. The generation of induced pluripotent stem cells for macular degeneration as a drug screening platform: identification of curcumin as a protective agent for retinal pigment epithelial cells against oxidative stress. Front Aging Neurosci [Internet]. 2014 [cited 2022 Jul 5];6. Available from: https://www.frontiersin.org/articles/10.3389/fnagi.2014.00191

341. Gomes L, Sorgine M, Passos CLA, Ferreira C, de Andrade IR, Silva JL, et al. Increase in fatty acids and flotillins upon resveratrol treatment of human breast cancer cells. Sci Rep. 2019 Sep 27;9(1):13960.

342. Ladak Z, Garcia E, Yoon J, Landry T, Armstrong EA, Yager JY, et al. Sulforaphane (SFA) protects neuronal cells from oxygen & glucose deprivation (OGD). PLOS ONE. 2021 Mar 18;16(3):e0248777.

343. Kuang Y, Zhang Y, Xiao Z, Xu L, Wang P, Ma Q. Protective effect of dimethyl fumarate on oxidative damage and signaling in cardiomyocytes. Mol Med Rep. 2020 Oct 1;22(4):2783–90.

344. Solana-Manrique C, Sanz FJ, Ripollés E, Bañó MC, Torres J, Muñoz-Soriano V, et al. Enhanced activity of glycolytic enzymes in Drosophila and human cell models of Parkinson's disease based on DJ-1 deficiency. Free Radic Biol Med. 2020 Oct 1;158:137–48.

345. Pratheeshkumar P, Son YO, Divya SP, Wang L, Turcios L, Roy RV, et al. Quercetin inhibits Cr(VI)-induced malignant cell transformation by targeting miR-21-PDCD4 signaling pathway. Oncotarget. 2016 Jun 17;8(32):52118–31.

346. Grossini E, Farruggio S, Raina G, Mary D, Deiro G, Gentilli S. Effects of genistein on differentiation and viability of human visceral adipocytes. Nutrients. 2018 Jul 27;10(8):978.

347. Pratheeshkumar P, Son YO, Divya SP, Roy RV, Hitron JA, Wang L, et al. Luteolin inhibits Cr(VI)-induced malignant cell transformation of human lung epithelial cells by targeting ROS mediated multiple cell signaling pathways. Toxicol Appl Pharmacol. 2014 Dec 1;281(2):230–41.

348. Harris GK, Qian Y, Leonard SS, Sbarra DC, Shi X. Luteolin and chrysin differentially inhibit cyclooxygenase-2 expression and scavenge reactive oxygen species but similarly inhibit prostaglandin-E2 formation in RAW 264.7 cells. J Nutr. 2006 Jun 1;136(6):1517–21.

349. Wojnar W, Zych M, Borymski S, Kaczmarczyk-Sedlak I. Chrysin reduces oxidative stress but does not affect polyol pathway in the lenses of type 1 diabetic rats. Antioxid Basel Switz. 2020 Feb 16;9(2):E160.

350. Gan Y, Fu Y, Yang L, Chen J, Lei H, Liu Q. Cyanidin-3-O-glucoside and cyanidin protect against intestinal barrier damage and 2,4,6-trinitrobenzenesulfonic acid-induced colitis. J Med Food. 2020 Jan;23(1):90–9.

351. Zeng Y, Song J, Zhang M, Wang H, Zhang Y, Suo H. Comparison of in vitro and in vivo antioxidant activities of six flavonoids with similar structures. Antioxidants. 2020 Aug;9(8):732.

352. Rice-Evans CA, Miller NJ, Paganga G. Structure-antioxidant activity relationships of flavonoids and phenolic acids. Free Radic Biol Med. 1996 Jan 1;20(7):933–56.

353. Platzer M, Kiese S, Tybussek T, Herfellner T, Schneider F, Schweiggert-Weisz U, et al. Radical scavenging mechanisms of phenolic compounds: A quantitative structure-property relationship (QSPR) study. Front Nutr. 2022;9:882458.

354. Xu D, Hu MJ, Wang YQ, Cui YL. Antioxidant activities of quercetin and its complexes for medicinal application. Molecules. 2019 Mar 21;24(6):1123.

355. Warnakulasuriya SN, Ziaullah, Rupasinghe HPV. Novel long chain fatty acid derivatives of quercetin-3-O-glucoside reduce cytotoxicity induced by cigarette smoke toxicants in human fetal lung fibroblasts. Eur J Pharmacol. 2016 Jun 15;781:128–38.

356. Wolfe KL, Liu RH. Structure−activity relationships of flavonoids in the cellular antioxidant activity assay. J Agric Food Chem. 2008 Sep 24;56(18):8404–11.

357. Pietta PG. Flavonoids as Antioxidants. J Nat Prod. 2000 Jul 1;63(7):1035–42.

358. Silva MM, Santos MR, Caroço G, Rocha R, Justino G, Mira L. Structure-antioxidant activity relationships of flavonoids: A re-examination. Free Radic Res. 2002 Jan 1;36(11):1219–27.

359. Kähkönen MP, Heinonen M. Antioxidant activity of anthocyanins and their aglycons. J Agric Food Chem. 2003 Jan 1;51(3):628–33.

360. Zhang H, Hassan YI, Liu R, Mats L, Yang C, Liu C, et al. Molecular mechanisms underlying the absorption of aglycone and glycosidic flavonoids in a Caco-2 BBe1 cell model. ACS Omega. 2020 May 6;5(19):10782–93.

361. Rodríguez-Ramiro I, Ramos S, Bravo L, Goya L, Martín MÁ. Procyanidin B2 and a cocoa polyphenolic extract inhibit acrylamide-induced apoptosis in human Caco-2 cells by preventing oxidative stress and activation of JNK pathway. J Nutr Biochem. 2011 Dec 1;22(12):1186–94.

362. Steffen Y, Schewe T, Sies H. (–)-Epicatechin elevates nitric oxide in endothelial cells via inhibition of NADPH oxidase. Biochem Biophys Res Commun. 2007 Aug 3;359(3):828–33.

363. Steffen Y, Gruber C, Schewe T, Sies H. Mono-O-methylated flavanols and other flavonoids as inhibitors of endothelial NADPH oxidase. Arch Biochem Biophys. 2008 Jan 15;469(2):209–19.

364. Park CH, Lee IS, Grippo P, Pandol SJ, Gukovskaya AS, Edderkaoui M. Akt kinase mediates the pro-survival effect of smoking compounds in pancreatic ductal cells. Pancreas. 2013 May;42(4):655–62.

365. Huang WC, Fang LW, Liou CJ. Phloretin attenuates allergic airway inflammation and oxidative stress in asthmatic mice. Front Immunol. 2017 Feb 13;8:134.

366. Dierckx T, Haidar M, Grajchen E, Wouters E, Vanherle S, Loix M, et al. Phloretin suppresses neuroinflammation by autophagy-mediated Nrf2 activation in macrophages. J Neuroinflammation. 2021 Jul 4;18(1):148.

367. Han L, Li J, Li J, Pan C, Xiao Y, Lan X, et al. Activation of AMPK/Sirt3 pathway by phloretin reduces mitochondrial ROS in vascular endothelium by increasing the activity of MnSOD via deacetylation. Food Funct. 2020 Apr 30;11(4):3073–83.

368. Zielinska D, Laparra-Llopis JM, Zielinski H, Szawara-Nowak D, Giménez-Bastida JA. Role of apple phytochemicals, phloretin and phloridzin, in modulating processes related to intestinal inflammation. Nutrients. 2019 May;11(5):1173.

369. Li Y, Chen LJ, Jiang F, Yang Y, Wang XX, Zhang Z, et al. Caffeic acid improves cell viability and protects against DNA damage: involvement of reactive oxygen species and extracellular signal-regulated kinase. Braz J Med Biol Res Rev Bras Pesqui Medicas E Biol. 2015 Jun;48(6):502–8.

370. Liu Q, Liu F, Zhang L, Niu Y, Liu Z, Liu X. Comparison of chicoric acid, and its metabolites caffeic acid and caftaric acid: In vitro protection of biological macromolecules and inflammatory responses in BV2 microglial cells. Food Sci Hum Wellness. 2017 Dec 1;6(4):155–66.

371. Chan WS, Wen PC, Chiang HC. Structure-activity relationship of caffeic acid analogues on xanthine oxidase inhibition. Anticancer Res. 1995 Jun;15(3):703–7.

372. Wang SH, Chen CS, Huang SH, Yu SH, Lai ZY, Huang ST, et al. Hydrophilic ester-bearing chlorogenic acid binds to a novel domain to inhibit xanthine oxidase. Planta Med. 2009 Sep;75(11):1237–40.

373. Shin H, Satsu H, Bae MJ, Totsuka M, Shimizu M. Catechol groups enable reactive oxygen species scavenging-mediated suppression of PKD-NFkappaB-IL-8 signaling pathway by chlorogenic and caffeic acids in human intestinal cells. Nutrients. 2017;

374. Varì R, Scazzocchio B, Santangelo C, Filesi C, Galvano F, D'Archivio M, et al. Protocatechuic acid prevents oxLDL-induced apoptosis by activating JNK/Nrf2 survival signals in macrophages. Oxid Med Cell Longev. 2015;2015:351827.

375. Pahlke G, Ahlberg K, Oertel A, Janson-Schaffer T, Grabher S, Mock H, et al. Antioxidant effects of elderberry anthocyanins in human colon carcinoma cells: A study on structure–activity relationships. Mol Nutr Food Res. 2021 Sep;65(17):2100229.

376. Okamoto Y, Hayashi T, Matsunami S, Ueda K, Kojima N. Combined activation of methyl paraben by light irradiation and esterase metabolism toward oxidative DNA damage. Chem Res Toxicol. 2008 Aug 1;21(8):1594–9.

377. Silva DC, Serrano L, Oliveira TMA, Mansano AS, Almeida EA, Vieira EM. Effects of parabens on antioxidant system and oxidative damages in Nile tilapia (Oreochromis niloticus). Ecotoxicol Environ Saf. 2018 Oct 30;162:85–91.

378. Bendary E, Francis RR, Ali HMG, Sarwat MI, El Hady S. Antioxidant and structure–activity relationships (SARs) of some phenolic and anilines compounds. Ann Agric Sci. 2013 Dec 1;58(2):173–81.

379. Valgimigli L, Amorati R, Fumo MG, DiLabio GA, Pedulli GF, Ingold KU, et al. The unusual reaction of semiquinone radicals with molecular oxygen. J Org Chem. 2008 Mar 1;73(5):1830–41.

380. Meng H, Li Y, Faust M, Konst S, Lee BP. Hydrogen peroxide generation and biocompatibility of hydrogel-bound mussel adhesive moiety. Acta Biomater. 2015 Apr 15;17:160–9.

381. Gambini J, Inglés M, Olaso G, Lopez-Grueso R, Bonet-Costa V, Gimeno-Mallench L, et al. Properties of resveratrol: In vitro and in vivo studies about metabolism, bioavailability, and biological effects in animal models and humans. Oxid Med Cell Longev. 2015 Jun 28;2015:e837042.

382. Kocher A, Schiborr C, Behnam D, Frank J. The oral bioavailability of curcuminoids in healthy humans is markedly enhanced by micellar solubilisation but not further improved by simultaneous ingestion of sesamin, ferulic acid, naringenin and xanthohumol. J Funct Foods. 2015 Apr 1;14:183–91.

383. Fança-Berthon P, Tenon M, Bouter-Banon SL, Manfré A, Maudet C, Dion A, et al. Pharmacokinetics of a single dose of turmeric curcuminoids depends on formulation: Results of a human crossover study. J Nutr. 2021 Jul 1;151(7):1802–16.

384. Langston-Cox A, Anderson D, Creek DJ, Palmer K, Wallace EM, Marshall SA. Measuring sulforaphane and its metabolites in human plasma: A high throughput method. Molecules. 2020 Feb 13;25(4):829.

385. Ak T, Gülçin İ. Antioxidant and radical scavenging properties of curcumin. Chem Biol Interact. 2008 Jul 10;174(1):27–37.

386. Gülçin İ. Antioxidant properties of resveratrol: A structure–activity insight. Innov Food Sci Emerg Technol. 2010 Jan 1;11(1):210–8.

387. Kim HJ, Barajas B, Wang M, Nel AE. Nrf2 activation by sulforaphane restores the age-related decrease of TH1 immunity: Role of dendritic cells. J Allergy Clin Immunol. 2008 May 1;121(5):1255-1261.e7.

388. Morimitsu Y, Nakagawa Y, Hayashi K, Fujii H, Kumagai T, Nakamura Y, et al. A Sulforaphane Analogue That Potently Activates the Nrf2-dependent Detoxification Pathway*. J Biol Chem. 2002 Feb 1;277(5):3456–63.

389. Ranaweera SS, Dissanayake CY, Natraj P, Lee YJ, Han CH. Anti-inflammatory effect of sulforaphane on LPS-stimulated RAW 264.7 cells and ob/ob mice. J Vet Sci. 2020 Nov;21(6):e91.

390. Ligen Z, Yuanfeng W, Yuke S, Lei Z, Mupunga J, Jianwei M, et al. Broccoli seed extracts but not sulforaphane have strong free radical scavenging activities. Int J Food Sci Technol. 2017;52(11):2374–81.

391. Zhu W, Cromie MM, Cai Q, Lv T, Singh K, Gao W. Curcumin and vitamin E protect against adverse effects of benzo[a]pyrene in lung epithelial cells. PLoS ONE. 2014 Mar 24;9(3):e92992.

392. Zhang Y, Wang G, Wang T, Cao W, Zhang L, Chen X. Nrf2–Keap1 pathway–mediated effects of resveratrol on oxidative stress and apoptosis in hydrogen peroxide–treated rheumatoid arthritis fibroblast-like synoviocytes. Ann N Y Acad Sci. 2019;1457(1):166–78.

393. Kubo E, Chhunchha B, Singh P, Sasaki H, Singh DP. Sulforaphane reactivates cellular antioxidant defense by inducing Nrf2/ARE/Prdx6 activity during aging and oxidative stress. Sci Rep. 2017 Oct 26;7(1):14130.

394. Green B, Parson WW, Parson WW. Light-harvesting antennas in photosynthesis. Springer Science & Business Media; 2003. 544 p.

395. Frank HA, Young AJ, Britton G, Cogdell RJ, editors. The photochemistry of carotenoids. Dordrecht: Springer Netherlands; 1999. (Govindjee, Amesz J, Aro EM, Barber J, Blankenship RE, Murata N, et al., editors. Advances in Photosynthesis and Respiration; vol. 8).

396. Chen P, Li L, Gao Y, Xie Z, Zhang Y, Pan Z, et al. β-carotene provides neuroprotection after experimental traumatic brain injury via the Nrf2-ARE pathway. J Integr Neurosci. 2019 Jun 30;18(2):153–61.

397. Park Y, Lee H, Lim JW, Kim H. Inhibitory effect of β-carotene on helicobacter pylori-induced TRAF expression and hyper-proliferation in gastric epithelial cells. Antioxidants. 2019 Dec;8(12):637.

398. Ros EO. The US FDA-approved drug dimethyl fumarate, an Nrf2 activator, for treating multiple sclerosis: The mechanisms of action revisited. React Oxyg Species. 2021 Feb 23;11:n7–8.

399. Bei D, An G. Pharmacokinetics and tissue distribution of 5,7-dimethoxyflavone in mice following single dose oral administration. J Pharm Biomed Anal. 2016 Feb 5;119:65–70.

400. Belcher JD, Chen C, Nguyen J, Zhang P, Abdulla F, Nguyen P, et al. Control of oxidative stress and inflammation in sickle cell disease with the Nrf2 activator dimethyl fumarate. Antioxid Redox Signal. 2017 May 10;26(14):748–62.

401. Brennan MS, Matos MF, Li B, Hronowski X, Gao B, Juhasz P, et al. Dimethyl fumarate and monoethyl fumarate exhibit differential effects on KEAP1, NRF2 activation, and glutathione depletion in vitro. PLOS ONE. 2015 Mar 20;10(3):e0120254.

402. Wang Q, Chuikov S, Taitano S, Wu Q, Rastogi A, Tuck SJ, et al. Dimethyl fumarate protects neural stem/progenitor cells and neurons from oxidative damage through Nrf2-ERK1/2 MAPK pathway. Int J Mol Sci. 2015 Jun 17;16(6):13885–907.

403. Traber MG, Stevens JF. Vitamins C and E: Beneficial effects from a mechanistic perspective. Free Radic Biol Med. 2011 Sep 1;51(5):1000–13.

404. Levine M, Wang Y, Padayatty SJ, Morrow J. A new recommended dietary allowance of vitamin C for healthy young women. Proc Natl Acad Sci U S A. 2001 Aug 14;98(17):9842–6.

405. Levine M, Conry-Cantilena C, Wang Y, Welch RW, Washko PW, Dhariwal KR, et al. Vitamin C pharmacokinetics in healthy volunteers: evidence for a

recommended dietary allowance. Proc Natl Acad Sci U S A. 1996 Apr 16;93(8):3704–9.

406. Levine M, Padayatty SJ, Espey MG. Vitamin C: a concentration-function approach yields pharmacology and therapeutic discoveries. Adv Nutr Bethesda Md. 2011 Mar;2(2):78–88.

407. Noroozi M, Angerson WJ, Lean ME. Effects of flavonoids and vitamin C on oxidative DNA damage to human lymphocytes. Am J Clin Nutr. 1998 Jun;67(6):1210–8.

408. You BR, Park WH. Arsenic trioxide induces human pulmonary fibroblast cell death via increasing ROS levels and GSH depletion. Oncol Rep. 2012 Aug 1;28(2):749–57.

409. Noh D, Choi JG, Huh E, Oh MS. Tectorigenin, a flavonoid-based compound of Leopard lily rhizome, attenuates UV-B-induced apoptosis and collagen degradation by inhibiting oxidative stress in human keratinocytes. Nutrients. 2018 Dec;10(12):1998.

410. Clapier CR, Cairns BR. The biology of chromatin remodeling complexes. Annu Rev Biochem. 2009;78:273–304.

411. Garcia-Canton C, Anadon A, Meredith C. Assessment of the in vitro γH2AX assay by High Content Screening as a novel genotoxicity test. Mutat Res Genet Toxicol Environ Mutagen. 2013 Oct 9;757(2):158–66.

412. Zhang J, Wang X, Bove KE, Xu M. DNA fragmentation factor 45-deficient cells are more resistant to apoptosis and exhibit different dying morphology than wild-type control cells. J Biol Chem. 1999 Dec 24;274(52):37450–4.

413. Hang B, Sarker AH, Havel C, Saha S, Hazra TK, Schick S, et al. Thirdhand smoke causes DNA damage in human cells. Mutagenesis. 2013 Jul;28(4):381–91.

414. Cloutier JF, Drouin R, Weinfeld M, O'Connor TR, Castonguay A. Characterization and mapping of DNA damage induced by reactive metabolites of 4-(methylnitrosamino)-1-(3-pyridyl)-1-butanone (NNK) at nucleotide resolution in human genomic DNA. J Mol Biol. 2001 Oct 26;313(3):539–57.

415. Chung FL, Xu Y. Increased 8-oxodeoxyguanosine levels in lung DNA of A/J mice and F344 rats treated with the tobacco-specific nitrosamine 4-(methylnitrosamine)-1-(3-pyridyl)-1-butanone. Carcinogenesis. 1992 Jul;13(7):1269–72.

416. Majidinia M, Bishayee A, Yousefi B. Polyphenols: Major regulators of key components of DNA damage response in cancer. DNA Repair. 2019 Oct 1;82:102679.

417. Sharma P, de Oca MKM, Alkeswani AR, McClees SF, Das T, Elmets CA, et al. Tea polyphenols for the prevention of UVB-induced skin cancer. Photodermatol Photoimmunol Photomed. 2018 Jan;34(1):50–9.

418. Yan S, Sorrell M, Berman Z. Functional interplay between ATM/ATR-mediated DNA damage response and DNA repair pathways in oxidative stress. Cell Mol Life Sci CMLS. 2014 Oct;71(20):3951–67.

419. Lu Y, Liu Y, Yang C. Evaluating in vitro DNA damage using comet assay. J Vis Exp JoVE. 2017 Oct 11;(128):56450.

420. Wölfle U, Esser PR, Simon-Haarhaus B, Martin SF, Lademann J, Schempp CM. UVB-induced DNA damage, generation of reactive oxygen species, and inflammation are effectively attenuated by the flavonoid luteolin in vitro and in vivo. Free Radic Biol Med. 2011 May 1;50(9):1081–93.

421. Roy M, Sinha D, Mukherjee S, Biswas J. Curcumin prevents DNA damage and enhances the repair potential in a chronically arsenic-exposed human population in West Bengal, India. Eur J Cancer Prev. 2011 Mar;20(2):123–31.

422. Suantawee T, Cheng H, Adisakwattana S. Protective effect of cyanidin against glucose- and methylglyoxal-induced protein glycation and oxidative DNA damage. Int J Biol Macromol. 2016 Dec 1;93:814–21.

423. Belhan S, Özkaraca M, Özdek U, Kömüroğlu AU. Protective role of chrysin on doxorubicin-induced oxidative stress and DNA damage in rat testes. Andrologia. 2020;52(9):e13747.

424. Manna K, Das U, Das D, Kesh SB, Khan A, Chakraborty A, et al. Naringin inhibits gamma radiation-induced oxidative DNA damage and inflammation, by modulating p53 and NF-κB signaling pathways in murine splenocytes. Free Radic Res. 2015 Apr 3;49(4):422–39.

425. Sakano K, Mizutani M, Murata M, Oikawa S, Hiraku Y, Kawanishi S. Procyanidin B2 has anti- and pro-oxidant effects on metal-mediated DNA damage. Free Radic Biol Med. 2005 Oct 15;39(8):1041–9.

426. Zhang Y, Guo L, Law BYK, Liang X, Ma N, Xu G, et al. Resveratrol decreases cell apoptosis through inhibiting DNA damage in bronchial epithelial cells. Int J Mol Med. 2020 Jun;45(6):1673–84.

427. Ding Y, Paonessa JD, Randall KL, Argoti D, Chen L, Vouros P, et al. Sulforaphane inhibits 4-aminobiphenyl-induced DNA damage in bladder cells and tissues. Carcinogenesis. 2010 Nov;31(11):1999–2003.

428. Min K, Ebeler SE. Quercetin inhibits hydrogen peroxide-induced DNA damage and enhances DNA repair in Caco-2 cells. Food Chem Toxicol. 2009 Nov 1;47(11):2716–22.

429. Bártíková H, Boušová I, Jedličková P, Lněničková K, Skálová L, Szotáková B. Effect of standardized cranberry extract on the activity and expression of selected biotransformation enzymes in rat liver and intestine. Molecules. 2014 Sep 18;19(9):14948–60.

430. Iwuchukwu OF, Tallarida RJ, Nagar S. Resveratrol in combination with other dietary polyphenols concomitantly enhances antiproliferation and UGT1A1 induction in Caco-2 cells. Life Sci. 2011 Jun 6;88(23–24):1047–54.

431. Chieli E, Romiti N, Rodeiro I, Garrido G. In vitro effects of Mangifera indica and polyphenols derived on ABCB1/P-glycoprotein activity. Food Chem Toxicol. 2009 Nov 1;47(11):2703–10.

432. Crampsie MA, Jones N, Das A, Aliaga C, Desai D, Lazarus P, et al. Phenylbutyl isoselenocyanate modulates phase I and II enzymes and inhibits 4-(methylnitrosamino)-1-(3-pyridyl)- 1-butanone–induced DNA adducts in mice. Cancer Prev Res (Phila Pa). 2011 Nov 2;4(11):1884–94.

433. Castell JV, Donato MT, Gómez-Lechón MJ. Metabolism and bioactivation of toxicants in the lung. The in vitro cellular approach. Exp Toxicol Pathol Off J Ges Toxikol Pathol. 2005 Jul;57 Suppl 1:189–204.

434. Stachel N, Skopp G. Formation and inhibition of ethyl glucuronide and ethyl sulfate. Forensic Sci Int. 2016 Aug 1;265:61–4.

435. Galijatovic A, Walle UK, Walle T. Induction of UDP-glucuronosyltransferase by the flavonoids chrysin and quercetin in Caco-2 cells. Pharm Res. 2000 Jan;17(1):21–6.

436. van der Logt EMJ, Roelofs HMJ, Nagengast FM, Peters WHM. Induction of rat hepatic and intestinal UDP-glucuronosyltransferases by naturally occurring dietary anticarcinogens. Carcinogenesis. 2003 Oct 1;24(10):1651–6.

437. Shih PH, Yeh CT, Yen GC. Anthocyanins induce the activation of phase II enzymes through the antioxidant response element pathway against oxidative stress-induced apoptosis. J Agric Food Chem. 2007 Nov 1;55(23):9427–35.

438. Samarghandian S, Azimi-Nezhad M, Samini F, Farkhondeh T. Chrysin treatment improves diabetes and its complications in liver, brain, and pancreas in

streptozotocin-induced diabetic rats. Can J Physiol Pharmacol. 2016 Apr;94(4):388–93.

439. Steele VE, Kelloff GJ, Balentine D, Boone CW, Mehta R, Bagheri D, et al. Comparative chemopreventive mechanisms of green tea, black tea and selected polyphenol extracts measured by in vitro bioassays. Carcinogenesis. 2000 Jan 1;21(1):63–7.

440. Gong Y qing, Huang W, Li K ran, Liu Y yuan, Cao G fan, Cao C, et al. SC79 protects retinal pigment epithelium cells from UV radiation via activating Akt-Nrf2 signaling. Oncotarget. 2016 Aug 9;7(37):60123–32.

441. Abeyrathna P, Su Y. The critical role of Akt in cardiovascular function. Vascul Pharmacol. 2015 Nov;74:38–48.

442. Li K ran, Yang S qing, Gong Y qing, Yang H, Li X miao, Zhao Y xia, et al. 3H-1,2-dithiole-3-thione protects retinal pigment epithelium cells against Ultra-violet radiation via activation of Akt-mTORC1-dependent Nrf2-HO-1 signaling. Sci Rep. 2016 May 6;6:25525.

443. Zhang F, Shao C, Chen Z, Li Y, Jing X, Huang Q. Low Dose of Trichostatin A Improves Radiation Resistance by Activating Akt/Nrf2-Dependent Antioxidation Pathway in Cancer Cells. Radiat Res. 2021 Jan;195(4):366–77.

444. Zheng K, Zhang Q, Sheng Z, Li Y, Lu H he. Ciliary Neurotrophic Factor (CNTF) Protects Myocardial Cells from Oxygen Glucose Deprivation (OGD)/Re-Oxygenation via Activation of Akt-Nrf2 Signaling. Cell Physiol Biochem. 2018;51(4):1852–62.

445. Feng J, Park J, Cron P, Hess D, Hemmings BA. Identification of a PKB/Akt hydrophobic motif Ser-473 kinase as DNA-dependent protein kinase. J Biol Chem. 2004 Sep 24;279(39):41189–96.

446. Sarbassov DD, Guertin DA, Ali SM, Sabatini DM. Phosphorylation and regulation of Akt/PKB by the rictor-mTOR complex. Science. 2005 Feb 18;307(5712):1098–101.

447. GPS 5.0 - Kinase-specific Phosphorylation Site Prediction [Internet]. [cited 2022 Jul 4]. Available from: http://gps.biocuckoo.cn/

448. Baba K, Morimoto H, Imaoka S. Seven in absentia homolog 2 (Siah2) protein is a regulator of NF-E2-related factor 2 (Nrf2). J Biol Chem. 2013 Jun 21;288(25):18393–405.

449. Zhuang S, Yu R, Zhong J, Liu P, Liu Z. Rhein from Rheum rhabarbarum inhibits hydrogen-peroxide-induced oxidative stress in intestinal epithelial cells partly through PI3K/Akt-mediated Nrf2/HO-1 pathways. J Agric Food Chem. 2019 Mar 6;67(9):2519–29.

450. Zhu L, Ding X, Zhu X, Meng S, Wang J, Zhou H, et al. Biphasic activation of PI3K/Akt and MAPK/Erk1/2 signaling pathways in bovine herpesvirus type 1 infection of MDBK cells. Vet Res. 2011 Apr 14;42(1):57.

451. Marino M, Acconcia F, Trentalance A. Biphasic estradiol-induced AKT phosphorylation is modulated by PTEN via MAP kinase in HepG2 cells. Mol Biol Cell. 2003 Jun;14(6):2583–91.

452. Wassmann S, Wassmann K, Nickenig G. Modulation of oxidant and antioxidant enzyme expression and function in vascular cells. Hypertension. 2004 Oct;44(4):381–6.

453. Wang L, Zhang F, Peng W, Zhang J, Dong W, Yuan D, et al. Preincubation with a low-dose hydrogen peroxide enhances anti-oxidative stress ability of BMSCs. J Orthop Surg. 2020 Sep 9;15(1):392.

454. Miguel F, Augusto AC, Gurgueira SA. Effect of acute vs chronic H2O2-induced oxidative stress on antioxidant enzyme activities. Free Radic Res. 2009 Apr;43(4):340–7.

455. Wen YD, Wang H, Kho SH, Rinkiko S, Sheng X, Shen HM, et al. Hydrogen sulfide protects HUVECs against hydrogen peroxide induced mitochondrial dysfunction and oxidative stress. PLOS ONE. 2013 Feb 5;8(2):e53147.

456. Wang F, Ke Y, Yang L, Wang F. Quercetin protects human oral keratinocytes from lipopolysaccharide-induced injury by downregulating microRNA-22. Hum Exp Toxicol. 2020 Oct 1;39(10):1310–7.

457. Xiao Y, Zhou L, Zhang T, Qin C, Wei P, Luo L, et al. Anti-fibrosis activity of quercetin attenuates rabbit tracheal stenosis via the TGF-β/AKT/mTOR signaling pathway. Life Sci. 2020 Jun 1;250:117552.

458. Ghafouri-Fard S, Shoorei H, Khanbabapour Sasi A, Taheri M, Ayatollahi SA. The impact of the phytotherapeutic agent quercetin on expression of genes and activity of signaling pathways. Biomed Pharmacother. 2021 Sep 1;141:111847.

459. Shi H, Li XY, Chen Y, Zhang X, Wu Y, Wang ZX, et al. Quercetin induces apoptosis via downregulation of vascular endothelial growth factor/Akt signaling pathway in acute myeloid leukemia cells. Front Pharmacol. 2020;11:e534171.

460. Dirimanov S, Högger P. Screening of inhibitory effects of polyphenols on Akt-phosphorylation in endothelial cells and determination of structure-activity features. Biomolecules. 2019 Jun 5;9(6):219.

461. Domae C, Ashida H, Yamashita Y. Black soybean seed coat polyphenols promote nitric oxide production in the aorta through the Akt/eNOS pathway. Funct Foods Health Dis. 2020 Aug 13;10(8):330–43.

462. Li YR, Li GH, Zhou MX, Xiang L, Ren DM, Lou HX, et al. Discovery of natural flavonoids as activators of Nrf2-mediated defense system: Structure-activity relationship and inhibition of intracellular oxidative insults. Bioorg Med Chem. 2018 Oct 1;26(18):5140–50.

463. Croft KD, Zhang D, Jiang R, Ayer A, Shengule S, Payne RJ, et al. Structural requirements of flavonoids to induce heme oxygenase-1 expression. Free Radic Biol Med. 2017 Dec 1;113:165–75.

464. Sutcliffe TC, Winter AN, Punessen NC, Linseman DA. Procyanidin B2 protects neurons from oxidative, nitrosative, and excitotoxic stress. Antioxidants. 2017 Oct 13;6(4):77.

465. Meng H, Forooshani PK, Joshi PU, Osborne J, Mi X, Meingast C, et al. Biomimetic recyclable microgels for on-demand generation of hydrogen peroxide and antipathogenic application. Acta Biomater. 2019 Jan 1;83:109–18.

466. Zhang Z, He X, Zhou C, Reaume M, Wu M, Liu B, et al. Iron Magnetic Nanoparticle-Induced ROS Generation from Catechol-Containing Microgel for Environmental and Biomedical Applications. ACS Appl Mater Interfaces. 2020 May 13;12(19):21210–20.

467. Thilakarathna WPDW, Rupasinghe HPV. Microbial metabolites of proanthocyanidins reduce chemical carcinogen-induced DNA damage in human lung epithelial and fetal hepatic cells in vitro. Food Chem Toxicol Int J Publ Br Ind Biol Res Assoc. 2019 Mar;125:479–93.

APPENDICES

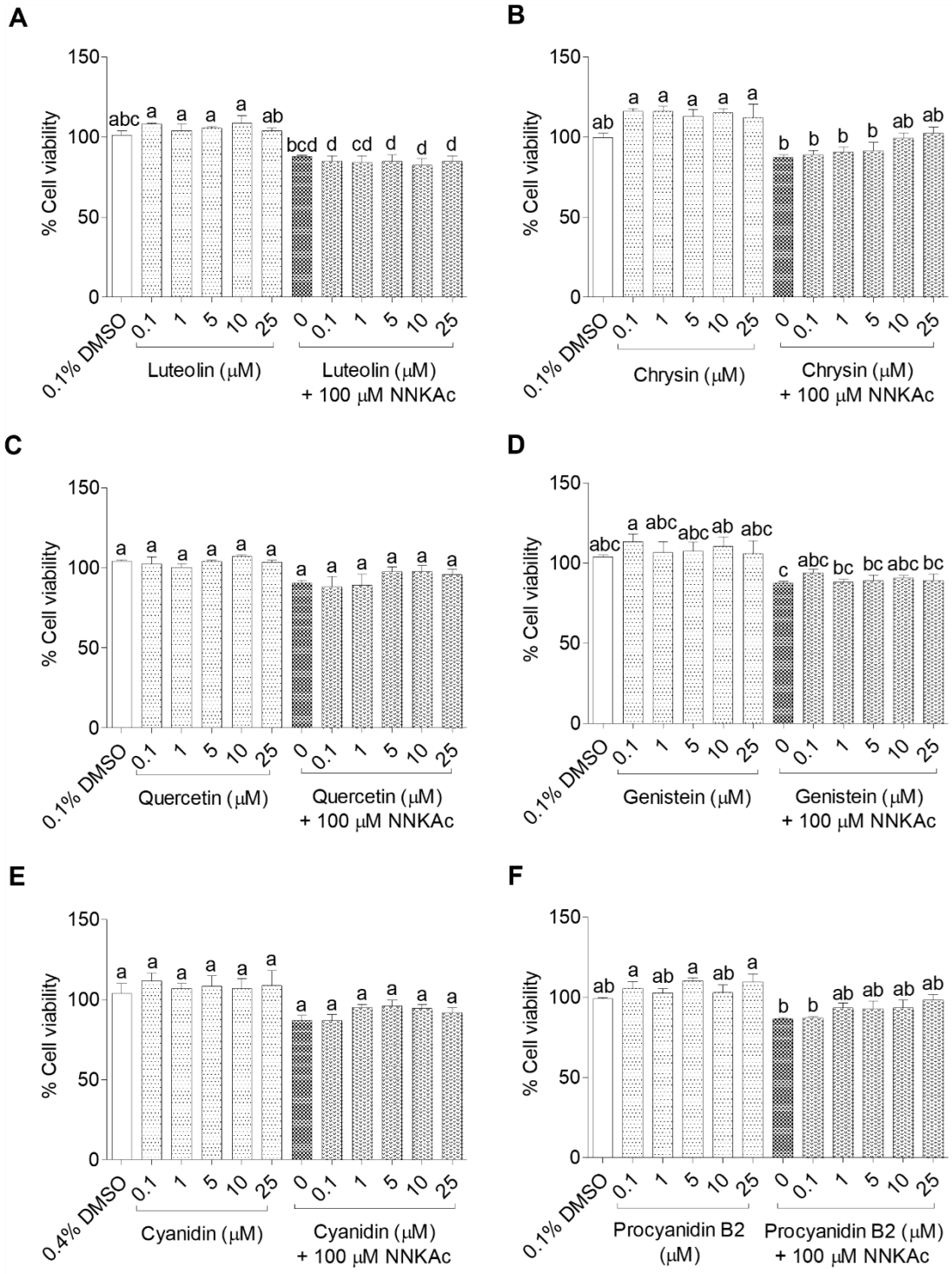

Appendix 1: Effect of luteolin (A), chrysin (B), quercetin (C), genistein (D), cyanidin (E), and procyanidin B2 (F) on cell viability against NNKAc in BEAS-2B cells

Cells were pre-treated with concentrations ranging from 0.1- 25 μM of selected compounds for 3 h. Pre-treated cells were exposed to 100 μM NNKAc for another 3 h. DMSO (0.1% or 0.4%) was used as the vehicle control. Effects on cell viability were quantified using the MTS assay. Three independent studies (each done in duplicates) were performed, and results were expressed as mean ± standard deviation. Statistical analysis of data was performed by one-way ANOVA and mean comparison was done by Tukey's mean comparison method (α=0.05) using Minitab 19 statistical software. Mean values that do not share similar letters (i.e., a-e) in bar graphs are significantly different ($p<0.05$). Abbreviations: NNKAc: 4-[(acetoxymethyl)nitrosamino]-1-(3-pyridyl)-1-butanone, DMSO: dimethyl sulfoxide.

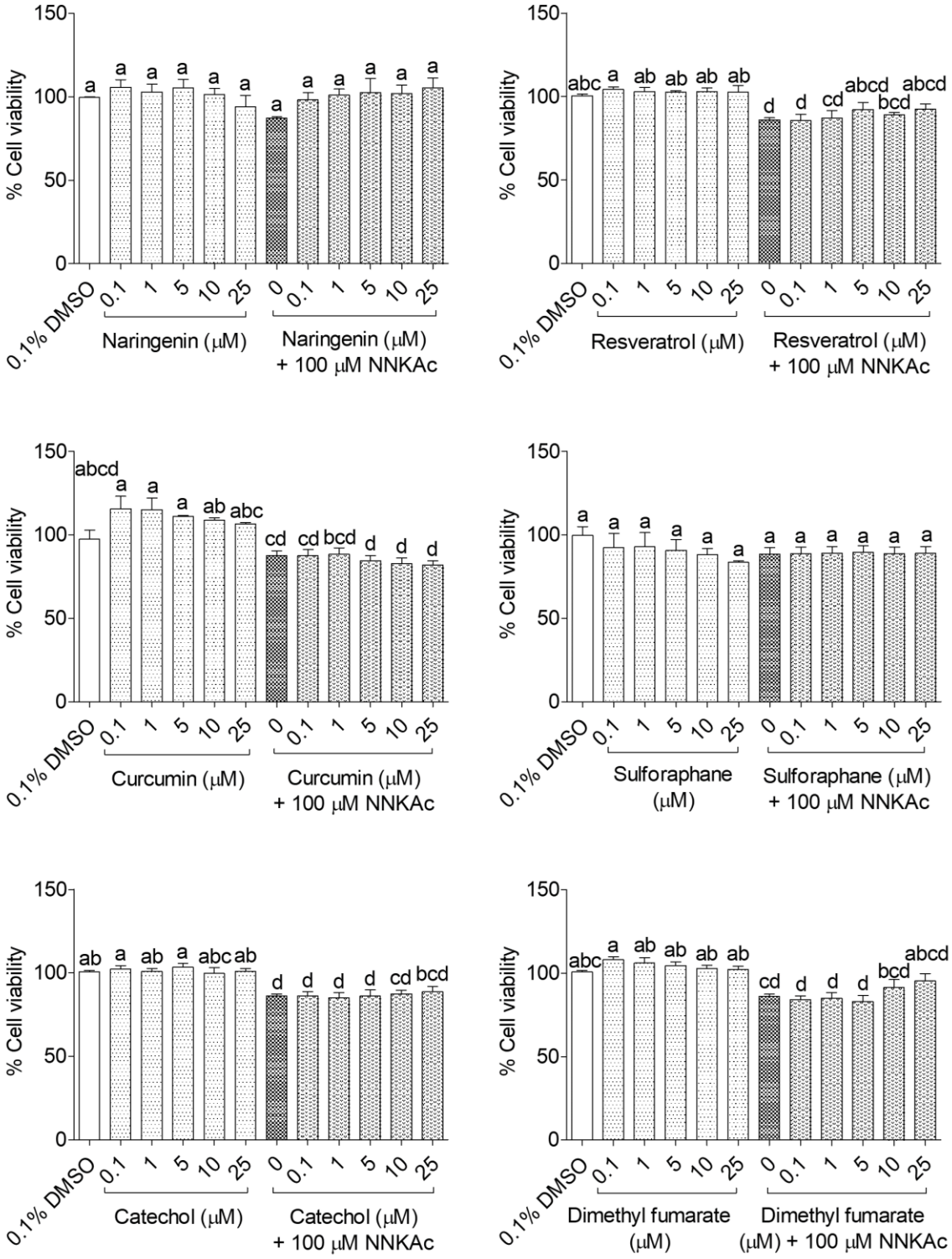

Appendix 2: Effect of naringenin (A), resveratrol (B), curcumin (C), sulforaphane (D), catechol (E), and dimethyl fumarate (F) on cell viability against NNKAc in BEAS-2B cells

Cells were pre-treated with concentrations ranging from 0.1- 25 µM of selected compounds for 3 h. Pre-treated cells were exposed to 100 µM NNKAc for another 3 h. DMSO (0.1%) was used as the vehicle control. Effects on cell viability were quantified using the MTS assay. Three independent studies (each done in duplicates) were performed, and results were expressed as mean ± standard deviation. Statistical analysis of data was performed by one-way ANOVA and mean comparison was done by Tukey's mean comparison method (α=0.05) using Minitab 19 statistical software. Mean values that do not share similar letters (i.e., a-e) in bar graphs are significantly different ($p<0.05$). Abbreviations: NNKAc: 4-[(acetoxymethyl)nitrosamino]-1-(3-pyridyl)-1-butanone, DMSO: dimethyl sulfoxide.

Appendix 3: Copyright permission from ACS publications to adapt a figure

4/6/22, 3:24 PM Rightslink® by Copyright Clearance Center

CCC RightsLink®

Home | Help | Live Chat | Tharindu Suraweera Arachchilage

ACS Publications
Most Trusted. Most Cited. Most Read.

Exposure and Metabolic Activation Biomarkers of Carcinogenic Tobacco-Specific Nitrosamines

Author: Stephen S. Hecht, Irina Stepanov, Steven G. Carmella
Publication: Accounts of Chemical Research
Publisher: American Chemical Society
Date: Jan 1, 2016

Copyright © 2016, American Chemical Society

PERMISSION/LICENSE IS GRANTED FOR YOUR ORDER AT NO CHARGE

This type of permission/license, instead of the standard Terms and Conditions, is sent to you because no fee is being charged for your order. Please note the following:

- Permission is granted for your request in both print and electronic formats, and translations.
- If figures and/or tables were requested, they may be adapted or used in part.
- Please print this page for your records and send a copy of it to your publisher/graduate school.
- Appropriate credit for the requested material should be given as follows: "Reprinted (adapted) with permission from {COMPLETE REFERENCE CITATION}. Copyright {YEAR} American Chemical Society." Insert appropriate information in place of the capitalized words.
- One-time permission is granted only for the use specified in your RightsLink request. No additional uses are granted (such as derivative works or other editions). For any uses, please submit a new request.

If credit is given to another source for the material you requested from RightsLink, permission must be obtained from that source.

BACK CLOSE WINDOW

© 2022 Copyright - All Rights Reserved | Copyright Clearance Center, Inc. | Privacy statement | Terms and Conditions
Comments? We would like to hear from you. E-mail us at customercare@copyright.com

https://s100.copyright.com/AppDispatchServlet 1/1

Appendix 4: Copyright permission from MDPI to use published literature review in the thesis

Re: Requesting permission to include published literature review in M.Sc. thesis

Antioxidants <antioxidants@mdpi.com>
Thu 3/3/2022 6:05 PM
To: Tharindu Suraweera Arachchilage <th992644@dal.ca>
Cc: Vasantha Rupasinghe <vrupasinghe@Dal.Ca>
CAUTION: The Sender of this email is not from within Dalhousie.

Dear Tharindu,

Thanks for your email. There is no need to send you the formal file since Antioxidants is open access journal and the copyright is retained by the authors.

You could check the copyright issue at the following link:
https://www.mdpi.com/authors/rights

You may see "the article may be reused and quoted provided that the original published version is cited" on the website above.

Therefore please feel free to use your published paper's content in your thesis.

Best regards,
Ms. Hortensia Hou
Managing Editor
E-Mail: hortensia.hou@mdpi.com
News: Antioxidants received increased Impact Factor of 6.312 and 5-year Impact Factor of 6.648 in 2020.

On 2022/3/4 3:38, Tharindu Suraweera Arachchilage wrote:
> Hi Hortensia,
>
> Thank you so much for your email. Is it possible to get a letter of
> permission emphasized on copy right permission to include in my thesis?
>
> Looking forward for your kind reply.
>
> Sincerely,
> Tharindu
>
> Get Outlook for Android <https://aka.ms/ghei36>
>
> ---
> *From:* Antioxidants <antioxidants@mdpi.com>

> *Sent:* Wednesday, February 23, 2022, 3:57 AM
> *To:* Tharindu Suraweera Arachchilage
> *Cc:* Vasantha Rupasinghe
> *Subject:* Re: Requesting permission to include published literature
> review in M.Sc. thesis
>
> CAUTION: The Sender of this email is not from within Dalhousie.
>
> Dear Tharindu,
>
> As the author of the published paper, you can reuse it in your M.Sc.
> thesis.
>
> Best regards,
> Hortensia
> On 2022/2/23 4:05, Tharindu Suraweera Arachchilage wrote:
>> Hi,
>>
>> I'm Tharindu Lakshan Suraweera Arachchilage, a M.Sc. student attached to
>> the Department of Plant, Food, and Environmental Sciences, Faculty of
>> Agriculture, Dalhousie University, Canada. I have published the
>> literature review related to my M.Sc. in Agriculture thesis in your
>> journal under the title of "Regulation of Nrf2/ARE pathway by Dietary
>> Flavonoids: A Friend or Foe for Cancer Management". Full reference for
>> the mentioned published literature review is given below.
>>
>> * *Suraweera, T.L.,*Rupasinghe, H. P. V., Dellaire, G*. *and Xu, Z.
>> (2020). Regulation of Nrf2/ARE Pathway by Dietary Flavonoids: A
>> Friend or Foe for Cancer Management? /Antioxidants/, 9(10), 973.
>> DOI: 10.3390/antiox9100973 <https://dx.doi.org/10.3390%2Fantiox9100973>
>>
>>
>> I wish to include texts and images of this review paper either as it is
>> or with some changes in my M.Sc. thesis. For that, I am glad if you can
>> provide me the required copy right permission to reproduce or use the
>> content as it is in my thesis.
>>
>> Looking forward for your kind reply.
>>
>> Sincerely,
>>
>> Tharindu
>>
>